NEW PERSPECTIVES ON FRACTIONAL QUANTUM HALL PHYSICS

BY

RAMANJIT SOHAL

DISSERTATION

Submitted in partial fulfillment of the requirements
for the degree of Doctor of Philosophy in Physics
in the Graduate College of the
University of Illinois Urbana-Champaign, 2021

Urbana, Illinois

Doctoral Committee:

Professor Michael Stone, Chair
Professor Eduardo Fradkin, Director of Research
Professor Vidya Madhavan
Associate Professor Bryce Gadway

Abstract

Despite having been discovered nearly four decades ago, fractional quantum Hall (FQH) states continue to provide platforms for the discovery of novel physical phenomena. In this thesis, I present a study of these remarkable phases of matter from three perspectives: (1) the role of an underlying lattice and its symmetries in engendering novel FQH states, (2) the description of non-Abelian FQH states using recently developed field theory dualities, and (3) the use of entanglement entropy in characterizing interfaces of FQH states.

In the first part, we examine phases of matter known as fractional Chern insulators (FCIs), lattice analogues of FQH states. We begin in Chapter 2 by formulating a composite fermion theory for FCI states in a kagome lattice model, making use of a recently developed lattice Chern-Simons theory to effect the flux attachment. We identify sequences of Abelian states, including states for which the Hall conductance does not match the filling fraction, which we characterize as realizing distinct translational symmetry fractionalization classes. Next, we apply this formalism in Chapter 3 to identify paired states of composite fermions in a square-lattice Hofstadter model. Magnetic translation symmetry is found to enforce finite-momentum pairing of the composite fermions, yielding pair-density wave (PDW) states with daughter charge-density wave order, analogous to the PDWs conjectured to describe the high-T_c cuprate superconductors. This constitutes a novel example of intertwined orders, in which topological order and broken symmetry order arise from a common microscopic origin.

In the second part, we apply a recently proposed web of Chern-Simons-matter theory dualities to develop effective field theories for a large class of non-Abelian FQH states. First, in Chapter 4, we demonstrate how these dualities can be used to construct bosonic Landau-Ginzburg theories of the Read-Rezayi and generalized non-Abelian spin singlet states by introducing interlayer interactions in a multilayer Abelian FQH system. Next, we extend this construction in Chapter 5 to develop a field theory and motivate a trial wave function for the elusive Fibonacci FQH state, which is the minimal model for realizing a universal topological quantum computer. We subsequently examine in Chapter 6 dual fermionic non-Abelian Chern-Simons-matter theories, allowing us to develop composite fermion descriptions of the Blok-Wen FQH states and a series of states which may be understood as arising from pairing in a dual Abelian composite fermion

theory. Our analysis reveals that dual fermionic theories can predict distinct ground states in a magnetic field, demonstrating the utility of dualities in mapping out regions of the phase diagram of electrons at fractional filling.

In the final part of this thesis, which comprises Chapter 7, we characterize interfaces of non-Abelian Moore-Read FQH states using entanglement entropy. We first employ a cut-and-glue approach to obtain the expected topological entanglement entropy (TEE) for a uniform Moore-Read state on the torus in each topological sector. This involves approximating the entanglement as arising purely from the coupled 1D chiral edge degrees of freedom at the entanglement cut. We next consider interfaces of distinct generalized Moore-Read states, identify when the interfaces can be gapped using an anyon condensation picture, construct explicit gapping interactions, and then compute the TEE for an entanglement cut along the interface. It is found that the value of the TEE is related to the total quantum dimension of a "parent" topological phase of the two generalized Moore-Read states between which the interface is formed.

To my parents

Acknowledgments

In these past few years, I have learned much more about physics and myself than I could have anticipated. For this, I have many friends and mentors to thank. I would like to acknowledge some of them here.

I am deeply grateful to my advisor, Eduardo Fradkin, for all his support and guidance. It has been a privilege to have had such a caring, respectful, and enthusiastic mentor with such a vast knowledge base in physics. Regardless of the problem at hand, he has always had something insightful to say that would help me appreciate new perspectives on my research. Eduardo taught me to think creatively and provided me with the latitude and encouragement to take risks and pursue my interests, which has helped me shape my own approach to physics. I am very grateful for his patience and for him displaying his faith in me as a researcher, even when I fell into self-doubt. I hope I have managed to integrate some amount of Eduardo's insight, tenacity, and good-natured approach to research and life more broadly during my time at Urbana.

Next I would like to acknowledge my collaborators, without whom this thesis would not have been possible. I thank Luiz Santos who, from the beginning of my graduate career, listened to my ideas with intent and respect and has been a constant source of positivity. I also thank Jeffrey Teo, who, throughout our collaboration, encouraged me to pursue my ideas while also pushing me to refine them. I am grateful to both Luiz and Jeffrey for always being in my corner and for providing models of tenacious researchers to which to aspire. I would also like to thank Hart Goldman for sharing his encyclopedic field theory knowledge and for his resolute approach to research that helped drive our work on non-Abelian quantum Hall states to completion. I thank Bo Han for sharing his conformal field theory expertise and helping initiate the collaboration with Jeffrey and Luiz. I further thank Jonah Kudler-Flam, Laimei Nie, and Xiao-Qi Sun for making my entry into the field of quantum chaos a more ordered one. I thank Eugeniu Plamadeala for introducing me to the physics of one-dimensional systems, which proved quite valuable for subsequent work.

I would like to thank Bryce Gadway, Vidya Madhavan, and Michael Stone for agreeing to serve on my committee and taking the time to read about my work. More broadly, I thank the members of the department and ICMT for creating such a stimulating environment including, in particular, Thomas Faulkner and Michael Stone for insightful courses and Taylor Hughes for helpful discussions.

I also thank Janice Benner and Wendy Wimmer for their exceedingly reliable help with administrative matters and Lance Cooper for his guidance and his commitment to the well-being of the graduate student body. They have been integral in making the department such a warm and welcoming environment.

I thank my fellow graduate students for making my time at Urbana an intellectually stimulating and enjoyable one through physics discussions, reading groups, and their friendship more broadly. I am grateful to all those I got to know and learn from including, in addition to those above, Oleg Dubinkin, Manthos Karydas, Saavanth Velury, Zach Weiner, and Penghao Zhu. I also thank Wladimir Benalcazar for helpful advice during my first year here.

I am also thankful for the continued companionship of my undergraduate friends – Afiny Akdemir, Matthias Yang He, Hubert Lin, Khoa Dang Nguyen, Pratyush Sarkar, and Freid Tong – from Toronto, as well as my long-lasting high school friendships. They have provided constant sources of motivation and helped me preserve (or regain) my sanity through the ups and downs of the past few years.

I would also like to thank my relatives – Navid, Tina, Neetu, and Paul – for providing a home away from home and their kids for providing welcome distractions from work.

Last but not least, I would like to thank my parents for their unconditional love and support. They instilled in me a fascination for science and learning at a young age. Through some combination of stubbornness and naïveté – neither of which I have really outgrown – that initial fascination led me on to a path to graduate studies in physics. Throughout all the anxieties and frustrations of this journey, they have been constant in their support of me and my goals and for that and so much more, I am deeply grateful.

Funding acknowledgments: I acknowledge the support of the Natural Sciences and Engineering Research Council of Canada (NSERC) [funding reference number PGSD3-516762-2018]. This work was also supported in part by the US National Science Foundation under Grant No. DMR-1725401 at the University of Illinois (awarded to Eduardo Fradkin).

Table of Contents

List of Tables

List of Figures

Chapter 1

Introduction

1.1 The Quantum Hall Effect and Topological Order

Perhaps one of the greatest surprises in condensed matter physics in recent decades has been the discovery of insulating phases of matter known as *topological orders*, which – at least to local probes – appear completely featureless. Lying outside the Landau paradigm, these phases do not exhibit spontaneous symmetry breaking and hence are not characterized by local order parameters. Instead, the defining feature of topologically ordered phases is that, in these states, the electron *fractionalizes* into quasiparticles known as anyons, which can carry fractional electric charge and interact via emergent gauge fields. The non-local correlations mediated by these gauge fields are made manifest in patterns of long-range quantum entanglement, a hallmark of topological order. Explaining the emergence and properties of these exotic phases of matter has resulted in a remarkable confluence of ideas from the fields of condensed matter physics, high-energy physics, and quantum information and continues to be a spring well for novel physics.

Given this impressive résumé and the central role played by topology in modern condensed matter physics, it is perhaps surprising that the theoretically most well understood and *only* experimental examples of topologically ordered phases are found in a seemingly mundane system, first encountered in one's undergraduate education: a two-dimensional electron gas (2DEG) in a strong magnetic field. At the single particle level, the energy spectrum of this system consists of equally spaced and highly degenerate Landau levels (LLs). Since the kinetic energy is quenched, one expects that on fractionally filling a LL, electronic interactions will break the degeneracy and select a strongly correlated state as the ground state. It was with this motivation that studies of 2DEGs in strong magnetic fields were carried out in the 1980s, with the expectation that one would find Wigner crystals of electrons – symmetry broken states in which electrons form a rigid lattice as a result of Coulomb repulsion. What was found was much more perplexing [3, 4]. At rational LL filling fractions $\nu = N_e/N_\Phi$, where N_e is the number of electrons and $N_\Phi = eB/hc$ the number of magnetic flux quanta piercing the system, insulating states were observed which *preserved* all symmetries of the two-dimensional system. Moreover, although these states necessarily had gapped charge carriers in the

bulk due to a vanishing longitudinal conductivity, $\sigma_{xx} = 0$, they nevertheless exhibited a Hall conductance *exactly* quantized to the LL filling fraction:

$$\sigma_{xy} = \nu \frac{e^2}{h}. \tag{1.1}$$

These states are now known as integer quantum Hall (IQH) states when ν is an integer and fractional quantum Hall (FQH) states when ν is a fraction. On one hand, the IQH states are readily explained within a single particle framework, as a fully filled Landau level is trivially gapped.[1] The Hall current can be computed within linear response theory and argued to be carried by chiral edge currents at the edge of the sample. On the other hand, strong correlation effects are needed to explain the FQH states, by virtue of their origin in a fractionally filled Landau level, necessitating a more sophisticated theoretical approach to explain their emergence. This also would suggest that they correspond to a more non-trivial phase of matter.

Indeed, the theoretical framework developed in the two decades following their discovery led to our understanding that FQH states constituted the first (and, as of writing, only) examples of entirely new phases of matter, the aforementioned topologically ordered phases. Although important questions remain regarding how topological order arises in generic many-body systems, there now exists an essentially complete classification of the properties of these phases.[2] As noted above, these are two-dimensional gapped insulators, which are locally indistinguishable from a trivial gapped state. Indeed, by virtue of the bulk gap, any local operator must exhibit exponentially decaying correlations, and so the defining features of a topological order must instead be hidden in non-local correlations. These phases are distinguished by the fact that electrons fractionalize into quasiparticles known as anyons, which exhibit fractional braiding statistics and can carry fractional electric charge.[3] There are in fact two classes of anyon, Abelian and non-Abelian, distinguished by their braiding properties. Abelian anyons provide direct generalizations of bosons and fermions, in that braiding one such anyon around another anyon results in the wave function accruing a phase of $e^{i\pi\delta}$, where $0 \leq \delta \leq 1$ is a rational number. Non-Abelian anyons, in contrast, support a topological degeneracy – that is to say, a particular spatial configuration of non-Abelian anyons defines a degenerate Hilbert subspace and braiding of these anyons results in rotations within this subspace. It is these braiding processes which lie at the heart of the proposal for employing topological phases for quantum computation [6].

The second manifestation of non-locality in topological phases is their sensitivity to the boundary con-

[1] That the IQH states persist for a range of magnetic field strengths and not only exactly at integer values of ν requires the presence of disorder.

[2] Formally speaking, in the same way that group theory provides the natural language for understanding broken symmetry orders, the mathematical language of unitary modular tensor categories provides a classification of topological orders [5].

[3] In the modern parlance, FQH states are topological orders *enriched* by a $U(1)$ charge conservation symmetry. That the anyons carry fractional charge means they transform under a *projective* representation of $U(1)$. In Chapter 2, we will see how anyons can transform projectively under lattice symmetries.

ditions of the spatial manifold on which they are defined. Indeed, these phases exhibit a *bulk-boundary correspondence*. On a manifold with boundary, while the bulk of a topological order remains gapped, the boundary will support (with some exceptions) gapless edge modes described, in general, by a strongly interacting conformal field theory. In the context of the FQHE, it is these edge modes which contribute to both the electrical and thermal Hall conductance. In the less experimentally relevant scenario of a closed spatial manifold, a topological order will exhibit a ground state degeneracy dependent on the genus (i.e. number of holes) of the manifold. For instance, a topological phase will have a unique ground state on the sphere and degenerate ground states on the torus. Note that if one slices open the torus to obtain a cylinder, the ground state degeneracy immediately disappears, no matter the system size – information about the topology of the manifold is somehow non-locally stored in the ground state wave functions. All these manifestations of non-locality just outlined are captured in the description of topological orders in terms of *topological quantum field theories* and, perhaps more fundamentally, reflect their long-range entanglement, a notion we will make precise later in this Chapter.

Perhaps one of the greatest theoretical advances in recent years has been the development of a framework – which we shall turn to shortly – predicting the emergence of the vast majority of experimentally observed FQH states and that they exhibit topological order. In a rare and beautiful display of accord between theory and experiment, many of the properties outlined above have been observed. As a non-exhaustive list, we note that quite recently, interferometry experiments have confirmed the fractional statistics of anyons [7, 8] and thermal Hall measurements have provided strong evidence in favor of non-Abelian topological order at $\nu = \frac{5}{2}$ [9].

In spite of these successes, many problems – new and old – remain to be explored in the FQH arena. Indeed, experimental advances in engineering so-called moiré materials have raised the possibility of realizing novel FQH states outside the LL context. Yet even in the LL problem, how the vast majority of conjectured non-Abelian FQH states could emerge remains poorly understood. Systems with *interfaces* between distinct FQH states have also come to the fore, as a result of the possibility of engineering non-Abelian zero modes at said interfaces. In this thesis, we will present work addressing these three broad problems using, accordingly, both old and new theoretical techniques. In the balance of this Chapter, we will set the stage for these studies by first briefly reviewing the main devices used in our understanding of the standard FQH states, emphasizing their surprising interconnections. This will permit us in the following section, which serves as an outline of this thesis, to then introduce the concepts specific to the three problems addressed in this thesis and emphasize the new perspectives they provide on the FQHE.

1.2 The Laughlin States: A Case Study

1.2.1 Wave Functions to Composite Particles

Developing a theoretical understanding of the emergence of FQH states seems to be, at first glance, a difficult undertaking. Indeed, the extensive degeneracy of states at fractional filling of a Landau level means the theorist's first recourse, Hartree-Fock theory, will generically be an unreliable approximation to the ground state and, beyond that, the absence of a small parameter implies there is no basis upon which to build a perturbative treatment of the system. A description of these exotic phases of matter evidently necessitates the use of non-perturbative techniques, keen physical insight, or some combination thereof.

In fact, one of the early crucial advances towards our understanding of the FQHE was provided by an *ansatz* wave function proposed by Laughlin [10]. Working in the symmetric gauge, Laughlin proposed that a system of N electrons in a FQH state at filling $\nu = \frac{1}{m}$, with m an odd integer, is described by the wave function,

$$\Psi_m(z_1, \dots z_N) = \prod_{i<j} (z_i - z_j)^m e^{-\sum_i |z_i|^2/4l_B}, \tag{1.2}$$

where $l_B = \sqrt{\hbar c/eB}$ is the magnetic length,[4] m is a "variational" parameter, which is in fact fixed by the filling fraction, and $z_j = x_j + iy_j$ describes the complex coordinate of the j^{th} electron. Indeed, if $m = 1$, this wave function reduces to one describing a fully filled Landau level of electrons, as expected. In addition, since m is odd, we see that the wave function is anti-symmetric under exchange of the coordinates of two electrons, as it should be. A crucial feature of this expression is that the factor multiplying the Gaussian is an *analytic* function of the z_i, which tells us that Ψ_m is a superposition of states lying in the lowest LL. Surprisingly, this simple wave function has remarkably high overlap with that numerically obtained via exact diagonalization for systems of a few electrons with Coulomb interactions. Moreover, this construction captures the properties of quasiparticles. As a *gedanken* experiment one can imagine inserting a solenoid of a single magnetic flux quantum at position η. This corresponds to multiplying Ψ_m by the factor $\prod_i (z_i - \eta)$, since braiding a single electron around the solenoid at η must yield an Aharnaov-Bohm phase of 2π. Using the so-called "plasma analogy", one can argue that a fractional charge of $-\frac{e}{m}$ is depleted at η. That is to say, the $\nu = \frac{1}{m}$ FQH state supports quasihole excitations with charge $\frac{e}{m}$. Historically, this wave function was the first step towards understanding the topological order of the FQH states.

Laughlin's ansatz, however, does not yet provide us with an understanding of *how* this gapped FQH

[4] Henceforth, we will work in natural units, $\hbar = c = 1$

state emerges. As a step towards answering this question, we follow Jain [11] in realizing that Laughlin's wave function can trivially be rewritten as

$$\Psi_m(z_1, \dots z_N) = \left(\prod_{i<j} (z_i - z_j) e^{-\sum_i |z_i|^2/4l_B} \right) \prod_{i<j} (z_i - z_j)^{m-1} \tag{1.3}$$

The first factor is simply the wave function of a fully filled Landau level of fermions. In analogy with the quasiholes described above, the second factor has the interpretation of describing solenoids attached to these fermions; indeed, since $m-1$ is even, the second factor contributes a phase of $e^{\pi i(m-1)} = 1$ on exchanging one fermion with another. This suggests an intuitive physical picture: a FQH state of electrons emerges as an IQH state of *composite fermions* – bound states of fermions with solenoids of an emergent gauge field.

This suggestive picture in fact has a solid grounding in a field theoretic description of the FQHE through the mapping known as *flux attachment*. This is the statement that a Lagrangian describing a system of electrons is equivalent to one describing *composite fermions* coupled to an emergent Chern-Simons gauge field [12]. Explicitly, letting Ψ represent the second-quantized electron field, ψ the composite fermions, A_μ the background electromagnetic (EM) field, and a_μ the emergent Chern-Simons field, we have the *duality*,[5]

$$\mathcal{L}_{\text{el}}[\Psi, \Psi^\dagger, A] \longleftrightarrow \mathcal{L}_{\text{CF}}[\psi, \psi^\dagger, a] + \frac{1}{2\pi(m-1)}(a - A)d(a - A)\,, \tag{1.4}$$

where we have employed differential form notation: $adA \equiv a_\mu \epsilon^{\mu\nu\lambda} \partial_\nu A_\lambda$. The left hand side describes interacting electrons in a background magnetic field while the right hand side describes a system of composite fermions. Note that the densities of the electrons and composite fermions are equal: $\rho \equiv \langle \Psi^\dagger \Psi \rangle = \langle \psi^\dagger \psi \rangle$. Crucially, the equation of motion for a_0 enforce the Gauss' law, or flux attachment constraint,

$$\rho = \frac{1}{2\pi(m-1)} \epsilon_{ij} \partial_i a_j, \tag{1.5}$$

which is precisely the statement that the composite fermions carry $m-1$ flux quanta of the emergent statistical gauge field a_μ. Now, suppose the electrons are at fractional filling $\nu = \frac{1}{m}$. We can perform a mean-field approximation in the composite fermion variables and assume that the emergent Chern-Simons flux is uniform throughout space. From Eq. (1.4), we see that the Chern-Simons field *screens* the magnetic

[5] Note that the Chern-Simons term has an improperly quantized coefficient. This can be rectified by introducing an auxiliary gauge field b_μ, known as the "hydrodynamic field", so as to rewrite $\frac{1}{2\pi(m-1)}(a-A)d(a-A) \sim -\frac{m-1}{4\pi} bdb + \frac{1}{2\pi} bd(a-A)$. Only with this correctly quantized action can one obtain the correct topological field theory described in the next subsection.

flux, so that the composite fermions feel a reduced flux of

$$N_\Phi^{CF} = N_\Phi - (m-1)N_e = mN_e - (m-1)N_e = N_e \tag{1.6}$$

which is to say, they fully fill a single Landau level in this effective flux, as suggested by the wave function picture! Hence, a FQH state of electrons corresponds (at mean-field level) to an IQH state of composite fermions. More generally, if the magnetic field was such that the composite fermions filled p Landau levels, then one would obtain a FQH state at filling $\nu = p/(p(m-1)+1)$. This describes the Jain sequence of states, the most stable FQH states observed in experiment.

Remarkably, a completely complementary description of the Laughlin states is accessible within a *composite boson* framework [13]. Indeed, letting Φ represent the composite boson field, we can apply the flux attachment transformation to the electronic system as follows:

$$\mathcal{L}_{\text{el}}[\Psi, \Psi^\dagger, A] \longleftrightarrow \mathcal{L}_{\text{CB}}[\Phi, \Phi^\dagger, a] + \frac{1}{2\pi m}(a-A)d(a-A)\,. \tag{1.7}$$

Now the flux attachment constraint attaches an odd number m of flux quanta to the Φ fields so that their bound state has fermionic statistics, as should be the case for an electron. Now, at filling $\nu = \frac{1}{m}$, again in a mean-field approximation, the Chern-Simons field *completely* screens the external magnetic field. This allows the composite bosons to condense, Higgsing the a_μ field. From the Lagrangian, we see that resulting gapped state has Hall conductance $\sigma_{xy} = \frac{1}{m}\frac{e^2}{h}$, and so we again arrive at the $\nu = \frac{1}{m}$ Laughlin state!

We have proceeded at a brisk pace, so let us pause and recapitulate what we have just done: starting from an *ansatz* wave function, we were able to motivate two distinct composite particle field theory perspectives on the emergence of the Laughlin states. This illustrates an underlying theme in the study of FQH physics which also pervades this thesis, namely that several complementary perspectives are often needed to build our understanding of FQH phenomena. The connections between these approaches ultimately hint at the underlying topological order of the FQH states.

1.2.2 Topological Order and Correspondences

Now, either by integrating out the matter fields in either the composite fermion or boson theories at $\nu = \frac{1}{m}$, one arrives at the hydrodynamic theory [14] of the Laughlin states:

$$\mathcal{L}_{\text{eff}} = -\frac{m}{4\pi}bdb + \frac{1}{2\pi}bdA. \tag{1.8}$$

Here b is a $U(1)$ gauge field, which is seen to describe the electronic current: $J_{\text{EM}} = \frac{1}{2\pi} db$. This $U(1)_m$ Chern-Simons action (where m denotes the "level") encodes all the key topological properties of the Laughlin state. Indeed, one can check that this action correctly predicts a Hall response of $\sigma_{xy} = \frac{1}{m}\frac{e^2}{h}$; that quasiparticles, represented by point charges with unit charge relative to b_μ, have electric charge $-\frac{e}{m}$ and braiding two such anyons yields a fractional phase of $e^{2\pi i/m}$; and a ground state degeneracy of m on the torus.

If this effective Chern-Simons action is placed on an open disk, then gauge invariance in fact mandates the existence of a single gapless bosonic mode ϕ on the edge, described by a $U(1)_m$ conformal field theory (CFT),

$$\mathcal{L}_{\text{edge}} = \frac{m}{4\pi}\partial_x\phi(\partial_t - v\partial_x)\phi. \tag{1.9}$$

The physical charge density is given by $\rho = \partial_x\phi/2\pi$, from which we see that this action describes the *chiral* propagation of charge along the edge, which is what leads to the Hall current. The *bulk-boundary correspondence* amounts to the statement that all topological data of the bulk is encoded in this edge theory. In particular, anyon excitations correspond to solitons on the edge, represented by vertex operators $e^{i\phi}$. Electron excitations are then given by composites of these operators: $e^{im\phi}$.

And with this, surprisingly, we come full circle. Indeed, the Laughlin wave function of Eq. (1.2) is in fact *equal* to an N-point correlation function of electron operators in this edge CFT. The other properties we have described hold for generic topological orders, but this correspondence between trial wave functions and the boundary theory is unique to FQH states. This relation is believed to hold for generic FQH states, whose bulk topological order is described by a G_k Chern-Simons theory, where G is an arbitrary Lie group. In these cases, trial wave functions can be constructed from correlation functions in the corresponding G_k Wess-Zumino-Witten CFT [1]. Though only a conjecture, this construction has received considerable mileage and forms the basis for much of our intuition about *non-Abelian* FQH states, as we shall soon describe.

What we have recounted in this section constitutes perhaps one of the crowning achievements of modern condensed matter physics. The composite fermion and boson theories provide explanations for the emergence of nearly all experimentally observed FQH states. The effective topological quantum field theory derived from these composite particle pictures provides a complete characterization of the fractionalized excitations, the gapless edge states, and the entanglement structure of these states. Moreover, the complementary wave function construction, aside from building our intuition about FQH states, has also served as a key tool in numerical simulations. In addition to laying the foundation for the modern theory of topological order, this nearly comprehensive theoretical understanding of the FQHE has largely stood the tests of experiment. And

yet, as we discuss next, there still is much left to be said about these remarkable states.

1.3 New Perspectives: An Outline of this Thesis

Lying just beyond the purview of the theoretical framework outlined in the previous section are a host of open problems – both old and new – and areas of exploration. Indeed, in the four decades since the discovery of the FQHE, new field theoretic tools have been developed which can shed light on hitherto poorly understood FQH states, while novel features of topological orders and new incarnations of the FQHE have gained relevance, both in theory and experiment. Our goal is to investigate these new perspectives on the FQHE. Specifically, in the three parts of this thesis, we wish to address the following problems:

(1) Recent experimental advances, especially in the engineering of moiré materials, have raised the prospect of realizing FQH states in topological Chern bands, rather than Landau levels. In such systems the lattice cannot be neglected. Can we still apply a composite fermion picture to understand FQH states in these settings? If so, can the presence of the lattice lead to novel FQH states? We investigate these states in Chapters 2 and 3, which are based on Refs. [15] and [16], respectively.

(2) The vast majority of experimentally observed FQH states are Abelian and can be described by the composite particle picture developed above. However, it is the non-Abelian states which are of interest for quantum computation applications. These exotic states have largely evaded description in terms of composite particle theories. In Chapters 4, 5, and 6, we employ new field theory tools to shed light on these states. These Chapters are based on Refs. [17], [18], and [19].

(3) Although the bulk-boundary correspondence generally implies the existence of gapless edge modes at the boundary of a topological phase, it has recently been shown that the edge modes of two distinct Abelian phases joined at an interface can be gapped out, provided the interface itself is nontrivial. In Chapter 7, which is based on Ref. [20], we extend this picture to interfaces of a class of non-Abelian interfaces, which we characterize using their entanglement properties.

In the balance of this Chapter we provide more context for these problems and motivate the tools with which we will attack them.

1.3.1 Fractional Chern Insulators and Composite Fermions

It is natural to ask to what extent a Landau level structure is needed to realize the FQHE in an electronic system. Indeed, it is now well established that an IQHE can be realized in non-interacting *lattice* systems known as Chern insulators in the *absence* of a magnetic field provided time-reversal symmetry is broken,

as first shown in the seminal work by Haldane [21]. Such systems exhibit a quantized Hall conductance of $\sigma_{xy} = C\frac{e^2}{h}$ when an integer number of bands are filled, where C is an integer invariant called the Chern number and characterizes the non-trivial topology of the Bloch states [22]. One can thus mimic a LL in a net zero magnetic field by realizing a nearly flat Chern band in a lattice system. By partially filling such a band in the presence of strong interactions, one might then expect to obtain analogues of FQH states. Indeed, numerical simulations over the past decade have provided concrete evidence for this scenario, with the resulting states naturally being called *fractional Chern insulators* (FCIs) [23–33]. These states exhibit all the hallmarks of FQH states, including anyon excitations and fractional Hall conductance.

Despite the striking similarities between FCIs and FQH states, there are several properties which make FCIs interesting phases of matter to study. Aside from the potential absence of a net non-zero magnetic field, a key difference between FCIs and continuum FQH states is the fact that the lattice structure can be ignored in the latter since the magnetic length is large relative to the lattice constant. In contrast, the lattice cannot be neglected in FCIs and can lead to novel physics. For instance, the breaking of Galilean invariance by the lattice can result in states with unequal Hall conductance and filling fraction [34]. Moreover, unlike Landau levels, Chern bands can have Chern number greater than unity, $|C| > 1$. It has been argued that these bands support FCIs with an emergent $|C|$-layer structure and that lattice defects in these states behave as non-Abelian objects known as *genons* [35,36]. Anyons can also interact non-trivially with the lattice in a phenomenon known as *symmetry fractionalization*, which means that the anyons carry fractional symmetry charges, such as fractional crystal momenta [37–40]. Aside from these topological aspects, FCIs also provide areas to investigate novel quantum critical points [41] and the competition or coexistence of topological order with conventional broken symmetry orders, such as charge density waves [42, 43].

Encouragingly, the observation of lattice FQH states was recently reported in a bilayer graphene/hexagonal boron nitride moiré heterostructure subjected to a magnetic field [44]. Although this experiment was conducted at non-zero magnetic field, the magnetic length was of the same order as the moiré super-lattice length, resulting in strong lattice effects. Indeed, states with $\sigma_{xy} \neq \nu$ were observed. More excitingly, recent years have seen significant advances in the engineering of Chern bands in solid-state moiré [44–49] and cold atom systems [50–54], raising the prospect of realizing genuine FCIs in zero magnetic field.

However, it is precisely the presence of the lattice, which makes FCIs worthy of interest, that also renders their analytical treatment a daunting theoretical challenge. Indeed, most studies of these states have relied on exact diagonalization and DMRG [23–33]. In particular, returning to our exposition of the continuum Laughlin states above, the simple form of the ansatz wave function – such as its analytic dependence on the electron coordinates – is crucially dependent on the properties of the lowest Landau level single-particle

eigenstates. Though a wave function approach to studying FCIs can be formulated [55], our goal will instead to be to develop a composite fermion theory, so as to provide a microscopic understanding of the dynamics behind the emergence of FCIs in specific lattice models.

This too, however, is fraught with its own difficulties. Indeed, the use of flux attachment on the lattice requires first understanding how to write down a lattice version of the Chern-Simons action. To see the issues inherent to this, let us consider the continuum Chern-Simons theory, expressed in Cartesian components:

$$S_{\text{continuum}}[a_\mu] = \frac{1}{2\pi}\int d^3x \left[a_0(x)\epsilon_{ij}\partial_i a_j(x) - \frac{1}{2}a_i(x)\epsilon_{ij}\dot{a}_j(x)\right]. \tag{1.10}$$

When coupled to fermions, the first term enforces the flux attachment constraint (note that a_0 has no dynamics of its own and is hence a Lagrange multiplier enforcing this constraint). The second term fixes the commutation relations of the spatial components of a_μ and ensures that the theory is gauge invariant. Now, let us attempt to write down a similar action on a lattice. In lattice gauge theory, the temporal (spatial) components of a gauge field are most naturally defined to live on the sites (links) of the lattice. Hence, fluxes are defined to live in the plaquettes. A natural candidate for a lattice Chern-Simons action then takes the form

$$S_{\text{lattice}}[a_\mu] = \frac{1}{2\pi}\int dt \sum_{\boldsymbol{x}} \left[a_0^\alpha(\boldsymbol{x},t)J_i^\alpha a_i(\boldsymbol{x},t) - \frac{1}{2}a_i(\boldsymbol{x},t)\mathcal{M}_{ij}\dot{a}_j(\boldsymbol{x},t)\right] \tag{1.11}$$

where, $\boldsymbol{x}$ labels the unit cell, α the sites within the unit cell, i labels the links within a unit cell, and J_i^α is a lattice version of the curl, such that $\Phi^\alpha(\boldsymbol{x}) \equiv J_i^\alpha a_i(\boldsymbol{x})$ is the flux through a plaquette adjacent to the site α. The first term will again enforce the flux attachment constraint, but also leads to the first issue. Since the $a_0^\alpha(\boldsymbol{x})$ are defined on the sites and the fluxes $\Phi^\alpha(\boldsymbol{x})$ on plaquettes, this action is only consistent if there exists a one-to-one assignment of sites to plaquettes. This is true for, say, the square and kagome lattices, but not for the triangular and honeycomb lattices. The second issue comes form the second term, in which the operator $\mathcal{M}_{ij}$ again fixes the commutation relations of the spatial components of a. Gauge invariance can be used to fix the form of $\mathcal{M}_{ij}$, which is lattice-dependent, though this is a non-trivial task and has been carried out first for the square lattice in Refs. [56, 57] and subsequently for all lattices satisfying the above vertex-face correspondence in Ref. [58]. So, flux attachment can be carried out on a large class of lattices, though perhaps not in as elegant a form as one may have hoped.

The aim of the first part of this thesis is to employ this formalism to investigate novel FCI states arising from gapped states of composite fermions in specific lattice models. In Chapter 2, we provide more details regarding lattice flux attachment and characterize FCI states in kagome lattice model arising (at mean-

field level) as Chern insulators of composite fermions and demonstrate how lattice translation symmetry is *fractionalized*, implying that anyons carry fractional crystal momenta. Although heuristic pictures of FCIs in terms of composite fermions have previously been proposed [59, 60], our work presents a more rigorous justification for these states, through use of the above lattice flux attachment procedure. In Chapter 3 we investigate FCI states in the square lattice Hofstadter model arising from superconducting states of composite fermions. Although a $p + ip$ paired state of composite fermions, known as the Pfaffian state, has been proposed to describe the continuum FQH state at $\nu = \frac{5}{2}$ [1, 61], we find that a richer set of superconducting phases appear on the lattice. Indeed, lattice symmetries naturally result in *pair-density waves* of composite fermions, states which form the basis for one proposal for describing the phase diagram of the high-T_c cuprate superconductors [62]. These states intriguingly exhibit a coexistence of topological and broken symmetry (namely, charge density wave) order. We also find a host of novel phases, including quantum Hall thermal semimetals and weak topological superconductors of composite fermions, illustrating the richness of the FCI phase diagram.

1.3.2 Non-Abelian States and Duality

Although FCIs present platforms for intriguing new physics, the continuum FQHE still presents many unresolved problems. Perhaps paramount among these is understanding the potential emergence of *non-Abelian* FQH states, which are characterized by their support of non-Abelian anyons. Although the vast majority of experimentally observed FQH states are believed to be Abelian, a multitude of non-Abelian FQH states have been proposed. However, these proposals are based primarily on conjectured wave functions, like that first proposed by Laughlin. Specifically, as noted in our discussion of the Laughlin states, trial wave functions can be constructed from correlators in an appropriate conformal field theory (CFT). A trial wave function for a FQH state with topological order characterized by a G_k Chern-Simons theory is obtained from correlators in the G_k Wess-Zumino-Witten theory. As was the case for Laughlin's ansatz, while these trial wave functions can provide us useful intuition about these states, including the properties of their non-Abelian excitations, they cannot inform us about the physical mechanisms underlying their emergence. Unfortunately, the vast majority of these proposed states lack composite particle field theory descriptions, like those describing Abelian states.

One prominent exception is provided by the aforementioned non-Abelian Pfaffian state, which may explain the experimentally observed FQH plateau at $\nu = \frac{5}{2}$. Its history begins with a trial wave function

constructed by Moore and Read [1] from a correlator in the CFT of a single Majorana and chiral boson[6]

$$\Psi(z_1, \ldots, z_N) = \mathrm{Pf}\left(\frac{1}{z_i - z_j}\right) \prod_{i<j} (z_i - z_j)^2. \tag{1.12}$$

Here, the first factor is the Pfaffian of the matrix A with entries $A_{ij} = (z_i - z_j)^{-1}$. As for the Laughlin state, one can construct wave function for anyon excitations, which can explicitly be shown to exhibit non-Abelian statistics [63]. An important feature of this wave function is that it vanishes only when at least *three* electrons are brought to the same point, in contrast to the Laughlin wave function, which vanishes when two electrons are coincident. At a heuristic level, this seems to suggest that this FQH state should be characterized by the Cooper pairing of some degrees of freedom. Indeed, the Pfaffian factor likewise appears in the BCS wave function for a $p + ip$ chiral superconductor of electrons, a rather suggestive coincidence.

Read and Green subsequently demonstrated that these connections go beyond mere analogy [61]. Indeed, if we apply the composite fermion mapping to a system of electrons at $\nu = \frac{1}{2}$ then, at mean-field level, the composite fermions will feel a *vanishing* net flux and hence form a composite Fermi liquid [64]. A natural path to a gapped state is through the formation of a superconductor of the composite fermions. Since they are spin polarized, a fully gapped state is obtained if the composite fermions pair in the $p + ip$ channel, exactly as suggested by the wave function picture! If the resulting composite fermion superconductor is in the weak-pairing regime, the result is the non-Abelian Pfaffian state. In particular, vortices in the Chern-Simons gauge field will trap Majorana zero modes and hence correspond to deconfined Ising anyons, which obey non-Abelian statistics. Excitingly, there is mounting experimental evidence that the observed FQH plateau at $\nu = \frac{5}{2}$ is indeed a paired composite fermion state (though perhaps not the Pfaffian state) [9].

Unfortunately, the composite particle theories we have discussed thus far have largely proved inadequate in describing non-Abelian states beyond the Pfaffian. Indeed, while the Pfaffian involves pairing, more exotic non-Abelian states are believed to involve *clustering* of electrons, based on their ideal wave function descriptions. For instance, the Read-Rezayi states, which have topological order described by an $SU(2)_k$ Chern-Simons theory, seem to arise from the formation of clusters of k electrons [65]. At a more elementary level, the flux attachment procedure we have employed, which involves Abelian gauge fields, appears ill-suited to describing non-Abelian FQH states, which necessarily involve emergent non-Abelian Chern-Simons gauge fields. Neither composite fermions nor bosons are the right set of variables to use, so to speak, to access these parts of the FQH phase diagram.

However, in the years since the initial proposal of these non-Abelian FQH states, parallel developments

[6] More precisely, the $[\mathrm{Ising} \times U(1)_8]/\mathbb{Z}_2$ CFT.

in the high-energy literature have led to what is effectively a *non-Abelian* generalization of flux attachment. Indeed, recent progress in the study of non-Abelian Chern-Simons-matter theories in their large-N ("planar") limit [66,67] has led to the proposal of non-Abelian Chern-Simons-matter theory dualities by Aharony [68]. The key feature of these dualities is that they can relate theories of composite fermions or bosons coupled to Abelian Chern-Simons gauge fields to theories of composite particles coupled to non-Abelian gauge fields. The upshot of this is that, starting with a system of electrons, we can first apply the standard flux attachment procedure to obtain a conventional theory of composite bosons. We can then employ these dualities to obtain an equivalent description in terms of a non-Abelian Chern-Simons-matter theory. In the same way that Abelian FQH states of electrons can be readily accessed in Abelian theories of composite fermions/bosons, it is natural to expect that non-Abelian states in the FQH phase diagram will be more easily accessible in these dual non-Abelian variables.

In the second part of this thesis, we task ourselves with demonstrating that this is indeed the case and carry out a program of developing effective field theories using these dualities to describe the emergence of a large class of non-Abelian FQH states. First, in Chapter 4, we develop Landau-Ginzburg theories for the Read-Rezayi states and their multicomponent extensions, the generalized non-Abelian spin-singlet states [69,70], which exhibit $SU(N)_k$ topological order. As was the case for the Pfaffian, our construction, which involves clustering of emergent particles in a multilayer system, finds motivation from the wave function description of these states. In Chapter 5, we extend this construction to develop a Landau-Ginzburg theory for a hitherto poorly understood FQH state, the *Fibonacci* state. The topological order supported by this state is the minimal one required to realize universal quantum computation. In a reversal of the standard story, we use this field theory to motivate a trial wave function for this novel state. Finally, in Chapter 6, we turn to investigating composite fermion theories coupled to non-Abelian Chern-Simons gauge fields, which are dual to the bosonic theories employed in the previous chapters. In addition to finding new descriptions of the so-called Blok-Wen states [71] and states typically arising from paired states of composite fermions, our analysis provides new insight into the dynamics of the composite fermion theories related by these dualities.

1.3.3 Gapped Interfaces and Entanglement

In Chapter 7, the final part of this thesis, we will change gears from pushing the composite particle picture to new settings and instead attempt to further our understanding of two other perspectives on the FQHE, namely, entanglement and the bulk-boundary correspondence. Specifically, we will be interested in investigating the exotic scenario where two, possibly distinct, FQH states are joined together along their edges, forming a one-dimensional *gapped interface*.

(a) (b)

Figure 1.1: (a) Cartoon of a gapped interface. The two cylinders support (possibly distinct) topological orders. The red and blue arrows denote the chiral edge states. The dotted lines between the inner edges represent electron scattering terms, which gap out the interface. (b) Spatial bipartition involved in computation of the entanglement entropy.

Such systems have been the subject of much theoretical interest in recent years [72–83]. Indeed, as we have described, a uniform topological order defined on a disk geometry will generically support chiral edge modes at its boundary. Suppose we consider two cylinders supporting the same topological order, say, the $\nu = \frac{1}{3}$ Laughlin state, which has a single chiral edge mode. If we bring two edges of the two cylinders together, one can introduce a simple electron tunneling term to gap the edges out, effectively "gluing" the cylinders together (see Fig. 1.1(a)). In particular, any anyon from one cylinder can freely propagate to the other. On the other hand, one can also gap out the interface through an electron *pairing* term via proximity coupling to a superconductor. In this case, an anyon passing from one cylinder to the other will be converted to its *conjugate* (the anyon with opposite electric charge). Intriguingly, it has been predicted that if one gaps out part of the interface with normal tunneling and the other part with superconducting pairing, the domain wall between these gapped regions will support a *parafermion* zero mode, generalizations of Majorana zero modes, which are sufficient platforms for universal topological quantum computation [73–75]. Excitingly, experimental progress has in fact been made in inducing superconductivity on the FQH edge [84].

More generally, one may consider the scenario raised above, in which the edges of two distinct topological orders are brought together to form a gapped interface. A systematic analysis of when the chiral edge modes at an interface can be fully gapped out via electron scattering has been conducted for the case where the two orders are both *Abelian* [85–87]. In this case, the gapped interface itself realizes a non-trivial symmetry-protected topological phase [88]. If one cuts open the cylinder such that the interface has endpoints terminating at the vacuum, these endpoints will generically again support parafermion zero modes.

The natural question we wish to ask is whether more exotic phenomena can occur at interfaces of *non-*

Abelian FQH states. The CFTs describing the edges of non-Abelian states are more complicated than those of their Abelian cousins, and so it seems difficult to directly describe the properties of a non-Abelian gapped interface. As it turns out, a useful perspective on characterizing the interface is given by the *entanglement* between the two phases which the interface separates. In order to motivate this, as well as to make more precise the notion of long-range entanglement of FQH states alluded to earlier in this Chapter, let us pause and provide a brief introduction to quantum entanglement.

At a fundamental level, entanglement is the key phenomenon distinguishing quantum and classical physics and is a reflection of the non-local correlations between observables in quantum systems. Many quantitative measures of entanglement have been proposed. Here we will concern ourselves with the most elementary one, the entanglement (or von Neumann) entropy. Let us consider a quantum system prepared in a pure state, $|\psi\rangle$, defined in a Hilbert space $\mathcal{H}$. The density matrix of this pure state is simply given by $\rho = |\psi\rangle\langle\psi|$. Now let us bipartition the system into the region A and its complement $\overline{A}$, such that the full Hilbert space is a product of the two subspaces associated with these subregions: $\mathcal{H} = \mathcal{H}_A \otimes \mathcal{H}_{\overline{A}}$ (see Fig. 1.1(b)). The reduced density matrix of $|\psi\rangle$ for region A is formed by tracing over the degrees of freedom in $\overline{A}$: $\rho_A = \mathrm{Tr}_{\overline{A}}\,\rho$. The entanglement entropy between A and $\overline{A}$ in the state $|\psi\rangle$ is then given by

$$S_A = -\,\mathrm{Tr}\,\rho_A \log \rho_A = -\sum_i \lambda_i \log \lambda_i, \tag{1.13}$$

where, after the second equality, we have expressed the entropy in terms of the eigenvalues, $0 \leq \lambda_i \leq 1$, of ρ_A. This latter expression is in fact the classical *Shannon* entropy and hence makes clear the physical content of the entanglement entropy: it is a measure of the number of bits of information stored between A and $\overline{A}$ in the state $|\psi\rangle$. As a simple example to illustrate this, let us consider a pair of spin-$\frac{1}{2}$ systems prepared in a Bell state: $|\psi\rangle = \frac{1}{\sqrt{2}}(|\uparrow\downarrow\rangle - |\downarrow\uparrow\rangle)$. It is easy to check that the entanglement entropy between the two systems is $\log 2$ and hence a single bit of information is stored in this state: specifying that one system is in the up state immediately determines the other state to be in the down state and vice versa.

As a probe of quantum correlations (at least at zero temperature), the entanglement entropy provides a useful tool to characterize quantum many-body phases. Let us restrict ourselves to ground states of *gapped* Hamiltonians in two-dimensional systems. If we bipartition the plane into two connected spatial regions, A and $\overline{A}$, then the entanglement entropy in such a ground state takes the general form

$$S_A = \alpha L - \gamma, \tag{1.14}$$

where L is the length of the *entanglement cut*, the line separating A from $\overline{A}$, while α and γ are non-

universal and universal constants, respectively. The first term is known as the *area law* and has a simple interpretation. In a ground state of a gapped Hamiltonian, the correlation length is vanishingly small, and so any entanglement between A and $\overline{A}$ should come primarily from degrees of freedom near the entanglement cut. Hence the entanglement entropy should have a term proportional to the length of the cut. The second term is known as the *topological entanglement entropy* (TEE) and, as the name suggests, is non-zero for topologically ordered phases [89, 90]. For a uniform topological phase, $\gamma = \log \mathcal{D}$, where $\mathcal{D}$ is the total quantum dimension, a number characterizing the anyon content of the phase. Note that γ is independent of both the sizes of A and $\overline{A}$ as well as the length of the entanglement cut and hence truly measures non-local correlations in the system. It is perhaps surprising that, as a signature of topological order, the TEE *decreases* the total entanglement entropy, a fact that appears to be at odds with our repeated claim that topological orders exhibit long-range entanglement. What the TEE is in fact encoding is that topological orders possess non-local *constraints* which reduce the information that can be stored in the system. For instance, in a FQH state in which we have excited some number of anyons, if we measure the net charge in A to be an integer multiple of e, then we immediately know that the net charge in $\overline{A}$ cannot be a fraction of e, since the full system must have an integer number of electrons. This is in contrast to the spin-$\frac{1}{2}$ example above, where *a priori* there is no restriction on the spins of the two systems – one can prepare the system in an arbitrary superposition of the two spins.

With this in mind, it is natural to expect that, in the scenario in which two distinct topological phases are joined at a gapped interface, that the entanglement entropy between the two phases should capture information about the interface. Indeed, the TEE has been computed [91] for an entanglement cut along the interface between two generic Abelian phases and shown to be directly connected with the emergence of the aforementioned symmetry-protected topological phase at the interface [88]. Our goal is to extend this calculation to non-Abelian phases. As is to be expected, this constitutes a much more challenging problem. In contrast to the Abelian case, the edge theories of non-Abelian phases are described by more complicated conformal field theories and an understanding of the possible gapped interfaces that can be formed is lacking. In Chapter 7 we will provide a first step towards tackling this problem, focusing on interfaces between a simple class of non-Abelian FQH states. In addition to classifying when gapped interfaces can be formed for any two given FQH states within this class, we compute the topological entanglement entropy for said interfaces, and illustrate how the properties of the interface are encoded in the entanglement.

Chapter 2

Chern-Simons Composite Fermion Theory of Fractional Chern Insulators

2.1 Introduction

One of the most exciting frontiers in fractional quantum Hall (FQH) physics is the study of FQH states realized in lattice systems, potentially in the absence of a magnetic field. As described in Chapter 1, these *fractional Chern insulators* (FCIs) exhibit the same features as their continuum FQH cousins, but can also support a richer set of phenomena as a result of the interplay of topological order with the underlying lattice. For instance, FCIs are expected to support non-Abelian states resulting from partial filling of Chern bands with $|C_0| > 1$ [36, 92], non-Abelian defects [35], and anyonic excitations with fractionalized symmetry quantum numbers, thus exhibiting 'symmetry fractionalization' [37–40]. However it is also the importance of the lattice which renders the development of an analytic and microscopic theory of FCIs a challenging endeavor.

The aim of this Chapter is to tackle this problem by developing an analytical description of FCI states on a specific kagome lattice model in terms of a Chern-Simons composite fermion (CF) theory. The CF approach has been used successfully in describing the conventional FQHE [11, 12]. As described in Chapter 1, in this picture the electrons nucleate fluxes of an emergent Chern-Simons gauge field such that at the mean field level, the CFs fill an integer number of Landau levels in the new effective flux. The IQH states of the CFs then correspond to FQH states of the original fermions. Quantum fluctuations about these IQH states endow the excitations with their correct fractionalized quantum numbers. Numerical studies suggest that a CF picture is also relevant for the lattice FQHE [59, 60] and so may be applicable to FCIs, as is also suggested by recent analytical work [93, 94], providing further motivation for our study. The methodology we use here is similar to that used in the continuum, but with a local and gauge-invariant Chern-Simons action on the lattice which we motivated in Chapter 1 [56, 58, 95, 96]. This is necessary as we work in the tight binding limit; in contrast, previous studies of the lattice FQHE [34] considered the opposite limit in which Landau levels are dressed by a lattice potential. Importantly, the theory we develop here will serve as a stepping stone towards investigating more exotic FCI states arising from paired states of composite

fermions in the following Chapter.

This Chapter is organized as follows. We begin by outlining in Section 2.2 the Chern insulator model on the kagome lattice to which we apply our analysis. Next, in Section 2.3, we review the CF mapping and the consistent definition of a Chern-Simons action on the kagome lattice as discussed in Refs. [96] and [58] (see Section 2.3.1). Special care will be given to the boundary conditions, focusing on the case of the torus. In Section 2.4 we construct gapped states of the CFs arising at the mean field level (i.e. the average field approximation) which are identified as candidate FCI states. The construction of the mean-field theory requires the self-consistent derivation of a class of Hofstadter states. In Section 2.5.1 we derive the effective topological field theory describing the gapped low-energy states, from which we can extract the Hall conductance, fractional excitations, and ground state degeneracy. In Section 2.5.2 we use the results of the previous sections to identify candidate FCI states from the composite fermion Hofstadter spectrum and characterize their topological properties. It is found that there are two classes of FCI states which can be realized: those with Hall conductance equal to the filling factor and those for which these two quantities are unequal. We then discuss how FCI states with the same topological order arising at different filling fractions can be viewed as realizing distinct symmetry fractionalization classes which are derived in Section 2.6. We provide concrete predictions arising from this classification which may be verified via numerical studies. Before concluding, we offer some remarks in Section 2.7 about the distinctions between FCIs and lattice FQHE states. Section 2.8 is devoted to our conclusions.

2.2 Model

The model we consider is a Chern insulator of spinless fermions with nearest-neighbor hopping on the kagome lattice, subject to a staggered magnetic field with net zero flux per unit cell [97]. The Hamiltonian of the model is

$$H = J \sum_{\langle \boldsymbol{x}, \boldsymbol{x}' \rangle} \left[\psi^\dagger(\boldsymbol{x}) e^{i\phi(\boldsymbol{x},\boldsymbol{x}')} \psi(\boldsymbol{x}') + h.c. \right] + \frac{g}{2} \sum_{\boldsymbol{x},\boldsymbol{y}} n(\boldsymbol{x}) V(\boldsymbol{x}-\boldsymbol{y}) n(\boldsymbol{y}) \tag{2.1}$$

Here J is the hopping amplitude on the kagome lattice, g is the coupling constant, and $V(\boldsymbol{x}-\boldsymbol{y})$ is the interaction between the fermions densities, the occupation numbers labeled by $n(\boldsymbol{x})$. For concreteness, we will assume that the interaction is for nearest-neighbors on the kagome lattice, but it can be a general interaction as well.

The staggered magnetic field is represented by the fixed phase field $\phi(\boldsymbol{x}, \boldsymbol{x}')$, defined on the links of the kagome lattice, such that the flux of this field is ϕ_+ (ϕ_-) into the page through the up (down) triangles of

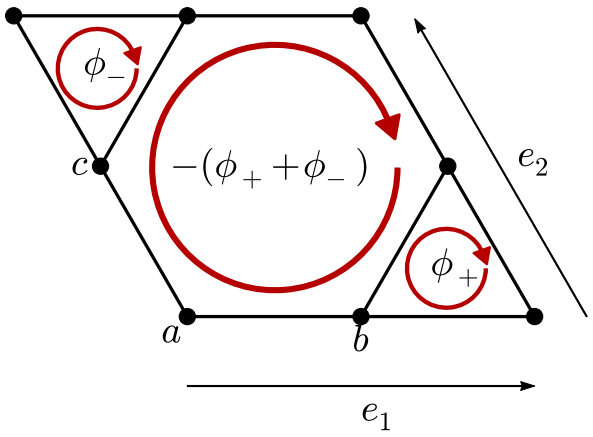

Figure 2.1: Kagome lattice unit cell with phases arising from a magnetic flux indicated by arrows. The net flux is zero.

the lattice as shown in Fig 2.1. Also illustrated in Fig. 2.1 are the sublattice structure and definition of the lattice vectors $\boldsymbol{e}_{1,2}$. We will focus on the case of $\phi_\pm = \pi/2$ which preserves the lattice point-group symmetry and yields three well-separated bands with the lowest band possessing Chern number $C_0 = +1$. The band structure is discussed further in Appendix A.1. We are interested in gapped topological phases arising from partially filling this lowest band; the fraction of it which is filled will be denoted by n_L.

In general, the formation of an FCI requires that the bandwidth of the partially filled Chern band is at most of the order of the band gaps of the non-interacting problem. Hence, the spinless fermions in the partially filled band can be regarded as being strongly correlated. Without this condition the system would be a metal, and not an FCI. In the specific staggered flux model we chose, the bandwidth is comparable to the gap between the bands. It is, however, still possible to stabilize an FCI, in principle, if interactions are strong enough.

2.3 Flux Attachment

The mapping of fermions to CFs is accomplished via a mapping onto an equivalent system of spinless fermions, the composite fermions, minimally coupled to a dynamical lattice Chern-Simons gauge field with a coupling parameter that we will denote by θ. We use the lattice Chern-Simons gauge theory on a kagome lattice on a 2D torus, as defined in Ref. [58] (a generalization of the approach of Refs. [56, 95]). This is an *exact* mapping provided the Chern-Simons theory can be well-defined on the lattice in a gauge-invariant fashion. That this is possible on a large class of lattices (including the kagome lattice) was shown in Ref. [58].

After performing this transformation our system is described by the action

$$S[\psi, \psi^\dagger, A_\mu, B_\mu] = S_F[\psi, \psi^\dagger, A_\mu] + S_{int}[A_\mu] + S_{CS}[A_\mu, B_\mu] \tag{2.2}$$

where ψ is the CF field, A_μ is the statistical gauge field, and B_μ is a hydrodynamic gauge field required for flux attachment to be defined consistently on a torus as described below [98]. Here S_F is the fermionic action, S_{int} is a fermion density-density interaction (as will be shown, flux attachment allows one to make a formal substitution of the densities with fluxes), and S_{CS} is the Chern-Simons action. In the following we will discuss in detail the actions S_F, S_{CS}, and S_{int} in turn.

The fermionic part of the action is of the usual form,

$$S_F[\psi, \psi^\dagger, A_\mu] = \int_t \sum_{\boldsymbol{x}} \psi^\dagger(\boldsymbol{x}, t) i D_0 \psi(\boldsymbol{x}, t) - \int_t J \sum_{\langle \boldsymbol{x}, \boldsymbol{x}' \rangle} (\psi^\dagger(\boldsymbol{x}, t) e^{i(A_j(\boldsymbol{x}, t) + \phi(\boldsymbol{x}, \boldsymbol{x}'))} \psi(\boldsymbol{x}', t) + h.c.), \tag{2.3}$$

where $D_0 = \partial_0 + iA_0$ is the covariant time derivative and $\langle \boldsymbol{x}, \boldsymbol{x}' \rangle$ indicates a sum over nearest neighbors. The temporal components of the gauge field, $A_0(\boldsymbol{x})$, live on the sites of the lattice whereas the spatial components, $A_i(\boldsymbol{x})$ $(i = 1, \ldots, 6)$, live on the links.

The form of the lattice Chern-Simons action is less intuitive. For a more detailed construction for a large class of lattices we direct the reader to Ref. [58]. In the following two subsections we will describe first the lattice formulation of the action for the statistical gauge field A_μ and subsequently the lattice formulation of an equivalent theory involving both A_μ and the hydrodynamic field B_μ which can can be defined on topologically non-trivial manifolds.

2.3.1 Lattice Chern-Simons

Broadly speaking, a theory of fermions coupled to a Chern-Simons field is a theory of flux-charge composites. Hence a Chern-Simons action must enforce a Gauss' Law constraint which attaches fluxes to the matter fields in addition to being gauge invariant. On the lattice, the fermions reside on the lattice sites and so it is natural to define the fluxes to live in the plaquettes (i.e. the sites of the dual lattice). So, in order to be able to consistently define a flux attachment condition, the lattice must be such that one can uniquely associate each site to a plaquette. This is indeed the case for the kagome lattice as well as the dice and square lattices but not, for instance, the honeycomb or triangular lattices.

As shown in Ref. [96] and [58], it follows from the above considerations that one consistent formulation

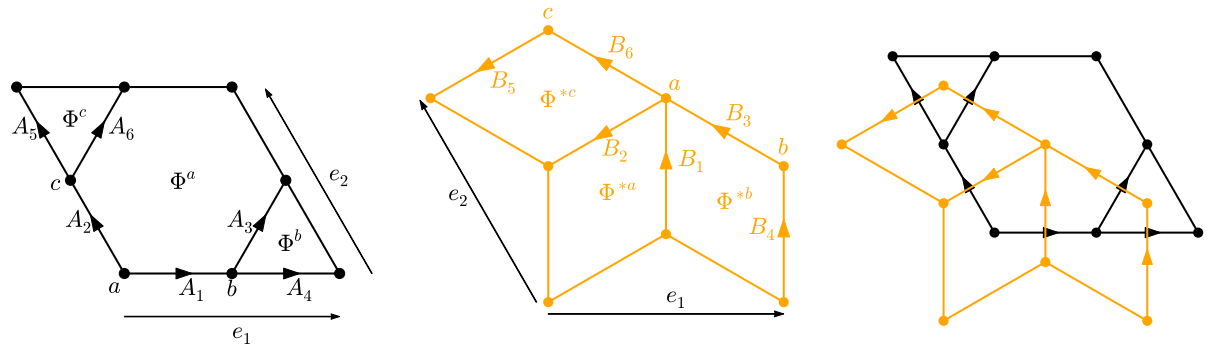

(a) (b) (c)

Figure 2.2: (a) Kagome lattice unit cell with spatial components of the statistical gauge field A_i and fluxes $\Phi^\alpha = J_i^\alpha A_i$. (b) Dice lattice unit cell with the hydrodynamic gauge field B_i and fluxes $\Phi^{*\alpha} = J_i^{*\alpha} B_i$. (c) Orientation of the dual (dice) lattice relative to the direct (kagome) lattice.

for a Chern-Simons action on the kagome lattice is given by[1]

$$S_{CS}[A_\mu] = \theta \int dt \sum_{\boldsymbol{x}} \left[A_0^\alpha(\boldsymbol{x},t) J_i^\alpha A_i(\boldsymbol{x},t) - \frac{1}{2} A_i(\boldsymbol{x},t) \mathcal{M}_{ij} \partial_t A_j(\boldsymbol{x},t) \right]. \tag{2.4}$$

Here the sum is over unit cell positions and the index $\alpha = a, b, c$ denotes the sublattice. As noted above, the temporal components of the gauge field, A_0^α, live on the lattice sites whereas the spatial components, A_i, live on the links. The orientation of the spatial gauge fields is shown in Fig. 2.2(a). In the context of flux attachment the coupling θ is given by $\theta = 1/2\pi(2k)$, $k \in \mathbb{Z}$. Now, the first term in the action enforces the flux-attachment (or Gauss' Law) constraint

$$n^\alpha(\boldsymbol{x}) = \theta J_i^\alpha A_i(\boldsymbol{x}) \equiv \theta \Phi^\alpha(\boldsymbol{x}). \tag{2.5}$$

The fluxes $\Phi^\alpha(\boldsymbol{x}) = J_i^\alpha A_i(\boldsymbol{x})$ live in the kagome lattice plaquettes as shown in Fig. 2.2(a). The J_i vectors may be viewed as discretized curl operators on the kagome lattice,

$$\begin{aligned} J^a &= (1, -1, 1, -s_2, -s_1, -1), \\ J^b &= (0, s_1, -1, 1, 0, 0), \\ J^c &= (-s_2, 0, 0, 0, -1, 1), \end{aligned} \tag{2.6}$$

[1]Note that what we call $\mathcal{M}_{ij}$ is the K_{ij} matrix of Refs. [56,58,96]; this is to avoid confusion with the K-matrix of Eq. 2.24. Additionally, as we have written the action, J_i^α and $\mathcal{M}_{ij}$ are operators while in Ref. [96] these objects are expressed as the functions $J_i(\boldsymbol{x}-\boldsymbol{y})$ and $\mathcal{M}_{ij}(\boldsymbol{x}-\boldsymbol{y})$ with the action containing a sum over $\boldsymbol{x}$ and $\boldsymbol{y}$. This is a matter of notation – in this and the following sections we will use one or the other convention depending on which is most convenient.

where we have used the lattice shift operators s_i which are defined as $s_i f(\boldsymbol{x}) = f(\boldsymbol{x} + \boldsymbol{e}_i)$. Hence the Gauss law ties the statistical fluxes in the hexagon, up triangle, and down triangle to the a, b, and c sites, respectively.

Note that the assignment of fluxes to sites necessarily breaks the rotational symmetry of the lattice. This will be true for any choice of assignment and so the lattice point-group symmetry is not respected by the lattice Chern-Simons formulation we have chosen. That being said, the mapping of fermions to composite fermions is an exact one at the level of the path integral and so the ground state predicted by our theory (at the full quantum level) should respect the lattice symmetries, provided there is no spontaneous symmetry breaking. We will return to this issue in the discussion of our mean field theory analysis.

The second term in the Chern-Simons action of Eq. (2.4) enforces the commutation relations. The matrix kernel $\mathcal{M}_{ij}$ must be chosen so as to make the theory gauge-invariant. This ensures that the Gauss' Law constraint can be applied consistently on different plaquettes, in other words, $[\Phi^{\alpha}(\boldsymbol{x}), \Phi^{\alpha'}(\boldsymbol{y})] = 0$. It was found previously [96] that on the kagome lattice the matrix kernel has the form

$$\mathcal{M}_{ij} = \frac{1}{2}\begin{pmatrix} 0 & -1 & 1 & -s_2 & s_1 + s_2^{-1} & -1 + s_2^{-1} \\ 1 & 0 & 1 - s_1^{-1} & -s_2 - s_1^{-1} & s_1 & -1 \\ -1 & s_1 - 1 & 0 & 1 - s_2 & s_1 & -1 \\ s_2^{-1} & s_1 + s_2^{-1} & s_2^{-1} - 1 & 0 & s_1 s_2^{-1} & s_2^{-1} \\ -s_2 - s_1^{-1} & -s_1^{-1} & -s_1^{-1} & -s_2 s_1^{-1} & 0 & 1 - s_1^{-1} \\ 1 - s_2 & 1 & 1 & -s_2 & s_1 - 1 & 0 \end{pmatrix}. \tag{2.7}$$

The standard canonical quantization procedure then yields $[A_i(\boldsymbol{x}), A_j(\boldsymbol{y})] = -\frac{i}{\theta}\mathcal{M}^{-1}_{ij}(\boldsymbol{x} - \boldsymbol{y})$ so that only neighboring gauge fields have non-trivial commutation relations. (See Appendix A.4 for a discussion of the spectrum of $\mathcal{M}_{ij}$.) This provides a fully consistent definition of a local Chern-Simons action on the kagome lattice with trivial topology.

2.3.2 Lattice Chern-Simons on a Torus

As noted above, when performing our mapping, the Chern-Simons parameter is given by $\theta = 1/2\pi(2k)$. This is the form of the flux attachment used in Ref. [96]. However, the coefficient θ is not properly quantized and so the theory cannot be defined on closed manifolds with non-zero genus [99]. Much as in the continuum case [98, 100], this problem is resolved by introducing the auxiliary, hydrodynamic field B_μ which lives on the dual lattice which, in our case, is the *dice lattice*. In particular, the temporal components, B_0^{α}, live on the sites of the dice lattice whereas the spatial components, B_k, live on the links. Following the conventions

of Ref. [58], the orientations of the B_k are obtained by rotating the arrows on the direct lattice counter-clockwise until they align with the links of the dual lattice. Fig. 2.2(b) shows the definition of the spatial components of the B_μ field while Fig. 2.2(c) illustrates the relative orientation of the direct and dual lattices. The resulting action is given by

$$\begin{aligned} S_{CS}[A_\mu, B_\mu] = &-\frac{2k}{2\pi}\int dt \sum_{\boldsymbol{x}} B_0^\alpha(\boldsymbol{x},t) J_i^{*\alpha} B_i(\boldsymbol{x},t) - \frac{1}{2} B_i(\boldsymbol{x},t)\mathcal{M}^*_{ij}\dot{B}_j(\boldsymbol{x},t) \\ &+ \frac{1}{2\pi}\int dt \sum_{\boldsymbol{x}} A_0^\alpha(\boldsymbol{x},t) J_i^{*\alpha} B_i(\boldsymbol{x},t) + B_0^\alpha(\boldsymbol{x},t) J_i^\alpha A_i(\boldsymbol{x},t) - \dot{B}_j(\boldsymbol{x},t) A_j(\boldsymbol{x},t). \end{aligned} \tag{2.8}$$

The first two terms give the Chern-Simons action for B_μ on the dual lattice whereas the remaining three terms give the 'BF' coupling between the A_μ and B_μ fields. This is the discretized form of the continuum action

$$\mathcal{L}^{\text{ctm}}_{CS}[A_\mu, B_\mu] = -\frac{2k}{4\pi}\epsilon^{\mu\nu\lambda} B_\mu \partial_\nu B_\lambda + \frac{1}{2\pi}\epsilon^{\mu\nu\lambda} A_\mu \partial_\nu B_\lambda. \tag{2.9}$$

known as the BF theory [101]. The objects $J_i^{*\alpha}$ and $\mathcal{M}^*_{ij}$ are the analogues of J_i^α and $\mathcal{M}_{ij}$ on the dice lattice. Explicitly, we have

$$\begin{aligned} J^{*a} &= (1, 1, 0, -s_1^{-1}, -s_2^{-1}, 0), \\ J^{*b} &= (-1, 0, 1, 1, 0, -s_2^{-1}), \\ J^{*c} &= (0, -1, -s_1^{-1}, 0, 1, 1) \end{aligned} \tag{2.10}$$

so that the B_μ fluxes are given by $\Phi^{*\alpha}(\boldsymbol{x}) = J_i^{*\alpha} B_i(\boldsymbol{x})$. Using the construction of Ref. [58], we find

$$\mathcal{M}^*_{ij} = \frac{1}{2}\begin{pmatrix} 0 & -1 & 1 & -1+s_1^{-1} & s_2^{-1} & s_2^{-1} \\ 1 & 0 & -s_1^{-1} & -s_1^{-1} & 1-s_2^{-1} & -1 \\ -1 & s_1 & 0 & 1 & s_1 & -s_1-s_2^{-1} \\ 1-s_1 & s_1 & -1 & 0 & s_1 s_2^{-1} & s_2^{-1} \\ -s_2 & -1+s_2 & -s_1^{-1} & -s_2 s_1^{-1} & 0 & 1 \\ -s_2 & 1 & s_2+s_1^{-1} & -s_2 & -1 & 0 \end{pmatrix}. \tag{2.11}$$

It can be seen that $\mathcal{M}^* = -\mathcal{M}^{-1}$ and so the $\mathcal{M}$ matrices are non-singular. Similar to the calculation shown in Appendix E of Ref. [58], one can integrate out B_μ in Eq. (2.8) to recover Eq. (2.4), and so the two theories are formally equivalent. However, Eq. (2.8) has properly quantized coefficients while Eq. (2.4) does not, and so the former is well-defined on topologically non-trivial manifolds whereas the latter is not. In

using Eq. (2.8) our flux attachment procedure can be performed on a toroidal geometry and so we will be able to safely infer the topological field theory describing our FCI states.

Having completed our description of the lattice Chern Simons action, we return to the flux attachment procedure. Due to their coupling to the statistical gauge field, the ψ fields have statistical angle $\delta = 2\pi k$ relative to the original fermionic statistics (as per the flux attachment constraint), and so by choosing the Chern Simons parameter k to be an integer, we ensure that the CFs are indeed fermions. The 2π periodicity of the statistical angle implies that theories with different integral values of k should be equivalent. This property is broken at the mean-field level but is recovered at the quantum level.

Lastly, S_{int} is assumed to describe a density-density interaction which, due to the flux attachment constraint Eq. 2.5, has the form

$$S_{int}[A_\mu] = -\frac{1}{2}\int_t \sum_{\boldsymbol{x},\boldsymbol{y}} \frac{g}{16\pi^2 k^2}\Phi^\alpha(\boldsymbol{x},t)V(\boldsymbol{x}-\boldsymbol{y})_{\alpha\beta}\Phi^\beta(\boldsymbol{y},t) \tag{2.12}$$

where the explicit sum is over unit cell positions and there is an implicit sum over the sublattices, $\alpha, \beta = a, b, c$. In this form, the interaction term does not enter in the fermionic part of the action. Instead, it is a parity-even contribution to the action of the gauge fields, similar in this sense to a Maxwell term for the fluxes. Since it involves more derivatives than the Chern-Simons term it is irrelevant as far as the long-wavelength fluctuations are concerned. However, it affects the local energetics and it enters in the mean-field equations (as we will see below). This analysis very much parallels what is done for the FQH states in the continuum, e.g. see Ref. [12], whose strategy we will follow closely. Hence, we will first identify the gapped FCI ground states, in the present formalism, with gapped composite fermion ground states, which will be analyzed in mean field theory in Sec. 2.4. After integrating out the gapped composite fermions, the universal contribution of the topological theory is encoded in an effective action $\mathcal{L}_{\text{eff}}[A_\mu, B_\mu]$ containing Chern-Simons terms [see Eq.(2.23)]. In Appendix A.3 we check for two examples of gapped states that, at the mean field level, the gap persists for a range of interactions strengths. Thus, the states that we will identify will not have any (infrared) instabilities since it is protected by the gap. In fact, for large enough interactions there should be a phase transition to a state with a broken translation symmetry. Nevertheless, since S_{int} is quadratic in fluxes, it is irrelevant relative to the Chern-Simons action of Eq. (2.23), and its presence does not affect the universal properties of the topological fixed points of the theory, provided the gap has not closed.

2.4 Mean Field Theory

Analogous to the approach taken for the CF theory of the conventional FQHE, we wish to identify gapped states of the CFs at the mean field level. These will correspond to candidate FCI states. The specific form of the interaction will determine whether these states remain gapped and if they are energetically favorable to other potential ground states.

We first note that after the Jordan-Wigner mapping the action has become quadratic in the fermions and so they may formally be integrated out, yielding the effective action

$$S_{\text{eff}}[\psi, \psi^\dagger, A_\mu, B_\mu] = -i \log \text{tr}\left[iD_0 - H(A)\right] + S_{CS}[A_\mu, B_\mu] \tag{2.13}$$

where $H(A)$ is the Hamiltonian describing fermions hopping on the lattice subject to the original magnetic fluxes as well as the statistical gauge field. The mean field ground states are solutions to the saddle point equations which are obtained by extremizing the effective action with respect to the gauge fields. We obtain

$$\langle n^\alpha(\boldsymbol{x})\rangle = \frac{1}{2\pi(2k)} \sum_{\boldsymbol{y}} J_i^\alpha(\boldsymbol{x}-\boldsymbol{y}) A_i(\boldsymbol{y}) = \theta \langle \Phi^\alpha(\boldsymbol{x})\rangle \tag{2.14}$$

$$\langle j_k(\boldsymbol{x})\rangle = \theta \sum_{\boldsymbol{y}} \left[A_0^\alpha(\boldsymbol{y},t) J_k^\alpha(\boldsymbol{y}-\boldsymbol{x}) - \mathcal{M}_{kj}(\boldsymbol{x}-\boldsymbol{y}) \dot{A}_j(\boldsymbol{y},t) \right] - g\theta^2 \sum_{\boldsymbol{y},\boldsymbol{z}} J_k^\alpha(\boldsymbol{z}-\boldsymbol{x}) V_{\alpha\beta}(\boldsymbol{z}-\boldsymbol{y}) B^\beta(\boldsymbol{y}) \tag{2.15}$$

where $\langle n^\alpha(\boldsymbol{x})\rangle$ and $\langle j_k(\boldsymbol{x})\rangle$ are the fermion density on sublattice α and current on link k, respectively. Explicitly,

$$\langle n^\alpha(\boldsymbol{x})\rangle = -\frac{\delta S}{\delta A_0^\alpha(\boldsymbol{x})}, \quad \langle j_k(\boldsymbol{x})\rangle = -\frac{\delta S}{\delta A_k(\boldsymbol{x})}. \tag{2.16}$$

Note that Eq. (2.14) is simply the flux attachment constraint imposed on average. Now, we are interested in time-independent solutions which preserve the translational symmetry of the lattice (i.e. $\langle n^\alpha(\boldsymbol{x})\rangle = \langle n^\alpha(\boldsymbol{x}+\boldsymbol{e}_i)\rangle$ for $i = 1, 2$ and likewise for all other gauge-invariant quantities). In addition we assume that the currents on all links are equal in magnitude and circulate with the same chirality around both up and down triangular plaquettes so that $j \equiv \langle j_{1,3,5}\rangle = -\langle j_{2,4,6}\rangle$. Since generically $j \neq 0$, we see from Eq. (2.15) that the A_0^α's can be different from one another, giving rise to unequal fermion densities on the three

sublattices. So, given this ansatz, the resulting mean field equations are satisfied by

$$\begin{aligned} n^a &= \theta\Phi^a = n_L/3 - 2\Delta, \\ n^b &= \theta\Phi^b = n_L/3 + \Delta, \\ n^c &= \theta\Phi^c = n_L/3 + \Delta, \end{aligned} \tag{2.17}$$

where Δ is the shift of the fermion density onto the b and c sublattices, and

$$A_0^a = \frac{j}{2\theta} + 4g\Delta, \quad A_0^b = A_0^c = -\frac{j}{2\theta} - 2g\Delta. \tag{2.18}$$

In our ansatz, by assuming the link currents, j_k, to be equal in magnitude and $n_b = n_c$, we have preserved as much of the lattice symmetry as possible (see Sec. 2.4.1 for more details about broken symmetries in our analysis).

For convenience we define

$$\Phi = (\Phi^a + \Phi^b + \Phi^c)/3 = 2\pi\frac{p}{q} = \frac{n_L}{3\theta} \tag{2.19}$$

to be the average statistical flux per unit plaquette where p and q are co-prime integers. Then one gauge choice which gives the flux configuration mandated by our mean field ansatz is

$$\begin{aligned} &A_1(\boldsymbol{x}) = 0,\ A_2(\boldsymbol{x}) = \Phi + \Delta/\theta, && A_3(\boldsymbol{x}) = 0 \\ &A_4(\boldsymbol{x}) = 0,\ A_5(\boldsymbol{x}) = 3\Phi x_1 - \Phi - \Delta/\theta,\ A_6(\boldsymbol{x}) = 3\Phi x_1 \end{aligned} \tag{2.20}$$

where x_i is the coordinate along the $\boldsymbol{e}_i$ direction. So at the mean-field level the problem reduces to one of fermions subject to constant magnetic and statistical fluxes and a staggered potential, the latter two of which must be solved for self-consistently, as described by the hopping Hamiltonian

$$\begin{aligned} H(A) = J\sum_{\boldsymbol{x}} (&\overline{\gamma}_- e^{iA_1(\boldsymbol{x})} |a,\boldsymbol{x}\rangle \langle b,\boldsymbol{x}| + \gamma_+ e^{iA_2(\boldsymbol{x})} |a,\boldsymbol{x}\rangle \langle c,\boldsymbol{x}| + \gamma_+ e^{iA_4(\boldsymbol{x})} |b,\boldsymbol{x}\rangle \langle a,\boldsymbol{x}+\boldsymbol{e}_1| \\ &+ \overline{\gamma}_+ e^{iA_3(\boldsymbol{x})} |b,\boldsymbol{x}\rangle \langle c,\boldsymbol{x}+\boldsymbol{e}_1| + \overline{\gamma}_- e^{iA_5(\boldsymbol{x})} |c,\boldsymbol{x}\rangle \langle a,\boldsymbol{x}+\boldsymbol{e}_2| + \gamma_- e^{iA_6(\boldsymbol{x})} |c,\boldsymbol{x}\rangle \langle b,\boldsymbol{x}+\boldsymbol{e}_2| + h.c.) \\ &+ \sum_{\boldsymbol{x},\alpha} A_0^\alpha |\alpha,\boldsymbol{x}\rangle \langle \alpha,\boldsymbol{x}|, \end{aligned} \tag{2.21}$$

where $\gamma_\pm = e^{i\phi_\pm/3}$ are the phases arising from the background magnetic field and $\overline{\gamma}_\pm$ denote their complex conjugates.

Now, as is explained in the previous section, the interaction term in the action is (formally) irrelevant

as it involves more derivatives than the Chern-Simons term. So, as is done in the analysis of the continuum FQHE, we look for gapped CF states of the kinetic term. Formally this amounts to setting $g = 0$. Note that this does not mean that the states we find can exist in the absence of interactions. As in the analysis of the continuum FQHE, there is a residual effect of the interactions in the composite fermion mapping which is what attaches the fluxes to the fermions. Additionally, at the mean field level, the interactions for $g \neq 0$ do affect the local energetics and and so can affect the sublattice imbalance Δ. However, the states that we find in the (formal) $g = 0$ limit should persist for finite $g \neq 0$. Indeed, we show explicitly in Appendix A.3 that the gapped states we find at a few sample fillings persist for finite interaction strength.

As the the filling of the lowest band of the original fermions n_L increases, so too will the statistical flux. Examining the resulting Hofstadter spectrum as a function of filling will allow us to identify gapped states of the CFs. For each gapped state we can then compute the Chern number of the filled composite fermions bands which is given explicitly by [22]

$$C = \frac{1}{2\pi} \sum_{n \text{ filled}} \int_{\text{BZ}} d^2\boldsymbol{k}\, \mathcal{F}^n_{12}(\boldsymbol{k}) \tag{2.22}$$

where the integral is performed over the Brillouin zone and $\mathcal{F}^n_{12}(\boldsymbol{k}) = \epsilon_{ij}\partial_{\boldsymbol{k}_i}\mathcal{A}_j$ is the Berry curvature of the n^{th} band. The Berry connection is defined as $\mathcal{A}_j = -i\,\langle n, \boldsymbol{k}|\, \partial_{\boldsymbol{k}_j}\, |n, \boldsymbol{k}\rangle$ where $|n, \boldsymbol{k}\rangle$ is the eigenvector in the n^{th} band of the Bloch Hamiltonian. We compute the Chern number numerically using the method of Ref. [102]. As discussed in the following section the Chern number appears in the effective topological theory of the FCI states.

We have plotted the Hofstadter spectrum, sublattice imbalance, and link currents as a function of in Fig. 2.3(a) for the case of $k = 1$. For now we simply note that we find a number of sequences of gapped states, with the gapped states highlighted by the vertical red and purple lines occurring at fillings corresponding to the Jain sequence: $n_L = p/(2p + 1)$, $p \in \mathbb{Z}$. In the following section we will discuss the topological field theory describing these states and the pattern of Hall conductances exhibited by them.

2.4.1 Symmetries and Mean Field Theory

At this point we return to the issue of the explicit lattice point-group symmetry breaking of the action which is made manifest by this mean-field analysis. In a gapped insulating phase, although the net current must vanish, the current on a link, $\langle j_k(\boldsymbol{x})\rangle$, need not be zero. Indeed, in a generic chiral phase we expect to find currents circulating around the plaquettes. Eq. (2.15) implies that non-zero currents require a staggered $A^a_0(\boldsymbol{x}, t)$ (i.e. a spatially modulated Chern-Simons electric field). This staggered sublattice potential will

create a staggered density of fermions. Hence our mean-field analysis would suggest that in general a ground state of CFs must necessarily break the point-group symmetry of the lattice (note that previous applications of this lattice Chern-Simons formalism, such as Ref. [96], did not self-consistently calculate the currents and so incorrectly found uniform states). The mean-field ansatz we have chosen preserves as much of the lattice symmetry as possible. This situation is to be contrasted with the CF theory of the continuum FQHE in which the mean-field ground state consists of fully filled CF Landau levels which have an exactly vanishing local current and hence a vanishing Chern-Simons electric field. Likewise, if we were to instead consider the problem of a square lattice in a uniform magnetic field then it would be possible to find a translationally invariant solution since such a state at the mean field level would have equal fluxes (the sum of the magnetic and statistical fluxes) through all plaquettes; it can be seen that the link currents must vanish in this state and hence the A_0's would also vanish as per the self-consistent equations. As a result, the mean-field analysis reduces to a simple Hofstadter problem, as was discussed in Ref. [60], without the need to self-consistently solve for the currents and density imbalance.

Although numerical studies have predicted FCI states which spontaneously break lattice symmetries [42], we suspect that the symmetry breaking in our analysis is an artifact of the mean field theory. In particular, note that in the $g = 0$ limit we considered, although our ansatz with $n_a \neq n_b = n_c$ satisfies the mean field equations, configurations corresponding to rotations of this ansatz (e.g. with $n_b \neq n_a = n_c$) are not solutions as is clear from Eq. (2.18) (which follows from only assuming that the link currents, j_k, are equal in magnitude). Hence there should not be an additional, trivial ground state degeneracy associated with this breaking of the point-group symmetry which suggests that this symmetry breaking is an artifact of the form of the lattice CS action. Furthermore, since the mapping of the fermions to CFs is exact at the level of the path integral, it should follow that all the symmetries of the original problem should be respected under the CF mapping at the full quantum level. Assuming that the effects of these corrections are not so large as to close the gap, the topological data we compute will be accurate. Since this is the focus of our study we will henceforth not concern ourself with the role played by the point-group symmetries, leaving a full analysis to future work. Evidently an improvement over the saddle-point approximation is needed to correctly describe the non-topological properties of the candidate FCI states predicted using our Chern-Simons theory.

2.5 Fractional Chern Insulator States

2.5.1 Topological Field Theory

In the cases where the CFs are gapped, we can integrate them out to obtain an effective low-energy, continuum theory. Doing so will yield a Chern-Simons term with coefficient equal to the Chern number, C, of the filled CFs bands [22]. Hence the effective continuum Lagrangian for fluctuations of the gauge fields about the mean field state is given by

$$\mathcal{L}_{\text{eff}}[A_\mu, B_\mu] = \frac{C}{4\pi}\epsilon^{\mu\nu\lambda}A_\mu\partial_\nu A_\lambda + \mathcal{L}^{\text{ctm}}_{CS}[A_\mu, B_\mu] + \dots \tag{2.23}$$

where $\dots$ represents irrelevant terms.

Adding in quasi-particle currents with gauge charges l_I and a coupling to an external probe gauge field $\tilde{A}_\mu$, we can write our theory in the conventional form:

$$\mathcal{L} = \frac{K_{IJ}}{4\pi}\epsilon^{\mu\nu\lambda}a^I_\mu\partial_\nu a^J_\lambda - \frac{q_I}{2\pi}\epsilon^{\mu\nu\lambda}\tilde{A}_\mu\partial_\nu a^I_\lambda + l_I j^\mu_{\text{qp}} a^I_\mu \tag{2.24}$$

where[2]

$$K_{IJ} = \begin{pmatrix} -2k & 1 & 0 \\ 1 & C & 0 \\ 0 & 0 & 1 \end{pmatrix}, \; q_I = \begin{pmatrix} 1 \\ 0 \\ 0 \end{pmatrix}, \; a^\mu_I = \begin{pmatrix} B^\mu \\ A^\mu \\ D^\mu \end{pmatrix}. \tag{2.25}$$

Here, we introduced the gauge field D^μ as the bare quasi-particles are CFs and so possess fermionic statistics. To account for this, and because the quasi-particles do not couple to B^μ, the flux vector is restricted to have form $\boldsymbol{l} = (0, l, l)^T$, $l \in \mathbb{Z}$ [100]. On integrating out the Chern-Simons fields, we find the Hall conductance to be (in units of e^2/h)

$$\sigma_{xy} = -\boldsymbol{q}^T K^{-1}\boldsymbol{q} = \frac{C}{2kC+1}. \tag{2.26}$$

Likewise, the quasi-particle charges and statistics are

$$Q_{\boldsymbol{l}} = -\boldsymbol{l}^T K^{-1}\boldsymbol{q}, \quad \theta_{\boldsymbol{l}\boldsymbol{l}'} = -2\pi\boldsymbol{l}^T K^{-1}\boldsymbol{l}'. \tag{2.27}$$

[2]This theory is equivalent to that arising from the standard hierarchical construction [14, 103]. In particular, the Hall conductance and anyon content of the theories are readily checked to be identical.

The ground state degeneracy g on a torus is then [14]

$$g = |\det K| = |2kC + 1|. \tag{2.28}$$

We can also extract the modular properties of the theory from the effective, topological action. In particular, the components of the modular $\mathcal{S}$ and $\mathcal{T}$ matrices (both of rank $|\det K|$, the number of anyons) are given by

$$\mathcal{S}_{ab} = \frac{1}{\sqrt{|\det K|}} e^{-2\pi i \boldsymbol{l}_a^T K^{-1} \boldsymbol{l}_b}, \quad \mathcal{T}_{aa} = e^{-\pi i \boldsymbol{l}_a^T K^{-1} \boldsymbol{l}_a} \tag{2.29}$$

where the total quantum dimension is $\mathcal{D} = \sqrt{|\det K|} = S_{00}^{-1}$, a topological invariant that determines the universal entanglement properties [89, 90, 104]. Moreover, the full topological structure of theory is encoded in $\mathcal{S}$ and $\mathcal{T}$. Hence the topological field theory for an FCI state which can be described by a gapped state of CFs is wholly determined by k, the number of attached fluxes, and C, the Chern number of the filled CF bands.

2.5.2 Fractionalized States from the CF Hofstadter Spectrum

Following the results of the previous sections, we now analyse the Hofstadter spectra of the CFs to identify candidate FCI states on the kagome lattice. Before inspecting the spectrum, we note that a gapped state of the CFs must satisfy the Diophantine equation

$$n_L = -\frac{3\Phi}{2\pi} C + r, \; r \in \mathbb{Z} \tag{2.30}$$

where C is the Chern number of the filled CF bands [60] and -3Φ is the net flux per unit cell (note that because of the coupling between the fermions and A_μ, if the statistical flux through a plaquette is ϕ, the fermions feel a flux $-\phi$). Combined with the flux attachment condition, this implies that a gapped state must satisfy

$$n_L = \frac{r}{2kC + 1} = \frac{r}{C} \sigma_{xy} \tag{2.31}$$

The existence of states satisfying $r \neq C$ is made possible due to the presence of the lattice.

Turning to our model, Fig. 2.3(a) depicts a portion of the Hofstadter spectrum on the kagome lattice and Fermi Energy for the case of $k = 1$ pair of attached fluxes. Figs. 2.3(b)-(c) depict the mean field sublattice

density shift, Δ, and link current, j, as a function of filling. It is clear from the Hofstadter spectrum that gapped states exist at fillings given by the principal Jain sequence and the gap sizes approach zero as n_L approaches $1/2$, as is the case in the continuum. We have also labelled the first few states in this sequence with the Chern number of the filled CFs bands and the filling factor. Using the expression for the Hall conductance given in Eq. (2.26), we find that $\sigma_{xy} = n_L$ (except for the state at $n_L = 2/3$). Hence we recover the principal Jain sequence despite the absence of a net non-zero magnetic field. We have not extensively analysed the spectrum of mean field states for $k \neq 1$ but our preliminary numerics suggest that for $|k| > 0$, there should generically exist gapped states of the CFs at filling factors corresponding to the Jain sequence of states $n_L = p/(2kp+1)$, $p \in \mathbb{Z}\backslash\{0\}$ with Hall conductances satisfying $\sigma_{xy} = \mathrm{sgn}(k) n_L$. These states are analogous to the FQH Jain sequences. We note, however, that there are exceptions to this rule. For instance, as noted above, the $k = 1$ state at $n_L = 2/3$ has $\sigma_{xy} = 1/3 \neq n_L$ and so is the not a typical Jain state. In Appendix A.2 we present for comparison the Hofstadter spectrum obtained if one assumes a uniform density of fermions (and hence uniform statistical flux configuration) and does not correctly solve for the link current self-consistently via the mean field equations.

Now, in the conventional FQH, one can condense quasiparticles in a Jain state to form a FQH state with a filling fraction which does not lie in the principal Jain sequence. On the lattice, we instead find what is presumably a dense set of FCI states not lying in the Jain sequences without invoking this condensation mechanism. In particular, this means that there exist FCI states with the same Hall conductance but at different fillings. For instance, we find gapped states at $n_L = 1/7, 2/7, 3/7, 5/7$, all with $\sigma_{xy} = 3/7$. The $n_L = 5/7$ state is highlighted in Fig. 2.3(a). It should be noted, however, that interactions will likely render the lattice-specific states with the smallest gaps energetically unfavorable relative to topologically trivial phases (e.g. Wigner crystals, CDWs, nematic states), which we have not considered.

2.6 Symmetry Fractionalization

The question now arises as to how states at different fillings but with the same topological order can be classified. In order to answer this question, we make use of the fact that topological phases enriched with symmetries (known as SETs) possess anyonic excitations which can transform projectively under symmetry operations [38]. This phenomenon is known as symmetry fractionalization and implies that anyons can carry fractional symmetry charges. In particular, SETs can be distinguished by their symmetry fractionalization class (i.e. the set of projective phases for each anyon). Given an SET with Abelian anyon group $\mathcal{A}$ and symmetry group $\mathcal{G}$, the set of distinct symmetry fractionalization classes is given by the second cohomology

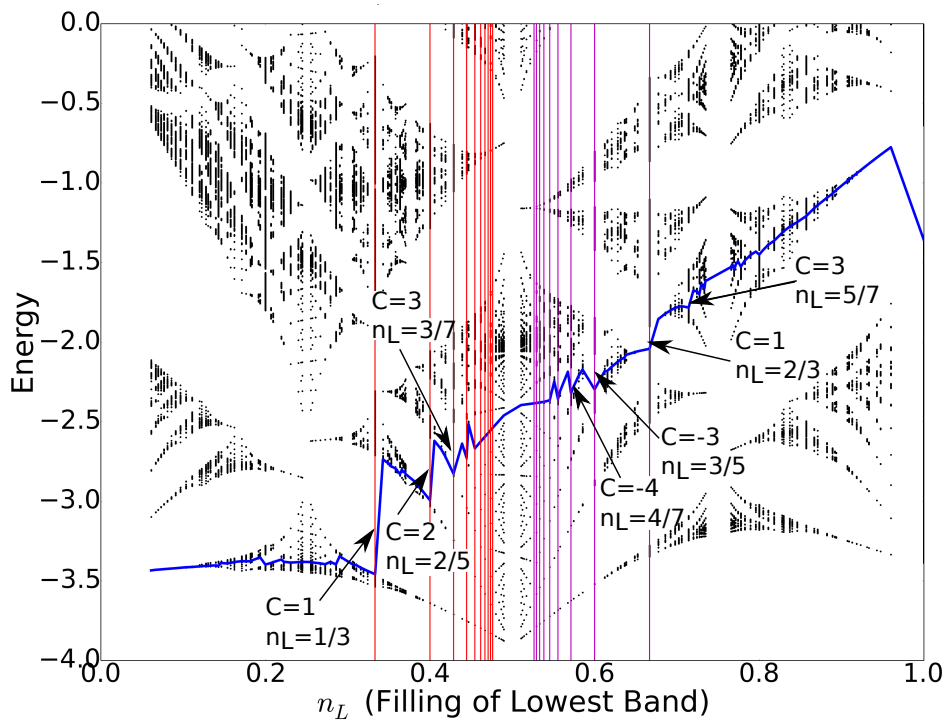

(a)

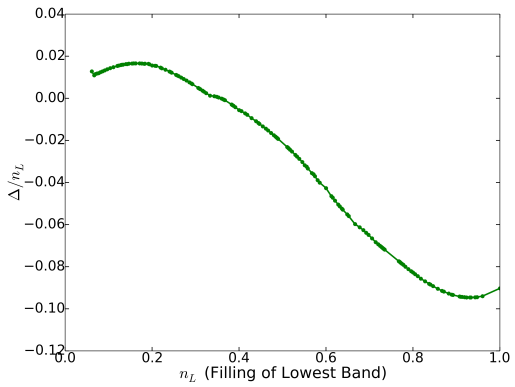

(b)

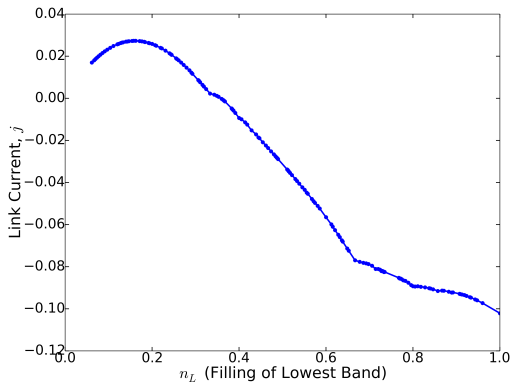

(c)

Figure 2.3: (a) Composite fermion Hofstadter spectrum on the kagome lattice with $k = 1$ and $\phi_\pm = \pi/2$. The blue line is the Fermi energy. Some examples of gapped states are labelled with their filling and Hall conductance. Vertical red (purple) lines are drawn at fillings corresponding to the principal particle (hole) Jain sequence. The ratio of the mean field sublattice shift, Δ, to the filling and the mean field current per link, k, are plotted in (b) and (c), respectively. All quantities are in units of $J = 1$.

group $H^2[\mathcal{G},\mathcal{A}]$ [37, 105].

Now, the anyon group of our FCI states is $\mathcal{A} = \mathbb{Z}_m$, where $m = |\det K|$, and the symmetry group is $\mathcal{G} = \mathbb{Z}^2 \times U(1)$ arising from lattice translation symmetry and $U(1)$ charge conservation, respectively.[3] Hence, the distinct fractionalization classes are given by $H^2[\mathbb{Z}^2 \times U(1), \mathbb{Z}_m] = \mathbb{Z}_m \times \mathbb{Z}_m$. The fractionalization is given on specification of the fluxon/vison F and the background anyon $\mathfrak{b}$ [106]. Physically speaking, the fluxon is the anyon created on the insertion of a 2π flux quantum; such an excitation carries charge equal to σ_{xy}. The fluxon specifies the $U(1)$ fractionalization in that the charge of an anyon, Q_a, is determined via the mutual statistics between a and F: $\exp(2\pi i Q_a) = \exp(i\theta_{F,a})$. Similarly, the background anyon specifies the translational symmetry fractionalization. This anyon possesses charge equal to the charge density per unit cell, n_L, and so physically one can view the ground state as a crystal of the background anyon $\mathfrak{b}$, with one $\mathfrak{b}$ residing in each unit cell [106, 107]. Braiding an anyon a around a single unit cell will give a phase $\exp(i\theta_{a,\mathfrak{b}})$ which implies

$$(T_2^a)^{-1}(T_1^a)^{-1}T_2^a T_1^a = e^{i\theta_{a,\mathfrak{b}}} \tag{2.32}$$

where $T_{1,2}^a$ are the local translations along the $e_{1,2}$ directions acting on anyon a. As an aside, we note that the fact that the system realizes a projective representation of the translation symmetry group may be viewed as an quantum anomaly of the discrete translational symmetry. Hence this effect may also lead to momentum pumping on a torus with tilted boundary conditions, a phenomenon which may be interesting to study in future work.

This analysis provides an interesting perspective on our spectrum of FCI states. The Jain states satisfy $\sigma_{xy} = n_L$ and so realize the fractionalization classes for which $F = \mathfrak{b}$. However, given $\mathcal{A} = \mathbb{Z}_{|\det K|}$ and the fluxon F (equivalently, σ_{xy}) there are a total of $|\det K|$ translational fractionalization patterns which can be realized from the choice of background anyon $\mathfrak{b}$. We have shown that these other fractionalization classes which have $\mathfrak{b} \neq F$ (i.e. $n_L \neq \sigma_{xy}$) can be realized on the lattice.

Moreover, we can use this language to make statements about the momenta of the topologically degenerate ground states [37]. Consider a gapped FCI state with $|\det K| = m$ and background anyon $\mathfrak{b}$ on a torus of size $N_1 N_2$ where $N_{1,2}$ are the number of unit cells in the $e_{1,2}$ direction, and N_2 is co-prime with m. Now, let $|0\rangle$ be the ground state labeled by the trivial anyon, and let $|\phi\rangle, \ldots, |\phi^{m-1}\rangle$ be the ground states generated by applying Wilson loop operators, $\mathcal{L}_2^{\phi^n}$, to $|0\rangle$ where ϕ is the minimal charge anyon. The Wilson loops can be viewed as operators creating anyon-antianyon pairs, braiding the anyons around a cycle of the torus, and

[3] The kagome lattice has a larger space group symmetry but, for simplicity, we will focus on the symmetry group $\mathcal{G} = \mathbb{Z}^2 \times U(1)$.

then fusing the anyon with the anti-anyon. We can thus make the identification

$$\mathcal{L}^a_\mu = (T^a_\mu)^{N_\mu} \tag{2.33}$$

where $\mu = 1, 2$. This implies that

$$T_1 \mathcal{L}^a_2 T_1^{-1} = T_1 (T^a_2)^{N_2} T_1^{-1} = e^{-iN_2\theta_{a,\mathfrak{b}}} \mathcal{L}^a_2. \tag{2.34}$$

Now, we have that $|\phi^n\rangle = (\mathcal{L}^\phi_2)^n |0\rangle$. Without loss of generality, suppose that the trivial ground state $|0\rangle$ has zero momentum. Hence,

$$T_1 |\phi^n\rangle = e^{-iN_2 n\theta_{\phi,\mathfrak{b}}} |\phi^n\rangle . \tag{2.35}$$

So, relative to the trivial state $|0\rangle$, the states $|\phi^n\rangle$ will have momenta $\boldsymbol{k}_n = (N_2 n\theta_{\phi,\mathfrak{b}}, 0)$. Since this momentum shift depends on the braiding angle with the background anyon, it provides a clear way to distinguish between two FCIs at different fillings possessing the same topological order.

As an explicit example, consider an FCI state with $\sigma_{xy} = C/(2kC+1)$ and $n_L = r/(2kC+1)$. In terms of the quasiparticle vectors $\boldsymbol{l}$, it is readily seen that the fluxon is represented by $\boldsymbol{l}_F = -(0, C, C)^T$, the background anyon by $\boldsymbol{l}_\mathfrak{b} = -(0, r, r)^T$, and the minimal charge anyon by $\boldsymbol{l}_\phi = -(0, 1, 1)^T$. The translational symmetry fractionalization for the minimal anyon is then obtained by using the fact that

$$\theta_{\boldsymbol{l}_\mathfrak{b}, \boldsymbol{l}_\phi} = -2rk\frac{2\pi}{2kC+1}. \tag{2.36}$$

We have listed the fractionalization patterns for observed FCI states with $\sigma_{xy} = 3/7$ in Table 2.1.

Table 2.1: Symmetry fractionalization for FCI states with $\sigma_{xy} = 3/7$. The third column gives the translational symmetry fractionalization for the minimal charge anyon ϕ. The fourth column gives the e_1 component of the crystal momentum of the ground state $|\phi\rangle$ relative to the trivial ground state.

n_L	σ_{xy}	$(T^\phi_2)^{-1}(T^\phi_1)^{-1}T^\phi_2 T^\phi_1$	$\widehat{k}_1 \|\phi\rangle$
1/7	3/7	$\exp\left(-2\frac{2\pi}{7}i\right)$	$-2\frac{2\pi}{7}N_2$
2/7	3/7	$\exp\left(-4\frac{2\pi}{7}i\right)$	$-4\frac{2\pi}{7}N_2$
3/7	3/7	$\exp\left(-6\frac{2\pi}{7}i\right)$	$-6\frac{2\pi}{7}N_2$
5/7	3/7	$\exp\left(-10\frac{2\pi}{7}i\right)$	$-10\frac{2\pi}{7}N_2$

2.7 Distinction between FCIs and the Lattice FQHE

Lastly, we would like to emphasize that the system we studied has a net zero external magnetic field and it is in this sense that the fractionalized states we find should be called FCI states. Conversely, fractionalized states found in lattice systems subject to a uniform magnetic field (i.e. in Hofstadter bands) should be considered lattice FQH states. Although both exhibit similar physics, it is important to make clear the distinction that one requires a net non-zero magnetic field while the other does not. In that regard, the states observed in Ref. [44] are lattice FQH states. The experimental observation of an FCI – in the absence of a net nonzero magnetic field – remains an open problem.

2.8 Conclusions

In this Chapter, we formulated a composite fermion theory of Fractional Chern Insulator states on the kagome lattice using a consistent lattice Chern-Simons theory. We find that partial filling of the lowest band yields two types of sequences of gapped states: those which satisfy $\sigma_{xy} = n_L$ and those which do not. Hence our theory provides a series of candidate FCI states whose stability against local interactions may be tested in numerical and experimental studies. Using the language of SETs we illustrated how these states may be viewed as realizing distinct symmetry fractionalization classes which exposes the rich structure of FCI states and allows for concrete, numerically verifiable, statements about ground state quantum numbers.

Chapter 3

Intertwined Order in Fractional Chern Insulators from Finite-Momentum Pairing of Composite Fermions

3.1 Introduction

In the preceding Chapter, we demonstrated that lattice analogues of fractional quantum Hall (FQH) states known as fractional Chern insulator (FCI) states can still be understood through the widely used composite fermion (CF) framework [11, 12], like most experimentally observed continuum FQH states, in spite of the importance of the underlying lattice. Specifically, much as in the case of the continuum FQH states, FCI states can also be represented in terms of a theory of composite lattice fermions coupled to a lattice version of Chern-Simons gauge theory [56–58, 95]. In this picture, the electrons nucleate fluxes of an emergent Chern-Simons gauge field. Just as continuum FQH states are formed when (at mean-field level) the composite fermions fill an integer number of Landau levels in the screened flux, Abelian FCI states are formed when the composite fermions fill an integer number of Hofstadter bands [15, 34, 59, 60].

With this lattice composite fermion formalism in hand, it is natural to ask whether composite fermions can exhibit more exotic dynamics on the lattice than in the continuum, leading to novel FCI states. We can glean some intuition for one route to new lattice states by recalling that certain (*non-Abelian*) continuum FQH states arise as *superconductors* of composite fermions. Specifically, at certain filling fractions in the continuum case, the composite fermions see no effective flux and so form a Fermi surface [64]. In higher Landau levels, this composite Fermi liquid yields to a pairing instability, resulting in a p_x+ip_y superconductor of composite fermions [61]. This gapped state is the non-Abelian Pfaffian state proposed by Moore and Read [1] to describe the experimentally observed FQH state at $\nu = 5/2$.

Although analogues of the Pfaffian state have been observed numerically in lattice systems [29, 108–111], we claim that more exotic paired phases of composite fermions may also be obtainable. Indeed, although the composite fermions may form a Fermi surface at certain filling fractions due to the vanishing of the net flux, at other filling fractions at which the net flux is non-zero, the composite fermions may partially fill a Hofstadter

This Chapter is adapted from Ramanjit Sohal and Eduardo Fradkin, Intertwined order in fractional Chern insulators from finite-momentum pairing of composite fermions, Phys. Rev. B **101**, 245154 (2020). This paper is also cited as Ref. [16] in this thesis.

band and so still form a Fermi surface. Magnetic translation symmetry implies, as we will review, that this Fermi surface must consist of multiple Fermi pockets, raising the possibility of finite-momentum pairing and the formation of Fulde-Ferrell-Larkin-Ovchinnikov (FFLO) [112,113] or pair-density wave (PDW) [114] like states. These statements may hold true even in zero magnetic field, as the composite fermions will still see a non-zero Chern-Simons flux. We should emphasize that the PDW states we investigate do not arise from a Zeeman effect (as in the conventional FFLO states) but rather have a purely orbital origin.

The goal of this Chapter is to illustrate the existence, at mean-field level, of a novel set of FCI phases which exhibit a *coexistence* of topological order (TO) and broken symmetry order (BSO) as a result of finite-momentum composite fermion pairing, taking as an example, for simplicity, the square-lattice Hofstadter model.[1] We find, for instance, topologically ordered states supporting CDWs, providing a new entry in the long history of stripe order in QH systems [119–123]. These states support a range of Abelian and non-Abelian topological orders, including the Pfaffian and PH-Pfaffian [124] states. We also find a phase which we call a quantum Hall thermal semimetal, as the charge sector is gapped, while the neutral sector is described by a theory of relativistic massless Majorana fermions. Such a state will possess a quantized Hall conductance, but will support unquantized transport of heat through the bulk.

Related phenomena have been exhibited in recent experiments [125–127], which revealed a competition between pairing and nematicity in continuum Landau levels. A subsequent theoretical study [128] proposed a $p_x + ip_y$ PDW state of composite fermions as a possible explanation for this observation. The distinguishing feature between the physics we present and that of, for instance, Ref. [128] is that we present FCIs as a platform in which to study *intertwining* of TO and BSO, in that they do not compete with nor are even independent of one another, but rather arise from a common microscopic origin, namely the interplay between the pairing of composite fermions and the commensurability of the lattice and magnetic length scales. We note that the competition and, in some cases, the coexistence of FCI states with more traditional broken symmetry orders, such as charge density waves (CDWs), has already been numerically established in Refs. [42,43] (though the underlying icrocopic mechanisms are likely distinct from those discussed here). This intriguing phenomenon of multiple orders that sometimes compete with each other but sometimes drive each other is reminiscent of the complex intertwined orders found in high temperature superconductors [114,129].

We emphasize that, although we focus on a particular lattice model, the basic mechanism of finite-momentum pairing of composite fermions is applicable to other experimentally relevant lattice systems. These include the aforementioned Moiré systems, such as bilayer graphene/hexagonal boron nitride heterostructures, in which Abelian fractionalized states have been observed in strong magnetic fields [44].

[1] See Refs. [115–118] for related studies of pairing of electrons in the spin-1/2 Hofstadter model.

Recent theoretical studies suggest that such states may even be found at zero magnetic field in twisted bilayer graphene systems [130–133]. On the cold atoms front, the Hofstadter model has already been experimentally realized [50–52]. Although fractionalized states have not yet been observed, the tunability of interactions in these systems make them a promising playground in which to search for our proposed finite momentum paired states. With this in mind, we look for both *fermionic and bosonic* FCI states in the Hofstadter model, the latter of which are of relevance to cold atom experiments. At the filling fractions we consider, the bosonic and fermionic phase diagrams exhibit roughly the same set of ordered states.

The remainder of this Chapter is structured as follows. First, we introduce the fermionic Hofstadter model and review the flux attachment transformation. We identify three example filling fractions at which the composite fermions form Fermi surfaces with multiple Fermi pockets. Next, we perform a self-consistent BCS calculation to produce phase diagrams at these fillings in the presence of attractive nearest-neighbor (NN) and repulsive next-nearest-neighbor (NNN) interactions. We then briefly repeat this analysis for the same lattice model, but with hardcore bosons. Lastly, we discuss our results and conclude.

3.2 Model, Flux Attachment, and Compressible FCI States

We consider the Hofstadter model [134–136] of spinless fermions hopping on a square lattice in a uniform magnetic field, as described by the Hamiltonian

$$H_0 = -t \sum_{\boldsymbol{x}} \sum_{j=x,y} \left[c^\dagger_{\boldsymbol{x}} c_{\boldsymbol{x}+\boldsymbol{e}_j} e^{-iA_j(\boldsymbol{x})} + H.c. \right], \tag{3.1}$$

where t is the hopping amplitude, $\boldsymbol{e}_j$ are the NN lattice vectors, and $A_j(\boldsymbol{x})$ is the electromagnetic vector potential. We choose the Landau gauge $\boldsymbol{A} = (0, \phi_0 x)$, where ϕ_0 is the flux per plaquette. We take

$$\phi_0 = 2\pi \frac{p_0}{q_0}, \quad p_0, q_0 \in \mathbb{Z}, \tag{3.2}$$

with p_0 and q_0 co-prime, so that the magnetic unit cell (MUC) consists of q_0 sites along the x direction. The energy spectrum therefore consists of q_0 bands. Additionally, the magnetic translation algebra [137] dictates that the single particle dispersion obeys the following periodicity in the magnetic Brillouin zone (MBZ):

$$\varepsilon(k_x, k_y) = \varepsilon(k_x, k_y - \phi_0). \tag{3.3}$$

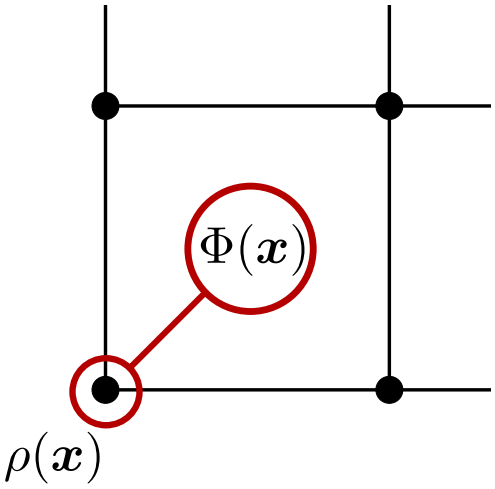

Figure 3.1: Flux attachment on the square lattice. The Chern-Simons flux, $\Phi(\boldsymbol{x})$, through the plaquette north-east of $\boldsymbol{x}$ is attached to the fermion density $\rho(\boldsymbol{x})$ via Gauss' law, $\rho(\boldsymbol{x}) = \theta\Phi(\boldsymbol{x})$.

The consequences of magnetic translation symmetry will play an important role when we turn to discussing pairing of composite fermions.

Now, the Chern number, C_0, of the first r filled bands of the Hofstadter Hamiltonian satisfies the Diophantine equation $r = C_0 p_0 + D_0 q_0$, $D_0 \in \mathbb{Z}$ [22]. The lowest Landau level (LLL) corresponds to the solution $(r, C_0, D_0) = (p_0, 1, 0)$. Hence, lattice effects split the LLL into p_0 sub-bands. We are interested in scenarios in which the LLL filling $\nu \equiv 2\pi n/\phi$, where n is the fermion density per site, is fractional. Here we are following the conventions of Ref. [60] by defining the filling relative to the bands below a certain gap (in this case, the gap above the manifold of states corresponding to the LLL), rather than in terms of the filling of a specific band.

We look for fractionalized phases at these filling fractions by performing an exact mapping of the system of fermions to a system of composite fermions coupled to an emergent Chern-Simons gauge field [12, 95]. Physically speaking, this flux attachment procedure amounts to attaching solenoids of $2k$, $k \in \mathbb{Z}$, flux quanta to each fermion so that the resulting bound state of a fermion and a solenoid, a composite fermion, still obeys Fermi statistics. The resulting action is given by

$$S[f, f^\dagger, a_\mu] = S_F[f, f^\dagger, a_\mu] + S_{CS}[a_\mu] \tag{3.4}$$

where f is the composite fermion field and a_μ the statistical gauge field. Explicitly,

$$S_F = \int_t \sum_{\boldsymbol{x}} \left[f^\dagger(\boldsymbol{x}, t)(iD_0 + \mu) f(\boldsymbol{x}, t) + \sum_{j=x,y} (f^\dagger(\boldsymbol{x}, t) e^{i(a_j(\boldsymbol{x},t) - A_j(\boldsymbol{x}))} f(\boldsymbol{x} + \boldsymbol{e}_j, t) + H.c.) \right], \tag{3.5}$$

where $D_0 = \partial_0 + ia_0$ is the covariant time derivative and μ is the chemical potential. The flux attachment procedure on the lattice is more subtle than that in the continuum due to the difficulties associated with defining a lattice Chern-Simons action. We make use of the action defined in Refs. [56, 58], which takes the form,

$$S_{CS} = \theta \int_t \sum_{\boldsymbol{x}} \left[a_0(\boldsymbol{x}, t)\Phi(\boldsymbol{x}, t) - \frac{1}{2} a_i(\boldsymbol{x}, t)\mathcal{M}_{ij}\dot{a}_j(\boldsymbol{x}, t) \right]. \tag{3.6}$$

Here,

$$\theta = 1/2\pi(2k),\ k \in \mathbb{Z} \tag{3.7}$$

and $\Phi(\boldsymbol{x}) \equiv \epsilon_{ij} d_i a_j(\boldsymbol{x})$ is the Chern-Simons flux through the plaquette north-east of the site $\boldsymbol{x}$, where the d_i are forward difference operators: $d_i a_j(\boldsymbol{x}) = a_j(\boldsymbol{x} + \boldsymbol{e}_i) - a_j(\boldsymbol{x})$. Likewise, we define backward difference operators, $\widehat{d}_i$, which have the action, $\widehat{d}_i a_j(\boldsymbol{x}) = a_j(\boldsymbol{x}) - a_j(\boldsymbol{x} - \boldsymbol{e}_i)$. The operator $\mathcal{M}_{ij}$ – the explicit form of which is unimportant for us and is relegated to Appendix B.1 – is chosen so as to make the theory gauge-invariant. What is important is that S_{CS} enforces the flux attachment constraint (or Gauss' law), $f^\dagger f(\boldsymbol{x}) = \theta\Phi(\boldsymbol{x})$, via the Lagrange multiplier field a_0, as depicted in Fig. 3.1.

We will defer the inclusion of interaction terms until the next section, as we first simply wish to understand the mean-field composite fermion band structure. Now, the saddle-point equations for the above action are given by (restricting to time-invariant solutions)

$$\langle f^\dagger(\boldsymbol{x}) f(\boldsymbol{x})\rangle \equiv \rho(\boldsymbol{x}) = \theta\Phi(\boldsymbol{x}) \tag{3.8}$$

$$\langle j_k(\boldsymbol{x})\rangle = \theta\epsilon_{ki}\widehat{d}_i a_0(\boldsymbol{x}) \tag{3.9}$$

where $j_k(\boldsymbol{x}) \equiv -\frac{\partial S_F}{\partial a_k(\boldsymbol{x})}$ is the gauge-invariant current. On the square lattice, there always exists a uniform solution at any filling fraction with

$$\rho(\boldsymbol{x}) \equiv n, \quad \Phi(\boldsymbol{x}) \equiv \phi = n\theta, \quad j_k(\boldsymbol{x}) = a_0(\boldsymbol{x}) = 0. \tag{3.10}$$

In this mean-field configuration the composite fermions feel a reduced effective flux of

$$\phi_* = \phi_0 - \phi \equiv 2\pi\frac{p_*}{q_*} \tag{3.11}$$

per plaquette, where we restrict ourselves to cases where p_* and q_* are integer and take them to be co-prime.

Table 3.1: Details of the three composite Fermi liquid states whose pairing instabilities we investigate. The names period two, three, and four refer to the periodicity of the MBZ. Here ϕ_0, n, ν, k, ϕ, and ϕ_* are the magnetic flux, fermion density per site, LLL filling fraction, number of pairs of attached statistical flux quanta, statistical flux, and effective flux seen by the composite fermions.

	$\phi_0/2\pi$	n	ν	k	$\phi/2\pi$	$\phi_*/2\pi$
Period two	3/4	1/8	1/6	1	1/4	1/2
Period three	2/3	1/6	1/4	1	1/3	1/3
Period four	5/8	3/16	3/10	1	3/8	1/4

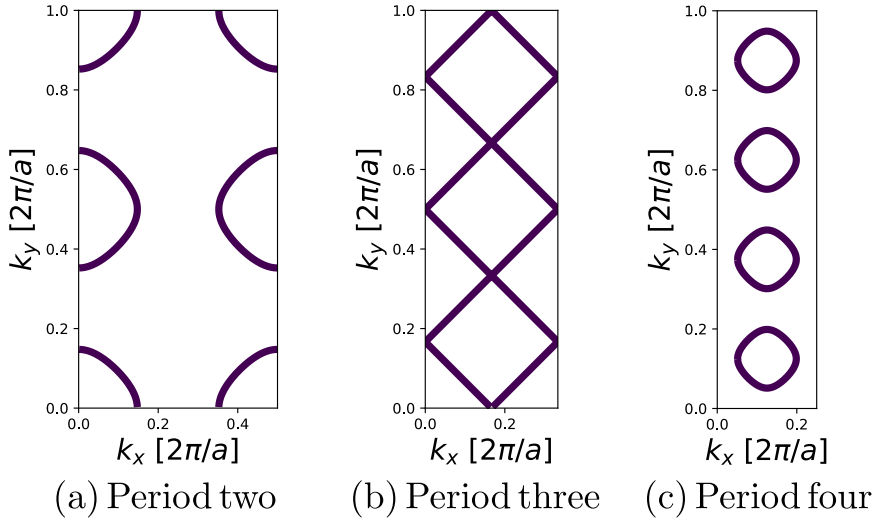

Figure 3.2: Composite Fermi surfaces for the period two, three, and four configurations given in Table 3.1.

So, the mean-field CF band structure is described by a Hofstadter Hamiltonian in the form of Eq. (3.1), but with a flux per plaquette of ϕ_*.

For appropriate choices of ν and k, the resulting mean-field spectrum consists of CFs partially filling a Hofstadter band, yielding a Fermi surface and hence a compressible state. In particular, if there is a CF pocket centered at, say, $\boldsymbol{k} = 0$, then magnetic translation symmetry implies, through Eq. (3.3), that there will be $q_* - 1$ additional CF pockets centered at momenta $\boldsymbol{Q}_l = (0,\, 2\pi l/q_*)$, $l \in \mathbb{Z}$, in the Landau gauge. This is illustrated in Fig. 3.2 for the three different configurations of magnetic flux and filling specified in Table 3.1. Given the number of Fermi pockets for each configuration, we will label them as period two, three, and four, respectively. It is clear that, in the presence of an attractive interaction, we have the possibility of the formation of Cooper pairs of CFs with center of mass momenta $\boldsymbol{Q}_l + \boldsymbol{Q}_m$.

3.3 Mean-field Theory of Paired States

Our goal now is to investigate the possible pairing instabilities when the composite fermions form a Fermi surface with multiple Fermi pockets, focusing, for simplicity, on the three configurations listed in Table 3.1. To that end, we introduce a NN attractive interaction,

$$\begin{aligned} S_{\text{pair}} &= -V \int_t \sum_{\boldsymbol{x},j} f^\dagger(\boldsymbol{x},t) f^\dagger(\boldsymbol{x}+\boldsymbol{e}_j,t) f(\boldsymbol{x}+\boldsymbol{e}_j,t) f(\boldsymbol{x},t) \\ &\sim -\int_t \sum_{\boldsymbol{x},j} \left[\Delta_{\boldsymbol{x},j} f^\dagger(\boldsymbol{x},t) f^\dagger(\boldsymbol{x}+\boldsymbol{e}_j,t) + \Delta^\dagger_{\boldsymbol{x},j} f(\boldsymbol{x}+\boldsymbol{e}_j,t) f(\boldsymbol{x},t) - \frac{1}{V} |\Delta_{\boldsymbol{x},j}|^2 \right] \end{aligned}$$

where $V < 0$ and we have performed a Hubbard-Stratonovich transformation to introduce the complex pair field $\Delta_{x,j}$. We will also consider the effect of NNN repulsive interactions,

$$\begin{aligned} S_{\text{int}} &= -\frac{g}{2} \int_t \sum_{\boldsymbol{x},\boldsymbol{x}'} f^\dagger(\boldsymbol{x},t) f(\boldsymbol{x},t) U(\boldsymbol{x}-\boldsymbol{x}') f^\dagger(\boldsymbol{x}',t) f(\boldsymbol{x}',t) \\ &\sim -g \int_t \sum_{\boldsymbol{x},\boldsymbol{x}'} \left[f^\dagger(\boldsymbol{x},t) f(\boldsymbol{x},t) U(\boldsymbol{x}-\boldsymbol{x}') \rho(\boldsymbol{x}',t) - \frac{1}{2} \rho(\boldsymbol{x},t) U(\boldsymbol{x}-\boldsymbol{x}') \rho(\boldsymbol{x}',t) \right] \end{aligned}$$

where $g > 0$, $\rho(\boldsymbol{x})$ is a Hubbard-Stratonovich field corresponding to the fermion density, and $U(\boldsymbol{x}-\boldsymbol{x}') = 1$ if $\boldsymbol{x}$ and $\boldsymbol{x}'$ are next-nearest-neighbors while $U(\boldsymbol{x}-\boldsymbol{x}') = 0$ otherwise. We include this repulsive interaction in order to stabilize additional striped solutions, which may be metastable at $g = 0$. Such a combination of short-range attractive and long-range repulsive interactions can be engineered in cold atom systems and has been shown numerically to be conducive to the formation of non-Abelian FCI states [111]. We will restrict our attention to the region of phase space in which $0 \leq g < -V$.

Now, in principle, we could perform a fully self-consistent calculation and solve the saddle-point equations for the Hubbard-Stratonovich fields and the Chern-Simons gauge fields. Indeed, the gauge fields should be expected to play an important dynamical role. Since they lead to repulsive interactions between the composite fermions, they will disfavor superconducting order [138] and possibly lead to phase separation [139]. However, we will instead adopt a more phenomenological approach, analogous to that used in the continuum [61], in which we simply take the uniform statistical gauge field flux as a fixed background and look for paired states on top of it. Our reasons for this are twofold. First, as in the continuum, our motivation is to look for potentially interesting pairing instabilities, not investigate dynamical questions of the stability of these states to gauge field fluctuations. Second, as discussed in Chapter 2, mean-field approximations of this type of lattice Chern-Simons action appear to be "too classical", in the sense that, although the mapping to composite fermions is an exact one, the choice of flux attachment breaks the lattice point-group

symmetries. This makes itself manifest in mean-field solutions and it is for this reason that we did not find uniform density FCI states in the preceding Chapter [15].[2] In the present problem, we are generally not able to find solutions with reasonably small unit cells, if we perform this fully self-consistent analysis. This may be indicative of a similar issue, or of the possibility that we are already seeing the effects of phase separation. In either case, this misses the main physics we which to address which, to reiterate, is the existence of interesting instabilities of the composite fermions.

It should also be noted that we have chosen specific channels into which to decompose the attractive and repulsive interactions. In a fully self-consistent variational calculation, it would be more appropriate to decompose both interactions into all possible channels since, as we shall see, the mean-field solutions typically exhibit CDWs and bond order waves (BOWs), even for $g = 0$.[3] We have adopted this simplified approach as our goal is not to provide a detailed, quantitative understanding of the phase diagram, but rather to highlight the qualitative features of the phases which may appear in these lattice systems.

With these assumptions and caveats out of the way, we are left with solving for mean-field configurations of spinless fermions in a uniform background magnetic field on a lattice, as described by the mean-field Hamiltonian

$$H_F = \sum_{\boldsymbol{x},j} \left[-t f^\dagger_{\boldsymbol{x}} f_{\boldsymbol{x}+\boldsymbol{e}_j} e^{-i a_{*,j}(\boldsymbol{x})} + \Delta_{\boldsymbol{x},j} f^\dagger_{\boldsymbol{x}} f^\dagger_{\boldsymbol{x}+\boldsymbol{e}_j} + \text{H.c.} \right] - \mu \sum_{\boldsymbol{x}} f^\dagger_{\boldsymbol{x}} f_{\boldsymbol{x}} + g \sum_{\boldsymbol{x},\boldsymbol{y}} f^\dagger_{\boldsymbol{x}} f_{\boldsymbol{x}} U(\boldsymbol{x}-\boldsymbol{y}) \rho(\boldsymbol{y}), \tag{3.12}$$

where we have defined $\boldsymbol{a}_* = \boldsymbol{A} - \boldsymbol{a} = (0, \phi_* x)$. We must look for solutions of the following self-consistent equations,

$$\rho(\boldsymbol{x}) = \langle f^\dagger(\boldsymbol{x}) f(\boldsymbol{x}) \rangle \tag{3.13}$$

$$\Delta_{\boldsymbol{x},j} = \langle f(\boldsymbol{x}+\boldsymbol{e}_j) f(\boldsymbol{x}) \rangle \tag{3.14}$$

$$\sum_{\boldsymbol{x}} \rho(\boldsymbol{x}) = N_f, \tag{3.15}$$

where N_f is the total number of fermions. For non-zero values of the pairing amplitudes, $\Delta_{\boldsymbol{x},j}$, the total fermion number is not conserved by the mean-field Hamiltonian, and so we fix the average density, n, by tuning the chemical potential, μ.

As noted in the previous section, we must allow for pair fields with COM momenta $\boldsymbol{Q}_l + \boldsymbol{Q}_m$, the smallest

[2] Theories of this type do not have small expansion parameters. A more correct treatment of quantum fluctuations can lead, presumably, to the partial melting of some of the broken symmetry states found in Ref. [15]. The same caveats apply to the problem under consideration here.

[3] Here we use a traditional (but inaccurate) terminology in which a CDW is meant a charge density wave on the sites of the lattice, and by a BOW charge density wave on the bonds of the lattice. In the case of an incommensurate CDW, the charge modulation has components both on sites and bonds.

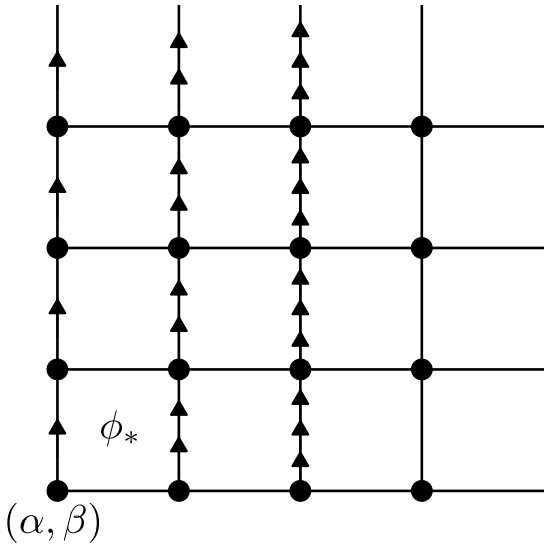

Figure 3.3: Unit cell used in the mean-field analysis. The net flux per unit cell is ϕ_* out of the page. Here we take $\phi_* = 2\pi\left(\frac{5}{8} - \frac{3}{8}\right) = 2\pi\frac{1}{4}$ so that the unit cell contains $q_* \times q_* = 4 \times 4$ lattice sites. The arrows represent our choice of the Landau gauge, with the net mean-field gauge field taking the form $\boldsymbol{a}_* = (0, \phi_* \alpha)$. Lastly, (α, β) represent the horizontal and vertical coordinates of the lattice sites within a unit cell.

of which is $(0, 2\pi/q_*)$ and corresponds to a period of q_* lattice sites in the y-direction. As such, we will take our unit cell to contain $q_* \times q_*$ lattice sites, as depicted in Fig. 3.3 for $q_* = 4$. This leaves us with q_*^2 densities, $\rho_{(\alpha,\beta)}$, and $2q_*^2$ pair fields, $\Delta_{(\alpha,\beta),j}$, to solve for, where $\alpha, \beta = 1, \ldots, q_*$ denote the horizontal and vertical coordinates of the sites within a unit cell (see Fig. 3.3). For given values of V and g, we numerically solve the saddle-point equations Eqs. (3.13)-(3.15), using several random *ansätze* for the densities and pair fields to ensure we identify the lowest energy solution. Note that the ground state is the solution which minimizes the energy – not the grand potential – since we are working at fixed particle number rather than fixed chemical potential. So, although we compute observables within the grand canonical ensemble, we must subtract $-\mu N_f$ from the mean-field Hamiltonian when comparing the energies of different mean-field configurations:

$$E = \langle H_F \rangle + \mu N_f - \frac{1}{V} \sum_{\boldsymbol{x},j} |\Delta_{\boldsymbol{x},j}|^2 - \frac{g}{2} \sum_{\boldsymbol{x},\boldsymbol{y}} \rho(\boldsymbol{x}) U(\boldsymbol{x} - \boldsymbol{y}) \rho(\boldsymbol{y}). \tag{3.16}$$

In the following, we will map out the mean-field phase diagrams as functions of V and g.

3.3.1 Role of Magnetic Translation Symmetry

As a brief interlude, let us investigate the role of the magnetic translation symmetry in determining the form of the pair fields [115]. In the Landau gauge we have chosen, the magnetic translation operators are given

by

$$\tilde{T}_1 = \exp\left(i\phi_* \sum_{\boldsymbol{r}} r_2 f^\dagger_{\boldsymbol{r}} f_{\boldsymbol{r}}\right) T_1, \qquad \tilde{T}_2 = T_2, \tag{3.17}$$

where $T_{1,2}$ are the ordinary translation operators and have the action $T_j^{-1} f_x T_j = f_{x-e_j}$. The magnetic translations $\tilde{T}_{1,2}$ commute with the kinetic part of the mean-field Hamiltonian. Under the action of $\tilde{T}_1$, the pair fields transform as

$$\begin{aligned} \tilde{T}_1 \Delta_{(\alpha,\beta),x} \tilde{T}_1^{-1} &= \Delta_{(\alpha+1,\beta),x} e^{-2i\phi_*\beta}, \\ \tilde{T}_1 \Delta_{(\alpha,\beta),y} \tilde{T}_1^{-1} &= \Delta_{(\alpha+1,\beta),y} e^{-2i\phi_*\beta} e^{-i\phi_*}. \end{aligned} \tag{3.18}$$

This implies that a mean-field state, $|\psi\rangle$, with, for instance, uniform $p_x + ip_y$ pairing actually breaks magnetic translations and the state $\tilde{T}_1 |\psi\rangle$ will have spatially modulated pair fields. We alert the reader to this fact now so it is clear, when we present real-space configurations of specific mean-field solutions, that the pair fields of the translated (and rotated) solutions will not take the same form. This is a consequence of the fact that magnetic translations (rotations) are translations (rotations) combined with a gauge transformation and the pair fields are not gauge-invariant quantities.

Let us now consider solutions which preserve the magnetic translation symmetry, so that $\tilde{T}_j \Delta_{(\alpha,\beta),j} \tilde{T}_j^{-1} = \Delta_{(\alpha,\beta),j}$. On defining the Fourier transform of the pair fields in the y-direction, $\Delta_{\alpha,P_l,j} = \sum_{\beta=1}^{q_*} \Delta_{(\alpha,\beta),j} e^{-iP_l\beta}$ with $P_l = \frac{2\pi l}{q_*}$, $l \in \mathbb{Z}$, and imposing the above magnetic translation symmetry constraints, we find

$$\Delta_{\alpha,P_l,j} = \Delta_{\alpha+1,P_l+2\phi_*,j} e^{-i\phi_*\delta_{j,y}}. \tag{3.19}$$

This implies that zero-momentum pairing will generically coexist with finite-momentum pairing, if magnetic translation symmetry is preserved. Of course, there is no guarantee that magnetic translations will be respected by the mean-field ground state and we will often find it to be the case that it is not. Nevertheless, this observation highlights the point that there is a predisposition to finite-momentum pairing in these lattice systems.

3.4 Fermionic Paired FCI Phase Diagrams

The results of our self-consistent mean-field analysis are summarized in the phase diagrams of Fig. 3.4. We find a host of translation symmetry breaking paired states of the composite fermions, the qualitative features of which we now describe in more detail. In addition to the site-centered charge density and pair

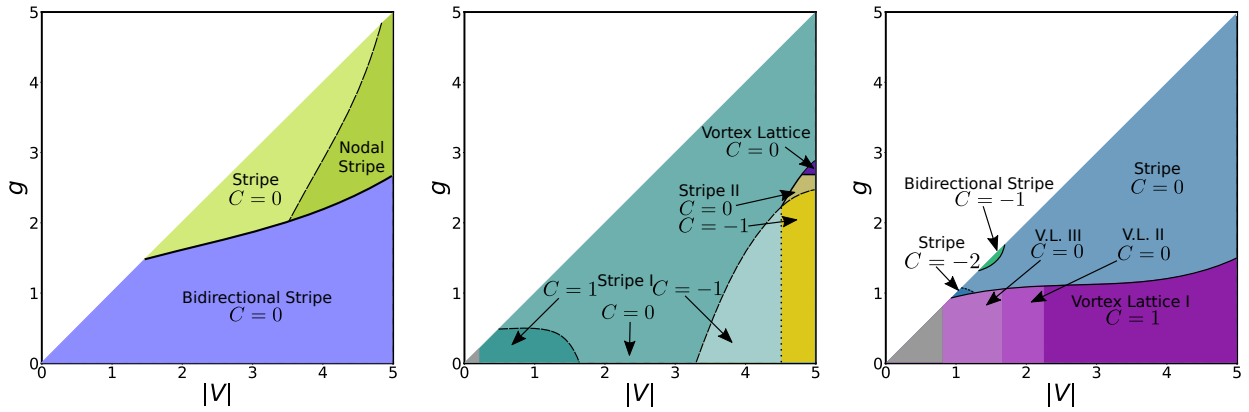

(a) Period two (b) Period three (c) Period four

Figure 3.4: Schematic mean-field phase diagrams as functions of the NN attraction, $|V| = -V$, and NNN repulsion, g, for the fermionic configurations of Table 3.1. Solid (dashed) black lines correspond to first order (continuous) transitions. The dotted line separating the Stripe I and II regions in (b) indicates a crossover. Gapped phases are labeled by the Chern number, C, of the BdG bands. The grey regions indicate where the energies of the saddle-point equation solutions are too close to numerically deduce which is the ground state. Details of the phases are presented in the main text and illustrated in Figures 3.5, 3.7, and 3.8.

field configurations, we characterize these phases by computing the link currents and the bond densities,

$$\langle j_{\boldsymbol{x},k} \rangle = \langle i f^\dagger_{\boldsymbol{x}} f_{\boldsymbol{x}+\boldsymbol{e}_k} e^{-i a_{*,k}(\boldsymbol{x},t)} + \text{H.c} \rangle, \tag{3.20}$$

$$\langle B_{\boldsymbol{x},k} \rangle = \langle f^\dagger_{\boldsymbol{x}} f_{\boldsymbol{x}+\boldsymbol{e}_k} e^{-i a_{*,k}(\boldsymbol{x},t)} + \text{H.c} \rangle, \tag{3.21}$$

as well as the Chern number, C, of the Bogoliubov-de Gennes (BdG) band structure, using the method of Ref. [102]. The latter quantity determines the number and chirality of Majorana edge modes in a system with open boundary conditions. This allows us to determine the topological order of the system via the bulk-boundary correspondence, on taking into account the presence of a charged chiral boson from the gapped charge sector. Equivalently, from the bulk perspective, vortices of the pair field will trap C Majorana zero modes (MZMs).

Much as in the well studied case of the paired FQH states in the continuum [61], due to the Higgsing of the dynamical Chern-Simons gauge field by the pairing amplitudes, vortices of the pair field are finite energy excitations and carry a charge $e/4k$, where e is the charge of the electron. So, states with an odd Chern number possess non-Abelian topological order, as these pair field vortices will possess one unpaired MZM. Conversely, states with an even Chern number possess Abelian topological order. In particular, since we have focused on FQH states arising from attaching a single pair of flux quanta ($k = 1$), states with $C = 1, -1$ possess the same topological order as the Pfaffian and PH-Pfaffian states [124], respectively, whereas those with $C = 0$ support the same topological order as the Abelian Halperin paired state [140].

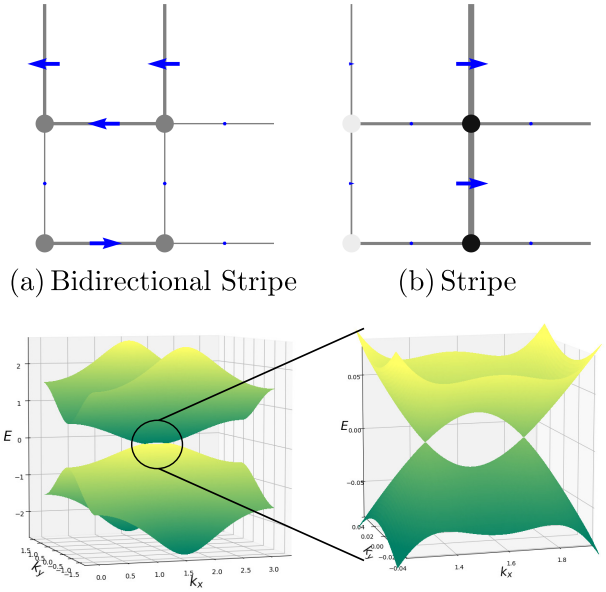

(a) Bidirectional Stripe (b) Stripe

(c) Nodal Stripe Dispersion

Figure 3.5: (a) and (b): Period-two mean-field configurations. In this and the following figures, the color of the sites indicates the charge density, with darker (lighter) sites corresponding to higher (lower) density. Likewise, the width of the links represent the magnitude of the bond density, $B_{\boldsymbol{x},j}$. The blue arrows represent the pair fields $\Delta_{\boldsymbol{x},j} = |\Delta_{\boldsymbol{x},j}|e^{i\theta_{\boldsymbol{x},j}}$, with length proportional to $|\Delta_{\boldsymbol{x},j}|$ and angle relative to the horizontal given by $\theta_{\boldsymbol{x},j}$. The link currents all vanish. (c): Spectrum of the BdG Hamiltonian for mean-field configuration (b). The left panel depicts the two bands closest to $E = 0$. The black circle highlights the presence of two Majorana cones along the line $k_y = 0$, which are depicted in more detail in the right panel.

The relation between the Higgsing of the Chern-Simons gauge field and the non-Abelian topological order is a subtle issue. Its root reason is the the fact that the pair field condensate leaves a local $\mathbb{Z}_2$ symmetry unbroken in a regime in which the theory is deconfined [141]. An example is the case of a conventional superconductor coupled to a dynamical gauge field which has $\mathbb{Z}_2$ topological order [142]. In the case of a relativistic field theory, the non-Abelian character can be described either through a similar pairing mechanism, or in terms of a topological phase of the partition function in the form of an η-invariant [143].

3.4.1 Period Two

We now turn to the non-uniform paired phases. We begin with the period-two phase diagram, depicted in Fig. 3.4(a), in which we find three striped phases. The real space configurations of these phases are depicted in Fig. 3.5. We note that the net (statistical plus magnetic) flux per plaquette is π and so, prior to the addition of interactions, the mean-field composite Fermi liquid solution [Fig. 3.2(a)] preserves time reversal symmetry (TRS). The mean-field paired ground states we find also preserve TRS since all the pair fields, $\Delta_{\boldsymbol{x},j}$, can be made real by a global $U(1)$ rotation.

Focusing on the individual phases in more detail, the ground state for small g is a bidirectional stripe phase. As depicted in Fig. 3.5(a), this state possesses a uniform site density but also a bidirectional BOW. In particular, $B_{\boldsymbol{x},x}$ and $B_{\boldsymbol{x},y}$ possess modulations at the wave vectors $(\pi, 0)$ and $(0, \pi)$, respectively. This is not surprising, as the pair fields take the forms $\Delta_{\boldsymbol{x},x} = \Delta e^{i\boldsymbol{q}_1\cdot\boldsymbol{x}} + \tilde{\Delta} e^{i\boldsymbol{q}_2\cdot\boldsymbol{x}}$ and $\Delta_{\boldsymbol{x},y} = \tilde{\Delta} e^{i\boldsymbol{q}_1\cdot\boldsymbol{x}} - \Delta e^{i\boldsymbol{q}_3\cdot\boldsymbol{x}}$, where $\tilde{\Delta} > \Delta > 0$, $\boldsymbol{q}_1 = (0, \pi)$, $\boldsymbol{q}_2 = (\pi, \pi)$ and $\boldsymbol{q}_3 = (0, 0)$. In general, the presence of pair fields at momenta $\boldsymbol{q}_1$ and $\boldsymbol{q}_2$ will induce a *daughter* CDW order with amplitude $\rho_{\boldsymbol{q}_1-\boldsymbol{q}_2} \sim \Delta_{\boldsymbol{q}_1}\Delta^*_{\boldsymbol{q}_2} + \Delta_{-\boldsymbol{q}_2}\Delta^*_{-\boldsymbol{q}_1}$, where $\rho_{\boldsymbol{q}}$ is the Fourier transform of the charge density, as can be shown through a simple free energy analysis [114,144]. However, in the present problem, we must be careful to note that the phases of the pair fields, and hence their Fourier components, depend on the choice of gauge for the background flux. In particular, as noted above, the pair fields transform non-trivially under magnetic translations and rotations. As such, we cannot directly use the free energy analysis of Ref. [144] to deduce the daughter orders of the spatially modulated superconducting order. A more careful treatment, which is beyond the scope of the present work, would require the analysis of a free energy which takes into account the transformations of the pair fields under the magnetic algebra. Nevertheless, it is clear that we can still identify the BOW as a daughter order of the striped superconducting order (and hence a consequence of finite momentum pairing of the composite fermions) by virtue of the fact that this phase exists as the ground state in the absence of the NNN repulsive interaction, at $g = 0$.

The band structure of the BdG Hamiltonian for this phase is less interesting. It is fully gapped with $C = 0$, implying there are no chiral Majorana edge states. We have also studied this mean-field configuration with open boundary conditions to confirm that there are indeed no edge states protected by the mean-field TRS or any other symmetry.

As g is increased, there is a first-order transition to a striped p_y phase, in which $\Delta_{\boldsymbol{x},x} = 0$, while $\Delta_{\boldsymbol{x},y} = \tilde{\Delta} + \Delta e^{i\boldsymbol{q}\cdot\boldsymbol{x}}$ with $\boldsymbol{q} = (\pi, 0)$ and $\tilde{\Delta} > \Delta > 0$. The modulation of the pair fields in this phase appears to be driven by the $(\pi, 0)$ CDW engendered by the repulsive NNN interactions, as this phase does not exist as a solution of the saddle-point equations at $g = 0$. Moreover, we have numerically checked that a similar stripe phase can be obtained in a square lattice system with the same interactions, but with a vanishing magnetic flux and hence a single Fermi pocket. Nevertheless, the BdG spectrum exhibits an interesting nodal structure. For large g and V, the system possesses two Majorana cones, as shown in Fig. 3.5(c). As g is increased further or V decreased, the cones approach and annihilate one another (indicated by the dashed black line in Fig. 3.5), yielding a fully gapped spectrum.

Although $C = 0$ in the gapped stripe phase, both the nodal and gapped phase band structures are in fact topologically non-trivial. This is demonstrated in Fig. 3.6, in which we plot the energy spectra for these

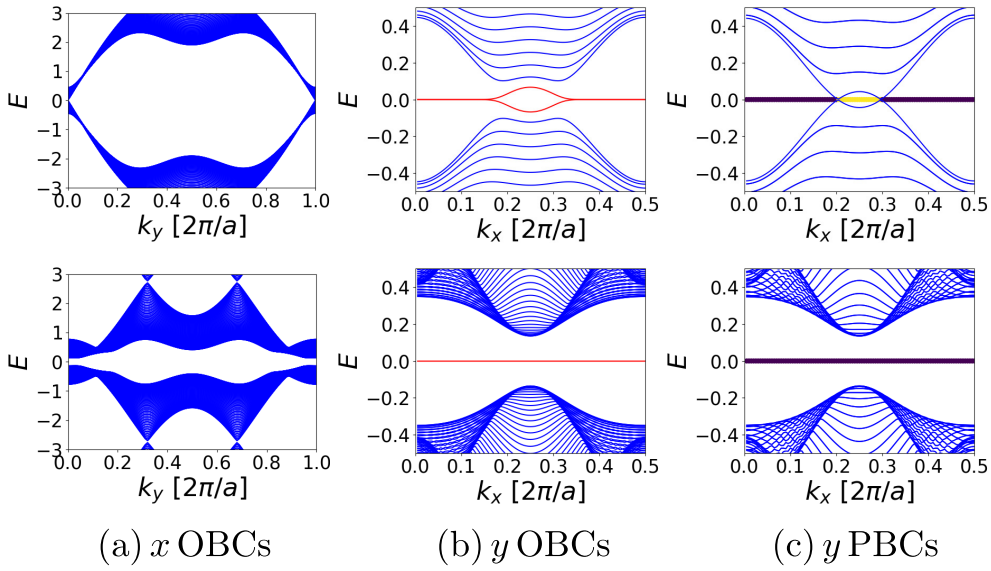

Figure 3.6: Dispersions of the (top row) nodal and (bottom row) gapped stripe phases on finite-size systems with different boundary conditions. In (c), we also plot a horizontal line at $E = 0$, representing the topological invariant $\mathcal{M}(k_x)$ defined in Appendix B.2.1. Purple (yellow) indicates $\mathcal{M}(k_x) = -1(+1)$.

phases on finite-size systems with open and periodic boundary conditions (OBCs and PBCs, respectively). In the nodal phase, on imposing OBCs along the direction parallel to the stripes, we find a Majorana flat band connecting the projections of the bulk nodes onto the edge Brillouin zone (BZ). In the gapped phase, we find a Majorana flat band spanning the entire surface BZ. These properties are typical of p_x-paired states [145]. We show in Appendix B.2.1 that a combination of the particle-hole symmetry of the BdG Hamiltonian and reflection symmetry, with the reflection axis taken along a stripe, are sufficient to protect these flat bands and the nodal points.

Physically, the existence of these flat bands is not surprising, as the mean-field ground state resembles an array of Kitaev chains [146]. At large values of g, hopping between the chains consisting of sites with high density, which also have non-zero $\Delta_{\boldsymbol{x},y}$, will be suppressed due to the intervening low density chains and the NNN repulsion. This yields an array of decoupled Kitaev chains which, in the topological regime, will host MZMs at their ends when OBCs are imposed, giving rise to the observed Majorana flat band. The gapped stripe phase thus describes a *weak* two-dimensional topological superconductor of composite fermions, in that it is formed from an array of one-dimensional topological superconductors (see Appendix B.2.2 for more details).

Since they both have $C = 0$, the bidirectional stripe phase and gapped stripe phases possess the topological order of the Abelian Halperin paired state. That being said, based on the physical picture of the gapped stripe phase as an array of nearly decoupled Kitaev chains, we expect that lattice dislocations should

bind MZMs (see Appendix B.2.2). This is a particularly intriguing possibility in the context of cold atom experiments, where lattice defects can be engineered directly. A somewhat similar nematic FQH phase was found in a coupled wire construction of paired FQH states in Ref. [147], although, in that case, the edge supported a pair of helical Majoranas with finite dispersion. Lastly, we note that the nodal striped phase is a quantum Hall thermal semi-metal in that charged excitations are gapped in the bulk, but the gapless Majoranas can still transport heat. The nodal striped phase is not strictly topologically ordered since it has a gapless spectrum. Nevertheless, it still supports gapped charge-1/2 Laughlin quasiparticles.

3.4.2 Period Three

We will now discuss the period-three inhomogeneous paired states. As shown in Fig. 3.4(b), the period-three phase diagram is dominated by unidirectional stripe phases. The real space configurations of these phases are depicted in Fig. 3.7. The stripe I and II configurations clearly belong to the same phase – they both possess a CDW at wave vector $(2\pi/3, 0)$. For small g, as $|V|$ is increased, there is a crossover from stripe I to stripe II, as the CDW order parameter continuously drops to zero around $|V| \approx 4.5$ and then changes sign. This crossover is indicated by the dotted black line in Fig. 3.4(b). As g is increased, however, this crossover changes to a first order transition around $g \approx 2.5$. The stripe I/II configurations are also characterized by finite momentum pairing and counter-propagating currents. The pair fields, in the chosen gauge, have the forms $\Delta_{\boldsymbol{x},x} = \Delta_0 + \Delta_1 \cos(2\pi x/3)$, where $\Delta_0 > \Delta_1 > 0$, and $\Delta_{\boldsymbol{x},y} = -i\Delta_2 - i\Delta_3 \cos(2\pi(x+1)/3)$, where $\Delta_3 > \Delta_4 > 0$. Note that the pair fields on the horizontal links of the rightmost two columns in Figures 3.7a and 3.7b do not vanish; they are simply about one to two orders of magnitude smaller than the pair fields on the other links. As in the example of the period-two bidirectional stripe, we identify the CDW order as a daughter order of the striped superconducting order, by virtue of the fact that the the stripe I/II phases persist down to $g = 0$. Aside from the stripe I/II phases, there is a small region of the phase diagram around $(V, g) = (-5, 3)$ which supports a vortex lattice phase and is separated from the other phases by a first order transition. As shown in Fig. 3.7(c), this phase consists of an array of clusters of four high density sites, around which there are circulating currents. As for the topological properties of these states, the stripe I/II phase supports regions with $C = -1, 0, 1$ and $C = 0, -1$, respectively, whereas the vortex lattice phase has Chern number $C = 0$. So, in contrast to the period-two case, non-Abelian phases with the topological orders of the Pfaffian and PH-Pfaffian are present in the period-three phase diagram.

We note that that we are not able to conclusively identify the ground state in the unlabeled grey region of Fig. 3.4(b). Here, several states (with $C = \pm 1$) compete with the stripe I configuration and all are nearly degenerate, up to our chosen numerical precision. This suggests that the system will likely be unstable to

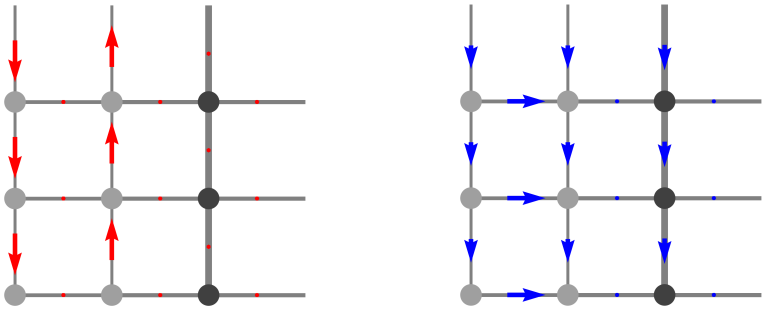

(a) Stripe I

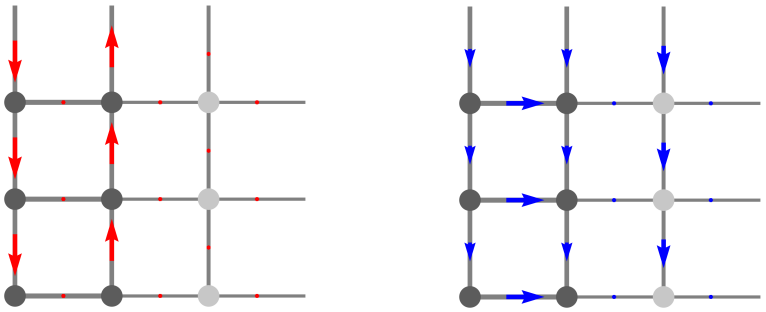

(b) Stripe II

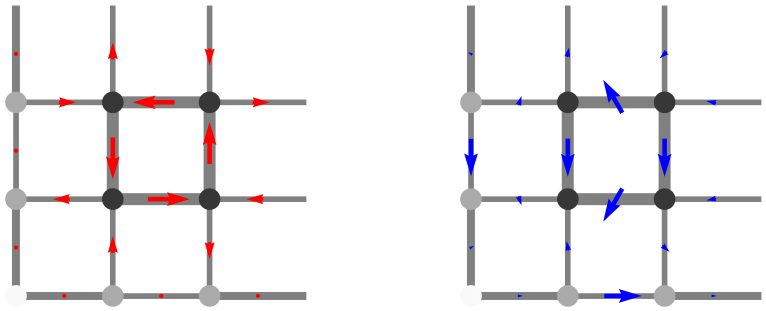

(c) Vortex Lattice

Figure 3.7: Period-three mean-field configurations. For each configuration, the left figure depicts the link currents, j_k, as red arrows, while the right figure depicts the pair fields in the same manner as Fig. 3.5.

phase separation in this regime.

3.4.3 Period Four

Lastly, we have the period-four phase diagram, shown in Fig. 3.4(c), which exhibits the greatest diversity of phases. A unidirectional stripe phase, shown in Fig. 3.8a, occupies most of the the $g \gtrapprox 1$ region. Of note is the fact that it supports a CDW and a BOW in the x-direction with a period of two lattice sites, while the pair field modulation has a period of four sites in the same direction (that is, the pair field pattern returns to itself after four *magnetic* translations). Explicitly, the pair fields on the y-links, $\Delta_{\boldsymbol{x},y}$, possess a uniform $\boldsymbol{q}_1 = (0,0)$ Fourier component and a modulation at wave vector $\boldsymbol{q}_2 = (\pi, 0)$, while the pair fields on the x-links are given by $\Delta_{\boldsymbol{x},x} = \Delta_{\boldsymbol{q}} e^{i\boldsymbol{q}\cdot\boldsymbol{x}} + \Delta_{-\boldsymbol{q}} e^{-i\boldsymbol{q}\cdot\boldsymbol{x}}$, where $\boldsymbol{q} = (\pi/2, 0)$ and $\Delta_{\boldsymbol{q}} = |\Delta| e^{-i\pi/4} = \Delta^*_{-\boldsymbol{q}}$. Note that the appearance of a CDW with half of the period of the pair field modulation is characteristic of PDW states [144]; indeed, the form of $\Delta_{\boldsymbol{x},x}$ is precisely that of a PDW, at least in the chosen gauge. In fact, this unidirectional stripe phase remains a solution of the saddle-point equations down to $g = 0$, and so it indeed owes its existence to finite-momentum pairing of the CFs – the NNN repulsive interactions are needed only to stabilize it as the ground state. Additionally, it is topologically trivial except for a small region of the phase diagram around $(V, g) = (-1.2, 1.2)$, where the BdG bands have $C = -2$. In this regime, the edge of the system supports a chiral boson from the charge sector and two counter-propagating Majorana fermions.

The NNN repulsion also helps stabilize a bidirectional stripe phase, shown in Fig. 3.8(b), in a small region of the phase diagram. This phase possesses CDWs at wave vectors $(0, \pi)$, $(\pi, 0)$, and (π, π) as well as modulations of the bond densities, $B_{\boldsymbol{x},x}$ and $B_{\boldsymbol{x},y}$, at wave vectors $(0, \pi)$ and $(\pi, 0)$, respectively. The pair fields take the form

$$\Delta_{\boldsymbol{x},x} = \tilde{\Delta} + \Delta + (\tilde{\Delta} - \Delta) e^{i\pi y} \tag{3.22}$$

$$\Delta_{\boldsymbol{x},y} = i\tilde{\Delta} \cos(\pi x/2 + \pi/2) + \Delta e^{i\pi y} \cos(\pi x/2), \tag{3.23}$$

with $\tilde{\Delta} > \Delta > 0$. Note that this mean-field configuration is invariant under two *magnetic* translations along both lattice directions, and so the CDW and BOW has the same periodicity as the pair field modulation, in contrast to the unidirectional stripe phase. However, we find that this phase exists as a (metastable) self-consistent mean-field solution at $g = 0$, and so it seems reasonable to view the CDWs and BOWs as daughter orders of the spatially modulated pairing. As far as its topological properties are concerned, this bidirectional stripe phase has Chern number $C = 1$, and so possesses the topological order of the Pfaffian.

In the region below $g \approx 1$, we find competition between various configurations with circulating currents,

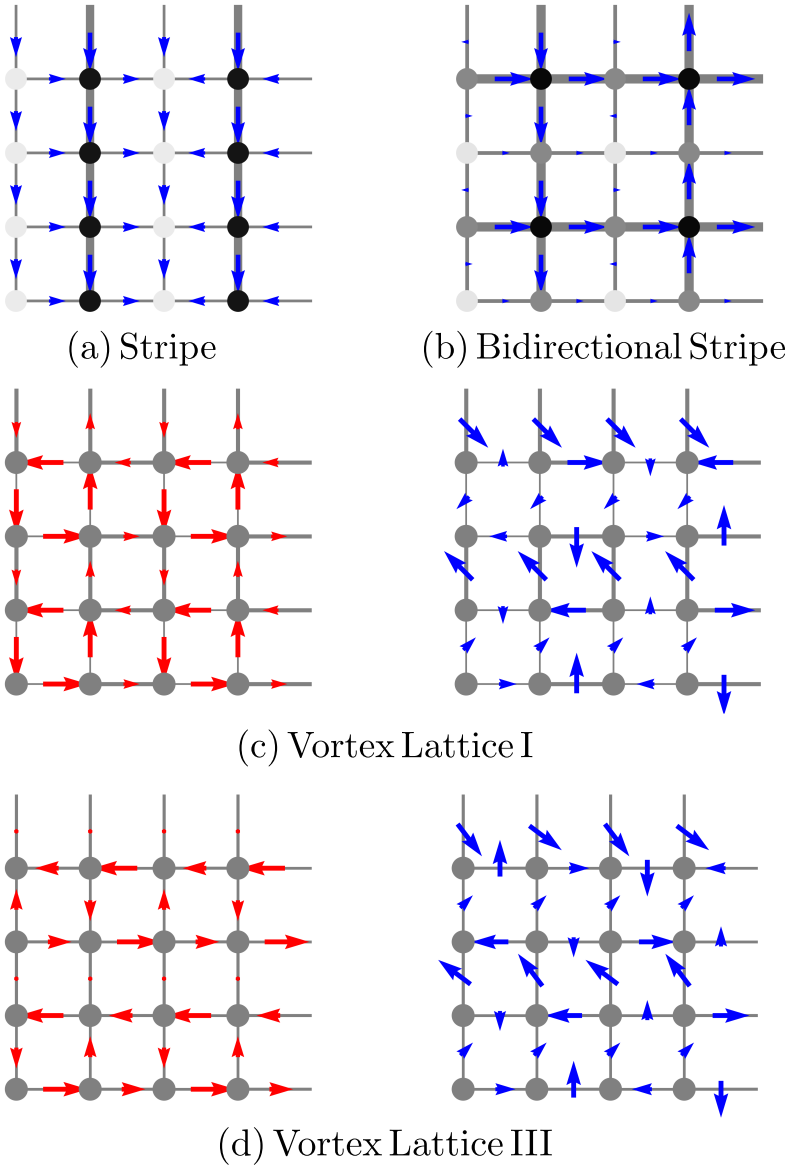

Figure 3.8: Period-four mean-field configurations. The link currents in the stripe configurations (a,b) all vanish.

Table 3.2: Details of the three composite Fermi liquid states for the bosonic system. Here, $2k' - 1$ is the number of attached statistical flux quanta.

	$\phi_0/2\pi$	n	ν	k'	$\phi/2\pi$	$\phi_*/2\pi$
Period two	3/4	1/4	1/3	1	1/4	1/2
Period three	2/3	1/9	1/6	2	1/3	1/3
Period four	5/8	1/8	1/5	2	3/8	1/4

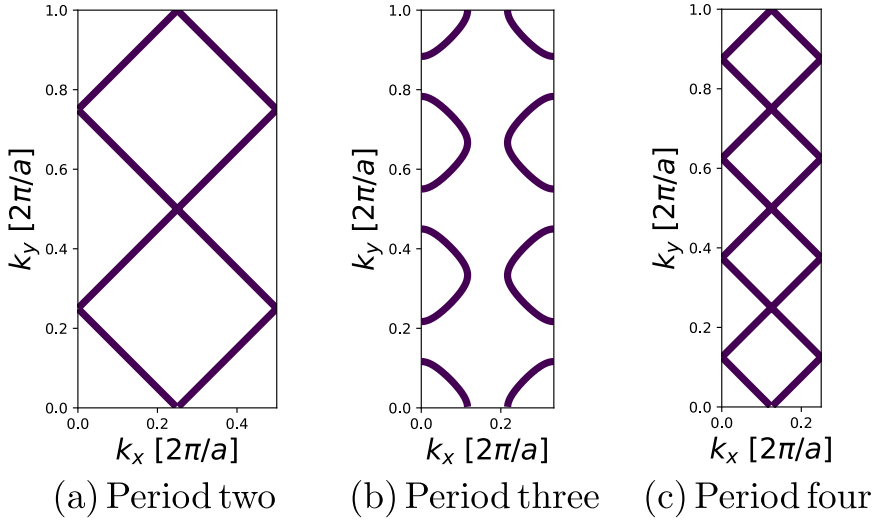

Figure 3.9: Composite Fermi surfaces for the period two, three, and four configurations given in Table 3.2.

which we refer to as vortex lattices. Two examples of these phases are shown in Fig. 3.8(c,d). For $|V| > 2.2$, the ground state is the vortex lattice I phase, which exhibits a square lattice of vortices. It also has $C = -1$, and so supports the same topological order as the PH-Pfaffian. As $|V|$ is lowered, the system transitions through other vortex lattice phases, including that of Fig. 3.8(d), in which there appears to be a triangular lattice of vortices. In the region $|V| \lessapprox 0.8$, marked by the color gray in Fig. 3.4(c), we find competition between several vortex lattice states, one of which has Chern number $C = -2$. These solutions appear to be degenerate (up to numerical precision), suggesting the system will likely be unstable to phase separation. It is thus unclear whether a uniform paired state of CFs can actually be stabilized in this regime, or if a proliferation of vortices will return the system to a composite Fermi liquid.

3.5 Bosonic Paired FCI Phase Diagrams

Thus far, we have considered paired FCI states in a tight-binding model of fermions. In this section, we repeat our analysis for a system of hardcore bosons in the same square-lattice Hofstadter model, which is of

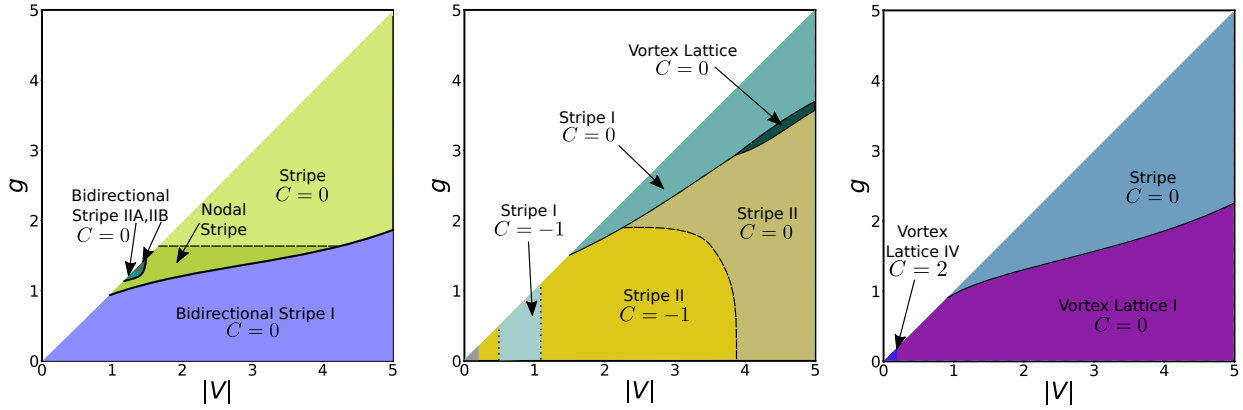

(a) Period two (b) Period three (c) Period four

Figure 3.10: Schematic mean-field phase diagrams as functions of the NN attraction, $|V| = -V$, and NNN repulsion, g for the bosonic configurations listed in Table 3.2. The bidirectional stripe I phase in (a) is the same as the bidirectional stripe phase present in Fig. 3.4(a).

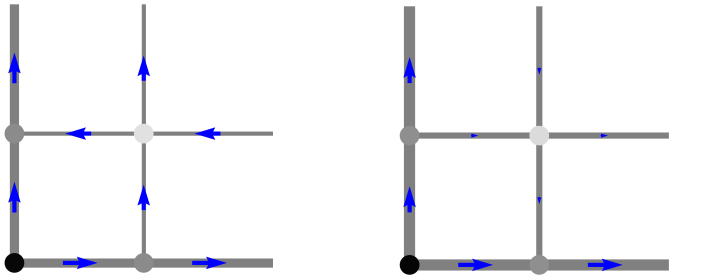

(a) Bidirectional Stripe IIA (b) Bidirectional Stripe IIB

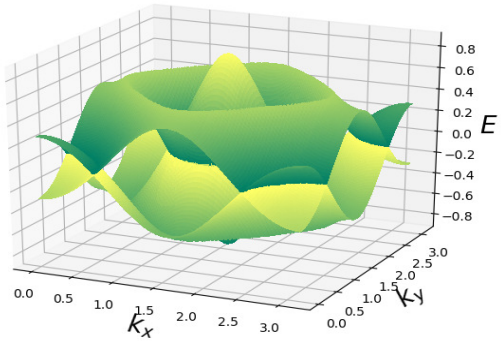

(c) BdG Spectrum

Figure 3.11: Real-space configuration of the bidirectional stripe (a) IIA and (b) IIB phases in the bosonic FCI period-two phase diagram (Fig 3.10a). The link currents vanish in both configurations. (c) The two BdG bands closest to $E = 0$ for IIB (the spectrum for IIA is similar). Despite appearances, there is a very small gap, as the pair fields are non-zero but small.

relevance for cold atom experiments [50–52]. The set-up is the same as that of the fermionic case considered above, with the only difference being that we must attach an odd number of flux quanta to the bosons to obtain a theory of composite fermions. Hence, we must take the Chern-Simons coupling to be

$$\theta = \frac{1}{2\pi(2k'-1)}, \quad k' \in \mathbb{Z}. \tag{3.24}$$

In gapped, paired states of the CFs, vortices of the pair field will thus carry charge $e/(4k'-2)$. We again consider three different configurations of filling and background magnetic flux, as summarized in Table 3.2, such that the composite fermions form Fermi surfaces with two, three, and four pockets, as shown in Fig. 3.9.

Repeating the same mean-field analysis as for the fermionic problem, we obtain the phase diagrams of Fig. 3.10, which exhibit nearly the same topology as the corresponding fermionic phase diagrams. One novel feature is the emergence of the bidirectional stripe IIA and IIB phases in the period-two phase diagram [Fig. 3.10(a)] around $(V, g) = (-1.3, 1.3)$, which support CDWs at wave vectors $(0, \pi)$, $(\pi, 0)$, and (π, π) and BOWs in $B_{\boldsymbol{x},x}$ and $B_{\boldsymbol{x},y}$ at wave vectors $(0, \pi)$ and $(\pi, 0)$, respectively. The real space configuration of these phases are depicted in Fig. 3.11; the differences between IIA and IIB are that, in the former, the $(0, 0)$ component of $\Delta_{\boldsymbol{x},y}$ is greater than the $(\pi, 0)$ component and the $(0, \pi)$ component of $\Delta_{\boldsymbol{x},x}$ is greater than the $(0, 0)$ component, while the opposite statements hold true in the latter. Unlike the other period-two phases, these phases spontaneously breaks TRS since the pair fields on the x-links, $\Delta_{\boldsymbol{x},x}$, are all real while those on the y-links, $\Delta_{\boldsymbol{x},y}$, are imaginary. The pair fields have very small magnitudes, yielding a minute gap which is not easily seen in Fig. 3.11(c). As such, even at low temperatures, the system will exhibit unquantized heat transport mediated by the Bogoliubov quasiparticles through the bulk.

Another new phase seems to appear at small $|V|$ and g in the period four diagram; since the order parameters are so small in this region, it is difficult to conclusively identify the nature of this phase, but we tentatively describe it as a vortex lattice and label it as Vortex Lattice IV. The BdG band structure has $C = 2$, and so this phase is Abelian. We note that a different $C = 2$ paired quantum Hall phase was studied in Ref. [128], which resulted from somewhat similar PDW physics.

3.6 Discussion and Conclusion

In this Chapter, we have presented a qualitative, mean-field picture of the intertwining of symmetry breaking and topological order in FCI states arising from the finite momentum pairing of composite fermions. This is a consequence of magnetic translation symmetry enforcing the presence of multiple composite Fermi pockets.

We find a diverse array of paired states, the most notable of which exhibit some subset of the following observable features:

1. Daughter CDW and/or BOW order arising from the modulated pair fields, similar to that in theories of PDW states in the cuprates.

2. Gapped neutral sectors possessing Chern numbers $C = -2, -1, 0, 1, 2$, resulting in C Majorana edge modes with chirality $\mathrm{sgn}(C)$, in addition to a charged chiral boson. Here, $C = -1, 0, 1$ correspond to the PH-Pfaffian, Halperin paired state, and Pfaffian topological orders, respectively.

3. Gapless neutral sectors, forming quantum Hall thermal semimetals (only the nodal stripe phase in Figures 3.4a and 3.10a possesses this property).

4. The possible trapping of MZMs by lattice dislocations (only the gapped stripe phase in Figures 3.4a and 3.10a possesses this property).

Although the more interesting phases we find occupy small regions of the phase diagram, there is some hope for observing these states in future cold atom experiments, in which the nature of the interactions can be finely tuned. At a minimum, our results demonstrate that the observation of BSO in an experimental setting need not rule out concomitant TO, as their coexistence is in fact a generic scenario in the composite fermion picture. In particular, the CDW patterns we discuss could be directly imaged in cold atom experiments [148].

Looking forward, it may prove interesting to better understand the properties of lattice defects in these systems. In particular, we found a stripe phase in the period-four phase diagram exhibiting a CDW with half the period of the pair field modulation, a feature shared by PDWs. In PDW states, a dislocation of the CDW pattern will require the pair field phase to wind by 2π about the dislocation, trapping a vortex [144]. It is possible that lattice dislocations in this phase, or related paired FCI states, may display similar properties. If the BdG band structure has Chern number C, such vortices would trap C MZMs and would provide a novel way of engineering non-Abelian defects in a manner distinct from previous proposals [35, 149].

Coupled wire constructions [147, 150–152] may also provide a means by which to demonstrate the existence of the striped states we find beyond mean-field, especially since, by definition, these are anisotropic states. However, while such constructions would allow us to identify regions of the phase diagram in which these states could in principle exist through the fine-tuning of interactions, there is still the issue of phase separation. As we have discussed, there appear to be nearly degenerate vortex lattice solutions in the fermionic period-four phase diagram, suggesting a tendency towards a proliferation of vortices and hence a destruction of superconducting order. Although the more interesting stripe phases can be stabilized, as we have seen, through long range repulsive interactions, such phases are also sensitive to the breaking of

translation symmetry via, for instance, disorder or the harmonic traps used in cold atom experiments. Such features would result in local variations of the density with periods which may be incommensurate with the expected stripe order in a clean system. So, while cold atoms experiments and solid state Moiré systems provide promising platforms in which to search for our proposed finite momentum paired FCI states, there are several physical hurdles which may disfavor the realization of said states.

Chapter 4

Landau-Ginzburg Theories of Non-Abelian Quantum Hall States from Non-Abelian Bosonization

4.1 Introduction

Our attention to this point has been directed towards understanding the novel properties of fractional quantum Hall (FQH) states realized in lattice systems. However, many unresolved questions still remain in the context of FQH states formed by two-dimensional electron gases in the continuum subjected to strong magnetic fields. Many of these loose threads lie in understanding the emergence of *non-Abelian* FQH states and it is this question we task ourselves with addressing in this and the following two Chapters of this thesis. Indeed, despite the success over the past several decades in understanding the Abelian FQH states, an understanding of the dynamics which can lead to non-Abelian FQH states has remained elusive, as such states cannot arise directly from the application of flux attachment, which is by definition Abelian. For example, while it is believed that the observed $\nu = 5/2$ FQH plateau is a non-Abelian state arising from composite fermion pairing [61], the origin and nature of the pairing instability leading to this state continues to be debated, with seemingly contradictory results between experiment and numerics [9,153–156]. Nevertheless, assuming a particular pairing channel, the non-Abelian Pfaffian phase appears quite naturally, as we outlined in Chapter 1 [1,61].

Unfortunately, this physical picture does not appear to translate simply to the other proposed non-Abelian states, such as the Read-Rezayi (RR) states [65]. Wave functions for these states can be constructed using conformal field theory (CFT) techniques [1], but it is not clear which of these states can be obtained starting from a (physically motivated) field theory of composite particles. To make matters worse, the wave functions for generic non-Abelian states are typically characterized by clustering of more than two particles [65, 157]. Naïvely, from perturbative scaling arguments, such states could not arise unless the clusters with fewer particles are disallowed by symmetry. Most theories of interest do not appear to have such a symmetry, implying that non-perturbatively strong interaction effects are required to give rise to such

This Chapter is adapted from Hart Goldman, Ramanjit Sohal, and Eduardo Fradkin, Landau-Ginzburg theories of non-Abelian quantum Hall states from non-Abelian bosonization, Phys. Rev. B **100**, 115111 (2019). This paper is also cited as Ref. [17] in this thesis.

states. While we note that projective/parton constructions can be used to formulate effective bulk theories of non-Abelian states [158–160], in such constructions the electron operator is fractionalized by hand, and it must be taken by fiat that the fractionalized degrees of freedom are deconfined. Consequently, although the projective approach can formally generate many candidate states, it does not shed much light on their dynamical origin.

Recent progress in the study of non-Abelian Chern-Simons-matter theories in their large-N ("planar") limit [66, 67] has led to the proposal of non-Abelian Chern-Simons-matter theory dualities by Aharony [68], which take the shape of level-rank dualities. Along with the Abelian web of dualities they imply [161, 162], these dualities constitute tools with which it may be possible to make non-perturbative progress on the above problem. Such dualities can relate theories of Abelian composite particles to theories of non-Abelian monopoles, and they have led to progress on several important problems in condensed matter physics [124, 163–170]. Of particular importance for us, pairing deformations of a dual non-Abelian theory can lead to non-Abelian topological phases which appear inaccessible to the original Abelian theory, in which this pairing corresponds to a highly non-local product of monopole operators.

In this Chapter, our strategy will be to use these non-Abelian dualities to begin to map the landscape of non-Abelian topological phases accessible from a "composite particle" picture, by way of "projecting down" from a multi-layer parent Abelian state. This type of approach, in which the transition to the non-Abelian phase can be physically interpreted as being driven by interlayer tunneling [61, 171–177] or pairing [69, 178], has formed the foundation of several lines of attack on the non-Abelian FQH problem. Such projections have been implemented at the formal level of the edge CFT ("ideal") wave function [179, 180] and in coupled wire constructions [70, 152]. Numerical studies of bilayer systems have also lent support to this idea [181–187]. However, a robust bulk LG description of generic non-Abelian FQH states continues to be lacking. In one major attempt to fill this gap, the authors of Ref. [178] constructed a non-Abelian LG theory for a subset of the bosonic RR states by considering layers of $\nu = \frac{1}{2}$ (bosonic) Laughlin states. Using the well-known level-rank duality of the (gapped) bulk Chern-Simons topological quantum field theory (TQFT) [188–190] (see Ref. [2] for a review), the authors motivated a description of these states involving $SU(2)$ Chern-Simons gauge fields coupled to scalar matter in the adjoint (matrix) representation, obtaining the non-Abelian QH state by pairing across the different layers. In this approach, the anyon content of the non-Abelian state is furnished by the vortices of the pairing order parameter. While this construction is conceptually appealing, it does not originate from a duality satisfied by the parent Abelian LG theory, which describes a quantum critical point, but, rather, a duality satisfied only deep in the gapped Abelian FQH phase. Moreover, in order to give the anyons electric charge in this approach, it is necessary for the external electromagnetic field

to couple to the $U(1)$ subgroup of the full non-Abelian gauge group, explicitly breaking the larger gauge invariance.

Using the non-Abelian bosonization dualities, we construct LG theories of the full bosonic RR sequence at filling fractions $\nu = k/(kM+2)$, $k, M \in \mathbb{Z}$, which do not suffer from these problems. These theories are obtained by starting with k layers of $\nu = 1/2$ bosonic QH states, using the dualities to obtain a LG theory of non-Abelian composite bosons, and attaching M fluxes to the resulting theory. For example, we obtain a LG theory of the bosonic $\nu = 1$ Moore-Read state consisting of two layers of bosons ϕ_n, $n = 1, 2$, which we call the "composite vortices," each at their Wilson-Fisher fixed point and coupled in the *fundamental* representation to a $SU(2)$ gauge field a_n,

$$\mathcal{L} = \sum_{n=1}^{2} \left[|D_{a_n - A\mathbf{1}/2}\, \phi_n|^2 - |\phi_n|^4 + \frac{1}{4\pi} \mathrm{Tr} \left(a_n da_n - \frac{2i}{3} a_n^3 \right) \right] - \frac{1}{4\pi} AdA \,. \tag{4.1}$$

where $D_{a_n - A\mathbf{1}/2} = \partial - i(a_n^b t^b - A\mathbf{1}/2)$ is the covariant derivative, we use the notation $AdB = \varepsilon^{\mu\nu\lambda} A_\mu \partial_\nu B_\lambda$, $t^b = \sigma^b/2$ are the $SU(2)$ generators, and $\mathbf{1}$ is the 2×2 identity matrix. We use the notation $-|\phi|^4$ to denote tuning to the Wilson-Fisher fixed point. Although the gauge fields a_n are non-Abelian, the topological phase accessed by simply gapping out the composite vortices will only support excitations with *Abelian* statistics. For a $SU(N)$ gauge group, non-Abelian statistics require the presence of a Chern-Simons term at level greater than one. To obtain the non-Abelian FQH state, we condense clusters of the non-Abelian composite vortices across the layers (see Fig. 4.1), in this case condensing $\phi_1^\dagger \phi_2$ without condensing ϕ_1, ϕ_2 individually. This Higgses the linear combination $a_1 - a_2$ of the $SU(2)_1$ gauge fields, causing the bilayer $SU(2) \times SU(2)$ gauge group to be broken down to its diagonal $SU(2)$ subgroup. The Chern-Simons levels of the resulting gapped phase add, leading to the desired $SU(2)_2$ Chern-Simons theory at low energies (the subscript refers to the Chern-Simons level). We will show below that the composite vortices individually have the proper quantum numbers to fill out the anyon spectrum of the theory. The clarity of the topological content of the non-Abelian states is a general advantage of the bosonic LG approach. However, alternative descriptions of non-Abelian FQH states involving dual non-Abelian composite *fermions* are also possible. We describe this complementary perspective in Chapter 6.

In addition to the the RR states, by considering N_f-component generalizations of the Halperin (2,2,1) spin-singlet states on each layer, we are able to generalize this approach to construct bulk LG descriptions of generalized non-Abelian $SU(N_f)$-singlet (NASS) states at fillings [70, 191],

$$\nu = \frac{kN_f}{N_f + 1 + kMN_f} \,, \qquad k, N_f, M \in \mathbb{Z} \,, \tag{4.2}$$

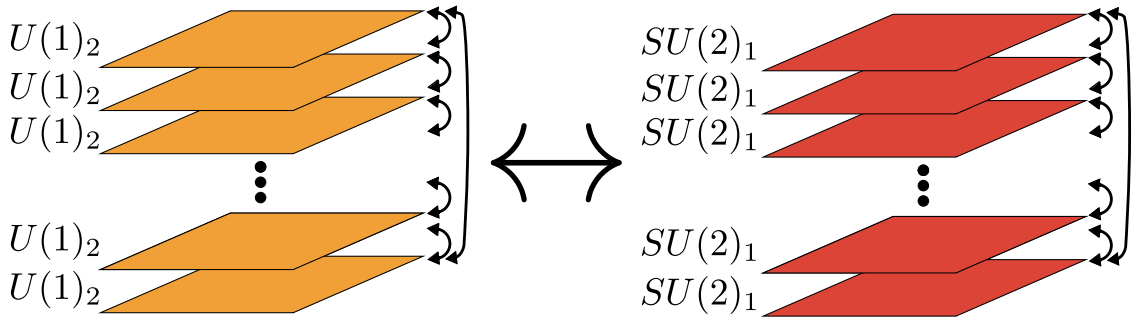

Figure 4.1: A schematic of our construction of LG theories for the RR states. k copies of the $\nu = \frac{1}{2}$ Laughlin state coupled to scalars (left) are dual to k copies of $SU(2)_1$ coupled to scalars (right). The $SU(2)_k$ Read-Rezayi states are obtained in the dual, non-Abelian language via pairing of the layers, represented by double-headed arrows. In the original Abelian theory, these correspond to non-local, monopole interactions.

which are bosonic (fermionic) for M even (odd). These states generalize the clustering properties of the RR states to N_f-component systems and, as their name suggests, are singlets under $SU(N_f)$ rotations. Indeed, for $N_f = 1$, these states reduce to the RR states while for $N_f = 2$, they describe the non-Abelian spin singlet (also NASS) states of Ardonne and Schoutens [69, 192]. These generalized NASS states morally possess $SU(N_f{+}1)_k$ topological order, and so support anyons obeying the fusion rules of Gepner parafermions [193], generalizations of the $\mathbb{Z}_k$ parafermions [194] found in the RR states. Although the physical relevance of an N_f-component FQH state may seem dubious for larger values of N_f, the generalized NASS states provide candidate ground states in systems of cold atoms [191, 195] and fractional Chern insulators [36]. In building LG theories of these states, we find a new duality relating (A) N_f Wilson-Fisher bosons coupled to $U(1)$ Chern-Simons gauge fields with Lagrangian given by the N_f-component generalization of the Halperin $(2, 2, 1)$ K-matrix theory to (B) a $SU(N_f + 1)_1$ Chern-Simons theory coupled to N_f Wilson-Fisher bosons in the fundamental representation. This non-Abelian dual description makes manifest the emergent $SU(N_f)$ global symmetry and reflects the fact that the edge theory of the N_f-component $(2, 2, 1)$ state supports an $SU(N_f + 1)_1$ Kac-Moody algebra.

The remainder of this Chapter is organized as follows. We begin in Section 4.2 by elaborating on the motivation for our construction both from the perspective of wave functions and that of the earlier Landau-Ginzburg approach of Ref. [178]. We then proceed to our analysis in Section 4.3 of the RR states using non-Abelian bosonization, resolving the lingering issues of the LG construction of Ref. [178]. We then extend our construction to the generalized NASS states in Section 4.4. Future directions are discussed in Section 4.5.

4.2 "Projecting Down" to Non-Abelian States

4.2.1 Perspective from the Boundary: Wave Functions and their Symmetries

If we wish to construct a LG description of non-Abelian FQH states involving pairing between Abelian states, it is first necessary to identify which Abelian states to pair. Such states can be motivated by considering "ideal" wave functions. These can be constructed from certain correlation functions, known as conformal blocks, of the edge CFT. In this language, the strategy of obtaining non-Abelian states from parent Abelian states through "projecting down" is well established [179].

Consider for example the bosonic RR states at $\nu = k/2$. The ideal wave functions of these states are defined as the ground states of ideal $k+1$-body Hamiltonians, which can be shown to be given by the conformal blocks of the $SU(2)_k$ Wess-Zumino-Witten (WZW) CFT [65]. This tells us that the RR wave functions describe FQH states with edges governed by $SU(2)_k$ WZW theories [1], corresponding in the bulk to a $SU(2)_k$ Chern-Simons gauge theory [99]. A natural way to obtain the ideal wave functions for the $\nu = k/2$ RR states uses the state with $k = 1$ – the $\nu = 1/2$ bosonic Laughlin state, which is Abelian – as a building block [179]. This state is described by the wave function

$$\Psi_{1/2}(\{z_i\}) = \prod_{i<j}(z_i - z_j)^2 e^{-\frac{1}{4}\sum_i |z_i|^2}, \tag{4.3}$$

where $z_j = x_j + iy_j$ denotes the complex coordinates of the j^{th} particle (a boson). The $\nu = k/2$ RR wave functions may be obtained from this one by "clustering" bosons across k copies of this state. This corresponds to taking $N = km$ bosons, dividing them into k groups, writing down a $\nu = \frac{1}{2}$ Laughlin wave function for each group, multiplying them together, and then symmetrizing over all possible assignments of bosons to groups. The resulting wave function is represented as

$$\Psi_k(\{z_i\}) = \mathcal{S}_k \left[\prod_{i=0}^{k-1} \Psi_{1/2}(z_{1+iN/k}, \ldots, z_{(i+1)N/k}) \right], \tag{4.4}$$

where $\mathcal{S}_k$ denotes symmetrization. It can be shown that this wave function is equivalent to that first proposed by Read and Rezayi [65] and exhibits the correct clustering properties: the wave function does not vanish unless the coordinates of $k+1$ bosons coincide. The RR wave functions for general k and M are obtained by multiplying Eq. (4.4) by a $\nu = \frac{1}{M}$ Laughlin factor.

The relation between the $k = 1$ and the $k > 1$ RR wave functions suggests that it should be possible to construct such a LG theory by considering k copies of the effective theory of the (*Abelian*) $k = 1$ state, the first attempt at which we describe in the next subsection. That a state with $SU(2)_k$ topological order

can be obtained from the Abelian $\nu = \frac{1}{2}$ Laughlin state is also made plausible by the fact that the latter has an alternative description as an $SU(2)_1$ Chern-Simons theory. This is a consequence of the level-rank duality between $U(1)_2$ and $SU(2)_1$, which is reflected in the above description by the fact that the $\nu = \frac{1}{2}$ wave function can be obtained from the $SU(2)_1$ WZW CFT [70, 178, 196, 197]. We review this level-rank duality in the subsection below.

4.2.2 Perspective from the Bulk: Early LG Theories from Level-Rank Duality

To approach the problem of constructing a bulk description of the Read-Rezayi states, the authors of Ref. [178] sought to obtain a non-Abelian Landau-Ginzburg theory of the $\nu = k/2$ RR states by also considering k layers of $\nu = 1/2$ bosonic Laughlin states, or $U(1)_2$ Chern-Simons theories and recognizing that each $U(1)_2$ theory is level-rank dual to a $SU(2)_1$ theory. They therefore conjectured that an alternate LG description was possible, one involving scalar matter coupled to $SU(2)_1$ gauge fields. These scalars could then pair and lead to the symmetry breaking pattern,

$$SU(2)_1 \times \cdots \times SU(2)_1 \to SU(2)_k \,. \tag{4.5}$$

What remained was to (1) determine how the scalars transformed under $SU(2)$ and how they coupled to the physical background electromagnetic (EM) field, and (2) determine precisely how to pair these fields to obtain non-Abelian states.

For simplicity, we consider first the case of $k = 2$, a bilayer of $\nu = 1/2$ bosonic FQH liquids. This will constitute a parent state for the $\nu = 1$ bosonic Moore-Read state. To motivate the level-rank duality to a non-Abelian representation, we again consider the edge physics. The edge theory of the $U(1)_2$ state is one of a chiral boson,

$$\mathcal{L}_{\text{edge}} = \frac{1}{4\pi\nu}\, \partial_x\varphi \left(\partial_t\varphi - v\partial_x\varphi\right), \tag{4.6}$$

where φ has compactification radius $R = 1$ and $\nu = 1/2$. The charge density is therefore $\rho = \frac{1}{2\pi}\partial_x\varphi$. The local particles (i.e. the physical bosons) of this theory are represented by the vertex operators,

$$\psi_1 = e^{i\varphi/\nu}. \tag{4.7}$$

In addition, the theory hosts anyonic quasiparticles, which are semions of charge $1/2$ and correspond to the vertex operators

$$\psi_{1/2} = e^{i\varphi}\,. \tag{4.8}$$

The $\psi_1, \psi_1^\dagger$, and ρ operators all have the same scaling dimension and furnish a $SU(2)_1$ Kac-Moody algebra. This is a manifestation of the level-rank duality at the level of the edge CFT, and we can write the bulk theory on each layer as a $SU(2)_1$ gauge theory with gauge field $a_\mu = a_\mu^b t^b$, where t^b are the generators of $SU(2)$. Importantly, the ρ operator appears as the diagonal generator of $SU(2)$. Therefore, the authors guessed that in the LG theory the background EM field couples through a BF term to the Cartan component of the bulk $SU(2)$ gauge field[1],

$$\mathcal{L}_{\text{EM}}[a^a, A] = \frac{1}{2\pi}\varepsilon^{\mu\nu\lambda} A_\mu \partial_\nu a_\lambda^3 \,. \tag{4.9}$$

This explicitly breaks gauge invariance and would indicate that the physical EM current is not conserved. We will eventually see in Section 4.3 that the new dualities will allow us to avoid this difficulty by granting us a gauge invariant way of coupling to the background electromagnetic field.

From this discussion, a natural guess for the matter variables for the bulk LG theory is a $SU(2)$ triplet on each layer consisting of boson creation and annihilation operators $B_n, B_n^\dagger$ and a boson number operator B_n^3 which essentially corresponds to the EM charge. Here $n = 1, 2$ is a layer index. If we write $B_n = B_n^1 + iB_n^2$ with $B_n^{1,2}$ real, the adjoint field B_n^a transforms like a vector under $SO(3)$. It is important to note, however, that any non-Abelian LG theory should be thought of as describing a (UV) quantum critical point proximate to the (IR) FQH state which shares universal features with the Abelian theory we started with. Since the level-rank duality is invoked deep in the FQH phase, it is a guess that these variables are the proper degrees of freedom at the UV quantum critical point (they may be alternatively understood as bound states – we will see later on that this interpretation is more accurate). Nevertheless, pairing these fields will lead to both the desired symmetry breaking pattern (4.5) as well as the existence of solitons with non-Abelian statistics.

The LG theory for the pairing of these fields can be explicitly constructed as follows. Each layer consists of a B_n^a field minimally coupled to its own $SU(2)_1$ gauge field,

$$\mathcal{L}_0[B_n, a_n] = \sum_{n=1,2} \left(|D_{a_n} B_n|^2 + \frac{1}{4\pi} \operatorname{Tr}\left[a_n da_n - \frac{2i}{3} a_n^3 \right] \right) + \cdots \,, \tag{4.10}$$

where we have suppressed Lorentz and $SU(2)$ indices, used the notation $AdC = \varepsilon^{\mu\nu\lambda} A_\mu \partial_\nu C_\lambda$, and defined the covariant derivative $D_{a_n} B_n \equiv \partial B_n^a - i\varepsilon^{abc} a_n^b B_n^c$. The ellipsis refers to additional contact terms, Maxwell terms, etc. These are set up so that, taken individually, when each layer is at filling $\nu = 1/2$, the diagonal color flux $b_I^3 = \langle f_{I,xy}^3 \rangle / 2\pi$, vanishes.

Although the B_n fields are bosons, we assume that they do not condense. Rather, we consider pairing them using a method analogous to that of Jackiw and Rossi [198], who considered pairing Dirac fermions by

[1]Note that, depending on context, we use a^3 to denote both the diagonal element of a as well as $a \wedge a \wedge a$.

coupling them to a scalar order parameter which mediates the pairing interaction. Let us introduce a field $\mathcal{O}^{ab}$ which transforms as an adjoint under each layer's $SU(2)$, $\mathcal{O} \mapsto G_1^{-1}\,\mathcal{O}\,G_2$, where $G_1, G_2 \in SO(3)$. Here we have used the fact that, as an adjoint field, $\mathcal{O}$ is blind to the $\mathbb{Z}_2$ centers of the two $SU(2)$ factors, and so effectively transforms under $SU(2)/\mathbb{Z}_2 \cong SO(3)$. The field $\mathcal{O}$ mediates a pairing interaction between the B_I^a fields as follows,

$$\mathcal{L}_{\text{pair}} = \lambda\, B_1^a \mathcal{O}^{ab} B_2^b\,. \tag{4.11}$$

We now require that $\mathcal{O}$ acquires a vacuum expectation value (VEV), which breaks $SU(2) \times SU(2)$ down to its diagonal subgroup $SU(2)_{\text{diag}}$, implementing the constraint $a_1 = a_2$. Any VEV equivalent to $\langle \mathcal{O} \rangle \propto \delta^{ab}$ is sufficient to achieve this. Therefore, in the final IR theory, the CS terms for a_1 and a_2 add, yielding a $SU(2)_2$ CS term, which describes precisely the $\nu = 1$ bosonic Moore-Read state. The authors of Ref. [178] then argued that, since the order parameter is valued on $[SO(3) \times SO(3)]/SO(3)$, that it can host non-trivial vortices which furnish the anyon content. This is in contrast to if we had chosen to pair fields in the fundamental representation, for which the order parameter has no non-trivial vortices. Finally, we note that because $\mathcal{O}$ is blind to the centers of the two original $SU(2)$ factors, the final gauge group is in fact $SU(2)_{\text{diag}} \times \mathbb{Z}_2$. This means that the resulting topological order is not quite that of the $\nu = 1$ bosonic Moore-Read state. We will elaborate on this point as well as the interpretation of the vortices in Section 4.3.3.

In spite of its successes, the LG theory described here has several problems. As mentioned above, the BF coupling between a_n^3 and the EM field A explicitly breaks the $SU(2)$ gauge symmetry. In addition, the theory of adjoint fields (4.10) cannot be the same as the Abelian LG theory of the original layers – the theories have different phase diagrams and so do not represent the same fixed point. Moreover, the final gauge group after pairing is not just $SU(2)$ but includes additional discrete gauge group factors. Finally, it is not entirely obvious how to generalize this approach to the rest of the Read-Rezayi states and beyond. In the work presented in this Chapter, using non-Abelian boson-fermion dualities, we repair all of these problems.

4.3 LG Theories of the RR States from Non-Abelian Bosonization

4.3.1 Setup

Our setup for obtaining LG theories of the RR states is depicted in Figure 4.1. We again consider k layers of bosonic quantum Hall fluids at $\nu = 1/2$. The standard LG theory [13] of these states consists of Wilson-Fisher bosons – the Laughlin quasiparticles – on each layer, denoted Φ_n, with $n = 1, \cdots, k$ being the layer index. Each of these fields is coupled to an *Abelian* $U(1)_2$ Chern-Simons gauge field a_n as follows (the total gauge group is $[U(1)]^k$),

$$\mathcal{L}_A = \sum_n \left(|D_{a_n} \Phi_n|^2 - |\Phi_n|^4 + \frac{2}{4\pi} a_n da_n + \frac{1}{2\pi} A da_n \right) . \tag{4.12}$$

where again $-|\Phi|^4$ denotes tuning to the Wilson-Fisher fixed point and $D_{a_n} = \partial - i a_n$ is the covariant derivative. Since we wish to impose particle-hole symmetry on the bosons in the FQH state, these theories are relativistic. We take the background EM field A_μ to couple to the sum of the global $U(1)$ currents on each layer $j_{\text{top}} = \frac{1}{2\pi} \sum_n da_n$, although we could have in principle coupled background fields to each of these currents individually [14]. Notice that there is no continuous flavor symmetry manifest in $\mathcal{L}_A$ since each Φ_n couples to its own gauge field a_n. Being a theory of Laughlin quasiparticles, the Abelian quantum Hall state arises when the Φ fields are gapped, or $\rho_\Phi = \sum_{I,n} \langle i(\Phi_n^\dagger \overleftrightarrow{D}_{a_n,t} \Phi_n) \rangle = 0$. We note here that throughout this Chapter we define the filling fraction with a minus sign $\nu = -2\pi\rho_e/B$, where ρ_e is the physical EM chage and B is the background magnetic field.

We call the Abelian theory whose Lagrangian $\mathcal{L}_A$ is shown in Eq. (4.12), **Theory A**. In order to obtain a non-Abelian $SU(2)_k$ theory, our strategy is to invoke a non-Abelian duality to trade $\mathcal{L}_A$ for a theory of k bosons which are charged under emergent non-Abelian gauge fields. Since these particles are non-Abelian analogues of the Laughlin quasiparticles (they are *gapped* in the Abelian QH state), we will refer to them as non-Abelian composite *vortices*. Indeed, we will see that these theories are the k-component generalizations of the theory of Eq. (4.1). We call this non-Abelian theory **Theory B**. By pairing these fields across the layers, we will obtain the final $SU(2)_k$ theory. Thus, the non-Abelian FQH states we obtain can be interpreted as clustered states of the dual non-Abelian composite vortices, in analogy to the clustering interpretation of the wave functions. Moreover, from products of the non-Abelian vortex fields, analogues of the adjoint B_n operators of Section 4.2 can be constructed and paired, leading to a "quartetted" non-Abelian state. We now turn to a procedure for obtaining these dualities.

4.3.2 A Non-Abelian Duality: $U(1)_2$ + bosons $\longleftrightarrow$ $SU(2)_1$ + bosons

The non-Abelian dualities presented by Aharony [68] relate Chern-Simons theories coupled to complex scalar fields at their Wilson-Fisher fixed point to dual Chern-Simons theories coupled to Dirac fermions,

$$N_f \text{ scalars} + U(N)_{k,k} \quad \longleftrightarrow \quad N_f \text{ fermions} + SU(k)_{-N+N_f/2}\,, \tag{4.13}$$

$$N_f \text{ scalars} + SU(N)_{k} \quad \longleftrightarrow \quad N_f \text{ fermions} + U(k)_{-N+N_f/2,-N+N_f/2}\,, \tag{4.14}$$

$$N_f \text{ scalars} + U(N)_{k,k+N} \quad \longleftrightarrow \quad N_f \text{ fermions} + U(k)_{-N+N_f/2,-N-k+N_f/2}\,, \tag{4.15}$$

where all matter is in the *fundamental* representation of the gauge group. These take the shape of level-rank dualities, but a crucial difference is that they relate critical theories of matter coupled to Chern-Simons gauge fields rather than gapped TQFTs. Across these dualities, baryons of the $SU(k)_{-N}$ theories are mapped to monopoles of the $U(N)_k$ theories. We list our conventions for the non-Abelian Chern-Simons gauge fields in Appendix F.

Using these dualities as building blocks, it is possible to obtain new dualities relating the Abelian **Theory A** to a non-Abelian **Theory B**. The dualities obtained in this section are described in Refs. [199, 200], although we show in Section 4.4 that new, more general dualities can be obtained with an analogous strategy. To begin, let us consider the case of a single layer $k = 1$ of bosons at $\nu = 1/2$. The Landau-Ginzburg theory for this state consists of Wilson-Fisher bosons Φ coupled to a $U(1)_2$ gauge field a,

$$\mathcal{L}_A = |D_a\Phi|^2 - |\Phi|^4 + \frac{2}{4\pi}ada + \frac{1}{2\pi}Ada\,. \tag{4.16}$$

We start by invoking an Abelian boson-fermion duality, Eq. (4.14) with $N = k = 1$, which relates a Wilson-Fisher boson to a Dirac fermion with a unit of flux attached [161, 162],

$$|D_A\Phi|^2 - |\Phi|^4 \longleftrightarrow i\overline{\psi}\not{D}_b\psi - \frac{1}{2}\frac{1}{4\pi}bdb + \frac{1}{2\pi}bdA - \frac{1}{4\pi}AdA\,, \tag{4.17}$$

where b is a new dynamical $U(1)$ gauge field[2] . Applying this duality to $\mathcal{L}_A$ by treating a as a background field, one obtains **Theory C**,

$$\mathcal{L}_A \longleftrightarrow \mathcal{L}_C = i\overline{\psi}\not{D}_b\psi - \frac{1}{2}\frac{1}{4\pi}bdb + \frac{1}{4\pi}ada + \frac{1}{2\pi}ad(b+A)\,. \tag{4.18}$$

We can integrate out a without violating the Dirac quantization condition: its equation of motion is simply

[2]Throughout this Chapter, we approximate the Atiyah-Patodi-Singer η-invariant by a level-1/2 Chern-Simons term and include it in the action.

$-da = db + dA$. Thus,

$$\mathcal{L}_A \longleftrightarrow \mathcal{L}_C = i\overline{\psi}\not{D}_b\psi - \frac{3}{2}\frac{1}{4\pi}bdb - \frac{1}{2\pi}bdA - \frac{1}{4\pi}AdA\,. \tag{4.19}$$

Theory C was motivated as a description of the $\nu = 1/2$ FQH-insulator transition in Ref. [201]. The duality (4.19) is a special case of more general Abelian dualities described (and derived) in Refs. [202,203]. However, of those dualities, it is one of the unique ones for which the Chern-Simons level is properly quantized. Notice also that this is the duality (4.15) with $N_f = N = k = 1$. The reason that we took a detour through the Abelian duality will become apparent in Section 4.4.

Applying the duality of Eq. (4.14) to **Theory C**, we obtain **Theory B**, which consists of bosons ϕ coupled to a $SU(2)_1$ gauge field u,

$$\mathcal{L}_A \longleftrightarrow \mathcal{L}_B = |D_{u-A\mathbf{1}/2}\phi|^2 - |\phi|^4 + \frac{1}{4\pi}\,\mathrm{Tr}\left[udu - \frac{2i}{3}u^3\right] - \frac{1}{2}\frac{1}{4\pi}AdA\,, \tag{4.20}$$

where $\mathbf{1}$ denotes the 2×2 identity matrix. Like its Abelian dual, Eq. (4.16), this theory describes a quantum phase transition between a $\nu = 1/2$ bosonic Laughlin state (gapped ϕ – the topological sector is decoupled) and a trivial insulator (condensed ϕ). Across this duality, the monopole current of **Theory A** is related to the baryon number current of **Theory B**,

$$\frac{\delta\mathcal{L}_A}{\delta A} = \frac{da}{2\pi} \longleftrightarrow \frac{\delta\mathcal{L}_B}{\delta A} = -\frac{i}{2}\,\phi^\dagger \overleftrightarrow{D}_{u-A\mathbf{1}/2}\,\phi - \frac{1}{2}\frac{dA}{2\pi} \tag{4.21}$$

Both of these currents correspond to the physical EM charge current J_e. We have suppressed Lorentz indices for clarity.

We can check explicitly that the $\nu = 1/2$ state has particle-hole symmetry in the composite vortex variables of **Theory B**. The physical EM charge density corresponds to the zeroth component of the currents (4.21),

$$\rho_e = \langle J_e^0\rangle = -\frac{1}{2}\,\rho_\phi - \frac{1}{2}\frac{B}{2\pi}\,, \tag{4.22}$$

where ρ_ϕ denotes the number density of the non-Abelian composite vortices, so, when $\rho_\phi = 0$, the filling fraction is

$$\nu = -2\pi\frac{\rho_e}{B} = \frac{1}{2}\,. \tag{4.23}$$

This means that the $\nu = 1/2$ bosonic Laughlin state can be thought of as a gapped, particle-hole symmetric phase of non-Abelian composite vortices just as well as Abelian ones! By copying this duality k times, we

will see in the next subsection how to obtain a non-Abelian LG theory of the RR states.

By applying the duality of Eq. (4.13) with $N = 1$ and $k = 2$ to **Theory A**, it is also possible to obtain a non-Abelian fermionic **Theory D** with gauge group $SU(2)_{-1/2}$. However, in this Chapter we focus on the non-Abelian bosonic LG theories, since in these theories the nature of the topological order and anyon content are manifest. Understanding the emergence of the RR states and other non-Abelian FQH states from the perspective of these non-Abelian composite fermion theories forms the subject of Chapter 6. Combining all of these dualities, we see that

$$\begin{array}{c} \textbf{Theory A:}\ \text{a scalar} + U(1)_2 \longleftrightarrow \textbf{Theory D:}\ \text{a fermion} + SU(2)_{-1/2} \\ \updownarrow \\ \textbf{Theory C:}\ \text{a fermion} + U(1)_{-3/2} \longleftrightarrow \textbf{Theory B:}\ \text{a scalar} + SU(2)_1\,. \end{array} \tag{4.24}$$

It is a miracle of arithmetic that, like the boson/fermion dualities, the boson/boson and fermion/fermion dualities above also have the flavor of level-rank dualities. Indeed, it is easy to show that the topological phases of these theories are all dual to one another [199]. This can be thought of as a consequence of the fact that we were able to integrate out the gauge field a above without violating flux quantization. It is an interesting question to ask whether there are more general dualities which exhibit the same miracle. We will show that this is indeed the case in Section 4.4. We finally note that the dualities of Eq. (4.24) also have the feature of hosting an emergent $SO(3)$ global symmetry, a consequence of the fact $SU(2) \simeq USp(2)$ [204,205]. This symmetry is manifest upon rewriting the theory in the $USp(2)$ language, which involves replacing the single complex matter field with two (pseudo)real ones [206].

4.3.3 Building Non-Abelian States from Clustering

Equipped with the duality (4.20), we now revisit the construction of Ref. [178], which we described in Section 4.2.2. We again start by considering the case where **Theory A** consists of $k = 2$ layers of $U(1)_2$ LG theories,

$$\mathcal{L}_A = \sum_n \left(|D_{a_n}\Phi_n|^2 - |\Phi_n|^4\right) + \frac{2}{4\pi} a_n da_n + \frac{1}{2\pi} A d(a_1 + a_2)\,, I = 1, 2\,. \tag{4.25}$$

Invoking Eq. (4.20), **Theory B** is two $SU(2)_1$ theories,

$$\mathcal{L}_B = \sum_n \left(|D_{u_n - A\mathbf{1}/2}\phi_n|^2 - |\phi_n|^4\right) + \frac{1}{4\pi}\sum_n \mathrm{Tr}\left[u_n du_n - \frac{2i}{3}u_n^3\right] - \frac{1}{4\pi} A dA\,, \tag{4.26}$$

The half-filling condition here is simply $\nu = 1$. Notice that the background gauge field A couples to the "baryon number" current of the ϕ's in a *gauge invariant* way, in contrast to the theory of Ref. [178]. This also means that the physical bosons can be interpreted as baryons, or color singlet bound states of two ϕ's. However, these are monopoles from the point of view of **Theory A**.

To obtain a $SU(2)_2$ bosonic Moore-Read state at $\nu = 1$, we again seek the symmetry breaking pattern

$$SU(2)_1 \times SU(2)_1 \to SU(2)_2 \,. \tag{4.27}$$

As described in Section 4.2.2, the authors of Ref. [178] achieved this via pairing of adjoint fields so that the theory would support vortices of the order parameter with non-Abelian statistics. Instead, we will argue that singlet pairing of our *fundamental* composite vortices is sufficient to both obtain this symmetry breaking pattern and to capture the full anyon spectrum from the matter content. Nevertheless, it is still possible to obtain an analogue of the theory described in Section 4.2.2 by "quartetting" the composite vortices. In this case, the order parameter contributes non-trivial vortex excitations which possess non-Abelian statistics. These vortices arise because the order parameter sees $SO(3)$ rather than $SU(2)$ gauge fields, as in Ref. [178], and the resulting topological order again does not quite match that of the RR states. We provide a brief account of the quartetted phase at the end of this section.

Singlet Pairing

We pair the non-Abelian composite vortices by adding to **Theory B**, Eq. (4.26), an interaction with an electromagnetically neutral fluctuating scalar field $\Sigma_{mn}(x)$,

$$\mathcal{L} = \mathcal{L}_B + \mathcal{L}_\Sigma + \mathcal{L}_{\text{singlet pair}} \,, \tag{4.28}$$

$$\mathcal{L}_\Sigma = \sum_{m,n} |\partial \Sigma_{mn} - i u_m \Sigma_{mn} + i \Sigma_{mn} u_n|^2 - V[\Sigma] \,, \tag{4.29}$$

$$\mathcal{L}_{\text{singlet pair}} = -\sum_{m,n} \phi_m^\dagger \Sigma_{mn} \phi_n \,, \tag{4.30}$$

where Σ_{mn} is Hermitian in the layer indices m, n, and $V[\Sigma]$ is the potential for Σ. The off-diagonal components, $\Sigma_{12} = \Sigma_{21}^\dagger$, induce interlayer pairing, while the diagonal components, Σ_{11} and Σ_{22}, induce intralayer pairing. Under a gauge transformation, Σ_{nn} (no summation intended) transforms in the adjoint representation of the $SU(2)$ gauge group on layer n, while Σ_{12} transforms as a bifundamental field under the bilayer

$SU(2) \times SU(2)$ gauge group,

$$\Sigma_{mn} \mapsto U_m \Sigma_{mn} U_n^\dagger, \quad U_m \in SU(2) \text{ on layer } m. \tag{4.31}$$

In both Eq. (4.29) and Eq. (4.31), left (right) multiplication indicates contraction with Σ's color indices in the fundamental (antifundamental) representation of $SU(2)$.

In order to achieve the symmetry breaking pattern (4.27), we choose the potential V so that Σ_{mn} condenses in such a way that $\langle \phi_1^\dagger \phi_2 \rangle \neq 0$ while $\langle \phi_1 \rangle = \langle \phi_2 \rangle = 0$. Explicitly,

$$\langle \Sigma_{nm} \rangle = M_{nm} \mathbf{1}, \qquad M_{11}, M_{22}, \det M > 0 \tag{4.32}$$

The requirement $M_{11}, M_{22}, \det M > 0$ guarantees that the resulting effective potential for $\phi_{1,2}$ is minimized only for $\langle \phi_1 \rangle = \langle \phi_2 \rangle = 0$, while the off-diagonal components $M_{12} = M_{21}^\dagger$ break the $SU(2) \times SU(2)$ gauge symmetry down to the diagonal $SU(2)$. As described in Section 4.2.2, in the low energy limit, this sets $u_1 = u_2$, and the Chern-Simons levels add to yield the correct $SU(2)_2$ Chern-Simons theory (the bosonic Moore-Read state) as the low energy TQFT.

Having obtained the $SU(2)_2$ RR state, we now show that its anyon spectrum is furnished by the non-Abelian composite vortices $\phi_{1,2}$. Both ϕ_1 and ϕ_2 carry electric charge $Q = \frac{1}{2}$ and transform in the spin-$\frac{1}{2}$ representation of the $SU(2)_2$ gauge group, endowing them with non-Abelian braiding statistics. These are precisely the properties of the minimal charge anyon in the $\nu = 1$ bosonic Moore-Read state, the half-vortex! Even though there are two bosonic fields $\phi_{1,2}$, these do not represent distinct anyons: ϕ_1 and ϕ_2 can be freely transformed into one another via the bilinear condensate $\langle \phi_1^\dagger \phi_2 \rangle$. In other words, their currents are no longer individually conserved, and the layer index is no longer a good quantum number. The remainder of the anyon spectrum is obtained by constructing composite operators of the ϕ fields or, equivalently, by fusing multiple minimal charge anyons. In the present case, the only remaining anyon is the Majorana fermion, which transforms in the spin-1 representation of $SU(2)$, and so is represented by the local bilinear $\chi_n^a = \phi_n^\dagger t^a \phi_n$ (see Table 4.1). We note that, unlike in Ref. [178], there are no non-trivial vortices in this approach, since an order parameter valued on $[SU(2) \times SU(2)]/SU(2)$ cannot host non-trivial vortices.

The reader might object to our identification of the individual particles making up the pairs with the fundamental anyons, since the energy cost to break up a pair will be on the order of the UV cutoff. However, this is not a significant shortcoming of our construction, since anyons are only well defined upon projecting into the (topologically ordered) ground state. They should therefore always be viewed as infinite energy excitations representated as Wilson lines.

Table 4.1: List of quasi-particles in the $\nu = 1$ bosonic Moore-Read state, their spin, θ, $U(1)_{EM}$ charges, Q, and the corresponding operator in our LG theory. We label the anyons by the corresponding operators in the edge CFT (see e.g. Refs. [1, 2]). Note that we do not sum over the layer index n.

	1 (vacuum)	$\sigma e^{i\varphi/2}$ (half-vortex)	χ (Majorana fermion)
θ	0	$\frac{3}{16}$	$\frac{1}{2}$
Q	0	$\frac{1}{2}$	0
Field theory	-	ϕ_n	$\phi_n^\dagger t^a \phi_n$

Quartetting and Vortices

Although singlet pairing is sufficient to obtain the RR states, it is interesting to consider an alternative mechanism for obtaining non-Abelian states that more closely resembles the construction of Ref. [178] that was discussed in Section 4.2.2. In this scenario, rather than pairing the non-Abelian bosons of **Theory B** (4.26), we imagine *quartetting* them. To do this, we define the adjoint operators,

$$B_n^a = \phi_n^\dagger t^a \phi_n \,, \tag{4.33}$$

where the repeated n index on the right hand side is not summed over. These operators are neutral under $U(1)_{\rm EM}$, and they will serve the same purpose for us here as the B_n^a fields disucussed in Section 4.2 and Ref. [178]. We thus consider a pairing interaction of the B_n^a's, or a *quartetting* interaction of the ϕ's, by introducing a scalar field $\mathcal{O}$ to mediate the pairing interaction

$$\mathcal{L}_{\rm quartet} = \lambda\, B_1^a\, \mathcal{O}^{ab}\, B_2^b = \lambda\, (\phi_1^\dagger t^a \phi_1)\, \mathcal{O}^{ab}\, (\phi_2^\dagger t^b \phi_2)\,. \tag{4.34}$$

The quartetted phase, where $\langle \mathcal{O}^{ab} \rangle = v\delta^{ab}$ and $\langle \phi_1 \rangle = \langle \phi_2 \rangle = 0$, is accessed by adding a suitable potential $V[\mathcal{O}]$ and ensuring that $\phi_{1,2}$ are gapped via a mass term $-m^2 \sum_n |\phi_n|^2$. Because $\mathcal{O}$ radiatively acquires a kinetic term of the form of a gauged nonlinear sigma model (NLSM), the resulting effective theory in the quartetted phase is

$$\mathcal{L}_{\rm eff} = \mathcal{L}_B + \mathcal{L}_{\rm quartet} - m^2 \sum_n |\phi_n|^2 - V[\mathcal{O}] + \kappa\ {\rm Tr}\left[\mathcal{O}^{-1} D_{u_1-u_2} \mathcal{O}\, \mathcal{O}^{-1} D_{u_1-u_2} \mathcal{O}\right] \tag{4.35}$$

where κ is a coupling constant defined so that $\mathcal{O}$ is properly normalized.

Since $\mathcal{O}$ transforms in the adjoint representation of the $SU(2)$ of each layer, it is blind to their $\mathbb{Z}_2$ centers. This means that the quartetted phase hosts not only the non-Abelian $SU(2)_2$ topological order (since $u_1 - u_2$ is again Higgsed), but also an additional Abelian $\mathbb{Z}_2$ sector. Explicitly, as noted in Section

4.2.2, the condensation of $\mathcal{O}$ yields the symmetry breaking pattern $SU(2) \times SU(2) \to SU(2)_{\text{diag}} \times \mathbb{Z}_2$, where the residual $\mathbb{Z}_2$ can be chosen to act on either ϕ_1 or ϕ_2 (amounting to a choice of basis). Hence, the full topological order of the ground state is $SU(2)_2 \times \mathbb{Z}_2$. This is also true of the original construction of Ref. [178], meaning that the singlet pairing mechanism discussed above carries the significant advantage that it yields the $\nu = 1$ Moore-Read state *alone*, with no additional Abelian sector. We therefore focus on singlet pairing for the remainder of this Chapter.

How do we account for the new Abelian anyon content? As discussed in Section 4.2.2, because of the order parameter's blindness to the $\mathbb{Z}_2$ centers, the NLSM above admits vortex solutions. These vortices can carry fluxes of *both* of the residual $\mathbb{Z}_2$ and $SU(2)$ gauge groups, and so they possess non-trivial braiding statistics with respect to each other and the scalar fields. However, since the B_n^a fields here are electrically neutral, the vortices of the order parameter should not carry any electric charge either. These vortices should therefore correspond to anyon excitations which are distinct from those that can be obtained from the $\phi_{1,2}$ fields alone, as these fields carry electric charge. We leave a detailed understanding of this Abelian sector to future work.

As in the singlet pairing case, this quartetting procedure can be generalized to the case of k layers, or $\nu = k/2$, which can be easily shown to have $SU(2)_k \times \mathbb{Z}_2^{k-1}$ topological order (each factor of $\mathbb{Z}_2$ corresponds to the unbroken center of a broken $SU(2)$). In the next subsection, we describe how both the singlet pairing and quartetting constructions can be generalized to the remaining RR fillings through a flux attachment transformation.

4.3.4 Generating the Full Read-Rezayi Sequence through Flux Attachment

By attaching M fluxes to the k-layer generalization of **Theory A** (4.25) and performing the same transformation on **Theory B** (4.26), it is possible to obtain LG theories of the remaining RR states at filling fractions

$$\nu = \frac{k}{Mk + 2}\,. \tag{4.36}$$

Flux attachment can be performed on **Theory A** as a modular transformation $\mathcal{S}\mathcal{T}^M\mathcal{S}$ [207, 208], where

$$\mathcal{S} : \mathcal{L}[A] \mapsto \mathcal{L}[b] + \frac{1}{2\pi} A db\,, \qquad \mathcal{T} : \mathcal{L}[A] \mapsto \mathcal{L}[A] + \frac{1}{4\pi} A dA\,, \tag{4.37}$$

where again A is the background EM field, and b is a new dynamical $U(1)$ gauge field. Thus, attaching M fluxes to **Theory A** amounts to

$$\mathcal{S}\mathcal{T}^M\mathcal{S} : \mathcal{L}_A[A] \mapsto \mathcal{L}_A[b] + \frac{1}{2\pi} cd(b+A) + \frac{M}{4\pi} cdc\,, \tag{4.38}$$

where c is a new dynamical $U(1)$ gauge field. It is straightforward to see that this transformation is equivalent to the usual attachment of M fluxes to the composite bosons (related to the composite vortex variables – or Laughlin quasiparticles – of **Theory A** by boson-vortex duality [209, 210]). One of the insights of Refs. [161, 162] was that the modular group $\mathrm{PSL}(2,\mathbb{Z})$ generated by $\mathcal{S}$ and $\mathcal{T}$ can generate new dualities from old ones. Restricting for the moment to $k = 2$ layers, the transformed **Theory A** is dual to

$$\tilde{\mathcal{L}}_B = \sum_n \left(|D_{u_n - b\mathbf{1}/2}\phi_n|^2 - |\phi_n|^4 \right) + \frac{1}{4\pi}\sum_n \mathrm{Tr}\left[u_n du_n - \frac{2i}{3} u_n^3 \right] - \frac{1}{4\pi} bdb + \frac{1}{2\pi} cd(b+A) + \frac{M}{4\pi} cdc\,. \tag{4.39}$$

We can repackage the $SU(2)$ gauge fields u_n as new $U(2)$ gauge fields u'_n with trace $\mathrm{Tr}[u'_1] = \mathrm{Tr}[u'_2] = b$. This gluing of the traces together can be implemented by introducing a new auxiliary gauge field α,

$$\begin{aligned} \tilde{\mathcal{L}}_B = &\sum_n \left(|D_{u'_n}\phi_n|^2 - |\phi_n|^4 \right) + \frac{1}{4\pi}\sum_n \mathrm{Tr}\left[u'_n du'_n - \frac{2i}{3} u'^3_n \right] \\ &- \frac{2}{4\pi}\mathrm{Tr}[u'_1] d\,\mathrm{Tr}[u'_1] + \frac{1}{2\pi} cd(\mathrm{Tr}[u'_1] + A) + \frac{M}{4\pi} cdc + \frac{1}{2\pi}\alpha d\left(\mathrm{Tr}[u'_1] - \mathrm{Tr}[u'_2]\right)\,. \end{aligned} \tag{4.40}$$

This transformation does not impact the singlet pairing nor the quartetting procedure discussed in the previous subsection, and it readily generalizes to k layers (more constraints need to be introduced in that case to glue the Abelian gauge fields together). We therefore obtain the $SU(2)_2$ Chern-Simons theory at low energies, albeit with the additional Abelian sector introduced above. For the general case of k layers, the u'_n's on each layer are set equal to one another, and the low energy TQFT is a $U(2)_{k,-2k} \times U(1)_M$ Chern-Simons-BF theory given by

$$\mathcal{L} = \frac{k}{4\pi}\mathrm{Tr}\left[u' du' - \frac{2i}{3} u'^3 \right] - \frac{k}{4\pi}\mathrm{Tr}[u'] d\,\mathrm{Tr}[u'] + \frac{1}{2\pi} cd(\mathrm{Tr}[u'] + A) + \frac{M}{4\pi} cdc\,. \tag{4.41}$$

This is indeed the proper bulk TQFT describing the RR states at filling (4.36), first described in Ref. [143]. As in the case of the $\nu = 1$ bosonic Moore-Read state discussed above, the fundamental scalars (i.e. the composite vortices) comprise the minimal charge anyons, here possessing electric charge $Q = 1/(Mk+2)$. This is the expected result for the minimal charge anyon in the general RR states.

4.4 Generalization to Non-Abelian $SU(N_f)$-Singlet States

Having derived a LG theory for the RR states, we will now demonstrate how our construction can be naturally extended to the generalized non-Abelian $SU(N_f)$-singlet states occuring at fillings

$$\nu = \frac{kN_f}{N_f + 1 + kMN_f}, \qquad k, N_f, M \in \mathbb{Z}. \tag{4.42}$$

These are clustered states in which k represents the number of local particles (fermions or bosons for odd and even M, respectively) in a cluster, M the number of attached Abelian fluxes, and N_f the number of internal degrees of freedom. Like the RR states, which correspond to $N_f = 1$, we will show that these states can also be obtained by pairing starting from a parent multi-layer Abelian LG theory. The particular Abelian states we will target are the N_f-component generalizations of the Halperin $(2, 2, 1)$ states. In parallel to Section 4.3, we will show that the LG theories of these Abelian states satisfy a new non-Abelian bosonization duality. This duality relates the Abelian LG theory of the generalized Halperin states to an $SU(N_f + 1)_1$ Chern-Simons-matter theory. That this is possible is perhaps not surprising given that the N_f-component $(2, 2, 1)$ state is known to have an edge theory which furnishes a representation of the $SU(N_f + 1)_1$ Kac-Moody algebra, as we shall review below [69, 70, 196, 197]. The generalized NASS states are then obtained by singlet pairing of the dual non-Abelian bosons.

4.4.1 Motivation: "Projecting Down" to the Generalized NASS States

Just as the RR states are naturally understood starting with the $\nu = 1/2$ Laughlin state by way of "projecting down," the generalized NASS states can be built up from N_f-component generalizations of the Halperin $(2, 2, 1)$ spin-singlet state [140]. These (bosonic) states are *Abelian* and correspond to $M = 0, k = 1$. These states are described by the wave functions

$$\Psi^{(221)}_{N_f}(\{z_i^\sigma\}) = \prod_{\sigma=1}^{N_f} \prod_{i<j} (z_i^\sigma - z_j^\sigma)^2 \prod_{\sigma<\sigma'}^{N_f} \prod_{i,j} (z_i^\sigma - z_j^{\sigma'})^1 e^{-\frac{1}{4}\sum_{\sigma,i} |z_i^\sigma|^2}, \tag{4.43}$$

where $z_i^\sigma = x_i^\sigma + iy_i^\sigma$ denotes the complex coordinates of the i^{th} boson with component index σ. In direct analogy with the $\nu = k/2$ RR states, the generalized NASS wave functions for general k (but still $M = 0$) may be obtained by symmetrizing over a product of k copies of the N_f-component $(2, 2, 1)$ wave function [36],

$$\Psi_{k,N_f} = \mathcal{S}_k \left[\prod_{i=0}^{k-1} \Psi^{(221)}_{N_f}(z_{1+iN/k}, \ldots, z_{(i+1)N/k}) \right]. \tag{4.44}$$

where the symmetrization operation $\mathcal{S}_k$ is morally the same as the one defined in Section 4.2.1. Again, the form of the wave function makes explicit the clustering of bosons characteristic of non-Abelian states. The wave functions for general M are obtained by multiplying Ψ_{k,N_f} by a $\nu = \frac{1}{M}$ Laughlin factor. Note that setting $N_f = 1$ recovers the RR wave functions (4.4).

The generalized NASS wave functions (4.44) should also be expresssible as correlators of the $SU(N_f+1)_k$ WZW CFT for $M = 0$ and of the $[U(1)]^{N_f} \times SU(N_f+1)/[U(1)]^{N_f}$ coset CFT for $M > 0$. Although this appears to have only been discussed explicitly for $N_f = 1, 2, 3$ [179, 191, 211], we will assume that this holds true for general N_f. We thus expect the corresponding bulk theories for the generalized NASS states to be $SU(N_f+1)_k$ Chern-Simons theories.

For the N_f-component Halperin states ($k = 1$), the presence of this "hidden" $SU(N_f+1)$ representation can be motivated as follows. These states are described by a $N_f \times N_f$ K-matrix and N_f-component charge vector q,

$$K = \begin{pmatrix} 2 & 1 & 1 & \dots & 1 & 1 \\ 1 & 2 & 1 & \dots & 1 & 1 \\ 1 & 1 & 2 & & & 1 \\ \vdots & \vdots & & \ddots & & \vdots \\ 1 & 1 & & & 2 & 1 \\ 1 & 1 & 1 & \dots & 1 & 2 \end{pmatrix}, \qquad q = \begin{pmatrix} 1 \\ \vdots \\ 1 \end{pmatrix}. \tag{4.45}$$

The form of the charge vector reflects the fact that the physical bosonic excitations of each species each carry the same EM charge, and it can read off that the Hall conductivity is $\sigma_{xy} = q^T K^{-1} q \frac{e^2}{h} = \frac{N_f}{N_f+1}\frac{e^2}{h}$. Under a particular change of basis $\tilde{K} = G^T K G$ and $\tilde{q} = Gq$, $G \in SL(N_f, \mathbb{Z})$, K can be shown to be related to the Cartan matrix of $SU(N_f+1)$ [70, 197],

$$G = \begin{pmatrix} 1 & -1 & & & & \\ & 1 & -1 & & & \\ & & \ddots & \ddots & & \\ & & & 1 & -1 & \\ & & & & 1 & \end{pmatrix} \Rightarrow \tilde{K} = \begin{pmatrix} 2 & -1 & 0 & \dots & 0 & 0 \\ -1 & 2 & -1 & \dots & 0 & 0 \\ 0 & -1 & 2 & & & 0 \\ \vdots & \vdots & & \ddots & & \vdots \\ 0 & 0 & & & 2 & -1 \\ 0 & 0 & 0 & \dots & -1 & 2 \end{pmatrix}, \qquad \tilde{q} = \begin{pmatrix} 0 \\ 0 \\ \vdots \\ 1 \end{pmatrix}. \tag{4.46}$$

Using this fact, one can show that the edge theory defined by $\tilde{K}$ supports a $SU(N_f+1)_1$ Kac-Moody

algebra (see e.g. Refs. [70, 212] for a derivation), and hence is equivalent to the $SU(N_f+1)$ WZW CFT. Consequently, the corresponding bulk theory of the N_f-component $(2,2,1)$ Halperin state is a $SU(N_f+1)_1$ Chern-Simons theory. This is the N_f-component generalization of the level-rank duality $U(1)_2 \leftrightarrow SU(2)_1$ described in Section 4.2.

This discussion indicates that we should expect the LG theories of the generalized NASS states can be obtained from pairing k copies of the N_f-component $(2,2,1)$ Halperin state. Because this state is level-rank dual to a $SU(N_f+1)_1$ theory, we might expect that there is a non-Abelian Chern-Simons-matter theory duality also taking this shape, from which we can build a LG theory of the non-Abelian states. We now show that this is indeed the case.

4.4.2 Non-Abelian Duals of N_f-Component Halperin $(2,2,1)$ States

The necessary non-Abelian duality can be constructed by starting with the Abelian LG theory for the N_f-component Halperin state, which we again call **Theory A**. This theory consists of N_f species of Wilson-Fisher bosons Φ_I, $I = 1, \ldots, N_f$, each coupled to a $U(1)$ Chern-Simons gauge fields a_I,

$$\mathcal{L}_A = \sum_{I=1}^{N_f} \left(|D_{a_I} \Phi_I|^2 - |\Phi_I|^4 \right) + \frac{1}{4\pi} \sum_{I,J=1}^{N_f} K_{IJ} a_I da_J + \frac{1}{2\pi} \sum_{I=1}^{N_f} q_I A da_I, \tag{4.47}$$

where K and q are given in Eq. (4.45). The N_f-component Halperin state corresponds to the phase in which all of the Φ_I fields – the Laughlin quasiparticles – are gapped. We emphasize that there is no continuous $SU(N_f)$ global symmetry rotating the Φ_I fields manifest in **Theory A**. Instead, there is only a discrete exchange symmetry of the Φ_I fields.

Following the reasoning laid out in Section 4.3.2, we now show that this theory is dual to one of N_f Wilson-Fisher bosons coupled to a *single* $SU(N_f+1)$ gauge field. Similar dualities have also been described in Ref. [213]. We start by applying the Abelian boson-fermion duality of Eq. (4.17) to each scalar Φ_I, treating the a_I's as background fields, to obtain the Dirac fermion **Theory C**,

$$\begin{aligned} \mathcal{L}_A \longleftrightarrow \mathcal{L}_C = & \sum_{I=1}^{N_f} i\overline{\psi}_I \not{D}_{b_I} \psi_I + \sum_{I=1}^{N_f} \frac{1}{4\pi} a_I da_I + \sum_{I=1}^{N_f} \sum_{J=I+1}^{N_f} \frac{1}{2\pi} a_I da_J + \sum_{I=1}^{N_f} \frac{1}{2\pi} A da_I \\ & + \sum_{I=1}^{N_f} \left[-\frac{1}{2} \frac{1}{4\pi} b_I db_I + \frac{1}{2\pi} b_I da_I \right]. \end{aligned} \tag{4.48}$$

As in the example discussed in Section 4.3.2, the a_I fields can be safely integrated out while respecting the Dirac flux quantization condition. This is because all of the Chern-Simons terms have coefficient equal to

unity. On integrating out one of the a_I fields,the remaining ones become Lagrange multipliers enforcing the constraints $b_I = b_1 \equiv b$. Integrating out the remaining a_I's, we find that **Theory C** can be rewritten as one of fermions coupled to a single dynamical gauge field,

$$\mathcal{L}_C = \sum_{I=1}^{N_f} i\overline{\psi}_I \not{D}_b \psi_I - \frac{N_f+2}{2}\frac{1}{4\pi} bdb - \frac{1}{2\pi} bdA - \frac{1}{4\pi} AdA. \tag{4.49}$$

In contrast to **Theory A**, **Theory C** has a manifest $SU(N_f)$ global flavor symmetry[3] since the fermions all couple in the same way to the gauge field b. This symmetry is thus an *emergent* symmetry from the point of view of **Theory A**.

We may now apply the non-Abelian duality (4.14) to **Theory C**, leading to a non-Abelian bosonic **Theory B**,

$$\mathcal{L}_B = \sum_{I=1}^{N_f} |D_{u-\frac{1}{N_f+1}A\mathbf{1}}\phi_I|^2 - |\phi|^4 + \frac{1}{4\pi}\mathrm{Tr}\left[udu - \frac{2i}{3}u^3\right] - \frac{1}{4\pi}\frac{N_f}{N_f+1}AdA\,. \tag{4.50}$$

where $-|\phi|^4$ denotes tuning to the Wilson-Fisher fixed point consistent with a global $SU(N_f)$ symmetry. We will again refer to the ϕ_I fields as the non-Abelian composite vortices. It will be convenient in the subsection below to re-express this theory as a $U(N_f+1)$ gauge theory with a constraint,

$$\mathcal{L}_B = \sum_{I=1}^{N_f} |D_u\phi_I|^2 - |\phi|^4 + \frac{1}{4\pi}\mathrm{Tr}\left[udu - \frac{2i}{3}u^3\right] + \frac{1}{2\pi}\alpha d(\mathrm{Tr}\,[u] - A) - \frac{1}{4\pi}AdA\,, \tag{4.51}$$

where we have introduced a $U(1)$ gauge field α. We have thus obtained a *new* triality,

$$\begin{aligned} &\textbf{Theory A: } N_f \text{ scalars} + U(1) \text{ } K\text{-matrix theory of Eq. (4.45)} \\ &\qquad\qquad\qquad\qquad \updownarrow \\ &\textbf{Theory C: } N_f \text{ fermions} + U(1)_{-\frac{N_f+2}{2}} \longleftrightarrow \textbf{Theory B: } N_f \text{ scalars} + SU(N_f+1)_1\,. \end{aligned} \tag{4.52}$$

This is the main result of this subsection. It is interesting that, for our particular choice of K-matrix in **Theory A**, we have obtained a non-Abelian dual theory in which the rank of the gauge group depends on the number of matter species and in which an emergent $SU(N_f)$ symmetry appears. Such trialities can be extended by applying the modular transformation $\mathcal{S}\mathcal{T}^{P-1}\mathcal{S}$ (flux attachment) to each side, transforming the K matrix of **Theory A** to that of the N_f-component $(P+1, P+1, P)$ Halperin states. The family of Abelian composite fermion theories obtained by this transformation has been conjectured to describe

[3]See Ref. [204] for a more detailed discussion of global symmetries in non-Abelian dualities.

plateau transitions in fractional Chern insulators [41].

Notice that Eq. (4.52) does not contain a non-Abelian fermionic theory analogous to **Theory D** in Eq. (4.24). That is not to say such a theory does not exist. We leave to future work a full inquiry into how the NASS states, to be discussed in the next section, may arise in a fermionic picture.

4.4.3 Generating the Non-Abelian $SU(N_f)$-Singlet Sequence from Clustering

With the non-Abelian composite vortex description of the N_f-component $(2,2,1)$ states in hand, we can follow the pairing procedure of Section 4.3.3 to generate the generalized NASS sequence. Unlike in Section 4.3, in this section we will consider LG theories for general k, M, and N_f from the outset. Our **Theory A** will thus consist of k layers of LG theories of the N_f-flavor Halperin $(2,2,1)$ states,

$$\mathcal{L}_A = \sum_{I,n} \left(|D_{a_{I,n}} \Phi_{I,n}|^2 - |\Phi_{I,n}|^4 \right) + \frac{1}{4\pi} \sum_{I,J,n} K_{IJ} a_{I,n} da_{J,n} + \frac{1}{2\pi} \sum_{I,n} q_I A da_{I,n}, \tag{4.53}$$

where again the K-matrix and charge vector are given by Eq. (4.45), and $n = 1, \ldots, k$ denotes the layer index. Applying the duality (4.51) to each layer, this theory is dual to the non-Abelian **Theory B**,

$$\mathcal{L}_B = \sum_{I,n} |D_{u_n} \phi_{I,n}|^2 - \sum_n |\phi_n|^4 + \sum_{I,n} \mathcal{L}_{U(N_f+1)}[u_n] + \frac{1}{2\pi} \sum_{I,n} \alpha_n d(\mathrm{Tr}\,[u_n] - A) - \frac{k}{4\pi} A dA. \tag{4.54}$$

Here, lower case Latin letters denote a layer index, upper case Latin letters a flavor index. We have also defined, for compactness,

$$\mathcal{L}_{U(N)}[u] \equiv \frac{1}{4\pi} \mathrm{Tr} \left[u du - \frac{2i}{3} u^3 \right]. \tag{4.55}$$

We introduce M via flux attachment, or application of the modular transformation $\mathcal{S}\mathcal{T}^M\mathcal{S}$, as in Section 4.3.4. This yields a sequence of descendant theories labelled by k, M, and N_f,

$$\begin{aligned} \tilde{\mathcal{L}}_B = &\sum_{I,n} |D_{u_n} \phi_{I,n}|^2 - \sum_n |\phi_n|^4 + \sum_n \mathcal{L}_{U(N_f+1)}[u_n] + \frac{1}{2\pi} \sum_n \alpha_n d(\mathrm{Tr}\,[u_n] - a) \\ &- \frac{k}{4\pi} a da + \frac{1}{2\pi} a db + \frac{M}{4\pi} b db + \frac{1}{2\pi} b dA. \end{aligned} \tag{4.56}$$

We are now in a position to consider singlet pairing between the different layers. One can also consider quartetting the composite vortices, but this only leads to additional Abelian sectors, as in the RR case.

Singlet pairing between the fundamental scalars is again mediated via a dynamical scalar field, $\Sigma_{m,n}(x) = \Sigma^\dagger_{n,m}(x)$, transforming in the bifundamental representation of the $SU(N_f+1)$ factor on layer m and on layer

n, i.e. $\Sigma_{m,n} \mapsto U_m \Sigma_{m,n} U_n^\dagger$, where $U_n, U_m \in SU(N_f+1)$. Note that the $U(1)$ gauge transformations cancel out, as the α_n fields force all the $U(1)$ gauge fields $\mathrm{Tr}[u_n]$ to be equal. If we require that $\Sigma_{m,n}$ be a flavor singlet, its coupling to the non-Abelian composite vortices is therefore

$$\mathcal{L}_{\text{singlet pair}} = -\sum_{m,n,I} \phi_{I,m}^\dagger \, \Sigma_{m,n} \, \phi_{I,n} \, . \tag{4.57}$$

As before, the off-diagonal terms induce inter-layer pairing, while the diagonal terms can be used to ensure that $\langle \phi_{I,n} \rangle = 0$. Thus, we obtain a non-Abelian state when $\Sigma_{m,n}$ condenses in such a way that it enforces the constraint $u_n \equiv u'$ for all n. Putting these pieces together, we find that the paired phase is governed by the TQFT

$$\mathcal{L}_{\text{eff}} = k \, \mathcal{L}_{U(N_f+1)}[u'] - \frac{k}{4\pi} \mathrm{Tr}[u'] d \mathrm{Tr}[u'] + \frac{1}{2\pi} \mathrm{Tr}[u'] db + \frac{M}{4\pi} b db + \frac{1}{2\pi} b dA \tag{4.58}$$

Integrating out the fluctuating gauge fields indeed yields the correct Hall response,

$$\sigma_{xy} = \frac{k N_f}{N_f + 1 + k M N_f} \frac{e^2}{h}, \tag{4.59}$$

which is the expected result for the generalized NASS states.

As in our LG theories of the RR states, the fundamental scalars $\phi_{I,n}$ correspond to the minimal charge anyons. Indeed, one can check from the equations of motion that the fundamental scalar fields each carry charge $Q = \frac{1}{N_f+1+MkN_f}$, which reduces to the expected result for the minimal charge anyons of the RR and non-Abelian spin singlet states for $N_f = 1$ and $N_f = 2$, respectively. Additionally, in the paired phase, the condensation of the bilinears $\phi_{I,m}^\dagger \phi_{I,n} + H.c.$ (no sum on I) ensures that all the $\phi_{I,n}$, for fixed I, are indistinguishable, removing the redundancy of the layer degree of freedom. In particular, because we took the pairing interaction to be diagonal in the flavor indices, there is no mixing between flavors on different layers. Hence the fundamental scalar excitations should still transform into each other under the diagonal $SU(N_f)$ subgroup of the original $SU(N_f) \times \cdots \times SU(N_f)$ global symmetry. Consequently, our theory reproduces the desired anyon spectrum, and we conclude that we have obtained a LG theory for the generalized NASS states.

4.5 Discussion

Using non-Abelian boson-fermion dualities, we have presented a physical pairing mechanism by which the non-Abelian Read-Rezayi states and their generalizations, the non-Abelian $SU(N_f)$-singlet states, may be obtained by "projecting down" from parent Abelian states. These dualities relate the usual Abelian LG theories of the parent state to theories of non-Abelian "composite vortices," which pair to form the non-Abelian FQH state. While this pairing amounts to condensing local operators in the non-Abelian theory, this is not the case in the original Abelian LG theory of Laughlin quasiparticles, in which the composite vortices are monopoles. In the process of developing these theories, we have described a new triality (4.52) which parallels a level-rank duality apparent from CFT/ideal wave function considerations and which has the interesting property that it involves a non-Abelian gauge theory with rank depending on the number of matter species. We believe that this approach for obtaining physically motivated bulk descriptions of non-trivial gapped phases represents a promising direction for future applications of duality to condensed matter physics which has thus far been under-explored.

Our construction contrasts with earlier bulk descriptions of non-Abelian FQH states in important ways. The use of non-Abelian boson-fermion dualities, which relate parent quantum critical points, or Landau-Ginzburg effective field theories, provides a clear mapping to theories of non-Abelian "composite vortex" variables which are manifestly gauge invariant, unlike in earlier approaches that invoked level-rank duality deep in the topological phase [69, 178]. Additionally, we showed that these earlier approaches in fact lead to a superfluous Abelian sector on top of the desired non-Abelian topological order. The use of non-Abelian dualities also avoids the issues inherent to parton constructions [158–160], which provide a perhaps larger class of fractionalized descriptions but rely on the assumption that the fractionalized particles are not confined. This is in spite of the fact that they are generally charged under non-Abelian gauge fields without Chern-Simons terms and, as such, are known to be confining in 2+1 dimensions. Consequently, it is likely that many partonic descriptions are on unstable dynamical footing.

We anticipate that many more exotic FQH and otherwise topologically ordered states can be targeted with our approach. Again, we can draw inspiration from edge CFT and ideal wave function approaches. For instance, the spin-charge separated spin-singlet states of Ref. [214] can both be related to a parent bilayer Abelian state and be obtained from conformal blocks of an $SO(5)$ WZW theory. There exist, in fact, Chern-Simons-matter dualities involving precisely $SO(N)$ (and many other) gauge groups [200, 215], which suggests that it may be possible to formulate non-Abelian Landau-Ginzburg theories of these states. It is perhaps also possible to apply our approach to generating bulk parent descriptions of the orbifold FQH states [176], which can involve an interesting interplay of usual gauge symmetries with gauged higher-form

symmetries [216, 217].

In this Chapter, we have focused on understanding non-Abelian states via pairing of non-Abelian bosonic matter. However, as described in Section 4.3, a non-Abelian composite fermion description is available for the $\nu = \frac{1}{2}$ Laughlin states. In the parent Abelian phase, these fermions feel a magnetic field and fill an integer number of Landau levels. Pairing across layers of these integer quantum Hall states in fact leads to $U(k)_2$ topological order, a demonstration of which we defer to Chapter 6. One may also consider starting not from multiple layers of FQH phases but instead of the (fermionic) compressible states at filling $\nu = 1/2n$, for which Dirac fermion theories have been proposed [124, 170]. It is possible that applying non-Abelian dualities to these theories may provide an avenue for developing exotic non-Abelian *excitonic* phases.

We lastly comment on the possible connection of the theories presented here to numerical studies of transitions between Abelian and non-Abelian states in bilayers [181–184, 186, 187]. To the extent that these transitions are continuous, it is an exciting possibility that they are in the universality class of the quantum critical theories presented here. However, since these theories are very strongly coupled, the only analytic techniques against which this can be checked are large-N approaches, which may describe a wholly different fixed point. Perhaps eventually the conformal bootstrap will be able to shed light on this issue.

Chapter 5

A Composite Particle Construction of the Fibonacci Fractional Quantum Hall State

5.1 Introduction

One of the many compelling motivations for studying non-Abelian topological orders is that they are among the most promising platforms for fault-tolerant quantum computation [6]. The non-Abelian anyon excitations in theses phases are quasiparticles with, as their name would suggest, non-Abelian braiding statistics [1]. Non-Abelian anyons therefore provide a source of *topological* degeneracy, allowing for non-local storage of information. Information can then be manipulated through braiding of the anyons, a process which is resilient against decoherence from local perturbations because of its topological nature [218–222]. Prime candidates for realizing non-Abelian topological order are the systems under consideration in this thesis – namely, two-dimensional gases of electrons in strong magnetic fields, which can form fractional quantum Hall (FQH) states. Excitingly, there is mounting experimental evidence for fractional statistics in FQH states [223], and for the non-Abelian Pfaffian state (introduced in Chapters 3 and 4) at filling fraction $\nu = 5/2$ supporting the simplest non-Abelian anyon, the Ising anyon [224–227].

Ising anyons, however, are not sufficient for universal quantum computation [6]. In contrast, topological orders supporting the so-called Fibonacci anyon can serve as universal quantum computers [228]. This follows from the Fibonacci anyon's fusion rule, $\tau \times \tau = 1 + \tau$, where τ is the Fibonacci anyon, 1 is the trivial anyon, and $\times$ denotes anyon fusion. For this reason, there has been much interest in the observed $\nu = 12/5$ FQH state, as numerics suggest this may correspond to the $\mathbb{Z}_3$ Read-Rezayi (RR) state [65], which supports the Fibonacci anyon among other, Abelian anyons [229, 230]. Unfortunately, the presence of the other anyons can complicate manipulation of the Fibonacci anyons by entering into braiding processes, a form of quasiparticle poisoning. It is thus of interest to understand if it is possible to realize a topological order supporting the Fibonacci anyon as its *only* excitation.

Several proposals have been put forward for realizing such a Fibonacci state. These include the nucleation

This Chapter is adapted from the following preprint, which is also cited as Ref. [18] in this thesis: Hart Goldman, Ramanjit Sohal, and Eduardo Fradkin, A composite particle construction of the Fibonacci fractional quantum Hall state, 2020, arxiv:2012.11611.

of a Fibonacci state on top of an Abelian FQH state using proximity coupled superconductors [231], chiral superconducting islands with special couplings [232], and the possible realization of the Fibonacci state at an integer filling of Landau levels [233]. Further studies have sought Fibonacci anyons via projective parton constructions [175,234], but all of these constructions lead to additional anyon content as well. All of the studies that realize a purely Fibonacci state follow the spirit of coupled wire constructions [152] which, although providing concrete and analytically tractable microscopic models with topologically ordered ground states, do not provide a physical picture for the dynamics that could lead to the emergence of such states in an isotropic system. A quantum loop model for a Fibonacci state was proposed in Ref. [235]. In the context of Abelian FQH states, such a picture is provided by composite fermion/boson field theories [11–13]. While a composite particle picture is lacking for most non-Abelian states, including the Fibonacci state, notable exceptions include the Moore-Read FQH state (and its cousins) at $\nu = 5/2$, which can be described as arising from the pairing of composite fermions [61], the Read-Rezayi sequence [17,178], the generalized non-Abelian spin singlet states [17,69,70], and a range of Blok-Wen states (which will be discussed in the following Chapter) [19,71,165]. Indeed, it is an open problem to establish a precise composite particle picture for any *purely* non-Abelian state, as flux attachment generically leads to Abelian anyon content.

In this Chapter, we continue the program initiated in Chapter 4 and employ the recently proposed Chern-Simons-matter field theory dualities [66–68] [see Eqs. (4.13)-(4.15)] to construct a composite particle theory for the emergence of the Fibonacci state in a QH system of bosons at $\nu = 2$. As we have seen, these dualities can be interpreted as non-Abelian analogues of flux attachment. In the present Chapter, we use duality to construct a Landau-Ginzburg description of a Fibonacci state of *bosons* starting from a trilayer of IQH states, using flux attachment to render the electric charges bosonic. In this setup, the dynamical mechanism leading to the Fibonacci state is manifest as interlayer clustering of dual bosonic "composite vortices," which couple to a fluctuating, non-Abelian gauge field. Our chosen clustering mechanism binds electric charges on two of the layers to holes on the third, breaking the interlayer exchange symmetry. Our flux attachment procedure similarly breaks this symmetry, rendering two of the layers topologically trivial and endowing the remaining layer with the topological order of the Halperin $(2, 2, 1)$ state.

Our dynamical mechanism therefore has an element of clustering, which underlies the interpretation of the RR states, while retaining the character of a multilayer state, as the $(2, 2, 1)$ state is commonly interpreted as a bilayer (it has a $\mathbb{Z}_2$ exchange symmetry). In parallel to this intuition, we motivate an ideal wave function for the Fibonacci state, an as-yet unprecedented achievement. This wave function superficially describes a bilayer state, but nevertheless has the clustering properties of the $\mathbb{Z}_3$ RR state, which describes clusters of three local quasiparticles.

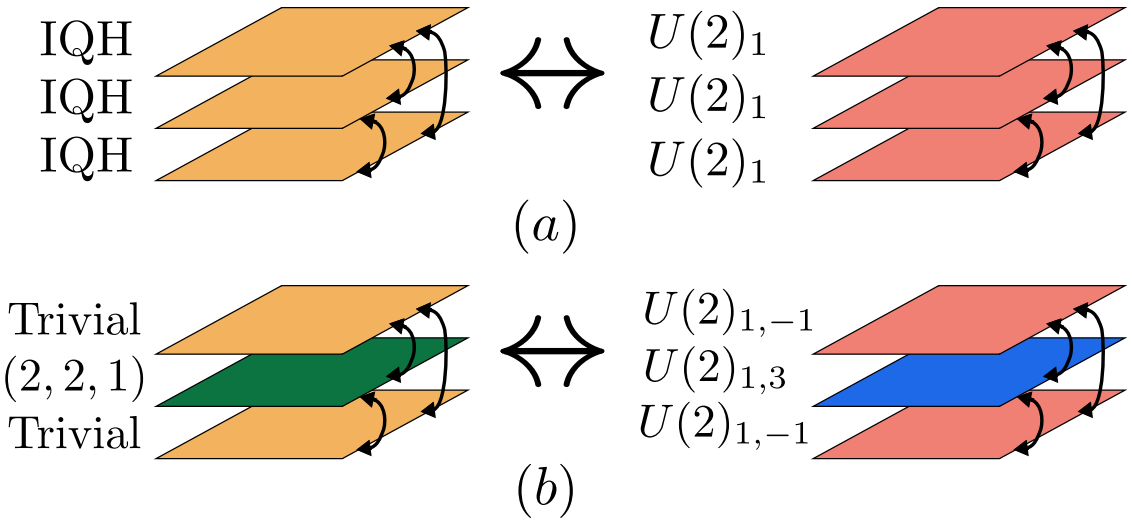

Figure 5.1: A schematic of our construction of the (a) $U(2)_3$ and (b) $U(2)_{3,1}$ Fibonacci states. Here $\leftrightarrow$ denotes duality between the theories of Laughlin quasiparticles and composite vortices. The non-Abelian state is obtained by clustering of the dual composite vortices between the layers.

5.2 Parent Model and Non-Abelian Duality

Our starting point is a trilayer of $\nu = 2$ IQH states, as shown in Fig. 5.1. We will take each layer layer to be near a $\nu = 2 \to 1$ transition described by a free Dirac fermion in the clean limit,

$$\mathcal{L}_{\text{IQH}} = \sum_{n=1}^{3} \left[\overline{\Psi}_n (i \not{D}_A - M) \Psi_n - \frac{3}{2} \frac{1}{4\pi} A dA \right] . \tag{5.1}$$

Here Ψ_n is a two-component Dirac fermion on layer n, A_μ is the background electromagnetic (EM) gauge field, and we use the notation $D_B^\mu = \partial^\mu - iB^\mu$, $BdC = \varepsilon^{\mu\nu\lambda} B_\mu \partial_\nu C_\lambda$, and $\not{B} = B^\mu \gamma_\mu$, where γ^μ are the Dirac gamma matrices. Integrating out the Dirac fermions yields a $\nu = 2$ ($\nu = 1$) IQH phase for $\text{sgn}(M) < 0$ ($\text{sgn}(M) > 0$). Note we define the filling as $\nu = -2\pi\rho_e/B$, $\rho_e = \langle \delta\mathcal{L}/\delta A_0 \rangle, B = \varepsilon^{ij}\partial_i A_j$. Our interest will be in the physics near the quantum phase transition at $M = 0$.

Near $M = 0$, this theory has been proposed to satisfy a large number of boson-fermion dualities [68], which are relativistic generalizations of the familiar flux attachment duality that relates the IQH transition of fermions to the condensation of composite bosons [13]. These relate the free Dirac fermion theory on each layer to one of a Wilson-Fisher boson, ϕ_n, coupled to a fluctuating $U(N)$ Chern-Simons (CS) gauge field, a_n, in the fundamental representation [199, 236, 237]. While a free Dirac fermion has a bosonic dual for any

value of N, our interest will be in the case of $N = 2$,

$$\tilde{\mathcal{L}}_{\rm IQH} = \sum_{n=1}^{3} \left[|D_a \phi_n|^2 - r|\phi_n|^2 - |\phi_n|^4 \right] + \sum_{n=1}^{3} \mathcal{L}_{\rm CS}[a_n] + A_\mu j^\mu_{\rm top} \,, \tag{5.2}$$

$$\mathcal{L}_{\rm CS}[a_n] = \frac{1}{4\pi} \,{\rm Tr}\left[a_n da_n - \frac{2i}{3}(a_n)^3 \right] \,, \tag{5.3}$$

$$A_\mu j^\mu_{\rm top} = \frac{1}{2\pi} A d \,{\rm Tr}[a_1 - a_2 + a_3] \,. \tag{5.4}$$

Here $-|\phi|^4$ denotes tuning such that the Wilson-Fisher fixed point occurs at $r = 0$, and traces are over color [i.e. $U(2)$] indices. We have also selected the BF terms in Eq. (5.4) such that the second layer has opposite EM charge from the other two. Because each layer is decoupled from one another, we may freely determine the signs in Eq. (5.4) because the partition function has a charge conjugation symmetry.

The fact that the theory in Eq. (5.2) has the same phase diagram as that of Eq. (5.1) follows from the so-called level-rank duality of topological quantum field theories (TQFTs) [188, 190, 199], which is an equivalence between $U(N)_k$ and $SU(k)_{-N}$ CS theories, where the subscript is the CS level. In particular, one can set $k = 1$, leading to a duality between a trivial (i.e. IQH) theory and a $U(N)_1$ CS theory,

$$\mathcal{L}_{\rm CS}[b] + \frac{1}{2\pi} A d \,{\rm Tr}[b] \longleftrightarrow -\frac{N}{4\pi} A d A \,, \tag{5.5}$$

where b is a $U(N)$ gauge field, and we have suppressed gravitational Chern-Simons terms.

Using level-rank duality, we can check the phase diagram of Eq. (5.2): for ${\rm sgn}(r) > 0$, the ϕ bosons are gapped, leading to a $U(2)_1$ theory on each layer, which describes a trilayer of $\nu = 2$ IQH states by Eq. (5.5). Similarly, for $r < 0$ the bosons condense, breaking the gauge group down to $U(1)$ on each layer. Integrating out the remaining $U(1)$ gauge fields leads to the desired trilayer $\nu = 1$ response. The equivalence of the phase diagrams of the theories in Eqs. (5.1) and (5.2) has led to the conjecture that the critical points at $r = M = 0$ are identical. Below we will assume this to be the case, our confidence bolstered by the large-N, k derivations of Refs. [66, 67] and the Euclidean lattice derivation of Ref. [236].

5.3 Landau-Ginzburg Theory

To target the Fibonacci phase, we first identify a CS TQFT representation of the state. It was recently shown [215] that one such representation is

$$U(2)_{3,1} = \frac{SU(2)_3 \times U(1)_2}{\mathbb{Z}_2} . \tag{5.6}$$

This is a $U(2)$ CS gauge theory where the Abelian and non-Abelian parts of the gauge field have different CS levels. The quotient by $\mathbb{Z}_2$ simply enforces that these two components are part of the same $U(2)$ gauge field (see Appendix F). The Lagrangian for this theory is written as

$$\mathcal{L}_{\text{Fib}} = 3\,\mathcal{L}_{\text{CS}}[a] - \frac{1}{4\pi}\,\text{Tr}[a]\,d\,\text{Tr}[a] + \frac{1}{2\pi}Ad\,\text{Tr}[a]\,, \tag{5.7}$$

where a is again a $U(2)$ gauge field. One can check that this theory has a single nontrivial anyon, besides the vacuum, which transforms in the spin-1 representation of $U(2)$, satisfies the Fibonacci fusion rule, $\tau \times \tau = 1 + \tau$, and has topological spin $h_\tau = 2/5$, as we illustrate explicitly in Appendix C.2. We also comment that this theory is known to be dual to a $(G_2)_1$ TQFT, where G_2 is the smallest exceptional simple Lie group [5, 215, 230].

To access the $U(2)_{3,1}$ state, we start by introducing interlayer clustering to the composite vortex theory, Eq. (5.2), via coupling to a scalar field, Σ_{nm},

$$\mathcal{L}_{\text{cluster}} = -\sum_{n,m}\phi^\dagger_m \Sigma_{mn}\phi_n - V[\Sigma]\,. \tag{5.8}$$

Under gauge transformations, $\Sigma_{nm} \mapsto U_m \Sigma_{mn} U_n^\dagger$, where U_n is a $U(2)$ gauge transformation on layer n. It can be understood as a Hubbard-Stratonovich field associated with the order parameter, $\phi^\dagger_m\phi_n$. We choose the potential $V[\Sigma]$ such that

$$\langle\Sigma_{mn}\rangle = M_{mn}\,\mathbf{1}_2\,, M_{mn} \neq 0\,,\; M_{nn} > 0\,, \det M > 0\,, \tag{5.9}$$

where $\mathbf{1}_2$ is the 2×2 identity matrix in color space and M_{mn} is a constant Hermitian matrix. In the resulting ground state, the ϕ_n fields are individually gapped, while the clustering order parameter, $\phi^\dagger_m\phi_n$ is condensed.

Because Eq. (5.9) is invariant under gauge transformations where $U_1 = U_2 = U_3$, the gauge group is broken as $U(2) \times U(2) \times U(2) \to U(2)$, Higgsing gauge field configurations except for those with $a_1 = a_2 = a_3 \equiv a$. As a result, the CS terms for each of the a_n gauge fields add, leading to a $U(2)_3$ theory,

$$\mathcal{L}_{U(3)_3}[a, A] = 3\,\mathcal{L}_{\text{CS}}[a] + \frac{1}{2\pi}Ad\,\text{Tr}[a]\,. \tag{5.10}$$

Computing the Hall response by integrating out $\text{Tr}[a] = \text{Tr}[\tilde{a}\mathbf{1}_2] = 2\tilde{a}$, one finds that the total filling fraction is now $\nu = 2/3$, rather than $\nu = 6$. The change in the filling fraction is related to our choice of charge assignments in Eq. (5.4), which results in the unit coefficient of the BF term in Eq. (5.10). While in the

decoupled trilayer theory this choice of signs was immaterial, upon clustering the EM charge densities on each layer, $\rho_n = \varepsilon_{ij}\partial^i \mathrm{Tr}[a_n^j]/2\pi$, $i,j = x,y$, are pinned as $\rho_1 = \rho_3 = -\rho_2$, thereby breaking the discrete symmetry exchanging the layers and altering the filling fraction. The resulting minimal EM charge will prove crucial to obtaining the Fibonacci state.

The Fibonacci state, Eq. (5.7), is a *descendant* of the $U(2)_3$ state at $\nu = 2/3$. To see this, we attach a single unit of flux to the "electrons," the charges which couple to the background EM vector potential, A_μ, and are understood to be the vortices of $\mathrm{Tr}[a]$ in the variables of Eq. (5.10). Since in our starting theory, Eq. (5.1), the EM charges are fermions, flux attachment shifts their statistics and renders the fundamental EM charges bosonic. Explicitly, introducing an Abelian statistical gauge field, b, we have

$$\mathcal{L} = \mathcal{L}_{U(3)_3}[a,b] + \frac{1}{4\pi} b db + \frac{1}{2\pi} b dA + \frac{1}{4\pi} A dA \,. \tag{5.11}$$

Integrating out b, one immediately finds the Lagrangian in Eq. (5.7), which displays a $\nu = 2$ Hall response. We have therefore found, using a combination of flux attachment and interlayer clustering, a Fibonacci state of bosons at $\nu = 2$.

The flux attachment transformation in Eq. (5.11) transmutes the original electric charges, which are fermions, to bosons, but it also mixes the three layers of the parent model, Eq. (5.1). A more physically transparent approach, which also leads to a Fibonacci state at $\nu = 2$, proceeds by first attaching a positive flux to each electron on the first and third layers of the theory in Eq. (5.1) while attaching a negative flux to each electron on the second layer, explicitly breaking the layer exchange symmetry outright and leading to the parent theory depicted in Fig. 5.1(b). On the first and third layers, this results in theories of electrically charged Wilson-Fisher bosons on top of a $\nu = -2$ IQH state. On the second layer, however, this leads to Wilson-Fisher bosons coupled to the Halperin $(2,2,1)$ CS gauge theory at filling $\nu = +2/3$. We show in Appendix C.1 that clustering of composite vortices starting from this trilayer state leads to a Fibonacci FQH state. We note that the Halperin $(2,2,1)$ state has appeared as a parent state for the Fibonacci order in related constructions [231, 238].

Using this bosonic parent description of Fig. 5.1(b), the final Landau-Ginzburg theory of the Fibonacci state can be expressed in terms of the clustering order parameter, Σ, after integrating out the composite vortices, ϕ, and the auxiliary gauge fields associated with flux attachment,

$$\begin{aligned}\mathcal{L} = &\sum_{m,n} \mathrm{Tr}\left[|\partial \Sigma_{mn} - i a_m \Sigma_{mn} + i \Sigma_{mn} a_n|^2\right] + \sum_n \mathcal{L}_{\mathrm{CS}}[a_n] \\ &+ \sum_n (-1)^n \left(\frac{1}{4\pi}\mathrm{Tr}[a_n] d\,\mathrm{Tr}[a_n] + \frac{1}{2\pi} A d\,\mathrm{Tr}[a_n]\right) - V_r[\Sigma]\,.\end{aligned} \tag{5.12}$$

where the first term is a kinetic term generated by quantum corrections due to integrating out ϕ, and V_r is the renormalized potential for Σ. The trace is again over color indices. The phase diagram can be understood as follows. For $\langle\Sigma\rangle = 0$, the theory consists of three decoupled layers: two IQH insulators and a single Halperin $(2,2,1)$ layer. For $\langle\Sigma\rangle = M \neq 0$, the theory finds itself in a phase with Fibonacci topological order.

Furthermore, one can identify the Fibonacci anyons with gapped degrees of freedom in the Landau-Ginzburg theory; namely, the excitations of the adjoint bilinear of composite vortices, $\phi^\dagger t^a \phi$, where t^a are the generators of $SU(2) \subset U(2)$. This can be observed from the fact that this operator transforms in the spin-1 representation of the gauge group and has vanishing electric charge, both properties of the Fibonacci anyon. Note that while the ϕ fields possess a layer index, in the Fibonacci state this does not lead to any unwanted degeneracy due to the condensation of $\langle\phi_m^\dagger \phi_n\rangle$, and so there is only one Fibonacci anyon.

5.4 Fibonacci Wave Function

Having developed an effective field theory that provides a concrete dynamical mechanism for how the Fibonacci state may be realized in a bosonic system at $\nu = 2$, we now seek to develop an ideal wave function, which until now has also proven elusive. Ideal wave functions encode information about the clustering properties of electrons in non-Abelian states and can be compared with numerically obtained ground states in order to identify the topological order realized in realistic Hamiltonians. Remarkably, the wave function we will obtain displays a number of physical features that parallel the above effective field theory construction.

To obtain a wave function, we employ the standard conformal field theory (CFT) approach, in which the wave function is constructed in terms of correlation functions of the edge $(G_2)_1 \cong U(2)_{3,1}$ Wess-Zumino-Witten (WZW) CFT, $\Psi(\{z_i^\sigma\}) = \langle \prod_{i=1}^N \Psi_\sigma(z_i^\sigma)\rangle$ [1]. Here, $z_i^\sigma = x_i^\sigma + i y_i^\sigma$ are the complex coordinates of the electrons, $\sigma = 1, \ldots, n_f$ a type of "flavor" index, $n_f N$ is the number of electrons, and $\Psi_\sigma(z_i)$ are operators in the CFT. Physically, $\Psi_\sigma(z)$ represents an electron operator and can in general be written as the product $\Psi_\sigma(z) = \chi_\sigma(z) e^{i\varphi(z)/\sqrt{\nu}}$, where ν is the filling fraction and φ is a compact boson. The $\chi_\sigma(z)$ operators are electrically neutral. From Eq. (5.6), we observe that for the case at hand the χ_σ's are operators in the $SU(2)_3$ CFT, and $e^{i\varphi/\sqrt{\nu}}$, with $\nu = 2$, is an operator in the $U(1)_2$ CFT.

The first step in constructing a wave function is therefore to determine the electron operators, Ψ_σ. We claim that the appropriate choice of electron operators is

$$\Psi_\uparrow \equiv \psi_2 e^{i\phi/\sqrt{6} + i\varphi/\sqrt{2}}, \quad \Psi_\downarrow \equiv \psi_1 e^{-i\phi/\sqrt{6} + i\varphi/\sqrt{2}}. \tag{5.13}$$

Here we have made use of the fact that operators in the $SU(2)_3$ CFT can be expressed as products of vertex

operators of another compact boson, ϕ, and so-called $\mathbb{Z}_3$ parafermions [239], ψ_1 and ψ_2, which satisfy the operator product expansions (OPEs),

$$\begin{aligned}\psi_1(z)\psi_1(z') &\sim (z-z')^{-2/3}\psi_2(z') + \dots \text{ (same for } 1 \leftrightarrow 2)\\ \psi_1(z)\psi_2(z') &\sim (z-z')^{-4/3} + \dots .\end{aligned} \tag{5.14}$$

The choice of the *two* electron operators (labeled by "spin" $\uparrow$ / $\downarrow$) in Eq. (5.13) is motivated by the effective field theory construction discussed above. Indeed, the $(2,2,1)$ Halperin state involved in the parent state in Fig. 5.1(b) has two species of vortices satisfying a $\mathbb{Z}_2$ exchange symmetry and is commonly understood as a bilayer state; the remaining two layers in Fig. 5.1(b) are topologically trivial. We therefore anticipate that the Fibonacci wave function "knows" about this exchange symmetry and choose electron operators as such.

More formally, the need for two electron species arises from the fact that the electron operators must correspond to generators of the $(G_2)_1$ current algebra, all of which represent local excitations. These can be labeled by the twelve roots of G_2, of which two are linearly independent. This suggests that we should have two distinct electron operators, as is the case for other FQH wave functions based on rank-two Lie algebras [69,160,214]. Following Refs. [69,214], we require that our choice of electron operators is such that they have the same electric charge and opposite $SU(2)$ spin. The first requirement is satisfied via the two $e^{i\varphi/\sqrt{2}}$ factors; the second by the fact that their $SU(2)_3$ factors are conjugate to one another. The details of the construction of these electron operators is somewhat technical, and so are relegated to Appendix C.3.

The Fibonacci wave function can thus be written as a $2N$-point correlation function of the $\Psi_{\uparrow/\downarrow}$ operators. The correlators of the vertex operators can be explicitly evaluated, and so we obtain (up to an overall Gaussian factor),

$$\Psi(\{z_i, w_i\}) = \langle \prod_{i=1}^{N} \psi_2(z_i)\psi_1(w_i)\rangle \prod_{i,j}(z_i - w_i)^{1/3} \prod_{i<j}(z_i - z_j)^{2/3} \prod_{i<j}(w_i - w_j)^{2/3}, \tag{5.15}$$

where z_i (w_i) labels the position of the up (down) "spin." This formal expression encodes key properties of the Fibonacci state. Indeed, the highest power of z_1 appearing in the factors multiplying the parafermion correlator is $2N(1/2)$, yielding a filling fraction of $\nu = 2$, consistent with our field theory construction. Additionally, one can use Eq. (5.14) to see that the wave function satisfies the same three-body clustering as the $\mathbb{Z}_3$ RR wave function [65] separately in each of the z_i and w_i coordinates, dovetailing with our description in terms of clustering of composite vortices. These parallels between our proposed wave function and our dynamical construction above are encouraging, giving us confidence that Eq. (5.15) does indeed describe

the Fibonacci state.

As we show in Appendix C.4, by using Eq. (5.14) to point-split ψ_2 into a product of ψ_1's, one can explicitly evaluate the above parafermion correlator to express Eq. (5.15) as

$$\Psi(\{z_i, w_i\}) = \frac{\Psi_{RR}^{k=3}(\{z_i, z_i, w_i\})}{\prod_{i<j}(z_i - z_j)^2 \prod_{i,j}(z_i - w_j)}, \tag{5.16}$$

where $\Psi_{RR}^{k=3}(\{z_i, z_i, w_i\})$ is the bosonic $\nu = 3/2$ RR wave function for $3N$ particles, with the coordinates of N pairs of particles set equal to one another. The apparent asymmetry in z_i and w_i is an artifact of choosing to point-split the ψ_2's. A manifestly symmetric wave function can be obtained via symmetric combination with the wave function obtained by point-splitting the ψ_1's. Note that while the wave function exhibits a simple pole as we bring $z_i \to w_i$, we expect that this short-distance singularity can be regularized without altering the topological properties of the wave function.

5.5 Discussion

In this Chapter, we have presented both a field-theoretic construction of the bosonic Fibonacci state at $\nu = 2$ based on non-Abelian composite particle dualities, as well as an explicit wave function for this state. Our construction involves a parent trilayer system, in which the Fibonacci state is realized via clustering of dual "composite vortices" coupled to fluctuating $U(2)$ gauge fields. Leveraging this construction, we obtain a wave function for the Fibonacci state sharing many of the physical properties of our field-theoretic construction. Our approach can therefore be used to generate many other exotic states in need of a microscopic construction, as well as to motivate their wave functions.

Unlike other non-Abelian states, short-distance constructions of the Fibonacci state, particularly in isotropic systems, have proven elusive. The fact that our construction is based on a parent state involving fairly germane bosonic FQH phases suggests that a Fibonacci state may be realizable in the laboratory. Furthermore, the fact that the wave function for the $\nu = 2$ bosonic Fibonacci state is manifestly holomorphic clearly suggests that it should be the ground state of a local Hamiltonian projected into a Landau level, and we hope that our wave function will motivate numerical studies in this direction. Additionally, going forward, it will be of interest to construct a transparent fermionic analogue of the bosonic Fibonacci state presented here, which would reproduce the fermionic Fibonacci state to be discussed in Chapter 6.

One may ask whether a different choice of electron operators would have yielded an equally reasonable candidate wave function. In particular, the $\Psi_{\uparrow/\downarrow}$ operators we defined are part of an $SU(2)$ quartet. For example, the wave function one obtains by choosing the other pair of operators within this quartet as the

electrons describes the *Abelian* Halperin $(2, 2, -1)$ state. While it is possible to obtain this state from our parent trilayer theory, it would be interesting to explore how different choices of electron operator in the CFT language may represent different parts of the bulk phase diagram.

Chapter 6

Non-Abelian Fermionization and the Landscape of Quantum Hall Phases

6.1 Introduction

Employing recently proposed Chern-Simons-matter field theory dualities, which we will review again shortly, we demonstrated in the proceeding two Chapters how one can construct Landau-Ginzburg theories describing the emergence of a host of non-Abelian fractional quantum Hall (FQH) states – namely, the Read-Rezayi, generalized non-Abelian spin singlet, and Fibonacci states – from a parent Abelian theory. A key feature of our approach is that the parent Abelian theory is described by a composite particle theory. The dualities we use then allow us to develop a picture of the *dynamics* underlying the emergence of these non-Abelian states, which turns out to rest on the clustering of bosonic objects we called "composite vortices". However, this is in some sense only half of the story, as the Chern-Simons-matter dualities of Eqs. (4.13)-(4.15) [see also Eqs. (6.2)-(6.4) below] often relate the bosonic composite vortex theories used in our Landau-Ginzburg theories of Chapter 4 to theories of composite *fermions* coupled to non-Abelian Chern-Simons gauge fields. This naturally leads one to wonder whether the non-Abelian phases found in Chapter 4 (or other non-Abelian states) are easily accessed within these dual composite fermion variables. As a capstone to our program of developing composite particle theories of non-Abelian FQH states, one goal of the present Chapter is to address this question. In pursuit of this question, we will in fact find a scheme by which these dualities allow us to make general claims about the phase diagrams of these composite fermion theories.

In order to set some context, we begin by first recapitulating the philosophy of the construction presented in Chapter 4. We developed Landau-Ginzburg theories for a large class of non-Abelian states which are related to Abelian composite particle theories via recently proposed Chern-Simons-matter theory dualities [68]. Motivated by the equivalence of $U(N)_k$ Chern-Simons theories coupled to gapless complex bosons and $SU(k)_{-N}$ theories coupled to gapless Dirac fermions in the 't Hooft (large-N, k) limit [66, 67], these dualities relate theories of gapless bosons or fermions coupled to Chern-Simons gauge theories in a manner

This Chapter is adapted from Hart Goldman, Ramanjit Sohal, and Eduardo Fradkin, Non-Abelian fermionization and the landscape of quantum Hall phases, Phys. Rev. B 102, 195151 (2020). This paper is also cited as Ref. [19] in this thesis.

which parallels the established level-rank dualities of pure Chern-Simons theories [188–190, 199]. Of these dualities, several relate theories with Abelian and non-Abelian gauge groups, meaning that they represent dualities between the conventional composite boson Landau-Ginzburg theories for certain Abelian FQH states and theories of dual bosons coupled to non-Abelian Chern-Simons gauge fields.[1] By stacking multiple copies of these Abelian states and introducing pairing in the dual non-Abelian composite boson language, we showed that one can access the Read-Rezayi [65] and generalized non-Abelian spin singlet states [69, 70, 192] in Chapter 4 as well as the Fibonacci state in Chapter 5. The success of this construction stems from the observation that phases naturally accessible by condensing local operators in the non-Abelian dual theory may not be visible in the original Abelian theory, in which these operators correspond to non-local monopole operators.

Lying at the heart of our construction in Chapter 4 was a string of dualities involving the usual Landau-Ginzburg theory for the $\nu = 1/2$ bosonic Laughlin state, a single flavor of Wilson-Fisher boson (describing the Laughlin quasiparticles) coupled to a $U(1)_2$ Chern-Simons gauge field. This theory has three duals,

$$\begin{array}{c} \text{a Wilson-Fisher scalar} + U(1)_2 \longleftrightarrow \text{a Dirac fermion} + SU(2)_{-1/2} \\ \updownarrow \\ \text{a Dirac fermion} + U(1)_{-3/2} \longleftrightarrow \text{a Wilson-Fisher scalar} + SU(2)_1 \,, \end{array} \tag{6.1}$$

where we use $\longleftrightarrow$ to denote duality and subscripts denote the Chern-Simons level (including the parity anomaly). The Abelian boson-fermion duality featured here and others like it were explored in Refs. [161, 162, 202, 203]. While most non-Abelian dualities are boson-fermion dualities, this *quadrality* – in which each of the four theories is dual to the others – is distinguished by its inclusion of non-Abelian boson-boson and fermion-fermion dualities. In Ref. [17], we focused on the non-Abelian boson-boson duality, in which the dual theory consists of non-Abelian bosonic "composite vortices" coupled to a $SU(2)_1$ Chern-Simons gauge field, obtaining the non-Abelian phases via inter-layer pairing of the composite vortices.

In this Chapter, we study the non-Abelian phases accessible to the dual theories of *composite fermions*. Of these, the theory of Dirac fermions coupled to a $U(1)_{-3/2}$ gauge field is a relativistic version of the standard composite fermion description of the $\nu = 1/2$ bosonic Laughlin state, while the theory of Dirac fermions coupled to a $SU(2)_{-1/2}$ gauge field constitutes a different kind of "flux attachment" in which the composite fermions possess charge under a fluctuating non-Abelian gauge field. Using this duality, we

[1] We emphasize here that it is possible for a Chern-Simons gauge theory to have a non-Abelian gauge group but an Abelian braid group, meaning that it represents an Abelian topological phase. For example, $SU(2)_1$ is Abelian in this sense, having the same anyon content as $U(1)_2$ by level-rank duality.

analyze two of the simplest paths to non-Abelian phases:

1. Forming integer quantum Hall (IQH) phases of the $SU(2)$ composite fermions, in analogy with Jain's construction of Abelian FQH phases as IQH states of composite fermions [11] and earlier projective parton constructions of non-Abelian FQH states [158–160].

2. Excitonic pairing between layers of $SU(2)$ composite fermions. This construction is a composite fermion version of the one presented in Ref. [17] for composite bosons.

In both constructions, we will find that the composite fermions yield the $\nu = k/2$ Blok-Wen states with $U(k)_2$ topological order [71], in contrast to the Read-Rezayi states obtained via inter-layer pairing of the $SU(2)$ bosons in Chapter 4. For many of these states, these are the first constructions starting from parent theories of Abelian composite particles, rather than projective parton constructions [159, 160, 175] or more general non-Abelian/non-Abelian dualities [165]. In addition, by considering more general non-Abelian dualities, we find not only the exotic Fibonacci state [6], but also composite fermion descriptions of a variety of non-Abelian states that have previously been understood via pairing instabilities of a composite Fermi liquid, including a new description of the anti-Pfaffian state [240, 241]. Remarkably, we find in these special cases that an IQH phase of the non-Abelian composite fermion theory is *dual* to pairing in the usual Abelian description. Our construction of all of these states using non-Abelian dualities represents the first category of main results of this Chapter.

In addition to revealing paths to different non-Abelian phases, these non-Abelian fermion-fermion dualities possess surprising information about the dynamics of composite fermions, leading to our second main family of results. These results relate to our first construction of the $U(k)_2$ states, in which a magnetic field and chemical potential are adjusted so that the $SU(2)$ composite fermions fill k Landau levels. This leads to a $SU(2)_{-k}$ spin topological quantum field theory (spin TQFT) at low energies, corresponding to $U(k)_2$ topological order by level-rank duality. However, this conclusion is immediately complicated by the duality with the Abelian composite fermion theory, IQH phases of which correspond to the bosonic Jain sequence states. Indeed, there are certain filling fractions ν_* of the underlying electric charges at which *both* types of composite fermions fill up an integer number of Landau levels. On integrating out the fermions in these two theories, one would then be led to conclude that the theory with an Abelian gauge group predicts an Abelian FQH state, while the non-Abelian theory predicts a non-Abelian FQH state. For instance, for a system of bosons at filling $\nu_* = 3/2$, the two theories appear to respectively predict $U(1)_{-2}$ and $U(3)_2$ topological order.

Because $U(3)_2$ and $U(1)_{-2}$ are distinct topological orders and are certainly not dual to one another, one

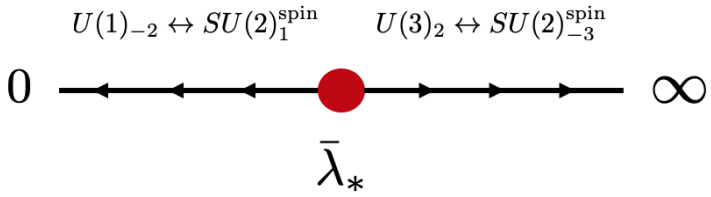

Figure 6.1: Proposed phase diagram for the $SU(2)$ composite fermion theory at filling $\nu = 3/2$. Here $\overline{\lambda} = g_{YM}^2/\omega_c$, where g_{YM}^2 is the Yang-Mills coupling (the fine structure constant) and $\omega_c \sim \sqrt{B}$ is the cyclotron frequency. When $\overline{\lambda} \to \infty$, the Yang-Mills term vanishes, and the picture of deconfined composite fermions filling (color degenerate) Landau levels is valid, leading to the $SU(2)_{-3}^{\text{spin}} \leftrightarrow U(3)_2$ state. When $\overline{\lambda}$ runs small, the Yang-Mills term becomes very large, Landau levels can mix, and the deconfinement of the composite fermions is no longer assured, leading ultimately to the $U(1)_2$ phase predicted in the dual Abelian theory. These states are separated by a critical point at $\overline{\lambda} = \overline{\lambda}_* \sim \mathcal{O}(1)$, which is likely first order.

might naïvely worry that these results signal a breakdown of the dualities, which postulate an equivalence of the infrared (IR) limits, or ground states, of the dual theories. On the other hand, it is very common for states with distinct topological orders to exist at the same filling fraction, with the ultimate choice of ground state depending on details of local energetics. Indeed, in this work we take the view that both topological orders are valid ground states at filling ν_*, and that the particular choice of ground state depends on the order in which the lowest Landau level ($B \to \infty$) and IR limits are taken. This order of limits is subtle, as the duality is only valid in the IR limit, while the statement that the composite fermions form a stable IQH state relies on the $B \to \infty$ limit. More precisely, on tuning the ratio of the Yang-Mills coupling to the cyclotron frequency in the non-Abelian theory, we argue that there is a phase transition between the Abelian and non-Abelian FQH states (see Figure 6.1). Such a transition, if continuous, would be quite exotic, as it would separate two very different topological orders and therefore lie beyond the Landau-Ginzburg paradigm. Thus, when the $U(1)$ composite fermions form an IQH state, the $SU(2)$ composite fermions experience an instability and find themselves on the *Abelian* side of this transition and vice versa.

Even if this transition is first order, our results demonstrate that QFT dualities can be used to infer non-trivial statements about the phase diagrams and dynamics of Chern-Simons-matter theories in the presence of background fields. Indeed, the phenomenon described above is a general feature of fermion-fermion dualities involving non-Abelian gauge groups, and we collect several additional examples. These appear both in the $SU(2)$ quadrality discussed above as well as in other dualities. In particular, we consider the case of the duality between a free Dirac fermion and a Dirac fermion coupled to a $U(N)_{-1/2}$ gauge field. We also comment that the scenario we present is reminiscent of recent proposals for the phase diagram of $SU(N)_k$ Chern-Simons theory with $N_f > 2k$ fermion flavors (at zero density and magnetic field) [242]

and recent follow-up work [243–246], in which it has been suggested that the Yang-Mills term can play a non-trivial role despite superficially appearing irrelevant (in the sense of the renormalization group).

This Chapter is organized as follows. In Section 6.2, we review the non-Abelian Chern-Simons-matter dualities, focusing on the quadrality in Eq. (6.1). In Section 6.3, we present a detailed description of the dual fermionic theories and the properties of their IQH states, and we present the cases in which they appear to predict different topological orders. We then present our proposed scenario for how this state of affairs can be made consistent and provide additional examples of dual fermionic theories displaying similar phenomena. In the process, we uncover an entire series of non-Abelian FQH states, including the anti-Pfaffian [240, 241], which we find can be simultaneously described as arising from IQH states of composite fermions in a non-Abelian theory and from pairing instabilities of a composite Fermi liquid in a dual Abelian theory. In Section 6.4, we demonstrate how the $U(k)_2$ states can be obtained through stacking and excitonic pairing in Abelian FQH states. Finally, we conclude with a discussion of our results and their implications.

6.2 Review of Non-Abelian Dualities and the Landau-Ginzburg Approach

6.2.1 Non-Abelian Dualities and the $\nu = 1/2$ Bosonic Laughlin State

In this section, we first briefly review the dualities relevant to describing the $\nu = 1/2$ bosonic Laughlin state. The recently proposed non-Abelian Chern-Simons-matter dualities relate theories of Wilson-Fisher bosons coupled to a Chern-Simons gauge field to theories of Dirac fermions also coupled to a Chern-Simons gauge field, with the matter content in the fundamental representation of the gauge group. These dualities are schematically given by Eqs. (4.13)-(4.15); for ease of access, we repeat them here:

$$N_f \text{ scalars} + U(N)_{k,k} \quad \longleftrightarrow \quad N_f \text{ fermions} + SU(k)_{-N+N_f/2}\,, \tag{6.2}$$

$$N_f \text{ scalars} + SU(N)_k \quad \longleftrightarrow \quad N_f \text{ fermions} + U(k)_{-N+N_f/2,-N+N_f/2}\,, \tag{6.3}$$

$$N_f \text{ scalars} + U(N)_{k,k+N} \quad \longleftrightarrow \quad N_f \text{ fermions} + U(k)_{-N+N_f/2,-N-k+N_f/2}\,. \tag{6.4}$$

Our conventions and notation concerning non-Abelian Chern-Simons theories are presented in Appendix F.

The dualities, Eqs. (6.2)-(6.4), can be shown to imply the quadrality described in the Introduction [199],

$$\begin{array}{ccc} \text{a scalar} + U(1)_2 & \longleftrightarrow & \text{a fermion} + SU(2)_{-1/2} \\ \updownarrow & & \\ \text{a fermion} + U(1)_{-3/2} & \longleftrightarrow & \text{a scalar} + SU(2)_1 \,. \end{array} \tag{6.5}$$

The first theory (top left) is the relativistic version of the usual Landau-Ginzburg theory for the $\nu = 1/2$ bosonic Laughlin state. Explicitly, it is described by the Lagrangian,

$$\mathcal{L}_\Phi = |D_a \Phi|^2 - |\Phi|^4 + \frac{2}{4\pi} a da + \frac{1}{2\pi} A da \,. \tag{6.6}$$

Here a is an emergent $U(1)$ gauge field; A the background electromagnetic (EM) field; we use the notation $D_a^\mu = \partial^\mu - i a^\mu$ and $adb = \varepsilon^{\mu\nu\lambda} a_\mu \partial_\nu b_\lambda$; and the term $-|\Phi|^4$ denotes tuning to the Wilson-Fisher fixed point. The dual non-Abelian bosonic theory (bottom right) is given by

$$\mathcal{L}_\phi = |D_{u - A\mathbf{1}/2}\phi|^2 - |\phi|^4 + \frac{1}{4\pi} \mathrm{Tr} \left[u du - \frac{2i}{3} u^3 \right] - \frac{1}{2} \frac{1}{4\pi} A dA \,, \tag{6.7}$$

where u is an $SU(2)$ gauge field, $\mathbf{1}$ is the 2×2 identity matrix in color space, and $-|\phi|^4$ again denotes tuning to the Wilson-Fisher fixed point. By turning on mass operators, both theories can be shown to describe the transition between the $\nu = 1/2$ bosonic Laughlin state and the trivial insulator, which correspond to their gapped ($\langle \Phi \rangle = 0$, $\langle \phi \rangle = 0$) and condensed ($\langle \Phi \rangle \neq 0$, $\langle \phi \rangle \neq 0$) phases, respectively. Essential to this conclusion is the fact that $SU(2)_1$, the TQFT obtained when Φ is gapped, is Abelian at the level of the braid group: it is equivalent to $U(1)_2$ by level-rank duality.

The $SU(2)$ theory, $\mathcal{L}_\phi$, served as the main building block in our construction of the Read-Rezayi states in Chapter 4 in which we considered multiple layers of the $\nu = 1/2$ bosonic Laughlin state and introduced an interlayer pairing interaction for the Φ particles. The paired phase of this theory yielded the Read-Rezayi states. However, in that work we did not consider the landscape of non-Abelian phases accessible by dual theories of Dirac fermions, which we now turn to.

6.2.2 A Comment on Level-Rank Duality and Topological Orders of Fermions

Before describing the composite fermion theories of interest, we mention here a subtlety that arises when considering topological orders of composite fermions. When assessing the anyon content of the corresponding gauge theory, it is necessary to account for the the fact that the degrees of freedom charged under the gauge

field are fermions, which affects the statistics of certain anyons by a minus sign. More technically, this is a result of the fact that gauge fields which couple to fermions are spin (actually spin$_c$, see Appendix F) connections, as opposed to the $U(1)$ connections that couple to bosons. We will refer to such gauge fields throughout this Chapter as spin gauge fields, and we will denote their associated TQFTs with the superscript 'spin.' In general, level-rank duality can be thought of as relating a TQFT with a spin gauge field (spin TQFT) to one with a $U(1)$ gauge field.[2] Therefore, since composite fermion theories give rise to spin TQFTs, we will frequently invoke level-rank duality below and refer to a state's topological order via its corresponding (non-spin) TQFT. For example, if a composite fermion theory yields a $SU(2)^{\text{spin}}_{-k}$ TQFT, we will refer to the associated topological phase by its level-rank dual, $U(k)_2$.

This formal discussion has physical implications. For example, consider the topological order of the $\nu = 1/2$ Laughlin state. The anyons of this state are semions, with $\pi/2$ statistics. This state can be equally well described by a $U(1)_2$ TQFT or a $U(1)_{-2}$ TQFT with a spin gauge field, which we will denote $U(1)^{\text{spin}}_{-2}$. As we will see below, this theory arises on integrating out a Landau level of composite fermions. While it appears that the anyons in this theory are antisemions (statistics $-\pi/2$), the π statistics of the composite fermions converts them into semions. This is a type of level-rank duality, relating $U(1)_2$ to $U(1)^{\text{spin}}_{-2}$. In this sense, level-rank dualities can generally be viewed as boson-fermion dualities, with some interesting exceptions, e.g. in the $SU(2)_1 \leftrightarrow U(1)_2$ duality mentioned above, neither theory is spin.

6.3 Non-Abelian Dualities and the Dynamics of Composite Fermions

6.3.1 The $\nu = 1/2$ Laughlin State and a Non-Abelian Fermion-Fermion Duality

The bosonic theories described above are dual to a theory of Dirac fermions coupled to a $U(1)_{-3/2}$ Chern-Simons gauge field. For clarity, we will refer to this theory as **Theory A**,

$$\mathcal{L}_A = i\overline{\psi}\not{D}_a\psi - \frac{3}{2}\frac{1}{4\pi}ada - \frac{1}{2\pi}adA - \frac{1}{4\pi}AdA + \cdots , \tag{6.8}$$

where a is a $U(1)$ gauge field and we use the notation $\not{D} = D_\mu\gamma^\mu$, where γ^μ are the Dirac gamma matrices. This theory is also dual to a theory of Dirac fermions coupled to a non-Abelian, $SU(2)_{-1/2}$ gauge field,

[2]Level-rank duality can be equivalently formulated to relate two spin-TQFTs by adding an invisible spin-1/2 line (also known in the condensed matter literature as a local spin-1/2 particle) to each side of the duality [199]. This formulation is less physical if we wish to view the fundamental charges at short distances as bosons, so we will refrain from using it.

which we will refer to as **Theory B**,

$$\mathcal{L}_B = i\overline{\chi}\not{D}_{b-A\mathbf{1}/2}\chi - \frac{1}{2}\frac{1}{4\pi}\mathrm{Tr}\left[bdb - \frac{2i}{3}b^3\right] - \frac{1}{4}\frac{1}{4\pi}AdA + \cdots\,, \tag{6.9}$$

where b is an $SU(2)$ gauge field and $\mathbf{1}$ is the 2×2 identity matrix.[3] Here the χ fields transform as a doublet under $SU(2)$, and they have charge $-1/2$ under the global EM symmetry, $U(1)_{\mathrm{EM}}$. The fundamental (unit) charges are therefore the baryons, $\varepsilon_{\alpha\beta}\chi^\alpha\chi^\beta$, where $\alpha,\beta = 1,2$ are $SU(2)$ color indices. Finally, the ellipses refer to irrelevant operators, such as Maxwell or Yang-Mills terms for the gauge fields. These operators are normally dropped since the duality is only valid in the IR limit, in which these operators are taken to zero, and their usual purpose is to provide UV regularization. However, we will see in the sections below that these operators can play important roles in determining low energy physics when background fields are turned on.

Being dual to the bosonic theories discussed in Section 2, **Theory A** and **Theory B** each describe a transition from the $\nu = 1/2$ bosonic Laughlin state, which has $U(1)_2$ topological order, to a trivial insulator. This can be seen by introducing mass terms, $-m_\psi\overline{\psi}\psi$ and $-m_\chi\overline{\chi}\chi$, to their respective theories. For $m_\psi > 0, m_\chi > 0$, integrating out ψ and χ can be seen to immediately yield an insulating state with vanishing Hall conductivity, $\sigma_{xy} = 0$. On the other hand, when $m_\psi < 0, m_\chi < 0$, integrating out the composite fermions yields a state with $\sigma_{xy} = -\frac{1}{2}\frac{1}{2\pi}$ $(m_\psi < 0, m_\chi < 0)$, with **Theory A** yielding a $U(1)^{\mathrm{spin}}_{-2}$ gauge theory and **Theory B** yielding $SU(2)^{\mathrm{spin}}_{-1}$. These constitute the same topological order as the $U(1)_2$ state by level-rank duality.

By differentiating this pair of Lagriangians with respect to the background EM gauge field, A_μ, to obtain the global EM charge current, J^μ, one observes that, under the duality, the monopole current of **Theory A** is related to the baryon number current of **Theory B**,

$$J^\mu_e = \frac{1}{2\pi}\varepsilon^{\mu\nu\lambda}\partial_\nu(a_\lambda - A_\lambda) \leftrightarrow -\frac{1}{2}j^\mu_\chi - \frac{1}{2}\frac{1}{2\pi}\varepsilon^{\mu\nu\lambda}\partial_\nu A_\lambda\,, \tag{6.10}$$

where $j^\mu_\chi = \overline{\chi}\gamma^\mu\chi$ is the χ charge current of the **Theory B**. The interpretation of this dictionary is analogous to charge-vortex duality [209,210]: flux of the gauge field a in **Theory A** maps to charge of the χ fermions in **Theory B**. The same interpretation applies to the pair of bosonic theories discussed in the previous Section.

[3] As in the preceding chapters of this thesis, we approximate the Atiyah-Patodi-Singer η-invariant as a level-$\frac{1}{2}$ Chern-Simons term and explicitly include it in the Lagrangian.

6.3.2 Abelian and Non-Abelian Jain Sequences

In contrast to their bosonic counterparts, these composite fermions each satisfy the Pauli exclusion principle. As a result, it is natural to consider the gapped phases accessible by filling up Landau levels and forming IQH states, in analogy to the construction of the Jain sequences, in which FQH phases are obtained as IQH states of composite fermions [11]. In particular, integer quantum Hall states of the $SU(2)$ doublet composite fermions, χ, can be expected to yield non-Abelian topological orders. This method of forming non-Abelian quantum Hall phases appears to be quite natural, but we will quickly learn that the non-Abelian dualities imply that things are not so simple, and the ultimate choice of ground state will be sensitive to the order in which the lowest Landau level and IR limits are taken.

To this end, we begin by relating the electronic filling fraction, ν, to the filling fractions of the ψ and χ fermions using the dictionary, Eq. (6.10). Focusing first on the Abelian **Theory A**, the physical electric charge density is given in terms of the magnetic flux felt by the composite fermions,

$$\rho_e = \left\langle J_e^0 \right\rangle = -\frac{1}{2\pi}\langle \varepsilon^{ij}\partial_i a_j\rangle - \frac{1}{2\pi}B, \tag{6.11}$$

where $B = \varepsilon^{ij}\partial_i A_j$ is the background magnetic field. We use brackets here to emphasize that that we define ρ_e to be the expectation value of the charge density operator. We can relate ρ_e to the composite fermion charge density through the equation of motion for a_0,

$$0 = \langle \psi^\dagger \psi\rangle - \frac{3}{4\pi}\langle \varepsilon^{ij}\partial_i a_j\rangle - \frac{1}{2\pi}B\,, \tag{6.12}$$

If we define the composite fermion filling fraction of **Theory A** to be

$$\nu_\psi = 2\pi\,\frac{\langle \psi^\dagger\psi\rangle}{\langle \varepsilon^{ij}\partial_i a_j\rangle}, \tag{6.13}$$

we obtain a relation between the composite fermion and electronic filling fractions,

$$\nu = -2\pi\,\frac{\rho_e}{B} = \frac{\nu_\psi - 1/2}{\nu_\psi - 3/2}\,. \tag{6.14}$$

Note that we have absorbed a minus sign into the definition of ν for notational convenience. From this formula, we see that IQH states of the ψ fermions, which occur at fillings $\nu_\psi = p - 1/2$, correspond to the

known (descendent) bosonic Jain sequence states,

$$\nu_p = \frac{p-1}{p-2}\,,\; p \in \mathbb{Z}\,. \tag{6.15}$$

Indeed, integrating out the composite fermions yields the Lagrangian,

$$\mathcal{L}_{A,\text{eff}} = \frac{p-2}{4\pi} ada - \frac{1}{2\pi} adA - \frac{1}{4\pi} AdA. \tag{6.16}$$

Each of these states (with the exception of the states at $p = 1, 2$, which are respectively a trivial insulator and a superfluid) is an Abelian FQH phase of the physical charges, which here are bosons.

The same type of analysis can be carried out for **Theory B**, leading to a non-Abelian version of the bosonic Jain sequence. Recalling Eq. (6.10), the electric charge density is directly related to the density of χ fermions, $\chi^\dagger\chi$, via

$$\rho_e = -\frac{1}{2}\langle\chi^\dagger\chi\rangle - \frac{1}{4}\frac{1}{2\pi}B. \tag{6.17}$$

Because the χ fermions are coupled to a Chern-Simons gauge field, they do not confine, meaning that a non-zero magnetic field, B, will cause them to form Landau levels with degeneracy,

$$d_{LL} = \frac{BA}{2\pi} \times |q_\chi| \times (\text{color degeneracy}) = \frac{BA}{2\pi}\,, \tag{6.18}$$

where A in this expression is the area of the system and $q_\chi = -1/2$ is the EM charge of the χ fermions. Therefore, the filling fraction of the χ fermions is

$$\nu_\chi = 2\pi\,\frac{\langle\chi^\dagger\chi\rangle}{B}\,. \tag{6.19}$$

Plugging this into Eq. (6.17) yields a relation between ν and ν_χ,

$$\nu = \frac{1}{2}\nu_\chi + \frac{1}{4}. \tag{6.20}$$

When the χ fermions fill an integer number of Landau levels, $\nu_\chi = s - 1/2$, and the filling of the physical charges is

$$\nu_s = \frac{s}{2}\,, s \in \mathbb{Z}\,. \tag{6.21}$$

On integrating out the composite fermions, one obtains a $SU(2)^{\text{spin}}_{-s}$ theory with Lagrangian,

$$\mathcal{L}_{B,\,\text{eff}} = -\frac{s}{4\pi}\text{Tr}\left[bdb - \frac{2i}{3}b^3\right] - \frac{s}{2}\frac{1}{4\pi}AdA\,, \tag{6.22}$$

which describes a non-Abelian, $U(s)_2$, topological order when $|s| > 1$. This approach recalls earlier approaches to non-Abelian FQH states using parton constructions [158–160]. However, unlike in those cases, in which the elctron operator is fractionalized by hand and it is necessary to require that the partons do not confine by fiat, here the duality provides a clear basis for the presence of a (deconfining) non-Abelian gauge field.

Having obtained the sequences of incompressible filling fractions associated with **Theory A** and **Theory B**, one can immediately observe several special (non-trivial) filling fractions, ν_*, at which *they coincide*, indicating the presence of competing ground states. Comparing Eqs. (6.15) and (6.21), these fillings occur when $\nu_p = \nu_s = \nu_*$, i.e.

$$s = 2\left(1 + \frac{1}{p-2}\right)\,,\; p, s \in \mathbb{Z}. \tag{6.23}$$

Here we recall that p and s are the number of Landau levels filled by the ψ and χ fermions, respectively. This equation has several solutions, which are organized in Table 6.1. Two of these solutions, $(p = 1, s = 0)$ and $(p = 0, s = 1)$, respectively correspond to the $\nu = 1/2$ bosonic Laughlin state, which has $U(1)_2 \leftrightarrow SU(2)^{\text{spin}}_{-1}$ topological order. This is consistent with the fact that at criticality these theories describe a plateau transition between these states.

It is the presence of other solutions, at $(p = 3, s = 4)$ and $(p = 4, s = 3)$, corresponding to $\nu_* = 2$ and $\nu_* = 3/2$ respectively, that reveals new physics. On the one hand, **Theory A** predicts the $\nu_* = 3/2$ and $\nu_* = 2$ states to have $U(1)_{-2}$ and $U(1)_1$ (i.e. trivial) topological orders. On the other hand, **Theory B** predicts the *same* states to have *non-Abelian* $SU(2)^{\text{spin}}_{-3} \leftrightarrow U(3)_2$ and $SU(2)^{\text{spin}}_{-4} \leftrightarrow U(4)_2$ topological orders. While it is common in quantum Hall physics for different competing states to be proposed for the same filling fraction, the duality of **Theory A** and **Theory B** identifies the two theories' ground states. Therefore, the consistency of the duality implies that the conditions under which the ψ fermions form an IQH state are not the same as those of the χ fermions, and the two possible states must be separated by a phase transition. A theory of this phase transition requires short-distance dynamical information not specified by, but consistent with, the duality. We now present a possible scenario for a transition of this kind.

Table 6.1: Solutions to Eq. (6.23), in which both the ψ and χ composite fermions form IQH states at special electronic filling fractions, ν_*. Also indicated are the topological orders predicted by the dual theories for each filling.

ν_*	0	$\frac{1}{2}$	$\frac{3}{2}$	2
$\nu_\psi + 1/2$	1	0	4	3
$\nu_\chi + 1/2$	0	1	3	4
Theory A	Trivial	$U(1)_2$	$U(1)_{-2}$	IQH
Theory B	Trivial	$U(1)_2$	$U(3)_2$	$U(4)_2$

6.3.3 Dynamical Scenario

We now provide a possible explanation of the physics occurring at the special filling fractions $\nu_* = 3/2, 2$. For now, we will work from the point of view of the non-Abelian **Theory B**, and we will begin by considering what happens as we fill Landau Levels. From Table 6.1, we see that filling the zeroth and first Landau Levels of the χ fermions corresponds to the expected trivial insulator ($\nu = 0$) and bosonic Laughlin ($\nu = 1/2$) states. What occurs when the non-Abelian composite fermions fill two Landau levels is also quite non-trivial, but we will table that discussion until the next subsection. For now, our concern will be what happens when we fill the third Landau level, corresponding to $\nu_* = 3/2$. Our proposal for $\nu_* = 2$ will prove to be essentially identical. At $\nu_* = 3/2$, **Theory B** predicts an incompressible state with $SU(2)^{\text{spin}}_{-3} \leftrightarrow U(3)_2$ topological order, while **Theory A** predicts $U(1)_2$. This suggests that it should be possible to trigger an instability in the non-Abelian theory as we fill this Landau level, which preempts the $U(3)_2$ topological order and yields the same Abelian phase predicted by **Theory A** (and vice versa). Consequently, both the $U(1)_2$ and $U(3)_2$ phases must exist in the $\nu = 3/2$ phase diagram. This is the only state of affairs consistent with the duality.

How might such an instability occur? It is here that the ellipses in Eqs. (6.8) and (6.9) become crucial.[4] These ellipses include operators that are irrelevant at tree level but may nevertheless play an important role in determining the low energy physics when a magnetic field and chemical potential are introduced. Indeed, there is no sense in which such fields are ever perturbative, as they reorganize the spectrum of a theory in dramatic ways. To make this discussion more precise, consider the Yang-Mills term in **Theory B**,

$$\mathcal{L}_{YM} = -\frac{1}{2g_{YM}^2}\,\mathrm{Tr}[f_{\mu\nu}f^{\mu\nu}]\,, \tag{6.24}$$

where $f_{\mu\nu} = \partial_\mu b_\nu - \partial_\nu b_\mu - i[b_\mu, b_\nu]$ is the field strength of the $SU(2)$ gauge field, b. At tree level, the mass dimension of the operator $\mathrm{Tr}[f^2]$ is 4, meaning that $[g_{YM}^2] = 1$: it is an energy scale. Commonly, the IR

[4] We thank Chong Wang for enlightening discussions on this point.

limit in which the duality of Eqs. (6.8) and (6.9) holds is phrased as the limit $g_{YM}^2 \sim \Lambda \to \infty$, where Λ is a UV cutoff, but strictly speaking this is only true in the absence of a background magnetic field, which provides its own energy scale in the form of the cyclotron frequency, $\omega_c \sim \sqrt{B}$ (for massless Dirac fermions).

Consequently, one can form a dimensionless coupling,

$$\overline{\lambda} = \frac{g_{YM}^2}{\omega_c}\,, \tag{6.25}$$

that can have non-trivial running as a result of strong interaction effects. This would mean that the ground state ultimately chosen by **Theory A** can depend on the order of the limits, $g_{YM}^2 \to \infty$ and $\omega_c \to \infty$. Importantly, one order of limits in **Theory B** may not correspond to an analogous order of limits in **Theory A**. In other words, **Theory B** may be in a strongly coupled regime ($0 \leq \overline{\lambda} < \infty$) while **Theory A** may behave as if all of the irrelevant operators have been taken to zero prior to taking $\omega_c \to \infty$.

This is the essence of our proposal[5] for the phase diagram of **Theory B**, shown schematically in Fig. 6.1. Whether the theory is in the $U(3)_2$ or $U(1)_2$ phase is determined by the value of $\overline{\lambda}$, with the two phases being separated by a phase transition at a value $\overline{\lambda} = \overline{\lambda}_* \sim \mathcal{O}(1)$. For $\overline{\lambda} > \overline{\lambda}_*$, $\overline{\lambda}$ runs large, corresponding to the limit $g_{YM}^2 \to \infty$ followed by $\omega_c \to \infty$. In this phase, the Yang-Mills term disappears, leaving the Chern-Simons term, which ensures that the composite fermions, χ, are deconfined. It is in this regime that we expect the picture described in the previous subsection of deconfined χ fermions filling Landau levels to hold, making this the phase with $U(3)_2$ topological order. On the other hand, for $\overline{\lambda} < \overline{\lambda}_*$, we propose that $\overline{\lambda}$ runs small. Here the Yang-Mills term becomes important, and the assumption of deconfined composite fermions breaks down: the Landau levels mix. As a result, the composite fermions will tend to form bound states that are neutral under $SU(2)$: the baryons, $\varepsilon_{\alpha\beta}\chi^\alpha\chi^\beta$. These are bosons of charge -1 since the fermions are doublets under $SU(2)$. Being the physical electric charges in this theory, these bosonic baryons will find themselves at filling $\nu = 3/2$, and the resulting topological order will ultimately be $U(1)_2$, as predicted by **Theory A**. Note that this final conclusion is conjecture based on the consistency of the duality – the physics in such a phase is very strongly coupled, and we cannot show explicitly that this is the true ground state. We also point out that $\overline{\lambda}$ may not run to zero in this phase, instead running to a small but finite value. This represents a very interesting but theoretically daunting possibility.

We now comment on what occurs in the dual description of **Theory A**, in which we can define a similar running coupling[6], $\overline{\lambda}_A = g_{\text{Maxwell}}^2/\omega_c$, where g_{Maxwell} is the coupling associated with the Maxwell term for

[5] We emphasize that while we focus on the example of the Yang-Mills term, there are many other operators that might be responsible for the behavior we propose, and it may be more correct to consider a linear combination of these operators as being responsible. Another likely family of examples is four-fermion operators, which have the same tree level dimension as the Yang-Mills operator.

[6] Note that unlike the fermions of **Theory B**, the magnetic field felt by the ψ fermions depends both on the background

the $U(1)$ gauge field, a. In this theory, the limit $\overline{\lambda}_A \to \infty$ corresponds to the $U(1)_2$ (IQH) state at filling $\nu_* = 3/2$ ($\nu_* = 2$), as the Maxwell term vanishes. However, since the Maxwell term is not dual to the Yang-Mills term, it is not clear whether the phase transitions described for **Theory B** correspond to transitions tuned by $\overline{\lambda}_A$ or another coupling, such as one associated with a linear combination of four-fermion operators. Nevertheless, unless $\overline{\lambda}_* = \infty$ in **Theory B** (in which case the non-Abelian phase is nowhere stable, having no basin of attraction), the duality indicates that the non-Abelian states should be accessible to **Theory A** as well, and that these transitions should also be present in that theory.

6.3.4 Comments on the Nature of the Transition

The nature of the transition between these phases depends on microscopic details, and it is not immediately clear how to study the strongly coupled physics when $\overline{\lambda} \sim \mathcal{O}(1)$. One exciting possibility is that the phase transition is continuous, which would exist beyond the Landau paradigm since it separates two distinct topological orders. Furthermore, this would imply the existence of an unstable conformal field theory (CFT) fixed point, which we expect would be quite exotic and perhaps involve emergent symmetries. In the spirit of universality, we attempt here to write down the simplest possible theory of such a transition. The theory we find consists of $N_f = 4$ flavors of electrically neutral Dirac fermions, ξ_i, coupled to a $SU(2)^{\text{spin}}_{-1}$ Chern-Simons gauge field, c,

$$\mathcal{L} = \sum_{i=1}^{N_f=4} \overline{\xi}_i (i \not{D}_c - m_\xi) \xi_i - \frac{1}{4\pi} \text{Tr} \left[cdc - \frac{2i}{3} c^3 \right] - \frac{3}{2} \frac{1}{4\pi} AdA \,. \tag{6.26}$$

We emphasize that the fields ξ and c need not have any local relationship with the fields in **Theory A** nor **Theory B**. This theory has a $U(4)$ global symmetry rotating the fermion flavors. For $m_\xi \gg 0$, the theory is in the Abelian, $SU(2)^{\text{spin}}_{+1} \leftrightarrow U(1)_{-2}$ phase, and for $m_\xi \ll 0$ the theory is in the non-Abelian, $SU(2)^{\text{spin}}_{-3} \leftrightarrow U(3)_2$ phase. While the flavor index can be interpreted as a kind of Landau level index, there is no *a priori* reason for this symmetry to be enforced, rendering this theory at best a multicritical point. What's more, this theory has $N_f > 2|k| = 2$, meaning that it falls outside of the Chern-Simons-matter dualities of Eqs. (6.2)-(6.4) and may spontaneously break the flavor symmetry at small values of m_ξ [242]. We therefore find the presence of a direct second-order transition unlikely, and we conjecture that any other possible CFT with these two phases also has an enlarged set of global symmetries compared to the underlying UV problem.[7] We also conjecture that this is the case for the other transitions discussed in this work.

Therefore, it is perhaps more natural to expect the mundane scenario in which the two phases are

chemical potential and magnetic field, so ω_c is not precisely the Landau level gap, which is determined by $\langle \varepsilon^{ij} \partial_i a_j \rangle$.

[7] While one may also wish to consider theories with bosonic matter, we note that it is not possible to condense bosonic operators to transition between $U(3)_2$ and $U(1)_{-2}$ due to the difference in the signs of the level. This cannot be repaired with level-rank duality because the $U(1)_{-2}$ gauge field is not spin.

Table 6.2: Solutions to Eq. (6.23) in which one of the two dual theories is metallic, i.e. is at infinite filling.

ν_*	-1	∞
$\nu_\psi + 1/2$	∞	2
$\nu_\chi + 1/2$	2	∞
Theory A	Metal	Superfluid
Theory B	$U(2)_2$	Metal

separated by a first order transition. Starting in, say, the $U(1)_2$ phase, as $\overline{\lambda}$ is increased, phase separation will set in, yielding bubbles and stripes of the $U(3)_2$ phase, which eventually fill the system. It is also possible that the transition is not direct, and that several different phases arise when $\overline{\lambda} \sim \mathcal{O}(1)$. We cannot exclude this possibility. That we cannot present a thorough description of the transition is not surprising, given the complexity of the phase diagrams for electrons in magnetic fields at fractional filling.

6.3.5 Non-Abelian Duality and Paired FQH Phases

In the above subsection, we conspicuously left out a discussion of the case when the χ composite fermions fill two Landau levels, corresponding to filling $\nu_* = 1$. At this filling, Eqs. (6.11) and (6.12) indicate that the ψ composite fermions of **Theory A** feel a vanishing magnetic field and therefore form a metallic state with density set by the background magnetic field, $\langle \psi^\dagger \psi \rangle = B/2\pi$. This is the well known metallic, composite Fermi liquid state of bosons with unit filling [247]. On the other hand, the analysis of Section 6.3.2 finds **Theory B** in an IQH state, yielding $U(2)_2$ topological order. Although one of the predicted phases is gapless, we nevertheless propose that the same scenario presented above holds in this theory: the ultimate choice of ground state is determined by the order in which the IR and $\omega_c \to \infty$ limits are taken. These states are again separated by a phase transition, which is tuned by the dimensionless coupling of the kind defined in Eq. (6.25).

In contrast to the cases in which both phases were gapped, here we can clearly understand this transition in terms of the ψ composite fermions of **Theory A**. Indeed, the $U(2)_2$ state can be shown to be one of a range of non-Abelian phases of bosons at $\nu = 1$ that can be obtained as paired states of the composite Fermi liquid [248], the most famous of which being the $SU(2)_2$ bosonic Pfaffian state [249]. The major difference between the $U(2)_2$ state and the $SU(2)_2$ state lies in the topological spin of the non-Abelian half-vortex, which is set by the pairing momentum channel. As we will explain in more detail in the following subsection, the appropriate channel to obtain the $U(2)_2$ order is $l = 2$. Consequently, this transition can be understood in terms of the flow of the pairing interaction, which is a four-fermion operator in the Abelian **Theory A**.

Interestingly, it is expected from numerical simulations and recent analytic calculations that the composite Fermi liquid state of bosons at $\nu = 1$ is unstable to pairing in the lowest Landau level limit [250,251], perhaps suggesting that the metallic state seen in **Theory A** has no basin of attraction unless the theory is modified in some way.

From the point of view of **Theory B**, it is natural to expect that $\overline{\lambda}$ is again the correct running coupling, with the choice of ground state again being viewed as a question of the order in which the lowest Landau level and IR limits are taken. As above, for $\overline{\lambda} > \overline{\lambda}_*$, the χ fermions find themselves in an IQH state, yielding the $U(2)_2$ topological order. For $\overline{\lambda} < \overline{\lambda}_*$, this picture breaks down, leading to a theory involving bosonic baryons, which we conjecture form the $\nu = 1$ metallic state.

Remarkably, at filling $\nu_* = 1$, we have observed a duality between composite fermion pairing in **Theory A** and the IQH effect in **Theory B**. This is surprising, as there is no known dictionary of local operators that makes this connection explicit. Indeed, while the $U(2)_2$ state has previously been obtined both in the Read-Green pairing picture [61,249] and as an IQH state of non-Abelian partons [158–160,252], it has never before been suggested that these two constructions may be dual to one another. We will see below that this duality is not limited to the particular case of bosons at $\nu = 1$: in Section 6.3.6, we will encounter a parallel story involving the anti-Pfaffian state of fermions at $\nu = 1/2$.

Similar competing ground states are found as the external magnetic field is turned off, i.e. $\nu_* \to \infty$ (see Table 6.2). In this case, the analysis of Section 6.3.2 indicates that **Theory A** predicts a superfluid state, the usual fate of bosons at finite density and $B = 0$. On the other hand, the composite fermions of **Theory B** form a metal with density equal to the background charge density, a far more exotic non-Fermi liquid state which surely requires that the fundamental bosonic charges be very strongly interacting. Nevertheless, the interpretation of the transition between these states is natural from the point of view of **Theory B**: again adopting the notation of Section 6.3.3, for $\overline{\lambda} > \overline{\lambda}_*$, the theory remains metallic, while for $\overline{\lambda} < \overline{\lambda}_*$, the χ fermions confine to form bosonic baryons. Since these bosons feel no magnetic field, they would then condense and spontaneously break $U(1)_{\text{EM}}$, forming the superfluid state seen in **Theory A**. Given how natural the state predicted in **Theory A** is, one might wonder if the metallic state predicted by **Theory B** is ever stable to baryon condensation. We leave this question for future work.

6.3.6 Examples in Other Fermion-Fermion Dualities

Thus far, we have focused our analysis on the dual fermionic theories appearing in the $SU(2)$ quadrality. However, the above considerations are broadly applicable to any pair of fermionic theories related by a Chern-Simons matter duality. To illustrate this point, we consider a more general composite fermion duality

Table 6.3: Fillings at which one of **Theory A′**, Eq. (6.27), and **Theory B′**, Eq. (6.28), predicts a metallic ground state and the other a nonmetallic state (first two columns), or where both predict distinct topological orders (last two columns). Here, N is the rank of the $U(N)$ gauge group in **Theory B′**, which is always equal to two in these examples. By Jain we mean a $U(1)^{\text{spin}} \times U(1)$ theory describing the usual Abelian Jain state at filling ν_*.

ν_*	$1/(k-1)$	$1/(k-2)$	$3/(3k-4)$	$2/(2k-3)$
$\nu_\psi + 1/2$	∞	2	4	3
$\nu_\eta + 1/2$	2	∞	3	4
Theory A′	Metal	$U(1)_{k-2}$ $(k \neq 2)$ Superfluid $(k = 2)$	Jain	Jain
Theory B′ $(N = 2)$	$U(2)_{2,2(k-1)}$	Metal	$U(3)_{2,3k-4}$	$U(4)_{2,2(2k-3)}$

describing a transition between the $\nu = 1/k$ Laughlin state and an insulator. This duality relates a theory of Dirac composite fermions with $k-1$ (Abelian) fluxes attached (**Theory A′**) to a theory of composite fermions coupled to a $U(N)$ gauge field (**Theory B′**) [167],

$$\mathcal{L}_{A'}(k) = i\overline{\psi}\not{D}_a\psi - \frac{1}{2}\frac{1}{4\pi}ada + \frac{1}{2\pi}adv + \frac{k-1}{4\pi}vdv + \frac{1}{2\pi}vdA + \dots, \tag{6.27}$$

$$\updownarrow$$

$$\mathcal{L}_{B'}(k,N) = i\overline{\eta}\not{D}_u\eta - \frac{1}{2}\frac{1}{4\pi}\,\mathrm{Tr}\left[udu - \frac{2i}{3}u^3\right] - \frac{N-k}{4\pi}bdb - \frac{1}{2\pi}\,\mathrm{Tr}[u]db + \frac{1}{2\pi}bdA + \dots \tag{6.28}$$

In **Theory A′**, ψ is a Dirac fermion charged under an emergent $U(1)$ gauge field a, and v is another $U(1)$ gauge field. In **Theory B′**, η is a Dirac fermion in the fundamental representation of $U(N)$, u is a $U(N)$ gauge field, and b is a $U(1)$ gauge field. These dualities are derived in Appendix D.1.1, where it is also shown that these theories are dual composite fermion descriptions of the bosonic Landau-Ginzburg theory for the $\nu = 1/k$ Laughlin state: when k is even, the fundamental charges are bosons, while when k is odd they are fermions (note that when $N = k = 2$, we recover **Theory A** and **Theory B**, which are associated with the $\nu = 1/2$ bosonic Laughlin state). We emphasize that the above duality holds *regardless* of the rank N of the gauge group $U(N)$ in **Theory B′**, and hence amounts to the statement that $\mathcal{L}_{A'}(k)$ is dual to an infinite number of theories $\mathcal{L}_{B'}(k,N)$ parameterized by the integer N.

As in the examples encountered thus far, we find special filling fractions, ν_*, at which the dual theories predict differing ground states. The details of this analysis are essentially identical to that of the preceding $SU(2)$ examples and are presented in detail in Appendix D.1.2. Our results are summarized in Table 6.3. For example, at the filling $\nu_* = 2/(2k-3)$, **Theory A′** predicts the usual Abelian Jain state, while **Theory B′** predicts the more exotic, non-Abelian $U(4)_{2,2(2k-3)}$ state. Our dynamical proposal for understanding the

transitions between these states, as well as the others featured in Table 6.3, is essentially identical to that of Section 6.3.3, and so we will not comment on it further.

One state of particular note is the $U(3)_{2,-1}$ topological order, which is level-rank dual to $U(2)^{\text{spin}}_{-3,-1}$, predicted by **Theory B′** with $k = 1$ at $\nu_* = -3$. Now, the non-spin $U(2)_{3,1}$ Chern-Simons theory is dual to the (also non-spin) $(G_2)_1$ Chern-Simons theory [253]. Remarkably, $(G_2)_1$ describes precisely the Fibonacci topological order, which supports a single non-trivial anyon, τ, obeying the fusion rule $\tau \times \tau = 1 + \tau$, and is of particular import from the perspective of topological quantum computation [6]. It is rather interesting that **Theory B′** predicts the (spin) Fibonacci topological order to appear in competition with the $\nu_* = -3$ IQH state. In Chapter 5, we likewise saw how the pure (non-spin) Fibonacci order can arise at filling $\nu = 2$ in a bosonic system.

Additionally, we wish to highlight the cases at fillings $\nu_* = 1/(k-1)$, in which the non-Abelian $U(2)_{2,2(k-1)}$ state predicted by **Theory B′** can again be understood as a pairing instability of the Abelian composite Fermi liquid state in **Theory A′**. The argument that $U(2)_{2,2(k-1)}$ can be obtained from pairing in **Theory A′** parallels that for the $U(2)_2$ state discussed in the previous subsection, which corresponds to the special case $k = 2$. Indeed, the non-Abelian part of $U(2)_{2,2(k-1)}$ is again $SU(2)_2$, and the major difference from this state lies in the topological spins of the non-Abelian half vortices, which are modified by the level of the Abelian sector. Moreover, one can check explicitly that pairing of the **Theory A′** composite fermions in the $l = 2$ angular momentum channel yields the expected $U(2)_{2,2(k-1)}$ topological order *for all* k by considering the edge spectrum: this topological order supports three chiral, charge-neutral Majorana fermions and one anti-chiral $U(1)_{k-1}$ bosonic charge mode. From the point of view of **Theory A′**, $l = 2$ pairing leads to the three chiral Majorana fermions, in addition to a $U(1)_{k-1}$ charge mode coming from the left over Abelian sector. That such a large class of non-Abelian topological orders which can be understood via pairing in a composite fermion theory, in this case **Theory A′**, has a dual description as IQH states of composite fermions in a dual non-Abelian theory, **Theory B′** is quite remarkable.

We close this section by commenting on some particular examples of physical interest. First, for $k = 1$ and $\nu_* = \infty$, **Theory A′** is a free Dirac fermion at finite chemical potential but vanishing magnetic field. In this case, in **Theory B′**, it is possible to integrate out the auxiliary gauge field b without violating flux quantization: its Chern-Simons level is $-(N - k) = -1$. This cancels the Chern-Simons term for the Abelian part of the $U(2)$ gauge field, $\text{Tr}[u]$, Higgsing the background EM field, A_μ, and leading to a chiral superconductor with topological order is $U(2)_{2,0} = [SU(2)_2 \times U(1)_0]/\mathbb{Z}_2 \cong SO(3)_1$, which is *Abelian*. This state contains only a single anyon, a Majorana fermion[8] [161, 254]. Such a state can be accessed via a

[8]This can be viewed as a consequence of the condensation of the Majorana fermion of the $SU(2)_2$ topological order, which confines the non-Abelian "half-vortex" of the $SU(2)_2$ factor.

pairing instability in **Theory A′**. It is natural to expect this instability to arise due to the effects of local four-fermion operators that destabilize **Theory A′** in the order of limits in which the η fermions of **Theory B′** form an IQH state.

For $k = -1$ and $\nu_* = -1/2$, **Theory A′** is Son's Dirac composite Fermi liquid theory of the half-filled Landau level [124]. In this case, the topological order predicted by **Theory B′** is $U(2)_{2,-4} = [SU(2)_2 \times U(1)_{-8}]/\mathbb{Z}_2$, which is the (time-reversed) topological order of the famous anti-Pfaffian state, another paired state of composite fermions [240, 241]! Additionally, for $k = 3$ and $\nu_* = 1/2$, **Theory B′** predicts the $[SU(2)_2 \times U(1)_8]/\mathbb{Z}_2 = U(2)_{2,4}$ order, which is that of Wen's (221) parton state [158,159], another proposed ground state of fermions at half filling that can be understood in terms of pairing in **Theory A′**, which now has additional attached fluxes. Now, although these states are all accessible within parton constructions (see, for example, Ref. [252]), we must again emphasize that the projective framework hinges on the dynamical assumption that the electron fractionalizes into partons which do not confine. Finally, another non-trivial bosonic example is $k = 0$ and $\nu_* = 1$, in which **Theory B′** predicts a $[SU(2)_2 \times U(1)_{-4}]/\mathbb{Z}_2 = U(2)_{2,-2}$ ground state, which describes the Ising topological order [143]. While these results are reminiscent of the parton constructions giving these states, the use of duality provides a connection between partonic intuition and the dynamics of pairing. Additionally, it is straightforward to check in these examples that $l = 2$ pairing in **Theory A′** yields the expected $U(2)_{2,2(k-1)}$ order by comparing the edge theories. It would be interesting to determine if other dual descriptions exist which yield the other proposed Pfaffian-like states, which arise from pairing the composite fermions of **Theory A′** in other angular momentum channels, as IQH phases of dual composite fermions, and we leave this to future work.

6.4 Building Non-Abelian States from Excitonic Pairing

In the preceding section, we illustrated how non-Abelian Chern-Simons matter dualities may be used to map out parts of the phase diagram for electrons (or bosons) in a magnetic field at certain fractional fillings, ν_*, finding gapless states as well as both Abelian and non-Abelian topological orders. We now turn to present an alternative means of constructing non-Abelian FQH states, still making use of the dual composite fermion theories employed above. Our goal here is to provide a complementary perspective to our previous work [17], in which we constructed Landau-Ginzburg theories for the Read-Rezayi states using bosonic Chern-Simons-matter using a multilayer pairing procedure. Specifically, we will consider condensing interlayer excitons (pairs of fermions in different layers which are neutral under the external EM gauge field) in **Theory B**, Eq. (6.9), to generate non-Abelian states. We will find, however, that the excitonic paired phases are not the

Read-Rezayi states constructed in Ref. [17], but rather the Blok-Wen states with $U(k)_2$ topological order, as in Section 6.3.

For simplicity, we again consider a bilayer system, with each layer being a $\nu = 1/2$ bosonic Laughlin state. We use the dual fermionic description of **Theory B** for each layer so that the (initially decoupled) multilayer system is described by the Lagrangian

$$\mathcal{L}_{B,2} = \sum_{n=1}^{2} \left(i\overline{\chi}_n \not{D}_{b_n - A\mathbf{1}/2} \chi_n - \frac{1}{2}\frac{1}{4\pi} \mathrm{Tr}\left[b_n db_n - \frac{2i}{3} b_n^3 \right] \right) - \frac{1}{2}\frac{1}{4\pi} AdA. \tag{6.29}$$

Here, χ_n and b_n are the composite fermions and $SU(2)$ gauge fields on layer n, respectively. Note that each layer couples in the same way to the external electromagnetic field, A. Moreover, we see from Table 6.1 that when each layer is at filling $\nu = 1/2$, so that the full multilayer system is at filling $\nu = 1$, the χ_n of each layer form an IQH state.

Now, following the standard approach [198], we introduce an interlayer excitonic pairing interaction mediated by an electrically neutral scalar field, Σ,

$$\mathcal{L}_{\text{exciton}} = \overline{\chi}_1 \Sigma \chi_2 + \text{H.c.} \tag{6.30}$$

The field Σ can be thought of as a Hubbard-Stratonovich field for the pairing interaction. It couples minimally to the gauge fields on either layer, and so has dynamics described by

$$\mathcal{L}_{\Sigma} = |\partial\Sigma - ib_1\Sigma + i\Sigma b_2|^2 - V[\Sigma], \tag{6.31}$$

where $V[\Sigma]$ is the potential for Σ. Under gauge transformations,

$$\Sigma \mapsto U_1 \Sigma U_2^{\dagger}, \qquad U_m \in SU(2) \text{ on layer } m. \tag{6.32}$$

The full multi-layer theory is therefore described by the Lagrangian,

$$\mathcal{L}_{\text{bilayer}} = \mathcal{L}_{B,2} + \mathcal{L}_{\text{exciton}} + \mathcal{L}_{\Sigma}\,. \tag{6.33}$$

The condensation of Σ yields the excitonic paired state, characterized by a non-zero expectation value for the operator $\overline{\chi}_1\chi_2$. It should be emphasized that in the dual descriptions of **Theory A** and the Landau-Ginzburg theory of Eq. (6.6), the interaction $\mathcal{L}_{\text{exciton}}$ will correspond to a highly nonlocal object involving monopole operators. In general, the fundamental fields do not map to local operators under the dualities of Eq. (6.2)-

(6.4) [68]. Hence, the upshot of examining this dual fermionic theory is that we can access regions of the phase diagram at a given filling fraction, which are less readily understood in the formulation of **Theory A** or the original bosonic Landau-Ginzburg theory, as they would require the inclusion of complicated, nonlocal interactions.

Now, suppose we have a nonzero magnetic field such that each layer is at filling $\nu = 1/2$, meaning the χ_n each fill a single Landau level, as indicated in Table 6.1. We assume that we can safely integrate out the occupied χ_n Landau levels, yielding additional level $-1/2$ Chern-Simons terms for the b_m gauge fields. The effective action describing this gapped state is then

$$\mathcal{L}_{\text{bilayer}} = -\sum_{n=1}^{2} \frac{1}{4\pi} \text{Tr}\left[b_n db_n - \frac{2i}{3} b_n^3\right] - \frac{1}{4\pi} AdA + \tilde{\mathcal{L}}_\Sigma + \dots , \tag{6.34}$$

where we have integrated out the fermions χ, leading to a renormalized Lagrangian for Σ, denoted $\tilde{\mathcal{L}}_\Sigma$. If the potential $V[\Sigma]$ is such that the field Σ is massive and does not condense, then we are simply left with an $SU(2)^{\text{spin}}_{-1} \times SU(2)^{\text{spin}}_{-1} \leftrightarrow U(1)_2 \times U(1)_2$ Chern-Simons theory at low energy, describing two decoupled layers of $\nu = 1/2$ Laughlin states. Now, suppose instead that the potential $V[\Sigma]$ is such that Σ obtains a non-zero vacuum expectation value, $\langle \Sigma \rangle \propto \mathbf{1}$. In this excitonic paired state, the gauge group $SU(2) \times SU(2)$ will be Higgsed down to the diagonal $SU(2)$ subgroup, as follows from the gauge transformations of Eq. (6.32). Explicitly, from the Lagrangian for Σ, the linear combination $b_1 - b_2$ of the gauge fields acquires a mass, effectively identifying the gauge fields of each layer: $b_1 \equiv b_2 \equiv b$. Hence, the Chern-Simons terms will add, resulting in a non-Abelian $SU(2)^{\text{spin}}_{-2} \leftrightarrow U(2)_2$ Chern-Simons theory at low energies.

It is possible to explicitly write out the anyon spectrum of this $U(2)_2$ topological order in terms of composite operators of the fundamental fermions. This requires identifying the operators which transform under the non-trivial spin-1/2 and spin-1 representations of the $SU(2)_{-2}$ gauge theory and taking into account additional spin factors coming from the underlying fermionic statistics of said operators. For reference, we denote the anyons transforming in the spin-1/2 and spin-1 representations of the $SU(2)_{-2}$ topological order as σ and ψ (not to be confused with the fermion field in **Theory A**), corresponding to the non-Abelian half-vortex (i.e. the Ising twist field) and Abelian Majorana fermion, respectively, in the time-reversed conjugate of the bosonic $\nu = 1$ Moore-Read state. They have spin[9] $h_\sigma = -3/16$ and $h_\psi = 1/2$, respectively, and satisfy the fusion rules $\sigma \times \sigma = 1 + \psi$ and $\psi \times \psi = 1$, where 1 represents the vacuum. Now, in our theory, the minimal charge anyons are represented by the fermions χ_1, which transform in the fundamental (or spin-1/2) representation of $SU(2)_{-2}$. The χ_1 operators will thus satisfy the same fusion rules as the σ

[9]Here, the spin of an anyon a is the phase factor $\exp(2\pi i h_a)$ picked up when rotating it through an angle of 2π. This is not to be confused with the spin-$j/2$ representations of $SU(2)$.

anyon in the $SU(2)_{-2}$ theory, but they have spin $-3/16+1/2=5/16$, due to the bare fermionic statistics of χ_1. The other non-trivial anyon is represented by the composite operator $\overline{\chi}_1\tau^a\chi_1$, where τ^a is the vector of generators of $SU(2)$. This operator is charge neutral and transforms in the spin-1 representation of $SU(2)$, meaning it obeys the same fusion rules as ψ. It also has the same spin as ψ, $h_\psi = 1/2$, since it has bare bosonic statistics, being a bilinear in fermion operators. Once can check that these anyons with these spins match the anyon spectrum expected for the $U(2)_2$ topological order. Finally, note that the fundamental fermions χ_1 and χ_2 are indistinguishable in the excitonic paired phase, as one can be transmuted into the other via the the $\langle\overline{\chi}_1\chi_2\rangle$ condensate. Hence, there is no double-counting of anyons.

Several remarks on this construction are in order. This excitonic pairing mechanism is somewhat unconventional and differs from the more common Read-Green construction [61] used to describe the Moore-Read states. In the latter picture, the electrons (or bosons) are mapped to composite fermions using non-relativistic flux attachment. At the appropriate filling fractions, the composite fermions see an effectively vanishing flux at mean-field level. The resulting composite Fermi liquid can give way to a pairing instability in the $p+ip$ channel, Higgsing the dynamical $U(1)$ Chern-Simons gauge field down to its $\mathbb{Z}_2$ subgroup and resulting in a gapped state. The non-Abelian Ising anyons in the Moore-Read state then have a description in terms of vortices of the Chern-Simons gauge field. In the present construction, we are instead pairing fermions on top of a filled Landau level, a gapped state. Hence, unlike the Read-Green picture, we cannot understand our exciton paired state as arising from some perturbative instability, since interactions must be sufficiently strong to overcome the gap. In addition, one can check from standard homotopy arguments that the symmetry breaking pattern $SU(2)\times SU(2)\to SU(2)_{\text{diagonal}}$ does not admit vortex configurations [17,178]. Instead, the anyon spectrum in our model is generated by composite objects formed from the fundamental fermions, as outlined above. It should be noted that even our earlier bosonic construction [17] required a similarly unconventional pairing mechanism, in which it was necessary to assume that composite bosons paired rather than condensed. Finally, it is clear that we can generalize our construction to a multilayer system with k copies of the $\nu=1/2$ Laughlin state; interlayer excitonic pairing in such a system would lead to a $U(k)_2$ topological order.

6.5 Discussion

Employing non-Abelian composite fermion dualities, we have presented two complementary pictures for describing a broad range of non-Abelian FQH states, which can be obtained either as IQH states of non-Abelian composite fermions or as excitonic states in multilayer systems. Along the way, we developed new

insights into the non-Abelian theories' dynamics, in which the order of the lowest Landau level ($B \to \infty$) and IR limits was seen to play a crucial role in determining the ultimate choice between the non-Abelian ground state and a competing Abelian state that is natural in a dual description. This subtlety has thus far received little attention in studies of non-Abelian dualities, yet we find it to be a ubiquitous feature of non-Abelian fermion-fermion dualities. It may be a worthwhile endeavour to see whether studying these theories at finite magnetic field in the 't Hooft limit, in the vein of Ref. [255], may provide an analytical handle on the physics of these transitions – we leave this for future work. Interestingly, related physics has been observed recently in numerics, where it has been argued that the ground state at certain fillings can exhibit effectively Abelian topological order for short-range interactions and non-Abelian order as the interaction range is increased [256, 257]. We hope that our work will motivate more numerical efforts in this direction.

Although we cannot make many concrete statements about the transitions we propose to occur between the Abelian and non-Abelian states, we remarkably find several examples in which the non-Abelian states – among them the anti-Pfaffian – can be understood in terms of pairing in a dual composite Fermi liquid description. Such dualities between composite fermion pairing and the IQH effect in a dual, non-Abelian theory are new, and finding new examples of such dualities will be a fruitful direction for future work. Looking forward, a natural question to ask is whether non-Abelian fermion-fermion dualities can be used to derive other non-Abelian FQH states, beyond the variations of the Blok-Wen states we find. Indeed, although the anti-Pfaffian is a member of the $U(2)_{2,2(k-1)}$ series of states, we do not seem to arrive at the Pfaffian or PH-Pfaffian states. To that end, it may be fruitful to apply our analysis using dualities involving Chern-Simons-matter theories with gauge groups other than $SU(N)$ or $U(N)$, as the family of Pfaffian states can naturally be described using $O(2)_{2,L}$ Chern-Simons theories [258]. It is also somewhat peculiar in that the Read-Rezayi and generalized non-Abelian spin singlet states, which are readily obtained through non-Abelian bosonic theories, do not appear to be accessible within the present approach. We leave the construction of fermionic theories for these states to future work.

Chapter 7

Entanglement Entropy of Generalized Moore-Read Fractional Quantum Hall State Interfaces

7.1 Introduction

Thus far, our focus has been on understanding the *emergence* of exotic fractional quantum Hall (FQH) states. In this, the final chapter of this thesis, we continue our investigation of non-Abelian FQH states, but we now shift the object of our inquiry to their *characterization*. Specifically, our focus will be on understanding systems in which distinct non-Abelian topological states are joined at a one-dimensional interface where all chiral edge modes are gapped out, forming a *gapped interface*. Such systems have been the subject of much theoretical interest, as we discussed in Chapter 1 and will briefly review below. As for conventional uniform topologically ordered states, the study of such systems and the properties of their one-dimensional interfaces is impeded by the fact that topological order, being characterized by non-local correlations, cannot be probed via local order parameters. Instead, we will endeavor to uncover the properties of these interfaces by characterizing the *entanglement* structure of the ground state, a calculation which has already been carried out in the corresponding Abelian problem [91]. As in this previous work, we will employ a "cut-and-glue" approach, which takes advantage of the bulk-boundary correspondence, to render the entanglement calculation a tractable one.

Let us briefly review the main concepts regarding quantum entanglement that will be of relevance for us in this Chapter. The most elementary measure of entanglement is provided by the entanglement entropy (EE). Given a state $|\psi\rangle$ and a bipartition of the Hilbert space $\mathcal{H} = \mathcal{H}_A \otimes \mathcal{H}_B$, the EE is given by

$$S = -\mathrm{Tr}_A(\rho_A \ln \rho_A) \tag{7.1}$$

where $\rho_A = \mathrm{Tr}_B |\psi\rangle \langle\psi|$ is the reduced density matrix of A. Specializing to $2+1$-dimensional systems, if $|\psi\rangle$ is the ground state of a local Hamiltonian and we choose a spatial bipartitioning of the Hilbert space, then

This Chapter is adapted from Ramanjit Sohal, Bo Han, Luiz H. Santos, and Jeffrey C. Y. Teo, Entanglement entropy of generalized Moore-Read fractional quantum Hall state interfaces, Phys. Rev. B **102**, 045102 (2020). This paper is also cited as Ref. [20] in this thesis.

the EE satisfies

$$S = \alpha L - \gamma \tag{7.2}$$

in the thermodynamic limit, where L is the length of the entanglement cut separating regions A and B. The first term in this expression is known as the area law, where α is a non-universal constant. In contrast, γ is a universal quantity known as the topological entanglement entropy (TEE) and is non-zero for topologically ordered systems [89,90]. If A has the topology of a smooth disc, then $\gamma = \ln \mathcal{D}$, where $\mathcal{D}$ is the total quantum dimension, a quantity which characterizes the anyon content of a topological order.

As a single number, the TEE provides a rather coarse grained description of a gapped state. A more descriptive object is provided by the entanglement spectrum (ES) [259], which is defined by first formally writing the reduced density matrix for region A in the form of a thermal density matrix,

$$\rho_A \propto e^{-\mathcal{H}_e}. \tag{7.3}$$

The ES is then given by the spectrum of the operator $\mathcal{H}_e$, which is known as the entanglement Hamiltonian. Remarkably, for (chiral) topological phases, the low-lying part [260] of the ES for a spatial entanglement cut corresponds to the physical spectrum of the conformal field theory (CFT) describing the edge of the topological order. This was first demonstrated numerically in fractional quantum Hall systems [259], while analytic arguments for the correspondence appeared shortly thereafter [261–265].

Of particular interest to us is the work of Qi, Katsura, and Ludwig [263], which employed a "cut-and-glue" approach to calculate the ES. These authors argued that one can compute the ES by physically cutting the system along the entanglement cut between A and B and turning on an interaction between the resulting gapless edge states. Since the correlation length vanishes in the bulk, any entanglement between A and B should come from the the coupled edges. Using boundary CFT techniques, Qi et. al. deduced the ground state of the coupled edge system and showed that the ES does indeed match that expected for the bulk topological order. Subsequent works applied this approach to the specific cases of *Abelian* topological phases, whose edges are described by multi-component Luttinger liquids [14]. In this case, one can write down explicit gapping terms for which the ground state can readily be approximated, without recourse to boundary CFT methods [91, 266].[1]

The utility of the cut-and-glue approach was made manifest in the work of Cano et. al. [91], in which the TEE for an entanglement cut along a gapped interface between *distinct* Abelian topological phases was

[1] See also Refs. [267, 268] for related calculations.

computed. The authors demonstrated that the TEE in fact receives (universal) corrections depending on the choice of interactions used to gap out the interface, even for an interface between two regions with the same topological order.[2] Gapped interfaces of topological phases are of physical interest, due to the possibility of realizing non-Abelian defects at their endpoints [72–83]. In fact, it was demonstrated that the aforementioned TEE corrections are directly related to the emergence of 1D SPTs along these interfaces [88]. Recently, progress has also been made in understanding (gapless) interfaces of topological phases beyond effective field theory constructions through numerical simulations [271–273].

The goal of this Chapter is to provide a first step towards extending the above story to non-Abelian topologically ordered phases of matter. Namely, we would like to, for some class of non-Abelian states, (1) use the cut-and-glue approach to compute the TEE in all topological sectors. Furthermore, we will aim to (2) identify when a gapped interface can be formed between these states and what interactions can generate these interfaces, as well as (3) compute the TEE for an entanglement cut along such an interface. The second of these issues – the construction of explicit gapping interactions – has been extensively studied for Abelian systems [85–87], but is less well understood for non-Abelian phases (although interfaces of non-Abelian states have been studied at an abstract level [274–282]).

To these ends, we focus on the generalized Moore-Read (MR) states [1], which provide examples of the simplest non-Abelian fractional quantum Hall (FQH) states. As described in Chapter 3, these states may be viewed as arising from $p + ip$ pairing of composite fermions [61] and, accordingly, their edge theories are described by a free compactified chiral boson and a free Majorana fermion [283]. One might then expect the computation of the TEE in the MR state to be an uneventful extension of the Abelian case. However, the choice of the local electron operator, which determines the allowed quasiparticles and provides the origin of the non-Abelian properties of these phases, glues the bosonic and fermionic sectors of the Hilbert space together in a non-trival manner. As we will see, the calculation of the EE requires a careful treatment of this organization of the Hilbert space. Before delving into these calculations, given the length of this Chapter, we first provide a summary of our results.

7.1.1 Summary of Results

(1) We first demonstrate that the correct ES and TEE is obtained for uniform MR interfaces on a torus in all topological sectors using the cut-and-glue approach. On a torus, the ground state of each topological sector, a, is a *minimum entropy state* [104, 284] and for an entanglement cut splitting the torus into two

[2] See also Ref. [269] for related considerations and Ref. [270] for a calculation using the bulk Chern-Simons theory.

cylinders, the TEE in these states is given by

$$\gamma = 2\ln(\mathcal{D}/d_a), \tag{7.4}$$

where d_a is the quantum dimension of the anyon associated to the a topological sector. For the MR state at filling $\nu = 1/n$, $\mathcal{D} = \sqrt{4n}$, while the allowed anyons have either $d_a = 1$ or $d_a = \sqrt{2}$ [104, 285]. The local interaction that gaps the interface corresponds to a single-electron backscattering term. This interaction is given by a sine-Gordon operator coupled to a Majorana mass and simultaneously gaps out the charged, chiral boson and neutral Majorana sectors. As in Refs. [91, 266], we will take the strong coupling limit and approximate this interaction to quadratic order in fluctuations of the fields about their vacuum expectation values. This approximation violates the requirement of electron locality alluded to above and must be supplemented by a projection into the correct topological sector.

(2) We investigate interfaces of MR states at filling fractions $\nu_A = 1/pb^2$ and $\nu_B = 1/pa^2$, where $p, a, b \in \mathbb{Z}$ and we take a and b to be coprime. Although gapped interfaces of non-Abelian states have been studied in the literature [274–282], a systematic understanding of interactions generating distinct classes of these interfaces is lacking. So, we use anyon condensation [286, 287] as a guide to deduce when gapped interfaces should exist and to motivate explicit gapping terms. Interestingly, although we can always gap out an interface between MR states at fillings ν_A and ν_B, we find that when a and b are both odd, a single interaction term is needed, whereas when one of a and b is even and the other odd, two terms are needed. Moreover, in the latter case, we find that the gapped interface is most easily constructed using an alternative representation of the $\nu = 1/n$ MR edge CFT which is topologically equivalent to its standard description in terms of a chiral Majorana and a $U(1)_n$ chiral boson. In particular, we will make use of the fact that we can rewrite the Ising CFT as

$$\text{Ising} = \frac{SO(N+1)_1}{SO(N)_1} \sim SO(N+1)_1 \boxtimes \overline{SO(N)}_1,$$

where G_k denotes a Wess-Zumino-Witten (WZW) theory with Lie group G at level k and the symbol $\boxtimes$ indicates a tensor product supplemented by the condensation of a particular set of bosons. The nature of the equivalence will be explained in more detail later on. This will allow us to express the MR edge in terms of a chiral boson and multiple chiral and anti-chiral Majorana fermions, which can be used to construct the appropriate gapping interactions.

(3) Combining the above results, it is then straightforward to compute the TEE for an entanglement cut along an interface between MR states at fillings ν_A and ν_B. In this calculation, we must take into account

the additional constraints on the ground states imposed by the specific forms of the gapping interactions, in a manner analogous to that of the calculation for Abelian interfaces [91]. Again working on the torus, we find the TEE in the vacuum sector to be given by

$$\gamma = 2\ln(2\sqrt{pa^2b^2}) \tag{7.5}$$

for a and b both odd while,

$$\gamma = 2\ln(4\sqrt{pa^2b^2}) \tag{7.6}$$

for one of a and b odd and the other even. Finally, we discuss the connection between these values of the TEE with the existence of a "parent" topological phase for the two MR states on either side of the interface.

It should be emphasized that ours is not the first work to investigate the EE of non-Abelian systems through a cut-and-glue type approach. The work of Qi et. al. applies to generic uniform chiral topological orders (both Abelian and non-Abelian) and demonstrated that the ground state of the coupled edge system at the interface should be described by so-called Ishibashi states [288,289]. Wen et. al. [290] later showed that appropriately regularized Ishibashi states furnish the correct entanglement structure for generic chiral phases and generic bipartitions on manifolds of arbitrary genus (a related, earlier calculation was also performed in Ref. [291]). Interfaces between distinct non-Abelian and/or Abelian orders have also been considered, where the interface was conjectured to be described by an appropriately constructed Ishibashi state [292]. Most recently (and concurrently with the completion of the work presented in this Chapter), Ref. [293] computed, using the bulk theory, the entanglement entropy for gapped interfaces between distinct non-Abelian Chern-Simons theories. One of our main contributions is a more microscopic justification of these results, for a specific set of non-Abelian phases, starting from an explicit effective field theory description of the interface.

The remainder of this Chapter is structured as follows. We begin by reviewing the MR edge theory, placing special emphasis on the interpretation of the distinct topological sectors in the CFT language in Section 7.2. Section 7.3 provides a review of the cut-and-glue approach and our handling of the topological sectors. We proceed to calculate the EE for a uniform MR state in Section 7.4. In Section 7.5 we identify the two distinct classes of interfaces between MR states at different fillings and write down explicit gapping terms. The computation of the EE for each of these interfaces is presented in Section 7.6. We provide a discussion of our results and conclude in Section 7.7. Finally, the appendixes collect some technical details.

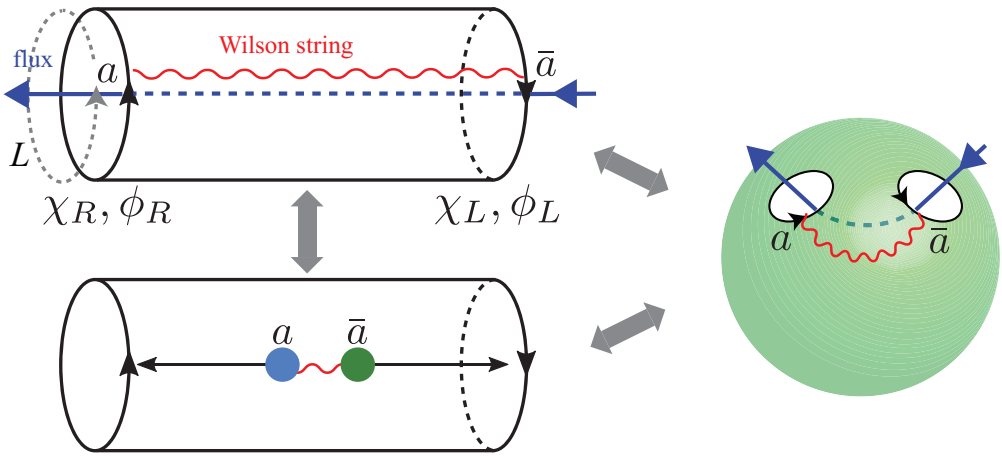

Figure 7.1: Moore-Read state on a cylinder with chiral edge states. The insertion of an anyon flux a through the cylinder (top) is equivalent to nucleating a conjugate anyon pair in the bulk of the cylinder and dragging them to opposite edges (bottom). The cylinder geometry is homotopic to a sphere with two punctures (right), which bounds the anyon pair.

7.2 Review of Moore-Read Edge Theory

We begin by reviewing the edge theory for the MR state at filling fraction $\nu = 1/n$ [283]. Note that n may be either even or odd. If n is even, we have a MR state of electrons (i.e. fermions) while, if n is odd, we have a MR state of bosons. In the following, we will often refer to the local particles comprising the MR FQH state as electrons, regardless of whether n is even or odd (and hence regardless of whether the local particles are fermions or bosons).

Now, let us consider a MR state defined on a cylinder with circumference L. Standard arguments imply that the edges of the cylinder will be described by CFTs of opposite chirality, $\mu = L, R = +, -$, as indicated in Fig. 7.1. Specifically, as described in the introduction, the edge theory contains both a neutral Majorana fermion χ sector and a charged $U(1)$ boson ϕ sector. The two edges are formally described by the Lagrangian densities

$$\mathcal{L}_\mu = \frac{i}{2}\chi_\mu(\partial_t - \mu v_n \partial_x)\chi_\mu + \frac{n}{4\pi}\partial_x\phi_\mu(\mu\partial_t - v_c\partial_x)\phi_\mu, \tag{7.7}$$

where $v_n > 0$ and $v_c > 0$ are the velocities of the Majorana and boson, respectively. The Majorana fermion and the $U(1)$ boson are Hermitian: $\chi^\dagger = \chi$, $\phi^\dagger = \phi$. The fields obey the equal-time (anti)commutation

relations

$$[\phi_\mu(x), \partial_y \phi_\mu(y)] = \frac{2\pi i \mu}{n} \delta(x-y) \tag{7.8}$$

$$\{\chi_\mu(x), \chi_\mu(y)\} = \delta(x-y). \tag{7.9}$$

The bosons are compactified on a circle of radius $R = 1$ so that $\phi_{L/R} \equiv \phi_{L/R} + 2\pi$, and the primary fields in the $U(1)$ sector are normal-ordered vertex operators $e^{ir\phi_\mu}$ with integral r. The charge densities on the two edges are given by $\rho_{L/R} = \partial_x \phi_{L/R}/(2\pi)$. Note that this means the *winding numbers* of the scalars around the length of the edges,

$$N_\mu \equiv \int_0^L \frac{\partial_x \phi_\mu(x)}{2\pi} dx = \int_0^L \rho_\mu(x) dx, \tag{7.10}$$

count the total charge carried by the edges (in units of e above the ground state) and so can only take values in the set of rational numbers, as determined by the charge of the minimal charge anyon.

At the level of the Lagrangian, it would appear that the charge and neutral sectors are decopuled and hence that the MR edge theory is described by an Ising $\times\, U(1)_n$ CFT. This is not the case, as the physical theory is not fully defined until the electronic (i.e. local) operators are specified. This determines the anyon content and hence the Hilbert space topological sectors, as all physical excitations must have trivial braiding statistics with respect to the electron. This constraint of electron locality is ultimately a consequence of the fact that the bulk topological state is constructed from electrons. In the MR edge theory, the charge e operators,

$$\psi_{e,L} = \chi_L e^{in\phi_L}, \quad \psi_{e,R} = \chi_R e^{-in\phi_R} \tag{7.11}$$

are defined to be electronic operators.

For later use, let us also define the fermion parity operator, $(-1)^F$, which anti-commutes with the fermions of *both* edges:

$$(-1)^F \chi_{R/L} = -\chi_{R/L} (-1)^F. \tag{7.12}$$

A similar operator for the bosonic sector is given by $(-1)^{N_R + N_L}$ which, using the commutation relations of

Eq. (7.8), is seen to have the action

$$(-1)^{N_R+N_L} e^{in\phi_\mu} = -e^{in\phi_\mu}(-1)^{N_R+N_L}. \tag{7.13}$$

Hence, the combined operator,

$$G \equiv (-1)^F (-1)^{N_R+N_L}, \tag{7.14}$$

which measures the relative parity between the fermion number and bosonic winding number (i.e. charge) of both edges, clearly commutes with the electron operators of both edges.

Having specified the electron operators, we can now enumerate the anyon content of the theory. Explicitly, the MR theory of the $\mu = L, R$ edge carries the following primary fields,

$$e^{ir\phi_\mu}, \quad \chi_\mu e^{ir\phi_\mu}, \quad \sigma_\mu e^{i(r+1/2)\phi_\mu}, \tag{7.15}$$

where $r = 1, \ldots, n$. We can restrict to these values of r, as two excitations are considered equivalent if they differ by fusion with an electron operator or a bosonic oscillator mode. Here, 1, χ and σ are the primary fields of the neutral Ising sector, where χ is the Majorana fermion and σ represents the non-Abelian Ising twist field. They obey the Ising fusion rules,

$$\begin{aligned} \chi \times \chi &= 1 \\ \chi \times \sigma &= \sigma \\ \sigma \times \sigma &= 1 + \chi. \end{aligned} \tag{7.16}$$

The vertex operators $e^{ir\phi}$ are charge-carrying Laughlin quasiparticles. In the bulk, the braiding phase between the fields $e^{ir_1\phi}$ and $e^{ir_2\phi}$ is $e^{2\pi i r_1 r_2/n}$. In contrast to the Laughlin $U(1)_n$ edge theory, the charge e boson (fermion) $e^{in\phi_\mu}$, for n even (odd), is fractional and is *not* a local excitation. This allows for the existence of the non-Abelian twist fields $\sigma e^{i(r+1/2)\phi}$, which exhibit -1 braiding with respect to the boson/fermion $e^{in\phi}$ (from the $e^{i\phi/2}$ factor) and the Majorana fermion χ (from the σ factor), but are local with respect to the electronic quasiparticles in Eq. (7.11). In the bulk language, $\sigma e^{i\phi/2}$ corresponds to a non-Abelian half vortex, which traps a Majorana zero-mode (MZM), represented by σ. The MZM flips the boundary condition of the Majorana fermion at the edge, since it exhibits a braiding phase of -1 with respect to χ. Note that, although the Ising $\times U(1)_n$ CFT is described by the same Lagrangian as the MR CFT, its anyon content is given by a direct product of that of the Ising and $U(1)_n$ topological orders, as the "electron operator" is the

vertex operator $e^{in\phi}$: $\{1, \sigma, \chi\} \times \{e^{ir\phi}\}_{r=1,\ldots,n}$.

The quantum dimension d_a of an anyon a is defined to respect the fusion rules so that $d_a d_b = \sum_c N_{ab}^c d_c$ if $a \times b = \sum_c N_{ab}^c c$. The $2n$ Abelian anyons $e^{ir\phi}$ and $\chi e^{ir\phi}$ have quantum dimension $d = 1$ while the remaining n non-Abelian Ising anyons $\sigma e^{i(r+1/2)\phi}$ have quantum dimension $d = \sqrt{2}$. The total quantum dimension $\mathcal{D}$ is defined as

$$\mathcal{D}^2 = \sum_c d_a^2. \tag{7.17}$$

For the MR state, $\mathcal{D} = \sqrt{4n}$. The conjugate $\overline{a}$ of an anyon a is the unique anyon type that annihilates a under fusion $a \times \overline{a} = 1 + \ldots$, i.e. $N_{a\overline{a}}^1 = 1$. For example, $\overline{\sigma_\mu e^{i(r+1/2)\phi_\mu}} \simeq \sigma_\mu e^{i(n-r-1/2)\phi_\mu}$. Note that, in any physical excited state supporting some number of anyons a_i, fusing together all the a_i's must yield the vacuum, since any physical state must ultimately be constructed from electrons.

As noted above, the choice of electron operator glues together the bosonic and fermionic sectors in a non-trivial way not specified at the level of the Lagrangian. In particular, we must restrict the edge CFT Hilbert space to states satisfying $G = 1$ [Eq. (7.14)]. That is, the parity of charge must match the fermion parity (as measured with respect to the ground state). Physically, this is just the statement that all physical states must be constructed out of electrons and acting with an electron operator changes the Majorana fermion parity by the same amount as the winding number parity. Loosely speaking, one may view the invariance of the electron operators under conjugation by G as reflecting a $\mathbb{Z}_2$ gauge symmetry and the constraint $G = 1$ as a projection to the gauge-invariant subspace. This rule organizes the states of the theory into topological sectors, which are in one-to-one correspondence with the fundamental anyon excitations. From the bulk perspective, these topological sectors are excited states corresponding to the insertion of Wilson lines connecting the two edges or, equivalently, the process of nucleating of an anyon and its conjugate in the bulk and dragging them to opposite edges, as shown in Fig. 7.1. (If one glues the edges together to form a torus as we shall do later, the Wilson line becomes a Wilson loop and the topological sectors now correspond to degenerate ground states.) In the following, we describe how these distinct sectors manifest themselves in the edge CFT.

Let us first consider the ground state of the MR theory on the cylinder (which implies there is no flux through the hole of the cylinder). Clearly, this state has $N_R = N_L = 0$ and no fermionic excitations; hence $G = 1$ in this state. Acting with the electron operator $\psi_{e,L} = \chi_L e^{in\phi_L}$ on the left edge of the cylinder, we obtain an excited state which is still, by definition, within the same topological sector. Since $\psi_{e,L}$ and G commute, it immediately follows that the application of the electron operator on the ground state can only

yield states in which the fermion parity has flipped *and* the bosonic winding has increased by one. All states in this topological sector can be obtained by the application of an arbitrary number of electron operators and $\partial_x \phi$ operators, the latter of which simply create charge density fluctuations without changing the charge or fermion parity. Hence, the states in the identity ($\mathbf{1}$) sector are characterized by having their fermion parity *equal* to the bosonic winding parity (equivalently, the parity of charge added above the ground state), individually on each edge. That is to say,

$$\mathbf{1} \text{ sector:} \quad (-1)^{N_{R/L}} (-1)^{F_{R/L}} = +1. \tag{7.18}$$

Here we have defined individual fermion parities for each edge, $(-1)^{F_{L/R}}$. This is possible because, in the untwisted sector, the fermions obey anti-periodic boundary conditions and so do not possess zero modes. So, acting on a state with, say, a right-moving fermion operator cannot change the left-moving fermion parity.

Let us now consider the states within the χ sector. Starting from the ground state, we can supply some energy to the bulk to nucleate a pair of neutral χ anyons and drag them to opposite edges (see Fig. 7.1). This defines a state in the χ sector, in which the fermion parity is odd but the bosonic winding is even (zero). Constructing the remaining states within this topological sector using the $\chi e^{in\phi}$ and $\partial_x \phi$ operators, we see that all states within the χ sector have fermion parity *opposite* to that of the bosonic winding number parity. In other words,

$$\chi \text{ sector:} \quad (-1)^{N_{R/L}} (-1)^{F_{R/L}} = -1. \tag{7.19}$$

Distinct topological sectors can also be obtained by inserting r magnetic flux quanta through the hole of the cylinder. This is equivalent to nucleating a Laughlin quasiparticle, $e^{ir\phi}$, and its conjugate in the bulk and dragging them to opposite edges. The Majorana fermions, being electrically neutral, are unaffected by this flux insertion. The winding number parity $(-1)^{N_{L/R}} = e^{i\pi N_{L/R}}$ becomes fractional in this sector. The anyon flux, which in low-energy is represented by the vertex combination $e^{ir\phi_L} e^{ir\phi_R}$ on the two edges, associates a phase $e^{i\pi\mu r/n}$ to the winding number parity because

$$(-1)^{N_\mu} e^{ir\phi_L} e^{ir\phi_R} = e^{i\pi\mu r/n} e^{ir\phi_L} e^{ir\phi_R} (-1)^{N_\mu}, \tag{7.20}$$

for $\mu = L, R = +, -$. In other words, the electron operators on both edges pick up a phase of $e^{2\pi ir}$ when

transported around the circumference of the cylinder. It is straightforward to see that this implies

$$\phi_\mu(x+L) = \phi_\mu(x) + 2\pi N_\mu \equiv \phi_\mu(x) + 2\pi\mu\frac{r}{n} \quad \text{modulo } 2\pi\mathbb{Z} \tag{7.21}$$

and so the winding numbers are quantized as

$$N_L = \tilde{N}_L + \frac{r}{n}, \quad N_R = \tilde{N}_R - \frac{r}{n}, \quad \tilde{N}_{L/R} \in \mathbb{Z}. \tag{7.22}$$

Hence, in the $e^{ir\phi}$ sector, we have

$$e^{ir\phi} \text{ sector:} \quad (-1)^{N_L}(-1)^{F_L} = [(-1)^{N_R}(-1)^{F_R}]^* = e^{i\pi r/n}. \tag{7.23}$$

Likewise, starting in the χ sector, we can insert r magnetic flux quanta in addition to the χ flux to obtain the $\chi e^{ir\phi}$ sectors:

$$\chi e^{ir\phi} \text{ sector:} \quad (-1)^{N_L}(-1)^{F_L} = [(-1)^{N_R}(-1)^{F_R}]^* = -e^{i\pi r/n}. \tag{7.24}$$

Note that in all of these sectors, we still have $G = 1$.

Thus far, we have only considered untwisted sectors – that is, topological sectors in which the Majorana fermions obey anti-periodic boundary conditions. The twisted sectors are obtained by inserting a π flux through the cylinder to which only the Majoranas are sensitive, flipping their boundary conditions from anti-periodic to periodic (note that the Majorana fermions, being real, can only see fluxes which are multiples of π). However, the electron operators, being local objects, cannot have their boundary conditions changed, which implies we must simultaneously insert a magnetic flux of (an odd integer multiple of) π to which the chiral bosons are sensitive. This particular flux insertion corresponds precisely to the half-vortex of the bulk theory, represented by $\sigma e^{i\phi/2}$ (or $\sigma e^{i(r+1/2)\phi}$ in general, for $r \in \mathbb{Z}$) in the CFT.

Now, it is clear that the effect on the chiral bosons is to simply change the quantization of their winding to

$$\phi_\mu(x+L) \equiv \phi_\mu(x) + 2\pi\mu\frac{r+1/2}{n}, \quad \text{modulo } 2\pi\mathbb{Z}, \tag{7.25}$$

and therefore the winding numbers are quantized as

$$N_L = \tilde{N}_L + \frac{r+1/2}{n}, \quad N_R = \tilde{N}_R - \frac{r+1/2}{n}, \quad \tilde{N}_{L/R} \in \mathbb{Z}. \tag{7.26}$$

The $\sigma e^{i(r+1/2)\phi}$ flux through the cylinder can be detected by

$$\sigma e^{i(r+1/2)\phi} \text{ sector:} \quad e^{2\pi i N_L} = e^{-2\pi i N_R} = e^{2\pi i (r+1/2)}. \tag{7.27}$$

The effect on the Majorana fermions, as stated above, is to change their boundary conditions to being periodic. As a result, each edge possesses a Majorana zero mode (MZM), $\chi_L(k=0) = c_0$, $\chi_R(k=0) = \tilde{c}_0$; these must be paired together to form a single, physical complex fermion mode, $f = (c_0 + i\tilde{c}_0)/\sqrt{2}$, which may be occupied or unoccupied. This is a reflection of the Ising fusion rules of the σ particles, Eq. (7.16). Note that this means we can no longer define separate fermion parities for the two edges, as the MZM operator changes the occupancy of this complex fermion mode, $\{c_0, (-1)^{N_f}\} = \{\tilde{c}_0, (-1)^{N_f}\} = 0$ for $(-1)^{N_f} = (-1)^{f^\dagger f}$. In the twisted sector, one can construct a physical state for given windings $N_{R/L}$ in (7.26) by filling up an arbitrary number of finite momentum Majorana fermion states on either edge, and then choosing the complex fermion zero mode f to be either occupied or unoccupied to satisfy the $G = 1$ condition.

Altogether, we see that there are $2n$ untwisted and n twisted sectors, corresponding to the $2n$ Abelian and n non-Abelian anyons of the $\nu = \frac{1}{n}$ MR state. The $2n$ Abelian anyon fluxes $e^{ir\phi}$ and $\chi e^{ir\phi}$ through the cylinder can be distinguished by the local edge combined parity $(-1)^{N_\mu}(-1)^{F_\mu}$, which is identical to a Wilson loop of anyon type $\sigma_\mu e^{i\phi_\mu/2}$ around the cylinder. The phases in (7.23) and (7.24) are identical to the monodromy braiding phases between $\sigma_\mu e^{i\phi_\mu/2}$ and $e^{ir\phi}$, $\chi e^{ir\phi}$

$$\mathcal{D}S_{\sigma_\mu e^{i\phi_\mu/2}, e^{ir\phi_\mu}} = e^{i\pi\mu r/n}. \tag{7.28}$$

As noticed previously, the remaining n non-Abelian fluxes $\sigma e^{i(r+1/2)\phi}$ through the cylinder cannot be detected by the same local edge combined parities because separate fermion parities for each edge, $(-1)^{F_\mu}$, cannot be defined in these twisted sectors. This is consistent with the trivial modular S-matrix entries $S_{\sigma e^{i\phi/2}, \sigma e^{i(r+1/2)\phi}} = 0$. Instead, the twisted sectors can be distinguished by their $U(1)$ sector according to $e^{2\pi i N_\mu}$, which is identical to a Wilson loop of anyon type $e^{i\phi_\mu}$ around the cylinder. The phases in (7.27) are identical to the monodromy braiding phases between $e^{i\phi_\mu}$ and $\sigma_\mu e^{i(r+1/2)\phi_\mu}$

$$\mathcal{D}S_{e^{i\phi_\mu}, \sigma e^{i(r+1/2)\phi_\mu}} = e^{2\pi i\mu(r+1/2)/n}. \tag{7.29}$$

Note that passing from one topological sector to another requires the application of a non-local Wilson line operator. In our computation of the EE using the cut-and-glue approach, we will thus need to ensure that

any approximations we make do not mix topological sectors since the "gluing" will be achieved via local electronic interactions. We describe this calculation and how we handle this subtlety next.

7.3 Cut-and-Glue Approach Review and Topological Sector Projection

As described in the introduction, our EE calculation is based on the cut-and-glue approach [263] as it is employed in Refs. [91,266] and which we now review in the context of the MR state. The application of this methodology to non-Abelian states such as the MR state brings with it new subtleties regarding the careful treatment of the edge theory's topological sectors, as noted above. We will discuss these issues below and describe in detail our approach for addressing them, which is an important new aspect of our work, in Sec. 7.3.1.

Consider a MR state on the torus. We wish to compute the EE associated with the entanglement cut splitting the torus into two cylinders, with the left and right halves labeled as regions A and B, respectively, as depicted in Fig. 7.2. The cut-and-glue approach employs the fact that, since the correlation length of the system is vanishingly small in a topological phase, we can approximate the EE as arising purely from entanglement between degrees of freedom near the entanglement cut. To that end, we can treat the entanglement cut as a physical cut and split the torus into two cylinders labeled as A and B. Adding electron tunneling interactions will gap out the edges and heal the cut. We can then compute the entanglement between the resulting coupled edge theories. In the case of a torus geometry, we will have two interfaces, as depicted in Fig. 7.2, which we label as the LA/RB and RA/LB interfaces, or interface 1 and interface 2, respectively.

The edges at interface 1, before coupling them through a tunneling term, are described by the Hamiltonians:

$$\begin{aligned} H_{\text{dec},1} = &\int_0^L dx \left[\frac{v_c}{4\pi} (\partial_x \phi_{RB})^2 - v_n \chi_{RB} \frac{i}{2} \partial_x \chi_{RB} \right] \\ &+ \int_0^L dx \left[\frac{v_c}{4\pi} (\partial_x \phi_{LA})^2 + v_n \chi_{LA} \frac{i}{2} \partial_x \chi_{LA} \right]. \end{aligned} \tag{7.30}$$

The Majorana fields have mode expansions

$$\chi_{RB}(x) = \frac{1}{\sqrt{L}} \sum_k e^{ikx} c_k, \quad \chi_{LA}(x) = \frac{1}{\sqrt{L}} \sum_k e^{ikx} d_k, \tag{7.31}$$

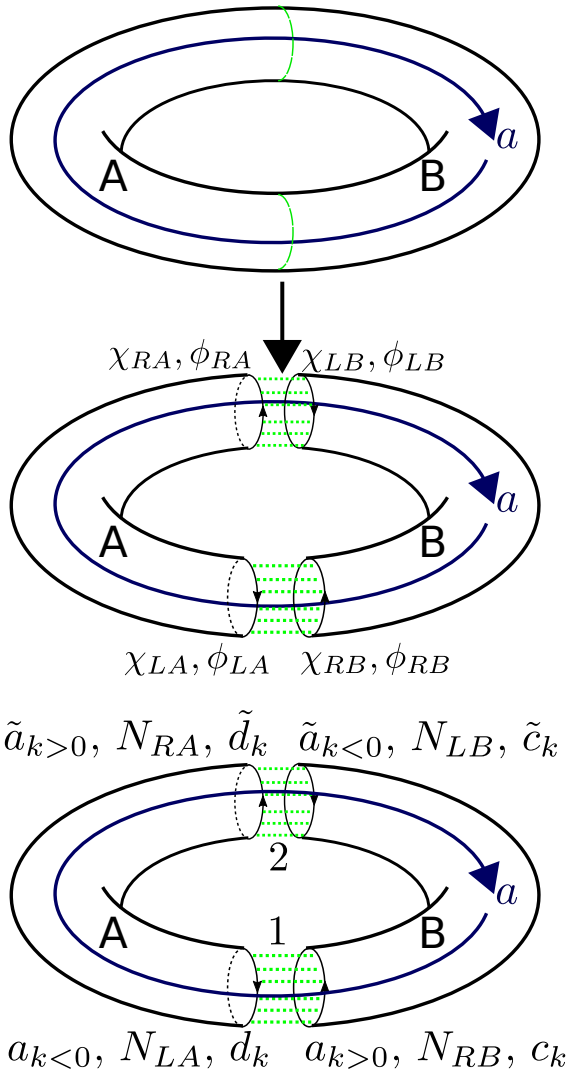

Figure 7.2: (Top) Moore-Read state on a torus. The arrow passing through the x-cycle (i.e. the vertical cycle) of the torus represents an anyon flux a. The green dashed lines represent an entanglement cut between regions A and B. In Sections 7.4 and 7.5, we will consider the situation in which regions A and B are occupied by MR states with equal and unequal, respectively, filling fractions. (Middle) A cartoon of the cut and glue approach to computing the entanglement entropy. The dotted green lines represent the electron tunneling terms added to glue the edges together. (Bottom) Same as the middle figure, but with each edge at interfaces 1 and 2 labelled by which mode operators act on them.

with half-integer quantized momenta in the untwisted sectors, $k = \frac{2\pi}{L}(j+1/2)$, $j \in \mathbb{Z}$, and integer quantized momenta in the twisted sectors, $k = \frac{2\pi}{L}j$, $j \in \mathbb{Z}$. The mode operators satisfy

$$c_k^\dagger = c_{-k}, \quad d_k^\dagger = d_{-k} \tag{7.32}$$

and obey the anti-commutation relations

$$\{c_k^\dagger, c_{k'}\} = \{d_k^\dagger, d_{k'}\} = \delta_{k,k'}, \quad \{c_k, d_{k'}\} = 0. \tag{7.33}$$

The boson fields have mode expansions

$$\begin{aligned} \phi_{RB} &= \phi_{RB,0} + 2\pi N_{RB}\frac{x}{L} + \sum_{k>0}\sqrt{\frac{2\pi}{nL|k|}}(a_k e^{ikx} + a_k^\dagger e^{-ikx}) \\ \phi_{LA} &= \phi_{LA,0} + 2\pi N_{LA}\frac{x}{L} + \sum_{k<0}\sqrt{\frac{2\pi}{nL|k|}}(a_k e^{ikx} + a_k^\dagger e^{-ikx}) \end{aligned} \tag{7.34}$$

with integer quantized momenta in all sectors: $k = \frac{2\pi}{L}j$, $j \in \mathbb{Z}/\ \{0\}$. The mode operators obey the commutation relations:

$$[a_k^\dagger, a_{k'}] = \delta_{k,k'}, \quad [a_k, a_{k'}] = 0, \tag{7.35}$$

$$[\phi_{RB,0}, N_{RB}] = -[\phi_{LA,0}, N_{LA}] = -\frac{i}{n}. \tag{7.36}$$

The quantization of the winding numbers is determined by the topological sector, as detailed in Section 7.2.

Likewise, before adding any couplings, interface 2 is described by

$$\begin{aligned} H_{\text{dec},2} = &\int_0^L dx \left[\frac{v_c}{4\pi}(\partial_x\phi_{LB})^2 - v_n\chi_{LB}\frac{i}{2}\partial_x\chi_{LB}\right] \\ &+ \int_0^L dx \left[\frac{v_c}{4\pi}(\partial_x\phi_{RA})^2 + v_n\chi_{RA}\frac{i}{2}\partial_x\chi_{RA}\right]. \end{aligned} \tag{7.37}$$

We write the mode expansions of the interface 2 fields as follows:

$$\chi_{LB} = \frac{1}{\sqrt{L}} \sum_k e^{ikx} \tilde{c}_k, \quad \chi_{RA} = \frac{1}{\sqrt{L}} \sum_k e^{ikx} \tilde{d}_k, \tag{7.38}$$

$$\begin{aligned} \phi_{RA} &= \phi_{RA,0} + 2\pi N_{RA} \frac{x}{L} + \sum_{k>0} \sqrt{\frac{2\pi}{nL|k|}} (\tilde{a}_k e^{ikx} + \tilde{a}_k^\dagger e^{-ikx}) \\ \phi_{LB} &= \phi_{LB,0} + 2\pi N_{LB} \frac{x}{L} + \sum_{k<0} \sqrt{\frac{2\pi}{nL|k|}} (\tilde{a}_k e^{ikx} + \tilde{a}_k^\dagger e^{-ikx}), \end{aligned} \tag{7.39}$$

where the quantization of the momenta and winding numbers are determined in the same way as for the interface 1 fields.

Now, the (quasi-)electron operators are given by

$$\psi_{e,L\alpha} = \chi_{L\alpha} e^{in\phi_{L\alpha}}, \quad \psi_{e,R\alpha} = \chi_{R\alpha} e^{-in\phi_{R\alpha}}. \tag{7.40}$$

We also define a $\mathbb{Z}_2$ symmetry operator for *each* cylinder:

$$G_\alpha = (-1)^{F_\alpha} (-1)^{N_{L\alpha} + N_{R\alpha}}, \quad \alpha = A, B, \tag{7.41}$$

where $(-1)^{F_\alpha}$ is the fermion parity operator on the two edges of cylinder α. Since we have physically split the torus into two cylinders, we require separately that $G_\alpha = 1$ for $\alpha = A, B$. As before, in the untwisted sectors, we can define separate fermion parities for each edge of either cylinder: $(-1)^{F_{L/R\alpha}}$.

We now wish to glue the two edges together to heal the cut. So, we add in the electron tunnelling terms

$$\begin{aligned} H_{AB} &= \int_0^L dx \left[\frac{2g}{2\pi} \left(\psi_{e,LA}^\dagger \psi_{e,RB} + h.c. \right) \right] + \int_0^L dx \left[\frac{2g}{2\pi} \left(\psi_{e,LB}^\dagger \psi_{e,RA} + h.c. \right) \right] \\ &= \int_0^L dx \left[\frac{2g}{\pi} i \chi_{LA} \chi_{RB} \cos[n(\phi_{RB} + \phi_{LA})] \right] + \int_0^L dx \left[\frac{2g}{\pi} i \chi_{LB} \chi_{RA} \cos[n(\phi_{RA} + \phi_{LB})] \right], \end{aligned} \tag{7.42}$$

where we take $g > 0$.[3]

Our task is to approximate the ground state of

$$H = H_{\text{dec},1} + H_{\text{dec},2} + H_{AB}, \tag{7.43}$$

which requires us to approximate H_{AB}. In the strong coupling limit, the ground state is assumed to give

[3]Note that this interaction is irrelevant in the renormalization group sense and so need not open up a gap. This can be remedied by adding in a density-density interaction of the form $U\partial_x\phi_{LA}\partial_x\phi_{RB}$. For a range of U, the scaling dimensions of the scalar fields will be renormalized so as to make the tunnelling term relevant. However, in the interest of simplicity, we will not include such terms and simply assume g to be large and the edges are gapped out by the interactions.

rise to individual expectation values of the bosonic operators $i\chi_{LA}\chi_{RB}$ and $\cos[n(\phi_{RB}+\phi_{LA})]$. Without loss of generality, the ground state for $g\to\infty$ is represented by the expectation values

$$\begin{aligned}&\langle n(\phi_{RB}+\phi_{LA})\rangle = \langle n(\phi_{RA}+\phi_{LB})\rangle = \pi\\ &\langle i\chi_{LA}\chi_{RB}\rangle,\, \langle i\chi_{LB}\chi_{RA}\rangle > 0\,,\end{aligned} \tag{7.44}$$

As such, expanding the fields around their classical expectations values yields a harmonic approximation of the interface interaction

$$\begin{aligned}H_{AB}\approx \int_0^L dx\Big[\text{const.}+v_n\tilde{g}i\chi_{LA}\chi_{RB}+v_n\tilde{g}i\chi_{LB}\chi_{RA}\\ +\frac{v_c\lambda\pi}{2}(\phi_{RB}+\phi_{LA}-\pi)^2+\frac{v_c\lambda\pi}{2}(\phi_{RA}+\phi_{LB}-\pi)^2\Big]\end{aligned} \tag{7.45}$$

where $\tilde{g}=-2g/(v_n\pi)<0$ and $\lambda>0$. Since we are considering only small fluctuations of $\phi_{RA}+\phi_{LB}$ and $\phi_{RB}+\phi_{LA}$ about their pinned values, they cannot have non-zero winding numbers, as this would imply they vary significantly over the length of the system. We thus have the constraint [266]

$$N_{RA}+N_{LB}=N_{LA}+N_{RB}=0, \tag{7.46}$$

in this strong coupling limit.

The harmonic approximation Eq. (7.45) plays a key role in this work, for it allows us to calculate the entanglement entropy and spectrum at the interface by analytical means. However, important issues underlying this approximation need to be accounted for. First, the approximated tunnelling Hamiltonian violates both the $\mathbb{Z}_2$ gauge symmetry gluing the fermionic and bosonic sectors together (as discussed above) and the $U(1)$ gauge symmetry associated with independent shifts of the bosonic fields[4]: $\phi_{L/R}\to\phi_{L/R}+2\pi P_{L/R}, P_{L/R}\in\mathbb{Z}$. Indeed, under conjugation by G_A, we see that $i\chi_{LA}\chi_{RB}\to -i\chi_{LA}\chi_{RB}$. This in turn means that the approximated tunnelling Hamiltonian mixes topological sectors. For instance, consider the identity ($\mathbf{1}$) and χ sectors of the MR theory. Recall that in the former sector, the fermionic parity matches the bosonic winding number parity on each edge, while these two quantities are opposite in the latter. Now, it is easy to see that the $\tilde{g}i\chi_{LA}\chi_{RB}$ term in the approximated interaction will change the fermionic parity on both edges and so will mix the identity and χ sectors on each half of the torus. The $(\phi_{RB}+\phi_{LA}-\pi)^2$ term also violates the $U(1)$ symmetry associated with the shift symmetry $\phi_{LA/RB}\to\phi_{LA/RB}+c_{LA/RB}$ and so, in principle, will also mix bosonic winding number sectors corresponding to distinct topological sectors.

[4]Note that, when we say the gauge symmetries are violated, we do not mean to imply that a gauge field is being Higgsed. As we explain, we mean simply that the harmonic approximation of H_{AB}, taken at face value, will mix topological sectors (that is, it is a non-local expression).

Hence the ground state of this approximated Hamiltonian *cannot* describe an approximation of the ground state of the interface theory in a definite anyon sector.

Our strategy for dealing with the $\mathbb{Z}_2$ gauge symmetry violation encoded in Eq. (7.45), is to promote the theory to an "expanded" Hilbert space in which the gauge symmetries are violated. In this expanded Hilbert space, the bosonic and fermionic sectors are genuinely decoupled and so we can compute the ground state of the approximated Hamiltonian using straightforward free field theory methods. Once this is done, we can project the resulting state into the appropriate topological sector of the gauge-invariant subspace. Restoring the $U(1)$ gauge symmetry amounts to projecting to states with appropriately quantized bosonic winding numbers. Restoring the $\mathbb{Z}_2$ symmetry means projecting to states obeying the appropriate matching of the fermion parity and bosonic winding number parity. We describe this in more detail next.

7.3.1 Description of the Projection

Let us denote the exact ground state of the coupled edge system, as described by the Hamiltonian of Eq. (7.43), in topological sector a as

$$|\psi_a\rangle = |\psi_{1,a}\rangle \otimes |\psi_{2,a}\rangle \,. \tag{7.47}$$

Here, $|\psi_{1,a}\rangle$ and $|\psi_{2,a}\rangle$ are the ground states of interfaces 1 and 2, respectively, in the topological sector a. Note that, although we can express the ground state as a tensor product of the two interfaces, the ground states of the interfaces are constrained to lie in the same topological sector. This is a consequence of the fact that the anyon flux a passing through one interface must necessarily pass through the other interface, as shown in Fig. 7.2. In particular, this means that we must have $G_A |\psi_a\rangle = G_B |\psi_a\rangle = |\psi_a\rangle$ – that is to say, each cylinder must, on its own, lie in the physical MR Hilbert space.

We can write the ground state of the approximated Hamiltonian, given by Eq. (7.43) with the approximation of H_{AB} by Eq. (7.45), in a similar form

$$|\widehat{\psi}_a\rangle = |\widehat{\psi}_{1,a}\rangle \otimes |\widehat{\psi}_{2,a}\rangle \,. \tag{7.48}$$

(Henceforth, symbols with hats will denote objects in the unprojected Hilbert space.) As emphasized above, our approximation of the gapping term violates the $\mathbb{Z}_2$ gauge symmetry, and so both $|\widehat{\psi}_{1,a}\rangle$ and $|\widehat{\psi}_{2,a}\rangle$ will be superpositions of states from different topological sectors of the MR theory. Nevertheless, we have written $|\widehat{\psi}_{1,a}\rangle$ and $|\widehat{\psi}_{2,a}\rangle$ as having dependence on a because they still retain some information about a through the boundary conditions of both the bosonic and fermionic fields. For instance, if we are working in one of

the twisted sectors, our approximation of the interaction term will not change the fact that the Majorana fermions obey periodic boundary conditions.

In order to obtain a state in a definite topological sector of the MR theory, we consider

$$|\psi_a\rangle \approx P_a |\widehat{\psi}_a\rangle \equiv P_{a,A} P_{a,B} |\widehat{\psi}_a\rangle \tag{7.49}$$

where $P_{a,\alpha}$ projects cylinder α to the topological sector a, and we have defined $P_a \equiv P_{a,A} P_{a,B}$. We will show in Section 7.4 that the projected state Eq. (7.49) correctly describes the universal entanglement properties of the MR state in each topological sector a (and takes the expected form of an Ishibashi state [263, 290]).

For a general topological sector a, the action of the projection is most easily understood when writing $|\widehat{\psi}_a\rangle$ in terms of a superposition of eigenstates of $N_{\mu\alpha}$ and $(-1)^{F_{\mu\alpha}}$, in which case the projection amounts to removing those states in the sum which do not satisfy the $\mathbb{Z}_2$ constraint appropriate to the topological sector in question. Focusing first on the untwisted sectors, we can, as noted above, define separate fermion parities for each edge:

$$(-1)^{F_\alpha} \equiv (-1)^{F_{L\alpha}} (-1)^{F_{R\alpha}}. \tag{7.50}$$

This permits us to define operators which project each edge to specific topological sectors of the untwisted sector. Indeed, we can formally write

$$P_{a,\alpha} \equiv P_{a,L\alpha} P_{a,R\alpha} \tag{7.51}$$

as the operator which projects cylinder α to the untwisted sector a, where $P_{a,\mu\alpha}$ are operators acting on edges $\mu\alpha$. Specialising momentarily to the sector $a = e^{ir\phi}$ and edge RB, we define $P_{e^{ir\phi},RB}$ via its action on a basis of states for the edge. An arbitrary state on edge RB can be written as a superposition of the states

$$|N_{RB}, \{n_{a,k}\}_{k>0}, \{n_{c,k}\}_{k>0}\rangle\,, \tag{7.52}$$

which are eigenstates of N_{RB}, $a_k^\dagger a_k$, and $c_k^\dagger c_k$ with eigenvalues N_{RB}, $\{n_{a,k}\}_{k>0}$, and $\{n_{c,k}\}_{k>0}$, respectively. We then define

$$P_{e^{ir\phi},RB} |N_{RB}, \{n_{a,k}\}, \{n_{c,k}\}\rangle = |N_{RB}, \{n_{a,k}\}, \{n_{c,k}\}\rangle \tag{7.53}$$

if $N_{RB} + \frac{r}{n} \in \mathbb{Z}$ and $(-1)^{N_{RB}+\frac{r}{n}+\sum_k n_{c,k}} = 1$, while

$$P_{e^{ir\phi},RB} \, |N_{RB}, \{n_{a,k}\}, \{n_{c,k}\}\rangle = 0 \tag{7.54}$$

otherwise. The first condition enforces that the winding number obey the appropriate quantization for the $a = e^{ir\phi}$ sector on edge RB, Eq. (7.22), while the second condition ensures that the $\mathbb{Z}_2$ constraint for sector $a = e^{ir\phi}$, Eq. (7.23), is satisfied. In physical terms, this operator ensures that the correct magnetic flux is threaded through the circle defined by the edge and that the fermion parity matches the integer part of bosonic winding on this edge. We similarly define for edge LB

$$P_{e^{ir\phi},LB} \, |N_{LB}, \{n_{\tilde{a},k}\}, \{n_{\tilde{c},k}\}\rangle = |N_{LB}, \{n_{\tilde{a},k}\}, \{n_{\tilde{c},k}\}\rangle \tag{7.55}$$

if $N_{LB} - \frac{r}{n} \in \mathbb{Z}$ and $(-1)^{N_{LB}-\frac{r}{n}+\sum_k n_{\tilde{c},k}} = 1$, while

$$P_{e^{ir\phi},LB} \, |N_{LB}, \{n_{\tilde{a},k}\}, \{n_{\tilde{c},k}\}\rangle = 0 \tag{7.56}$$

otherwise. The operators $P_{e^{ir\phi},\mu A}$ are defined in an analogous manner. Likewise, the $P_{\chi e^{ir\phi},\sigma\alpha}$ operators are defined in a similar way, but by instead enforcing the $\mathbb{Z}_2$ constraint of Eq. (7.24) on each edge.

As for the twisted sectors, since we cannot define separate fermion parities for each edge, we cannot write down a projection operator as a product of operators acting on the two edges of the cylinder. Let us first consider cylinder B. We define a complex fermion from the Majorana zero modes of each edge (recall that the Majorana fermions obey periodic boundary conditions in the twisted sectors),

$$f_B = \frac{1}{\sqrt{2}}(c_0 + i\tilde{c}_0), \tag{7.57}$$

which explicitly ties together the $\mu = L, R$ Hilbert spaces of the cylinder. An arbitrary state on cylinder B can then be written as a superposition of states of the form

$$|N_{RB}, \{n_{a,k}\}_{k>0}, \{n_{c,k}\}_{k>0}\rangle \otimes |N_{LB}, \{n_{\tilde{a},k}\}_{k<0}, \{n_{\tilde{c},k}\}_{k<0}\rangle \otimes |n_B\rangle \tag{7.58}$$

which are eigenstates of $N_{R/L,B}$, $a_k^\dagger a_k$, $\tilde{a}_k^\dagger \tilde{a}_k$, $c_k^\dagger c_k$, $\tilde{c}_k^\dagger \tilde{c}_k$, $f_B^\dagger f_B$ with eigenvalues, $N_{R/L,B}$, $\{n_{a,k}\}_{k\neq 0}$, $\{n_{c,k}\}_{k>0}$, $\{n_{\tilde{c},k}\}_{k<0}$, and n_B respectively. We then define the operator $P_{a,B}$, which projects cylinder B to the twisted

topological sector $a = \sigma e^{i(r+1/2)\phi}$, via its action on these states:

$$P_{\sigma e^{i(r+1/2)\phi},B} \, |N_{\mu B}, \{n_{a/\tilde{a},k}, n_{c/\tilde{c},k}\}, n_B\rangle = |N_{\mu B}, \{n_{a/\tilde{a},k}, n_{c/\tilde{c},k}\}, n_B\rangle \tag{7.59}$$

if $N_{\mu B} + \mu \frac{r}{n} \in \mathbb{Z}$ and $(-1)^{\sum_\mu N_{\mu B} + \sum_k (n_{c,k} + n_{\tilde{c},-k}) + n_B} = 1$, while

$$P_{\sigma e^{i(r+1/2)\phi},B} \, |N_{\mu B}, \{n_{a/\tilde{a},k}, n_{c/\tilde{c},k}\}, n_B\rangle = 0 \tag{7.60}$$

otherwise. Again, the first constraint ensures that the bosonic winding numbers satisfy the quantization of Eq. (7.26) while the second condition enforces the $\mathbb{Z}_2$ constraint $G_B = 1$. Physically, $P_{\sigma e^{i(r+1/2,\phi)},B}$ ensures the correct magnetic flux passes through the cylinder and that the total fermion parity across both edges matches the total bosonic winding of the two edges. An analogous operator, $P_{\sigma e^{i(r+1/2)\phi},A}$, for cylinder A can be defined, after forming a complex fermion, f_A, defined from the Majorana zero modes of the two edges:

$$f_A = \frac{1}{\sqrt{2}}(d_0 + i\tilde{d}_0). \tag{7.61}$$

One can write down explicit expressions for the projection operators defined above but, for our purposes, the above operational definitions will prove more convenient. We also note that there is a bit of an ambiguity in defining the projection operators for the twisted sectors in that there is a choice as to whether one defines an occupied $f_{A/B}$ state as corresponding to odd or even fermion parity. We will return to this point in Section 7.4.2, when we calculate the EE in the twisted sectors, and in Appendix E.2.2, where we present explicit expressions for the twisted sector ground states.

7.4 Uniform Interface Entanglement Entropy

We are now prepared to move on to the actual computation of the ES and EE of the MR states. We first recall that, for an entanglement cut of the torus of the type we are considering (Fig. 7.2), the TEE in the ground state of topological sector a is given by

$$\gamma_a = 2\ln(\mathcal{D}/d_a), \tag{7.62}$$

where $\mathcal{D}$ is again the total quantum dimension and d_a is the quantum dimension of the anyon a. These states (on the torus) are known as *minimum entropy states*, as they maximize the TEE within the space of degenerate ground states [104, 284]. As noted in Section 7.2, a MR state at filling $\nu = 1/n$ has $\mathcal{D} = 2\sqrt{n}$,

the Abelian anyons $e^{ir\phi}$ and $\chi e^{ir\phi}$ all have $d_a = 1$, and the non-Abelian anyons $\sigma e^{i(r+1/2)\phi}$ have $d_a = \sqrt{2}$. Hence, in the untwisted sectors, we expect to find the TEE

$$\gamma_a = 2\ln 2\sqrt{n}, \quad a = e^{ir\phi}, \chi e^{ir\phi}, \tag{7.63}$$

while in the twisted sectors we expect

$$\gamma_a = 2\ln \sqrt{2n}, \quad a = \sigma e^{i(r+1/2)\phi}\,. \tag{7.64}$$

We can glean some intuition for these results by contrasting them with the TEE for the Abelian system consisting of a $p+ip$ superconductor stacked with (and decoupled from) a $\nu = \frac{1}{n}$ Laughlin state. Such a state has $\mathcal{D} = \sqrt{n}$ and an edge is also described by Eq. (7.7), but with local (electronic) operators given by χ and $e^{in\phi}$. The TEE in, for instance, the trivial sector on the torus of this theory is thus $\gamma_1 = 2\ln\sqrt{n}$, in contrast to $\gamma_1 = 2\ln 2\sqrt{n}$ for the MR state. As we will see explicitly, the factor of two difference in the argument of the logarithm arises precisely from the the projection discussed in Section 7.3.1. Indeed, when writing the approximated ground state $|\widehat{\psi}_a\rangle$, as a superposition of states with definite bosonic winding and fermion occupation numbers, we will find that the projection to the physical MR Hilbert space, Eq. (7.49), will remove exactly *half* of the states appearing in the superposition. This increases the TEE by $\ln 2 + \ln 2$, with each interface contributing a single $\ln 2$.

A heuristic understanding of the difference between the TEEs of the untwisted and twisted sectors follows from the fact that a cylinder with a $\sigma e^{i(r+1/2)}$ flux traps a MZM at each edge. Gluing two cylinders together to form a torus, as we do, hybridizes the MZMs on the edges. On tracing out one cylinder to compute the EE, one is, loosely speaking, tracing out half of a qubit for each pair of edges, giving a contribution of $2\ln\sqrt{2}$ to the EE.

In the following subsections, we proceed to compute the entanglement spectrum and TEE of the ground state of the MR theory for the Abelian and non-Abelian topological sectors. We will compute the ground state for the interface 1 explicitly; the calculations for interface 2 are identical.

7.4.1 Abelian (Untwisted) Sectors

We begin by considering a MR state on a torus in one of the untwisted topological sectors: $e^{ir\phi}$, $\chi e^{ir\phi}$. The Majorana fields satisfy anti-periodic boundary conditions while the bosons obey the boundary conditions of Eq. (7.21) and hence the winding numbers are quantized as in Eq. (7.22). Now, using the field mode expansions, the full approximated Hamiltonian describing interface 1 decouples into fermionic and bosonic

terms:

$$H_1 \equiv H_{1,f}^{\text{osc}} + H_{1,b}^{\text{osc}} + H_{1,b}^{\text{zero}}. \tag{7.65}$$

The bosonic zero mode Hamiltonian is given by

$$H_{1,b}^{\text{zero}} = \frac{\pi v_c n}{2L}(N_{RB} - N_{LA})^2 + \frac{\pi \lambda v_c L}{2}(\phi_{RB,0} + \phi_{LA,0})^2, \tag{7.66}$$

where we have made use of the constraint of Eq. (7.46). The bosonic oscillator part takes the form

$$H_{1,b}^{\text{osc}} = \frac{v_c}{2}\sum_{k\neq 0}(a_k^\dagger \quad a_{-k}) \begin{pmatrix} A_k & B_k \\ B_k & A_k \end{pmatrix} \begin{pmatrix} a_k \\ a_{-k}^\dagger \end{pmatrix}, \tag{7.67}$$

where

$$A_k = |k| + \frac{2\lambda\pi^2}{n|k|}, \quad B_k = \frac{2\lambda\pi^2}{n|k|}. \tag{7.68}$$

Lastly, the fermion oscillator modes are governed by the Hamiltonian

$$H_{1,f}^{\text{osc}} = v_n \sum_{k>0}(c_k^\dagger \quad d_{-k}) \begin{pmatrix} k & -i\tilde{g} \\ i\tilde{g} & -k \end{pmatrix} \begin{pmatrix} c_k \\ d_{-k}^\dagger \end{pmatrix}. \tag{7.69}$$

Since, within our harmonic approximation, the bosons and fermions decouple, we can compute the ground state of these two sectors separately. However, as emphasized above, this decoupling is a manifestation of the violation of the $\mathbb{Z}_2$ gauge symmetry by our approximation. As discussed in Section 7.3.1, we will have to perform a projection to obtain a state in a definite untwisted topological sector. Having done so, it will then be straightforward to obtain the reduced density matrix for subregion B, as the projected ground state will take a simple Schmidt decomposed form.

Bosonic Sector Ground State

In the expanded Hilbert space, the computation of the ground state in the bosonic sector is identical to the calculation carried out by Lundgren et. al. [266] for the Laughlin states at filling $\nu = 1/n$. For completeness, we briefly review the calculation here.

Starting with the oscillator sector, we can diagonalize Eq. (7.67) via a Bogoliubov transformation,

$$\begin{pmatrix} a_k \\ a_{-k}^\dagger \end{pmatrix} = \begin{pmatrix} \cosh\theta_k & \sinh\theta_k \\ \sinh\theta_k & \cosh\theta_k \end{pmatrix} \begin{pmatrix} b_k \\ b_{-k}^\dagger \end{pmatrix}, \tag{7.70}$$

where $\cosh(2\theta_k) = A_k/\varepsilon_k$, $\sinh(2\theta_k) = -B_k/\varepsilon_k$, and $\varepsilon_k = \sqrt{|k|^2 + 4\lambda\pi^2/n}$. With these definitions, we can write $H_{1,b}^{\text{osc}} = v_c \sum_{k\neq 0} \varepsilon_k (b_k^\dagger b_k + \frac{1}{2})$, so that the ground state is defined by $b_k |G_{b,\text{osc},1}\rangle = 0$. It is readily checked that the ground state is given by the coherent state

$$|G_{b,\text{osc},1}\rangle = \exp\left(\sum_{k>0} e^{-u_k/2} a_k^\dagger a_{-k}^\dagger\right)|0\rangle, \tag{7.71}$$

where $u_k = \ln\coth^2(2\theta_k)$ and $|0\rangle$ is the ground state of the decoupled system, satisfying $a_k|0\rangle = 0$ for all $k \neq 0$. For $|k| \ll \lambda$,

$$u_k \approx \frac{2}{\pi}\sqrt{\frac{n}{\lambda}}k \equiv v_e k, \tag{7.72}$$

where we have defined the entanglement velocity $v_e = \frac{2}{\pi}\sqrt{\frac{n}{\lambda}}$.

As for the zero-mode sector, on defining $X = n(N_{RB} - N_{LA})/2$ and $P = \phi_{LA,0} + \phi_{RB,0}$ so that $[X, P] = i$, we see that Eq. (7.66) describes a simple harmonic oscillator. In the $L \to \infty$ limit, we can ignore the discretization of X and simply write down the ground state:

$$|G_{b,\text{zero},1}\rangle = \sum_{N\in\mathbb{Z}-\frac{r}{n}} e^{-v_e \pi n N^2/2L} |N_{RB} = N, N_{LA} = -N\rangle, \tag{7.73}$$

where we have again made use of the constraint $N_{RB} + N_{LA} = 0$ [Eq. Eq. (7.46)] and enforced the quantization of the winding numbers given in Eq. (7.21).

Majorana Sector Ground State

Turning next to the Majorana fermions, we can perform a unitary transformation to diagonalize Eq. (7.69). We define $\gamma_k = \cos\varphi_k c_k + i\sin\varphi_k d_{-k}^\dagger$, where $\sin\varphi_k = \tilde{g}/\lambda_k$, $\cos\varphi_k = k/\lambda_k$, and $\lambda_k = \sqrt{k^2 + \tilde{g}^2}$. The Hamiltonian, in this basis, becomes $H_{1,f}^{\text{osc}} = v_n \sum_{k\neq 0} \lambda_k(\gamma_k^\dagger\gamma_k - \frac{1}{2})$. The ground state is defined by $\gamma_k |G_{f,\text{osc},1}\rangle = 0$. Explicitly, we can write the ground state of $H_{1,f}^{\text{osc}}$ in BCS form:

$$|G_{f,\text{osc},1}\rangle = \exp\left(\sum_{k>0} i e^{-w_k/2} d_{-k}^\dagger c_k^\dagger\right)|0\rangle, \tag{7.74}$$

where we have defined w_k through $e^{-w_k/2} = -\tan\varphi_k$ (recalling that $\tilde{g} < 0$) and $|0\rangle$ is the ground state of the decoupled system, satisfying $c_k|0\rangle = d_{-k}|0\rangle = 0$ for all $k > 0$. For $|k| \ll \tilde{g}$, we have that

$$w_k \approx \frac{2k}{|\tilde{g}|} \equiv \tilde{v}_e k, \tag{7.75}$$

where we have defined $\tilde{v}_e = 2/|\tilde{g}|$.

Projecting to the Physical Hilbert Space

We can now construct the full ground state of the coupled edge system in the expanded Hilbert space by combining the above results with the analogous results for interface 2 (i.e. the RA/LB interface). Explicitly,

$$\begin{aligned} |\widehat{\psi}_a\rangle &= |\widehat{\psi}_{1,a}\rangle \otimes |\widehat{\psi}_{2,a}\rangle\,, \\ |\widehat{\psi}_{i,a}\rangle &= |G_{b,\mathrm{zero},i}\rangle \otimes |G_{b,\mathrm{osc},i}\rangle \otimes |G_{f,\mathrm{osc},i}\rangle\,,\ i = 1,2 \end{aligned} \tag{7.76}$$

where,

$$|G_{b,\mathrm{zero},2}\rangle = \sum_{N\in\mathbb{Z}-\frac{r}{n}} e^{-\frac{v_e \pi n N^2}{2L}} |N_{LB} = -N, N_{RA} = N\rangle\,, \tag{7.77}$$

$$|G_{b,\mathrm{osc},2}\rangle = \exp\left(\sum_{k>0} e^{-v_e k/2} \tilde{a}_k^\dagger \tilde{a}_{-k}^\dagger\right)|0\rangle\,, \tag{7.78}$$

$$|G_{f,\mathrm{osc},2}\rangle = \exp\left(\sum_{k>0} i e^{-\tilde{v}_e k/2} \tilde{c}_{-k}^\dagger \tilde{d}_k^\dagger\right)|0\rangle\,. \tag{7.79}$$

Note that in the expressions for the oscillator sector ground states, we have taken the low-energy limit by expanding u_k and w_k to linear order in k. This is because the correspondence between the entanglement spectrum and the physical edge CFT spectrum only holds for the low lying entanglement spectrum eigenvalues.

In order to obtain an approximation to the true ground state $|\psi_a\rangle$ ($a = e^{ir\phi}$ or $\chi e^{ir\phi}$), we must apply the projection operator $P_a \equiv P_{a,A}P_{a,B}$ defined in Eq. (7.49). Now, since $|\widehat{\psi}_a\rangle$ is a superposition of states with winding number and fermion parity eigenvalues satisfying $N_{RB} = -N_{LA}$ and $(-1)^{F_{RB}} = (-1)^{F_{LA}}$ as well as $N_{LB} = -N_{RA}$ and $(-1)^{F_{LB}} = (-1)^{F_{RA}}$, it is straightforward to see that

$$|\psi_a\rangle = P_a|\widehat{\psi}_a\rangle = P_{a,A}|\widehat{\psi}_a\rangle = P_{a,B}|\widehat{\psi}_a\rangle\,. \tag{7.80}$$

In more physical terms, this expresses the fact that the electron tunneling term enforces that the two cylinders

reside in the same topological sector.

The explicit form of $|\psi_a\rangle = P_{a,B}\,|\widehat{\psi}_a\rangle$ is rather cumbersome, and so we leave it for Appendix E.2.1. However, on expanding out the exponentials in $|G_{b,\mathrm{osc},1/2}\rangle$ and $|G_{f,\mathrm{osc},1/2}\rangle$, it is not too difficult to see that $|\psi_a\rangle = P_{a,B}\,|\widehat{\psi}_a\rangle$ is in a Schmidt decomposed form. Indeed, we have that

$$|\psi_{1,a}\rangle = e^{-\mathcal{H}_e^{RB}/2} \sum_{\substack{N_{RB},\\ \{n_{a,k},n_{c,k}\}}} i^{\sum_k n_{c,k}} P_{a,RB}\Big[\,|N_{RB}=-N_{LA}\rangle \otimes |\{n_{a,k}=n_{a,-k}, n_{c,k}=n_{d,-k}\}_{k>0}\rangle\Big], \tag{7.81}$$

$$|\psi_{2,a}\rangle = e^{-\mathcal{H}_e^{LB}/2} \sum_{\substack{N_{LB},\\ \{n_{\tilde{a},k},n_{\tilde{c},k}\}}} i^{\sum_k n_{\tilde{c},k}} P_{a,LB}\Big[\,|N_{LB}=-N_{RA}\rangle \otimes |\{n_{\tilde{a},-k}=n_{\tilde{a},k}, n_{\tilde{c},-k}=n_{\tilde{d},k}\}_{k>0}\rangle\Big] \tag{7.82}$$

where,

$$\mathcal{H}_e^{RB} = v_e\left(\frac{\pi n}{L}N_{RB}^2 + \sum_{k>0} k a_k^\dagger a_k - \frac{\pi}{12L}\right) + \tilde{v}_e\left(\sum_{k>0} k c_k^\dagger c_k - \frac{\pi}{24L}\right) \tag{7.83}$$

and

$$\mathcal{H}_e^{LB} = v_e\left(\frac{\pi n}{L}N_{LB}^2 + \sum_{k<0} |k| \tilde{a}_k^\dagger \tilde{a}_k - \frac{\pi}{12L}\right) + \tilde{v}_e\left(\sum_{k<0} |k| \tilde{c}_k^\dagger \tilde{c}_k - \frac{\pi}{24L}\right). \tag{7.84}$$

Note that we have multipled $|\psi_{a,i}\rangle$ by unimportant overall constants, $e^{-v_e\pi/24L}$ and $e^{-\tilde{v}_e\pi/48L}$, for later convenience. For readers familiar with boundary CFT methods, it should hopefully be clear that $|\psi_{1/2,a}\rangle$ are essentially regularized Ishibashi states for the a topological sectors of the MR CFT [263, 290] (up to unimportant relative phases). In other words, $|\psi_a\rangle = |\psi_{1,a}\rangle \otimes |\psi_{2,a}\rangle$ is a superposition of all states in the a topological sector, regulated by the operator $\exp[-(\mathcal{H}_e^{LB}+\mathcal{H}_e^{RB})/2]$. We can thus deduce that the reduced density matrix for, say, cylinder B is given by

$$\rho_{a,B} = \mathrm{Tr}_A\left[|\psi_a\rangle\langle\psi_a|\right] = \frac{1}{Z_{a,e}} P_{a,B} e^{-\mathcal{H}_e^{RB}-\mathcal{H}_e^{LB}} P_{a,B}, \tag{7.85}$$

So, the form of the entanglement Hamiltonian precisely matches that of the physical edge Hamiltonian in the topological sector a, as expected. The projection operator $P_{a,B}$ ensures the reduced density matrix only acts on states within the topological sector a of the physical Hilbert space.

Entanglement Spectrum and Entropy

At this point in the calculation, we are actually done. Indeed, we have argued that the entanglement spectrum exactly matches the physical edge CFT spectrum (taking into account the projection into the appropriate topological sector), and so we will necessarily obtain the correct TEE. Nevertheless, for completeness, we will show explicitly that we obtain the correct TEE for the $e^{ir\phi}$ sectors.

Introducing the fictitious inverse temperature $\beta = 1/T$, we wish to compute

$$Z_{e^{ir\phi},e} = \mathrm{Tr}_B \left[P_{e^{ir\phi},B} e^{-\beta(\mathcal{H}_e^{RB} + \mathcal{H}_e^{LB})} P_{e^{ir\phi},B} \right] = Z^{RB}_{e^{ir\phi},e} Z^{LB}_{e^{ir\phi},e} \tag{7.86}$$

where we have defined[5]

$$Z^{RB}_{e^{ir\phi},e} = \mathrm{Tr}_{RB} \left[P_{e^{ir\phi},RB} e^{-\beta \mathcal{H}_e^{RB}} P_{e^{ir\phi},RB} \right], \tag{7.87}$$

$$Z^{LB}_{e^{ir\phi},e} = \mathrm{Tr}_{LB} \left[P_{e^{ir\phi},LB} e^{-\beta \mathcal{H}_e^{LB}} P_{e^{ir\phi},LB} \right]. \tag{7.88}$$

In the following, we will focus on the computation of $Z^{RB}_{e^{ir\phi},e}$, as the calculation of $Z^{LB}_{e^{ir\phi},e}$ is virtually identical. First, we define the modular parameters

$$\tau = i\tau_2 = i\frac{\beta v_e}{L}, \quad \tilde{\tau} = i\tilde{\tau}_2 = i\frac{\beta \tilde{v}_e}{L} \tag{7.89}$$

and the variables

$$q = e^{2\pi i \tau}, \quad \tilde{q} = e^{2\pi i \tilde{\tau}}. \tag{7.90}$$

We compute the trace using eigenstates of N_{RB}, $a_k^\dagger a_k$, and $c_k^\dagger c_k$. Keeping in mind that that the role of the projection operator $P_{e^{ir\phi},RB}$ is to exclude those states which do not satisfy the constraint of Eq. (7.23), we compute the entanglement partition function to be

$$Z^{RB}_{e^{ir\phi},e} = \frac{1}{2}\chi_0^{\mathrm{Ising}}(\tilde{q})[\chi^+_{r/n}(q) + \chi^-_{r/n}(q)] + \frac{1}{2}\chi_{1/2}^{\mathrm{Ising}}(\tilde{q})[\chi^+_{r/n}(q) - \chi^-_{r/n}(q)], \tag{7.91}$$

[5]We emphasize that the trace is taken over all states in the physical MR Hilbert space on cylinder B. In particular, this means that we cannot, in general, separate the trace into separate traces over the edges RB and LB, since the states appearing in the trace must lie in a definite topological sector. However, the presence of the $P_{e^{ir\phi},\mu B}$ operators within the trace ensures that only states on edge μB satisfying the winding number quantization of Eq. (7.22) contribute, ensuring we do not mix topological sectors. So, in this case, we are justified in splitting the trace over B into two traces over its two edges.

where, employing the notation of Ref. [283], we have defined

$$\chi_0^{\text{Ising}}(\tilde{q}) = \frac{1}{2}\tilde{q}^{-\frac{1}{48}}\left[\prod_{j=0}^{\infty}(1+\tilde{q}^{j+1/2}) + \prod_{j=0}^{\infty}(1-\tilde{q}^{j+1/2})\right] \tag{7.92}$$

$$\chi_{1/2}^{\text{Ising}}(\tilde{q}) = \frac{1}{2}\tilde{q}^{-\frac{1}{48}}\left[\prod_{j=0}^{\infty}(1+\tilde{q}^{j+1/2}) - \prod_{j=0}^{\infty}(1-\tilde{q}^{j+1/2})\right] \tag{7.93}$$

and

$$\chi_{r/n}^{\pm}(q) = q^{-\frac{1}{24}}\left(\sum_{N\in\mathbb{Z}}(\pm 1)^N q^{n(N-\frac{r}{n})^2/2}\right)\prod_{j=1}^{\infty}\left(1-q^j\right)^{-1}. \tag{7.94}$$

Let us take a moment to unpack these expressions. The terms $\chi_0^{\text{Ising}}(\tilde{q})$ and $\chi_{1/2}^{\text{Ising}}(\tilde{q})$ are the contributions from the fermionic sector. Focusing first on $\chi_0^{\text{Ising}}(\tilde{q})$, we note that the first product appearing within the square brackets is simply the partition function for a free Majorana fermion with momenta quantized as $k = 2\pi(j+1/2)/L$. The second product is the partition function for a free Majorana, but with each state weighted by its fermion parity, $(-1)^F$. So, when these two products are added together, all terms corresponding to a state with an *odd* number of excited Majorana oscillator modes will cancel out. In other words, $\chi_0^{\text{Ising}}(\tilde{q})$ is the partition function for a free Majorana, with the trace restricted to states with an *even* fermion parity, $(-1)^F = +1$. Likewise, $\chi_{1/2}^{\text{Ising}}(\tilde{q})$ is the partition function for a free Majorana, with the trace restricted to states with an *odd* fermion parity, $(-1)^F = -1$. In more formal terms, $\chi_{0,1/2}^{\text{Ising}}(\tilde{q})$ are the characters of the 1 and χ sectors of the Ising CFT, respectively. Similarly, $\chi_{r/n}^{+}(q)$ are the characters for a $U(1)_n$ boson in the $e^{ir\phi}$ sector. In particular, the term in large rounded brackets in Eq. (7.94) results from the trace over the winding number sector, while the product outside the brackets results from the trace over the oscillator modes. The term $\chi_{r/n}^{-}(q)$ is the character for a $U(1)_n$ boson in the $e^{ir\phi}$ sector, but with each term in the trace weighted by the parity of the integer part of its winding number, $(-1)^N$. Hence, $\chi_{r/n}^{+}(q) \pm \chi_{r/n}^{-}(q)$ correspond to the partition functions for $U(1)_n$ bosons in the $e^{ir\phi}$ sector with the trace over the winding numbers restricted to states with the integer part of the winding being even and odd, respectively. Altogether, the first (second) line of Eq. (7.91) corresponds to a trace of $e^{-\mathcal{H}_e^{RB}}$ over states with even (odd) fermion number and an even (odd) integer part of the bosonic winding number. This accounts for all states in the $e^{ir\phi}$ topological sector. So, the entanglement partition function of the right-movers of the MR theory in the $e^{ir\phi}$ sector is indeed given by Eq. (7.91).

Now, we can write Eq. (7.91) in terms of the Dedekind η and Jacobi θ functions (see Appendix E.1):

$$\begin{aligned} Z^{RB}_{e^{ir\phi},e} =& \frac{1}{4}\left[\sqrt{\frac{\theta_0^0(\tilde{\tau})}{\eta(\tilde{\tau})}}+\sqrt{\frac{\theta_{1/2}^0(\tilde{\tau})}{\eta(\tilde{\tau})}}\right]\frac{\theta_0^{-r/m}(n\tau)+e^{-\frac{i\pi r}{m}}\theta_{1/2}^{-r/m}(n\tau)}{\eta(\tau)} \\ &+\frac{1}{4}\left[\sqrt{\frac{\theta_0^0(\tilde{\tau})}{\eta(\tilde{\tau})}}-\sqrt{\frac{\theta_{1/2}^0(\tilde{\tau})}{\eta(\tilde{\tau})}}\right]\frac{\theta_0^{-r/m}(n\tau)-e^{-\frac{i\pi r}{m}}\theta_{1/2}^{-r/m}(n\tau)}{\eta(\tau)}. \end{aligned} \tag{7.95}$$

Using the modular transformation properties of the η and θ functions given in Eqs. (E.4) and (E.7), as well as their asymptotic behaviour in the limit $L\to\infty$ as given in Eqs. (E.11) and (E.12), we find

$$\lim_{L\to\infty} Z^{RB}_{e^{ir\phi},e} \to \frac{1}{2\sqrt{n}} e^{\frac{\pi L}{12\beta}\left(\frac{1}{v_e}+\frac{1}{2\tilde{v}_e}\right)}. \tag{7.96}$$

Essentially identical calculations yield $Z^{RB}_{e^{ir\phi},e} = Z^{LB}_{e^{ir\phi},e}$ in this limit. Hence,

$$S_{e^{ir\phi}} = \left.\frac{\partial[T\ln Z_{e^{ir\phi},e}]}{\partial T}\right|_{T=1} = -2\ln(2\sqrt{n}) + \frac{\pi L}{3}\left(\frac{1}{v_e}+\frac{1}{2\tilde{v}_e}\right), \tag{7.97}$$

and so we obtain the expected TEE [see Eq. (7.63)].

7.4.2 Non-Abelian (Twisted) Sectors

Next we turn to the twisted sectors, corresponding to the insertion of a $\sigma e^{(r+1/2)\phi}$ anyon flux through the torus. The mode expansions of the fields have the same form as that in Eq. (7.31) and Eq. (7.34), except that the quantization of the quantum numbers has changed. The Majorana fields are now periodic and so have integer-quantized momenta $k=\frac{2\pi}{L}j$, $j\in\mathbb{Z}$. As for the bosons, the momenta will still be quantized as $k=\frac{2\pi j}{L}$, $j\in\mathbb{Z}$. The winding numbers, however, now obey the quantization of Eq. (7.26).

Let us again first focus on interface 1. The full approximate Hamiltonian takes the form

$$H_1 \equiv H^{\text{osc}}_{1,f} + H^{\text{zero}}_{1,f} + H^{\text{osc}}_{1,b} + H^{\text{zero}}_{1,b}. \tag{7.98}$$

Here, $H^{\text{osc}}_{1,f}$, $H^{\text{osc}}_{1,b}$, and $H^{\text{zero}}_{1,b}$ are again given by Eqs. (7.66)-(7.69), with appropriate changes to the quantization of the momenta and winding numbers. The new addition is a contribution from the Majorana zero modes

$$H^{\text{zero}}_{1,f} = i\tilde{g}d_0c_0. \tag{7.99}$$

We now proceed to derive the reduced density matrices for each sector, following the same methodology as was employed for the untwisted sectors.

Bosonic Sector Ground State

Aside from the change in the quantization of the winding modes, the calculation of the bosonic sector ground state proceeds as before. Hence, we can immediately write the zero mode ground state as

$$|G_{b,\text{zero},1}\rangle = \sum_{N\in\mathbb{Z}-\frac{r+1/2}{n}} e^{-\frac{v_e\pi n N^2}{2L}} |N_{RB}=N, N_{LA}=-N\rangle\,, \tag{7.100}$$

with the only change being the quantization of N_{RB}. Similarly, the oscillator mode ground state is again given by Eq. (7.71).

Majorana Sector Ground State

Likewise, the ground state for the Majorana oscillator mode sector is again given by Eq. (7.74), where now $k=\frac{2\pi}{L}j$, $j\in\mathbb{Z}$. The new aspect of the calculation in the twisted sector is the presence of the Majorana zero modes. Constructing complex fermion operators as

$$f=\frac{1}{\sqrt{2}}(c_0+id_0), \quad \tilde{f}=\frac{1}{\sqrt{2}}(\tilde{d}_0+i\tilde{c}_0) \tag{7.101}$$

the Hamiltonian describing the zero modes of interfaces 1 and 2 can be expressed as

$$H_{1,f}^{\text{zero}}+H_{2,f}^{\text{zero}} = i\tilde{g}d_0c_0+i\tilde{g}\tilde{c}_0\tilde{d}_0 = -\tilde{g}(f^\dagger f+\tilde{f}^\dagger\tilde{f}-1) \tag{7.102}$$

where $\tilde{g}<0$. Now, a complete basis for the zero-mode Hilbert space is given by $|n,\tilde{n}\rangle$ where n ($\tilde{n}$) denotes the occupation of the f ($\tilde{f}$) fermion. The ground state is then given by $|G_{f,\text{zero}}\rangle = |0,\tilde{0}\rangle$.

We can also form a different pair of complex fermions from the above Majorana zero modes, localized in the two halves of the torus, as defined in Eq. (7.57) and Eq. (7.61):

$$f_A=\frac{1}{\sqrt{2}}(d_0+i\tilde{d}_0), \quad f_B=\frac{1}{\sqrt{2}}(c_0+i\tilde{c}_0).$$

Calculating the reduced density matrix for cylinder B will require us to trace out the f_A degree of freedom from the state $|0,\tilde{0}\rangle$, and so we must express $|G_{f,\text{zero}}\rangle$ in terms of the basis states $|n_A,n_B\rangle$, where $n_{A/B}$

denotes the occupation of the $f_{A/B}$ fermion:

$$|G_{f,\text{zero}}\rangle = \frac{1}{\sqrt{2}}(|0_A, 0_B\rangle + i\,|1_A, 1_B\rangle). \tag{7.103}$$

Projecting to the Physical Hilbert Space

Putting everything together, we can write the ground state of the approximated Hamiltonian, Eq. (7.98), as

$$\begin{aligned}|\widehat{\psi}_a\rangle = &|G_{b,\text{osc},1}\rangle \otimes |G_{b,\text{zero},1}\rangle \otimes |G_{f,\text{osc},1}\rangle \\ &\otimes |G_{b,\text{osc},2}\rangle \otimes |G_{b,\text{zero},2}\rangle \otimes |G_{f,\text{osc},2}\rangle \otimes |G_{f,\text{zero}}\rangle\end{aligned} \tag{7.104}$$

where the explicit forms of $|G_{b,\text{zero},1}\rangle$, $|G_{b,\text{osc},1}\rangle$, $|G_{f,\text{osc},1}\rangle$, and $|G_{f,\text{zero}}\rangle$ are given above, while

$$|G_{b,\text{zero},2}\rangle = \sum_{N\in\mathbb{Z}-\frac{r+1/2}{n}} e^{-\frac{v_e\pi n N^2}{2L}}\,|N_{LB} = -N, N_{RA} = N\rangle\,, \tag{7.105}$$

$|G_{b,\text{osc},2}\rangle$ is again given by Eq. (7.78), and $|G_{f,\text{osc},2}\rangle$ is given by Eq. (7.79) with $k = \frac{2\pi}{L}j$, $j \in \mathbb{Z}$.

We now obtain an approximation to the physical ground state, $|\psi_a\rangle$, through the projection $P_a = P_{a,A}P_{a,B}$ defined in Section 7.3.1, with $a = \sigma e^{i(r+1/2)\phi}$. As in the untwisted sector problem, it suffices to apply only one of the projection operators acting on one of the cylinders, say, $P_{a,B}$, due to the form of $|\widehat{\psi}_a\rangle$. Indeed, from its explicit form, we see that every state appearing in $|\widehat{\psi}_a\rangle$ has $(-1)^{N_{RB}+N_{LB}} = (-1)^{N_{RA}+N_{LA}}$ and $(-1)^{F_B} = (-1)^{F_A}$. Hence, following the same reasoning given in the untwisted sector calculation, we have that

$$|\psi_a\rangle = P_a\,|\widehat{\psi}_a\rangle = P_{a,A}P_{a,B}\,|\widehat{\psi}_a\rangle = P_{a,B}\,|\widehat{\psi}_a\rangle \tag{7.106}$$

Again, we reserve the explicit form of $|\psi_a\rangle$ for Appendix E.2.2. We also discuss, in Appendix E.2.2, an important subtlety regarding the definition of the fermion parity of the complex fermion zero mode. Now, as we did in the untwisted sector problem, we can make use of the fact that $|\psi_a\rangle = P_a\,|\widehat{\psi}_a\rangle = P_{a,B}\,|\widehat{\psi}_a\rangle$ is in a Schmidt decomposed form to deduce the form of the reduced density matrix for, say, cylinder B. Explicitly,

$$\rho_{a,B} = \frac{1}{Z_{\sigma e^{i(r+1/2)\phi},e}} P_{a,B}\rho_{\text{zero},B}e^{-\mathcal{H}_e^{RB}-\mathcal{H}_e^{LB}}P_{a,B}, \tag{7.107}$$

where,

$$\mathcal{H}_e^{RB} = v_e \left(\frac{\pi n}{L} N_{RB}^2 + \sum_{k>0} k a_k^\dagger a_k - \frac{\pi}{12L} \right) + \tilde{v}_e \left(\sum_{k>0} k c_k^\dagger c_k + \frac{\pi}{12L} \right), \tag{7.108}$$

$$\mathcal{H}_e^{LB} = v_e \left(\frac{\pi n}{L} N_{LB}^2 + \sum_{k<0} |k| \tilde{a}_k^\dagger \tilde{a}_k - \frac{\pi}{12L} \right) + \tilde{v}_e \left(\sum_{k<0} |k| \tilde{c}_k^\dagger \tilde{c}_k + \frac{\pi}{12L} \right), \tag{7.109}$$

$$\rho_{\text{zero},B} = |0_B\rangle \langle 0_B| + |1_B\rangle \langle 1_B| . \tag{7.110}$$

We have again shifted the entanglement spectrum by a constant for convenience.

Entanglement Spectrum and Entropy

Now, introducing the fictitious inverse temperature $\beta = 1/T$, we wish to compute (for $a = \sigma e^{i(r+1/2)\phi}$)

$$Z_{a,e} = \text{Tr}_B \left[P_{a,B} \rho_{\text{zero},B} e^{-\beta(\mathcal{H}_e^{RB} + \mathcal{H}_e^{LB})} P_{a,B} \right]. \tag{7.111}$$

When computing the trace, the presence of the $P_{a,B}$ projection operators requires that we only sum over states in the $a = \sigma e^{i(r+1/2)\phi}$ sector. Now, consider a state $|\beta\rangle$ which obeys the correct quantization of winding numbers for the $\sigma e^{i(r+1/2)\phi}$ sector, but has a fermion parity such that $(-1)^{F_B} \neq (-1)^{N_{RB}+N_{LB}}$, implying it does not lie in the physical MR Hilbert space and so will not contribute to the trace. It follows that by applying either f_B or $f_B^\dagger$ (recall that these are the zero-mode operators on cylinder B) to $|\beta\rangle$ will yield a state that *does* satisfy the parity selection rule $(-1)^{F_B} = (-1)^{N_{RB}+N_{LB}}$. Moreover, whichever of $f_B |\beta\rangle$ or $f_B^\dagger |\beta\rangle$ is non-zero will have the same eigenvalue as $|\beta\rangle$ under $\rho_{\text{zero},B} e^{-\beta(\mathcal{H}_e^{RB} + \mathcal{H}_e^{LB})}$, since $\rho_{\text{zero},B}$ is simply the identity operator in the zero-mode sector. It is then not too difficult to see that we obtain

$$Z_{\sigma e^{i(r+1/2)\phi},e} = Z^{RB}_{\sigma e^{i(r+1/2)\phi},e} Z^{LB}_{\sigma e^{i(r+1/2)\phi},e} \tag{7.112}$$

where, focusing on edge RB and recalling the definitions of Eq. (7.90),

$$Z^{RB}_{\sigma e^{i(r+1/2)\phi},e} = \chi^{\text{Ising}}_{1/16}(\tilde{q}) \chi^{+}_{(r+1/2)/n}(q). \tag{7.113}$$

Here,

$$\chi^{\text{Ising}}_{1/16}(\tilde{q}) = \tilde{q}^{\frac{1}{24}} \prod_{j=1}^{\infty}(1+\tilde{q}^{j}) \tag{7.114}$$

results from the trace over the (anti-periodic) Majorana oscillator modes and is the character of the Ising CFT in the twisted sector. The quantity $\chi^{+}_{m}(q)$ was defined in Eq. (7.94). It should be emphasized that the entanglement partition function can be expressed as a product of traces over edges RB and LB because the the Majorana zero modes have been traced over; the Hilbert spaces of edges RB and LB are not genuinely decoupled.

This expression for the entanglement partition function matches the character of the appropriate topological sector in the MR CFT [283], and so it follows immediately that we will obtain the correct EE. Indeed, as usual, we can express the entanglement partition function in terms of modular functions:

$$Z^{RB}_{\sigma e^{i(r+1/2)\phi},e} = \sqrt{\frac{\theta_0^{1/2}(\tilde{\tau})}{2\eta(\tilde{\tau})}} \frac{\theta_0^{-(r+1/2)/n}(n\tau)}{\eta(\tau)}. \tag{7.115}$$

Making use of the modular transformation and asymptotic properties of the θ and η functions (see Appendix E.1), we obtain, in the $L \to \infty$ limit,

$$\lim_{L\to\infty} Z^{RB}_{\sigma e^{i(r+1/2)\phi},e} \approx \frac{1}{\sqrt{2n}} e^{\frac{\pi}{24\tilde{\tau}_2}} e^{\frac{\pi}{12\tau_2}}. \tag{7.116}$$

One finds that $Z^{LB}_{\sigma e^{i(r+1/2)\phi},e}$ is given by the same expression in this limit. So,

$$S_{\sigma e^{i(r+1/2)\phi}} = \lim_{L\to\infty} \frac{\partial[T \ln Z_{\sigma e^{i(r+1/2)\phi},e}(\beta)]}{\partial T}\bigg|_{T=1} = -2\ln(\sqrt{2n}) + \frac{\pi L}{3}\left(\frac{1}{v_e} + \frac{1}{2\tilde{v}_e}\right), \tag{7.117}$$

as required [see Eq. (7.64)].

7.5 Non-Uniform Moore-Read Gapped Interfaces

Thus far, we have demonstrated that the cut-and-glue approach can be extended to the computation of the EE in all topological sectors of the MR theory. However, the utility of this approach is that it may be used to compute the EE for an entanglement cut lying along the interface between two *different* topological phases. This was demonstrated for interfaces of arbitrary Abelian phases in Ref. [91]. The focus of the remainder of this Chapter is to conduct a similar analysis of interfaces of MR states at different filling fractions.

As a prerequisite to computing the EE for non-uniform interfaces, it is necessary to first deduce which pairs of MR states actually admit gapped interfaces and what interaction terms can generate such a gap. The corresponding question for arbitrary Abelian states has been studied in great detail [85–87, 294]. It is now well established that an interface between Abelian topological orders $\mathcal{A}$ and $\mathcal{B}$ can be gapped if and only if (i) $\mathcal{A}$ and $\mathcal{B}$ have identical chiral central charge $c(\mathcal{A}) = c(\mathcal{B})$, which is related to the thermal Hall conductance [295–297] by $\kappa = dI_{\text{energy}}/dT = c\frac{\pi^2 k_B^2}{3h}T$, and (ii) the topological order $\mathcal{A} \times \overline{\mathcal{B}}$ (where the overbar indicates time-reversal) possesses a *Lagrangian subgroup*, a maximal set of mutually local bosons which, when condensed, confine all other anyons. Such subgroups, when they exist, are related to the so-called null vectors [298], which label sine-Gordon interactions corresponding to tunneling of integer numbers of electrons.

Interfaces of non-Abelian states have also been studied intensively [274–282], although many open questions still remain. Indeed, in contrast to Abelian edge theories, which are described by multi-component Luttinger liquids [14], non-Abelian edge theories are described by generic CFTs [1], whose primary fields need not have free-field representations. As such, a comprehensive approach to classifying gapped interfaces via explicit gapping interactions seems difficult to develop (although specific examples have been considered before, such as those in Ref. [299]). Our goal in this section is to use anyon condensation, which we will briefly review, to understand when interfaces between MR states can be gapped, and then to use this picture to propose explicit gapping interactions.

7.5.1 Anyon Condensation Picture of Gapped Interfaces

Suppose we wish to determine whether one can form a gapped interface between topological phases $\mathcal{A}$ and $\mathcal{B}$, assuming they have identical chiral central charges. This is equivalent to asking whether one can gap out an interface between the phase $\mathcal{A} \times \overline{\mathcal{B}}$ and the vacuum by the folding trick [80, 287]. In the case where $\mathcal{A}$ and $\mathcal{B}$ are both Abelian, the necessary and sufficient criterion for the existence of such an interface is the existence of a Lagrangian subgroup, $\mathcal{L} \subset \mathcal{A} \times \overline{\mathcal{B}}$. If $\mathcal{A} \times \overline{\mathcal{B}}$ is a bosonic topological order (i.e. the local "electron" operators have bosonic statistics), then a Lagrangian subgroup is a set of anyons defined by the requirements that (1) for all $a \in \mathcal{L}$, $e^{i\theta_a} = 1$, where θ_a is the spin of a, (2) for all $a, b \in \mathcal{L}$, $e^{i\theta_{a,b}} = 1$, where $\theta_{a,b}$ is the braiding phase between a and b, and (3) for any $b \notin \mathcal{L}$, there exists some $a \in \mathcal{L}$ such that $e^{i\theta_{a,b}} \neq 1$. Now, in the anyon condensation picture of Bais and Slingerland [286], if one condenses all anyons in $\mathcal{L}$, all other anyons in the theory will become confined. If $\mathcal{A} \times \overline{\mathcal{B}}$ is fermionic, then condition (1) is relaxed to the constraint $e^{i\theta_a} = \pm 1$ – that is, the anyons in $\mathcal{L}$ can have bosonic or fermionic self-statistics. This is because a fermionic anyon $a \in \mathcal{L}$ can be fused with a local fermion (an electron) to obtain a bosonic quasiparticle

which can be condensed. In either case, $\mathcal{A} \times \overline{\mathcal{B}}$ can be reduced to the vacuum or a trivial state *without* the closing of a gap, implying the existence of a gapped interface between $\mathcal{A}$ and $\mathcal{B}$.

It is believed that a similar anyon condensation criterion can be used to identify gapped interfaces of non-Abelian states [279,280]. In this case, the picture is a bit more subtle as non-Abelian anyons may "split" under condensation, and so the maximal set of condensable anyons may not be closed under fusion. For this reason, we will call such a set of anyons a Lagrangian subset, as opposed to a subgroup. Although, to the best of our knowledge, there is no rigorous proof of connection between the existence of a Lagrangian subset and the gappability of a non-Abelian interface, we can use this picture as motivation for writing down explicit gapping terms for the Moore-Read states. After first reviewing gapped Laughlin interfaces, this will be the next order of business.

Review of Laughlin Interfaces

Let us consider an interface between Laughlin states at fillings $\nu_1 = 1/k_1$ and $\nu_2 = 1/k_2$, as studied in Ref. [81]. The free part of the Lagrangian describing the interface is given by

$$\mathcal{L}_0 = \frac{k_1}{4\pi}\partial_x\phi_L(\partial_t - \partial_x)\phi_L + \frac{k_2}{4\pi}\partial_x\phi_R(-\partial_t - \partial_x)\phi_R. \tag{7.118}$$

The interaction term we add in to gap out the interface must be constructed from local degrees of freedom (i.e. electron operators). It will be sufficient to restrict our attention to an electron tunneling term:

$$\mathcal{L}_{\text{int}} = (\psi_L^\dagger)^a \psi_R^b + \text{H.c.} = \cos(ak_1\phi_L + bk_2\phi_R), \tag{7.119}$$

where $\psi_L = e^{-ik_1\phi_L}$ and $\psi_R = e^{ik_2\phi_2}$ are the local electron operators. Here, $\Lambda = (a, b)$ must satisfy Haldane's null vector criterion [298]

$$\begin{pmatrix} a & b \end{pmatrix} \begin{pmatrix} k_1 & 0 \\ 0 & -k_2 \end{pmatrix} \begin{pmatrix} a \\ b \end{pmatrix} = 0. \tag{7.120}$$

This ensures the argument of the cosine argument behaves as a classical variable and so can obtain an expectation value in the strongly interacting limit, gapping out the scalar fields. In the present case, this means

$$a^2 k_1 - b^2 k_2 = 0. \tag{7.121}$$

We also require Λ to be primitive [300], so as to not introduce a spurious ground state degeneracy, meaning that a and b must be co-prime. These two requirements can be shown to constrain the fillings to be [81]

$$\nu_1 = k_1^{-1} = \frac{1}{pb^2}, \quad \nu_2 = k_2^{-1} = \frac{1}{pa^2}. \tag{7.122}$$

Hence, there exists a gapped interface between Laughlin states $\mathcal{A}$ and $\mathcal{B}$ at the filling fractions:

$$(\mathcal{A}) \quad \nu = \frac{1}{pb^2} \qquad | \qquad (\mathcal{B}) \quad \nu = \frac{1}{pa^2}. \tag{7.123}$$

Let us now confirm that there indeed exists a Lagrangian subgroup for $\mathcal{A} \times \overline{\mathcal{B}}$, which is condensed by Eq. (7.119). The anyon content of $\mathcal{A} \times \overline{\mathcal{B}}$ is

$$\mathcal{A} \times \overline{\mathcal{B}} = \{e^{ir\phi_L}\}_{r=1,\ldots,pb^2} \times \{e^{is\phi_R}\}_{s=1,\ldots,pa^2}. \tag{7.124}$$

For concreteness, r and s will henceforth always index the $\mathcal{A}$ and $\overline{\mathcal{B}}$ factors, respectively. These anyons have spin

$$h_{r,s} = \frac{1}{2}\left(\frac{r^2}{pb^2} - \frac{s^2}{pa^2}\right). \tag{7.125}$$

Hence, anyons of the form $(r,s) = l(b,a)$ have trivial spin; it is also straightforward to see that they have trivial braiding statistics with each other and non-trivial statistics with respect to all other anyons. So, the anyons

$$\mathcal{L} = \{e^{ilb\phi_L} e^{ila\phi_R}\}_{l=1,\ldots,pab} \tag{7.126}$$

form a Lagrangian subgroup and their condensation fully gaps the interface. Note, in particular, that

$$(e^{ib\phi_L} e^{ia\phi_R})^{pab} = e^{ipab^2\phi_L} e^{ipa^2b\phi_R} \tag{7.127}$$

corresponds to the composite electron operator $\psi_L^a \psi_R^b$ appearing in Eq. (7.119) and will obtain an expectation value when the argument of the cosine is pinned, resulting in the condensation of all anyons in $\mathcal{L}$. This makes explicit the connection between Lagrangian subgroups and electron tunneling terms.

Extension to Moore-Read Interfaces

We would now like to identify gapped interfaces between generalized MR states at different filling fractions. Absent a correspondence between gapping terms and Lagrangian subsets, as exists in the Abelian case, we can at best use the anyon condensation picture as a source of intuition for identifying candidate gapping terms. As a first step, however, we can restrict which filling fractions to consider by focusing on gapping terms that correspond to tunneling of electrons. Indeed, if we consider an interface between MR states at filling fractions $\nu_1 = 1/k_1$ and $\nu_2 = 1/k_2$, the most general electron tunneling term we can write down is given by

$$\mathcal{L}_{\text{int}} = (\psi_L^\dagger)^a \psi_R^b + \text{H.c.} = i\chi_L^a \chi_R^b \cos(ak_1\phi_L + bk_2\phi_R). \tag{7.128}$$

We will analyze this interaction term in more detail in the following subsection. For now, we emphasize that our implementation of the cut-and-glue approach required that the Majorana and bosonic parts of the interaction term were separately bosonic and so separately obtained expectation values in the strongly interacting limit [see the discussion around Eq. (7.44)]. Using our analysis of Laughlin interfaces above, we see that this is only possible if $k_1 = pb$ and $k_2 = pa$, with a and b co-prime [6]. So, we will restrict our attention to gapped interfaces (GIs) between two MR phases, $\mathcal{A}$ and $\mathcal{B}$, at filling fractions

$$(\mathcal{A}) \quad \nu = \frac{1}{pb^2} \qquad | \qquad (\mathcal{B}) \quad \nu = \frac{1}{pa^2}. \tag{7.129}$$

This is not to say that GIs cannot be formed between MR states at other filling fractions, only that these GIs are those most obviously amenable to our cut-and-glue approach to the calculation of the EE.

In this case, the anyon content of $\mathcal{A} \times \overline{\mathcal{B}}$ is

$$\mathcal{A} \otimes \overline{\mathcal{B}} = \{e^{ir\phi_L}, \chi_L e^{ir\phi_L}, \sigma_L e^{i(r+1/2)\phi_L}\}_{r=1,\ldots,pb^2} \otimes \{e^{is\phi_R}, \chi_R e^{is\phi_R}, \sigma_R e^{i(s+1/2)\phi_R}\}_{s=1,\ldots,pa^2}. \tag{7.130}$$

Again, our goal is to condense a set of bosonic anyons such that all other anyons will be confined. Our strategy is as follows: we will first condense all possible Abelian anyons. This will yield a new topological order in which all of the non-Abelian anyons will have, hopefully, either become confined or have split into Abelian ones. It will then be straightforward to see whether that order can be reduced to a trivial one.

Motivated by our analysis of the Laughlin problem, we start by condensing the following set of Abelian

[6] The condition that a and b be co-prime arose in the Abelian case by requiring primitivity of the gapping term. We do not have a systematic understanding of what constitutes a primitive gapping term in the MR case, but we can at least justify requiring a and b being co-prime by noticing that any tunneling term of the form $(\psi_L^\dagger)^{qa}\psi_R^{qb} + H.c.$ with q integer will necessarily be less relevant (in the renormalization group sense) than Eq. (7.128).

anyons:

$$\mathcal{L}_0 = \{e^{ilb\phi_L} e^{ila\phi_R}\}_{l=1,\ldots,pab} \times \{1_L 1_R, \chi_L \chi_R\} \tag{7.131}$$

It follows immediately that all anyons of the form $e^{ir\phi_L} e^{is\phi_R}$ and $\chi_L e^{ir\phi_L} \chi_R e^{is\phi_R}$ not lying in $\mathcal{L}_0$ will be confined. The condensation pattern of the remaining anyons depends on whether a and b are odd or even. Since we have assumed a and b to be coprime, there are only two cases to consider: (i) one of a and b even, the other odd and (ii) both a and b odd.

Case (i): One of a and b even, the other odd

Without loss of generality, let us take a to be even and b odd. In this case, the anyons in the set

$$\{\chi_L e^{ilb\phi_L} e^{ila\phi_R}, e^{ilb\phi_L} \chi_R e^{ila\phi_R}\}_{l=1,\ldots,pab}, \tag{7.132}$$

despite being fermionic, can be condensed after combining them with (fermionic) electrons. In fact, they are all *equivalent* to products of anyons in $\mathcal{L}_0$, up to fusion with electron operators. For instance,

$$\begin{aligned} 1_L \chi_R &\sim 1_L \chi_R \times (\chi_L e^{ipb^2\phi_L})^a \times (\chi_R e^{ipa^2\phi_R})^b \\ &= e^{ipab^2\phi_L} e^{ipa^2 b\phi_R}, \end{aligned} \tag{7.133}$$

where the tilde indicates an equivalence up to fusion with electrons. Here we made use of the fact that $\chi^a \sim 1$, since $a \in 2\mathbb{Z}$. Thus, we should extend the Lagrangian subset from $\mathcal{L}_0$ to

$$\mathcal{L} = \{e^{ilb\phi_L} e^{ila\phi_R}\}_{l=1,\ldots,2pab} \times \{1_L 1_R, \chi_L \chi_R\}. \tag{7.134}$$

It immediately follows that all of the non-Abelian anyons will be confined. Indeed, any anyons of the form

$$\sigma_L e^{i(r+1/2)\phi_L} e^{is\phi_R} \sim \sigma_L e^{i(r+1/2)\phi_L} \chi_R e^{is\phi_R} \tag{7.135}$$

and

$$e^{ir\phi_L} \sigma_R e^{i(s+1/2)\phi_R} \sim \chi_L e^{ir\phi_L} \sigma_R e^{i(s+1/2)\phi_R} \tag{7.136}$$

will be confined, since they all possess non-trivial braiding with $\chi_L\chi_R$. As for anyons of the form,

$$\sigma_{L,r}\sigma_{R,s} \equiv \sigma_L e^{i(r+1/2)\phi_L}\sigma_R e^{i(s+1/2)\phi_R}, \tag{7.137}$$

we can compute their braiding with $e^{ilb\phi_L}e^{ila\phi_R}$ and $\chi_L e^{ilb\phi_L}\chi_R e^{ila\phi_R}$ to be

$$e^{i\theta_{(r,s),l}} = \exp\left(2\pi i\frac{l}{pab}\left[ar - bs + \frac{1}{2}(a-b)\right]\right). \tag{7.138}$$

Since a is even while b is odd, this phase can never be trivial. Hence all anyons of the form $\sigma_{L,r}\sigma_{R,s}$ will be confined. Thus, we obtain a gapped interface, but one which is opaque to non-Abelian anyons since they are all confined.

Case (ii): a, b both odd

As a first step, we again condense $\mathcal{L}_0$. Upon doing so, the anyon

$$f \equiv \chi_L e^{ilb\phi_L}e^{ila\phi_R} \sim \chi_L 1_R \sim 1_L\chi_R \sim e^{ilb\phi_L}\chi_R e^{ila\phi_R} \tag{7.139}$$

remains deconfined, where the equivalences come from fusion with elements of $\mathcal{L}_0$. However, any other anyon of the form $\chi_L e^{ir\phi_L}e^{is\phi_R}$ or $e^{ir\phi_L}\chi_R e^{is\phi_R}$ will clearly be confined, as the chiral boson factors will yield non-trivial braiding with the elements of $\mathcal{L}_0$. It is also straightforward to see that any anyons of the form $\sigma_L e^{i(r+1/2)\phi_L}e^{is\phi_R} \sim \sigma_L e^{i(r+1/2)\phi_L}\chi_R e^{is\phi_R}$ and $e^{ir\phi_L}\sigma_R e^{i(s+1/2)\phi_R} \sim \chi_L e^{ir\phi_L}\sigma_R e^{i(s+1/2)\phi_R}$ will be confined, since they all possess non-trivial braiding with $\chi_L\chi_R$.

This leaves us with the anyons of Eq. (7.137). Their braiding with $e^{ilb\phi_L}e^{ila\phi_R}$ and $\chi_L e^{ilb\phi_L}\chi_R e^{ila\phi_R}$ is again given by Eq. (7.138). Since a and b are both odd, it follows that $a-b \in 2\mathbb{Z}$ and so this phase can be trivial for an appropriate choice of r and s. Specifically, we need to look for $r, s \in \mathbb{Z}$ satisfying the Diophantine equation

$$ar - bs + \frac{1}{2}(a-b) = pabt, \quad t \in \mathbb{Z} \tag{7.140}$$

in order to identify the deconfined non-Abelian anyons. One can show that solutions to this equation for arbitrary t are equivalent to those for $t = 0$, up to fusion with electrons. It is easy to see that, for the $t = 0$ case, one solution to the Diophantine equation is given by

$$r_0 = \frac{b-1}{2}, \quad s_0 = \frac{a-1}{2}. \tag{7.141}$$

All other solutions can be parameterized as

$$r_u = r_0 + ub, \quad s_u = s_0 + ua \tag{7.142}$$

and correspond to fusing $\sigma_{L,r_0}\sigma_{R,s_0}$ with a condensed anyon in $\mathcal{L}_0$. Hence, after condensing $\mathcal{L}_0$, $\sigma_{L,r_0}\sigma_{R,s_0}$ is the only non-Abelian anyon (up to fusion with electrons and condensed anyons) which is not confined.

In order to understand the fate of $\sigma_{L,r_0}\sigma_{R,s_0}$ after condensing the anyons in $\mathcal{L}_0$, let us check the fusion of $\sigma_{L,r_0}\sigma_{R,s_0}$ with itself. We have that

$$\sigma_{L,r_0}\sigma_{R,s_0} \times \sigma_{L,r_0}\sigma_{R,s_0} = (1 + \chi_L 1_R + 1_L \chi_R + \chi_L \chi_R) e^{ib\phi_L} e^{ia\phi_R} \to 2 \times 1 + 2 \times f \tag{7.143}$$

where, in the last step, we applied the identifications arising from condensing $\mathcal{L}_0$. Since the vacuum appears twice in this fusion rule, $\sigma_{L,r_0}\sigma_{R,s_0}$ must split [286] into two Abelian anyons: $\sigma_{L,r_0}\sigma_{R,s_0} \to e + m$, with the fusion rules $e^2 = m^2 = f^2 = 1$ and $e \times m = f$. So, after condensing the Abelian anyons in $\mathcal{L}_0$, we are left with the Abelian anyons $\{1, e, m, f\}$. Now, since $\sigma_{L,r_0}\sigma_{R,s_0}$ has bosonic self-statistics,

$$e^{i\theta_{(r_0,s_0)}} = \exp\left(\pi i \left[\frac{(r_0 + 1/2)^2}{pb^2} - \frac{(s_0 + 1/2)^2}{pa^2}\right]\right) = 1, \tag{7.144}$$

it follows that the daughter e and m anyons must also be self-bosons. Additionally, the monodromy associated with braiding f around $\sigma_{L,r_0}\sigma_{R,s_0}$, and hence also around either e or m, is -1. So, this condensation pattern is essentially that of the Ising $\times$ $\overline{\text{Ising}}$ $\to$ Toric code transition. We can then condense either e or m to fully gap out the interface. In contrast to the previous case, however, a subset of non-Abelian anyons *can* pass through this interface.

We thus conclude that we can always form a GI between Moore-Read states at filling fractions $\nu^{-1} = pa^2$ and $\nu^{-1} = pb^2$, although the nature of the interface depends on whether or not $a - b \in 2\mathbb{Z}$.

7.5.2 Gapping Terms for $\nu_1^{-1} = pb^2$ and $\nu_2^{-1} = pa^2$ MR Interfaces

We now turn to the problem of constructing explicit interactions which can gap out these interfaces by drawing some intuition from the above anyon condensation pictures.

Equal Parity Interface: $a, b \in 2\mathbb{Z}+1$

Let us first focus on the interface between $\nu_1^{-1} = pb^2$ and $\nu_2^{-1} = pa^2$ with a and b both odd. In this case, the naïve electron tunneling term of Eq. (7.128) takes the form

$$\mathcal{L}_{\text{int}} = i\chi_L\chi_R \cos(pab^2\phi_L + pa^2b\phi_R), \tag{7.145}$$

where we used the fusion rule $\chi^2 = 1$. [To be more careful about this, one should point-split Eq. (7.128) and perform an operator product expansion to obtain Eq. (7.145)]. It is straightforward to see that, in the strongly interacting limit, this interaction term will gap out both the scalar fields and Majorana fermions.

How does this interaction term connect with the anyon condensation picture described above? As a start, one may ask what anyon (or anyons) generate the set of anyons, $\mathcal{L}_0$, of Eq. (7.131). First, we note that up to the electronic combinations $\chi_L e^{-ipb^2\phi_L}$ and $\chi_R e^{-ipa^2\phi_R}$,

$$e^{ipab^2\phi_L}e^{ipa^2b\phi_R} \sim (\chi_L e^{-ipb^2\phi_L})^a \times (\chi_R e^{-ipa^2\phi_R})^b \times e^{ipab^2\phi_L}e^{ipa^2b\phi_R} = \chi_L\chi_R. \tag{7.146}$$

So, all anyons in $\mathcal{L}_0$ can be obtained by fusing the anyon $e^{ib\phi_L}e^{ia\phi_R}$ with itself some number of times, which is to say, $\mathcal{L}_0$ is generated by a single anyon. Additionally, we observed above that

$$\sigma_{L,r_0}\sigma_{R,s_0} \times \sigma_{L,r_0}\sigma_{R,s_0} = (1 + \chi_L 1_R + 1_L\chi_R + \chi_L\chi_R)e^{ib\phi_L}e^{ia\phi_R}, \tag{7.147}$$

which means the elements of $\mathcal{L}_0$, and hence the full Lagrangian subset, can all be generated from this single non-Abelian anyon. This suggests that the corresponding gapped edge can be obtained using a single gapping term, namely that given by Eq. (7.145). Indeed, in the strong coupling limit, the argument of the cosine will be pinned and $\chi_L\chi_R$ will obtain an expectation value, corresponding to the condensation of $\chi_L\chi_R$ and all anyons of the form $e^{ilb\phi}e^{ila\overline{\phi}}$, as suggested by the Lagrangian subset picture. That, roughly speaking, $\sigma_{L,r_0}\sigma_{R,s_0}$ is condensed can be inferred from Eq. (7.147), since $e^{ib\phi}e^{ia\overline{\phi}}$ is also condensed, or by analogy with the standard Ising model, in which the condensation of $\chi_L\chi_R$ implies a gap for the full theory.

Opposite Parity Interface: $a \in 2\mathbb{Z}$, $b \in 2\mathbb{Z}+1$

In contast to the previous case, the naive tunneling term of Eq. (7.128) will not serve to gap out the interface. Indeed, since a is even and b is odd, we have that $\psi_L^a\psi_R^b$ is fermionic and so cannot obtain a non-zero expectation value. In order to identify an appropriate gapping interaction, let us try to draw some intuition from the above anyon condensation picture. In particular, we may ask which anyons generate the

set $\mathcal{L}$ of Eq. (7.134). By inspection, we see that $\mathcal{L}$ has the group structure $\mathbb{Z}_{2pab} \times \mathbb{Z}_2$. (Note that $\chi_L\chi_R$ is *not* equivalent up to fusion with electrons with $e^{ipab^2\phi_L}e^{ipa^2b\phi_R}$ when one of a and b is even and the other odd.) In particular, $\mathcal{L}$ is generated by $e^{ib\phi_L}e^{ia\phi_R}$ and $\chi_L\chi_R$. This suggests that we will need two distinct tunneling terms to condense the anyons in each of the $\mathbb{Z}_{2pab}$ and $\mathbb{Z}_2$ factors and hence fully gap the interface.

Motivated by this observation, we can write down what is effectively the square of the naïve electron tunneling operator of Eq. (7.128):

$$\mathcal{L}_c = (\psi_L^\dagger)^{2a}\psi_R^{2b} + H.c. = \cos(2pab^2\phi_L + 2pa^2b\phi_R), \tag{7.148}$$

where we again used the fusion rule $\chi^2 = 1$. It is clear that this interaction can gap out the charged sector (i.e. the scalar fields) and the pinning of the argument of the cosine will correspond to the condensation of the anyons $e^{ilb\phi_L}e^{ila\phi_R}$ in Eq. (7.134).

We are thus left with the task of gapping out the neutral degrees of freedom, namely the Majorana fermions. The naïve expectation, on inspection of Eq. (7.134), is that the neutral sector should be gapped out by a term of the form $(\chi_L\chi_R)^2$, since $\chi_L^2 = 1$ and $\chi_R^2 = 1$ are local quasi-particles and $(\chi_L\chi_R)^2$ obtaining an expectation value would correspond to the condensation of $\chi_L\chi_R$. But, it is precisely due to these fusion rules that $(\chi_L\chi_R)^2 \sim 1$ cannot introduce a gap. More precisely, on point-splitting the interaction, one finds $(\chi_L\chi_R)^2 \sim \chi_L\partial\chi_L\chi_R\partial\chi_R$, which is an irrelevant interaction (in the RG sense) and cannot perturbatively introduce a gap [7]. Evidently, we must employ a more indirect approach to fully gap out the interface.

Indeed, we will make use of an alternative representation of the Ising CFT

$$\text{Ising} = \frac{SO(N+1)_1}{SO(N)_1} \sim SO(N+1)_1 \boxtimes \overline{SO(N)}_1, \tag{7.149}$$

where $N = 2r$ is an even number with $r > 1$, $SO(N)_1$ denotes the $SO(N)$ Kac-Moody algbera at level one, and the tensor product $\boxtimes$ denotes a usual tensor product combined with the condensation of a particular set of bosonic anyons to tie the two factors together. The details of this representation are reviewed in Appendix E.3. This representation allows us to to re-express the Majorana sector of the MR theory in terms of $N+1$ left-moving and N right-moving Majorana fermions. The topological data of theory (i.e. the anyon content) will remain the same in this alternative reprsentation due to the choice of condensed operators encoded in the $\boxtimes$ notation. In particular, all $2N+1$ Majorana operators belong to a single topological sector. So, we expect to obtain the correct TEE in our entanglement calculation. However, the total central charge will change

[7] In the Ising model, this interaction induces a flow from the tricritical to the critical Ising CFT, all along which the fermions remain massless [301]. Beyond the tricritial Ising CFT fixed point, this interaction does open a gap. Although a similar situation may arise here, we are interested in writing down relevant interactions, which we know will perturbatively introduce a gap

and will alter the area law term in the entanglement entropy. This, of course, is not distressing since the coefficient of the area law term is a non-universal quantity. The upshot of this alternative representation is that we can write down current-current backscattering interactions which are manifestly local and marginally relevant, which means they *can* induce a gap.

Explicitly, in this alternative reprsentation, we can write the free part of the $\nu = 1/n$ MR edge theory as

$$\mathcal{L} = \frac{n}{4\pi}\partial_x\phi(\partial_t - \partial_x)\phi + \frac{1}{4\pi}\sum_{j=1}^{r}\partial_x\phi^j(\partial_t - \partial_x)\phi^j + \frac{1}{4\pi}\sum_{j=1}^{r}\partial_x\overline{\phi}^j(-\partial_t - \partial_x)\overline{\phi}^j + \chi\frac{i}{2}(\partial_t - \partial_x)\chi, \tag{7.150}$$

with the local operators being the electron operator

$$\psi_e = \chi e^{in\phi}, \tag{7.151}$$

the SO currents of Eqs. (E.32)-(E.34), as well as the condensed operators of Eqs. (E.35)-(E.36). As usual, it is important to understand the organization of the Hilbert space. To that end, let us place this MR phase on a cylinder so that we have chiral and anti-chiral copies on the left (L) and right (R) edges of the cylinder. We then define the operator

$$G' = G(-1)^{\sum_j(N_R^j+N_L^j)}(-1)^{\sum_j(\overline{N}_R^j+\overline{N}_L^j)} = (-1)^{N_R+N_L}(-1)^F(-1)^{\sum_j(N_R^j+N_L^j)}(-1)^{\sum_j(\overline{N}_R^j+\overline{N}_L^j)}, \tag{7.152}$$

where N_μ, N_μ^j, and $\overline{N}_\mu^j$ are the winding modes of ϕ_μ, ϕ_μ^j, and $\overline{\phi}_\mu^j$, respectively. One can check that G' commutes with all the local-electronic operators in this theory. Hence, similar to the conventional MR edge theory, the physical Hilbert space is defined by the constraint $G' = 1$. This simply states that the charge (i.e. the winding number parity of the ϕ field) must match the combined fermion number parity and neutral boson winding number parity. In particular, in the $\mathbf{1}$ sector we can define separate fermion parities for each edge. As such, we can define the operators

$$G'_\mu = (-1)^{N_\mu}(-1)^{F_\mu}(-1)^{\sum_j N_\mu^j} \times (-1)^{\sum_j \overline{N}_\mu^j}. \tag{7.153}$$

The $\mathbf{1}$ sector is then defined by the constraint $G'_\mu = 1$. For later convenience, we can define the operator

$$P_{\mathbf{1}} = P_{\mathbf{1},R}P_{\mathbf{1},L} \tag{7.154}$$

which projects states the cylinder to the $\mathbf{1}$ sector of the MR edge theory. Here, $P_{\mathbf{1},\mu}$ acts on edge μ of the

cylinder and for $|\psi\rangle$ an eigenstate of $(-1)^{F_\mu}$, $(-1)^{N_\mu}$, $(-1)^{N_\mu^j}$, and $(-1)^{N_\mu^j}$, we have that, schematically,

$$P_{\mathbf{1},\mu}|\psi\rangle = |\psi\rangle \tag{7.155}$$

if $G'_\mu|\psi\rangle = |\psi\rangle$ and

$$P_{\mathbf{1},\mu}|\psi\rangle = 0 \tag{7.156}$$

otherwise.

Returning to the non-uniform interface, we can now employ the current-current interactions described in Appendix E.3 to gap out the neutral modes [302]:

$$\mathcal{L}_n = u\sum_{j_1\neq j_2}\cos(2\Theta^{j_1})\cos(2\Theta^{j_2}) + u\sum_{j=1}^{r}\cos(2\Theta^j)i\chi_L\chi_R + u\sum_{j_1\neq j_2}\cos(2\overline{\Theta}^{j_1})\cos(2\overline{\Theta}^{j_2}) \tag{7.157}$$

where we have defined

$$2\Theta^j \equiv \phi_R^j - \phi_L^j, \quad 2\overline{\Theta}^j = \overline{\phi}_R^j - \overline{\phi}_L^j. \tag{7.158}$$

In its fermionized form, as presented in Eq. (E.40) of Appendix E.3, we see that $\mathcal{L}_n$ does indeed, heuristically, represent a $(\chi_L\chi_R)^2$ interaction, in line with our intuition from the anyon condensation picture. It is clear that, taken together, the charge sector and neutral sector interaction terms,

$$\mathcal{L}_{\text{gap}} \equiv \mathcal{L}_c + \mathcal{L}_n, \tag{7.159}$$

will fully gap the interface.

7.6 Non-Uniform Interface Entanglement Entropy

Having established which interfaces of MR states can be gapped and which explicit interactions can induce these gaps, we can proceed to apply the cut-and-glue approach to the calculation of the EE for these interface systems. We again consider the geometry of Fig. 7.2 except, now, region A (B) will be occupied by a $\nu^{-1} = pb^2$ ($\nu^{-1} = pa^2$) MR state. The entanglement cut thus lies on the interface between these two distinct topological orders. We will consider the two classes of interfaces discussed in the previous section in turn. Our analysis will parallel that of Ref. [91], in that we will first illustrate how the gapping interactions

place constraints on the ground state. Aside from these constraints, the actual computation of the ground state and the EE then proceeds in essentially the same way as for the uniform interfaces. We will focus, for simplicity, on the trivial (**1**) sector.

7.6.1 Equal Parity Interface

We begin by considering the case where both a and b are odd. As in the uniform interface calculation, we will focus on the LA/RB interface (i.e. interface 1). For ease of access, we restate here the free Lagrangian,

$$\begin{aligned}\mathcal{L}_{\text{dec},1} = \chi_{LA}\frac{i}{2}(\partial_t - v_n\partial_x)\chi_{LA} + \frac{pb^2}{4\pi}\partial_x\phi_{LA}(\partial_t - v_c\partial_x)\phi_{LA} \\ + \chi_{RB}\frac{i}{2}(\partial_t + v_n\partial_x)\chi_{RB} + \frac{pa^2}{4\pi}\partial_x\phi_{RB}(-\partial_t - v_c\partial_x)\phi_{RB},\end{aligned} \tag{7.160}$$

and the gapping interaction,

$$\mathcal{L}_{\text{gap},1} = -\frac{2g}{\pi}i\chi_{LA}\chi_{RB}\cos(pab^2\phi_{LA} + pa^2b\phi_{RB}). \tag{7.161}$$

Gapping Term Constraints

As in the uniform interface problem, we will take the strongly interacting limit and approximate

$$H_{\text{gap},1} \approx \int_0^L \left[\text{const.} + v_n\tilde{g}i\chi_{LA}\chi_{RB} + \frac{v_c\lambda\pi}{2}(b\phi_{LA} + a\phi_{RB} - \pi/pab)^2\right]dx, \tag{7.162}$$

where $\tilde{g} = -2g/(v_n\pi) < 0$ and we have expanded about the vacuum

$$\begin{aligned}\langle pab^2\phi_{LA} + pa^2b\phi_{RB}\rangle = \pi \\ \langle i\chi_{LA}\chi_{RB}\rangle > 0.\end{aligned} \tag{7.163}$$

We perform a similar approximation for interface 2. As before, this violates the $\mathbb{Z}_2$ gauge symmetries generated by the G_α operators [Eq. (7.41)], and so the ground state to the approximated Hamiltonian will need to be projected to the $G_\alpha = 1$ subspace. However, following Ref. [91], an additional constraint is imposed by the gapping interaction.

Indeed, as in the case of the uniform interface problem, the pinning of the cosine term implies the linear combination of the scalar fields $b\phi_{LA} + a\phi_{RB}$ cannot fluctuate significantly from its vacuum expectation

value over the length of the system. In particular, it cannot have a non-zero winding, which requires that

$$bN_{LA} + aN_{RB} = 0. \tag{7.164}$$

Since a and b are coprime, this relation fixes the quantization of the winding numbers to be

$$N_{LA} = az, \quad N_{RB} = -bz, \quad z \in \mathbb{Z}. \tag{7.165}$$

The physical content of this restriction is clear in view of the form of the gapping interaction, which involves scattering a electrons from edge LA with b holes from edge RB. The ground state of the interface will then naturally consist of a superposition of states consisting of multiples of $(\psi^\dagger_{LA})^a \psi^b_{RB}$ particle-hole pairs. This is precisely what is expressed by the above constraint, once we also enforce the $\mathbb{Z}_2$ gauge symmetry constraint, which ties the bosonic winding to the fermionic parity.

Entanglement Entropy Calculation

The calculation of the EE is nearly identical to that of the uniform interface case, with the primary difference being that we must take into account the above constraints on the winding numbers. The approximated Hamiltonian again takes the decoupled form

$$H_1 \equiv H^{\text{osc}}_{1,f} + H^{\text{osc}}_{1,b} + H^{\text{zero}}_{1,b}. \tag{7.166}$$

The fermionic part of the approximated Hamiltonian, $H^{\text{osc}}_{1,f}$, is identical to that for the uniform interface problem, Eq. (7.69), and so the ground state of the fermionic sector will again be given by Eq. (7.74). The bosonic parts of the Hamiltonian are now given by:

$$H^{\text{zero}}_{1,b} = \frac{\pi v_c p}{2L}(aN_{RB} - bN_{LA})^2 + \frac{\pi \lambda v_c L}{2}(a\phi_{RB,0} + b\phi_{LA,0})^2, \tag{7.167}$$

$$H^{\text{osc}}_{1,b} = \frac{v_c}{2}\sum_{k\neq 0}(a^\dagger_k \quad a_{-k}) \begin{pmatrix} A_k & B_k \\ B_k & A_k \end{pmatrix} \begin{pmatrix} a_k \\ a^\dagger_{-k} \end{pmatrix}, \tag{7.168}$$

where

$$A_k = |k| + \frac{2\lambda\pi^2}{p|k|}, \quad B_k = \frac{2\lambda\pi^2}{p|k|}. \tag{7.169}$$

Dispensing with the details, we simply jump to writing down the ground state for the approximated Hamiltonian (including both interfaces):

$$|\widehat{\psi}_{\mathbf{1}}\rangle = |\widehat{\psi}_{1,\mathbf{1}}\rangle \otimes |\widehat{\psi}_{2,\mathbf{1}}\rangle\,, \tag{7.170}$$

$$|\widehat{\psi}_{1/2,\mathbf{1}}\rangle = |G_{b,\text{zero},1/2}\rangle \otimes |G_{b,\text{osc},1/2}\rangle \otimes |G_{f,\text{osc},1/2}\rangle \tag{7.171}$$

where

$$\begin{aligned} |G_{b,\text{zero},1}\rangle &= \sum_{N\in\mathbb{Z}} e^{-\frac{v_e \pi p a^2 b^2 N^2}{2L}} |N_{RB} = bN, N_{LA} = -aN\rangle\,, \\ |G_{b,\text{zero},2}\rangle &= \sum_{N\in\mathbb{Z}} e^{-\frac{v_e \pi p a^2 b^2 N^2}{2L}} |N_{LB} = -bN, N_{RA} = aN\rangle\,, \end{aligned} \tag{7.172}$$

while $|G_{b,\text{osc},1/2}\rangle$ and $|G_{f,\text{osc},1/2}\rangle$ are again given by Equations (7.71), (7.78) and (7.74), (7.79), respectively. The constraint imposed by the gapping interaction manifests itself in the sums over the winding mode states. The entanglement velocities are given by

$$v_e = \frac{2}{\pi}\sqrt{\frac{p}{\lambda}}, \qquad \tilde{v}_e = \frac{2}{|\tilde{g}|}. \tag{7.173}$$

Following the now standard procedure, we must apply the projection operator $P_{\mathbf{1}} \equiv P_{\mathbf{1},A} P_{\mathbf{1},B}$ defined in Eq. (7.49) to obtain a physical state in the MR Hilbert space. As in the uniform interface case, we again have that $P_{\mathbf{1}}\,|\widehat{\psi}_{\mathbf{1}}\rangle = P_{\mathbf{1},A}\,|\widehat{\psi}_{\mathbf{1}}\rangle = P_{\mathbf{1},B}\,|\widehat{\psi}_{\mathbf{1}}\rangle$. Indeed, we see that every state appearing in $|\widehat{\psi}_{\mathbf{1}}\rangle$ has $(-1)^{F_{RB}} = (-1)^{F_{LA}}$ and $(-1)^{F_{LB}} = (-1)^{F_{RA}}$. Additionally, since *both* a and b are *odd*, we have that $(-1)^{bN} = (-1)^{aN}$, and so the states also satisfy $(-1)^{N_{RB}} = (-1)^{N_{LA}}$, as well as $(-1)^{N_{LB}} = (-1)^{N_{RA}}$. It then readily follows that

$$|\psi_{\mathbf{1}}\rangle = P_{\mathbf{1}}\,|\widehat{\psi}_{\mathbf{1}}\rangle = P_{\mathbf{1},A}\,|\widehat{\psi}_{\mathbf{1}}\rangle = P_{\mathbf{1},B}\,|\widehat{\psi}_{\mathbf{1}}\rangle\,. \tag{7.174}$$

As in the uniform interface problem, $P_{\mathbf{1},B}\,|\widehat{\psi}_{\mathbf{1}}\rangle$ is again in a Schmidt decomposed form, and so we can directly read off the entanglement spectrum and hence the reduced density matrix for B (the only difference with the uniform interface calculation is the winding mode sector. We have that

$$\rho_{\mathbf{1},B} = \frac{1}{Z_{e^{ir\phi},e}} P_{\mathbf{1},B} P_b e^{-\mathcal{H}_e^{RB} - \mathcal{H}_e^{LB}} P_b P_{\mathbf{1},B}, \tag{7.175}$$

where $\mathcal{H}_e^{RB}$ and $\mathcal{H}_e^{LB}$ are given by Equations (7.83) and (7.84), respectively, with the substitution $n = pa^2$.

The operator P_b enforces the constraint of Eq. (7.165):

$$P_b \left| N_{RB}, N_{LB} \right\rangle = \delta_{N_{RB},0 \bmod b} \delta_{N_{LB},0 \bmod b} \left| N_{RB}, N_{LB} \right\rangle . \tag{7.176}$$

It is now a straightforward matter to derive the entanglement partition function. As before, we can write $Z_{\mathbf{1},e}$ as a product of contributions from the right and left edges:

$$Z_{\mathbf{1},e} = Z^{RB}_{\mathbf{1},e} Z^{LB}_{\mathbf{1},e}. \tag{7.177}$$

Explicitly,

$$\begin{aligned} Z^{RB}_{\mathbf{1},e} = \chi^{\text{Ising}}_0(\tilde{q}) \left(\sum_{N \in \text{even}} q^{pa^2(bN)^2/2} \right) q^{-\frac{1}{24}} \prod_{j=1}^{\infty} \left(1 - q^j\right)^{-1} \\ + \chi^{\text{Ising}}_{1/2}(\tilde{q}) \left(\sum_{N \in \text{odd}} q^{pa^2(bN)^2/2} \right) q^{-\frac{1}{24}} \prod_{j=1}^{\infty} \left(1 - q^j\right)^{-1}, \end{aligned} \tag{7.178}$$

where $\chi^{\text{Ising}}_0(\tilde{q})$ and $\chi^{\text{Ising}}_{1/2}(\tilde{q})$ were defined in Eqs. (7.92) and (7.93), respectively, and $Z^{LB}_{\mathbf{1},e}$ is given by a similar expression. As in the entanglement partition function for the untwisted sectors of the uniform interface problem, the first (second) line of Eq. (7.178) arises from the states in the trace which have both an even (odd) fermion parity and winding number parity. It is immediate to see that Eq. (7.178) is formally equivalent to Eq. (7.91) with the substitutions $n \to pa^2b^2$ and $r \to 0$. This implies that Eq. (7.178) is in fact the partition function in the trivial sector for a MR state at inverse filling $\nu^{-1} = pa^2b^2$. We will have more to say on this point later in this section but, for now, this observation allows us to immediately deduce the EE in the present non-uniform interface problem to be,

$$S_{\mathbf{1}} = -2 \ln(2\sqrt{pa^2b^2}) + \frac{\pi L}{3} \left(\frac{1}{v_e} + \frac{1}{2\tilde{v}_e} \right). \tag{7.179}$$

We thus find the TEE for this nonuniform interface on the torus (in the vacuum sector) is given by

$$\gamma_1 = 2 \ln(2\sqrt{pa^2b^2}), \tag{7.180}$$

which is one of the main results of this Chapter.

7.6.2 Opposite Parity Interface

We now turn to the class of interfaces in which one of a and b is even and the other odd. Without loss of generality, we will again take a to be even and b to be odd. We will also employ the topologically equivalent representation of the MR CFT, as discussed in Section 7.5.2 and detailed in Appendix E.3. Again focusing on interface 1, the free part of the Lagrangian is given by,

$$\begin{aligned}\mathcal{L}_{\text{dec},1} = \sum_{\mu} \Bigg[&\frac{k_\mu}{4\pi}\partial_x\phi_\mu(\mu\partial_t - v_c\partial_x)\phi_\mu + \chi_\mu \frac{i}{2}(\partial_t - \mu v_n\partial_x)\chi_\mu \\ &+ \frac{1}{4\pi}\sum_{j=1}^{r}\left\{\partial_x\overline{\phi}_\mu^j(-\mu\partial_t - v_n\partial_x)\overline{\phi}_\mu^j + \partial_x\phi_\mu^j(\mu\partial_t - v_n\partial_x)\phi_\mu^j\right\}\Bigg],\end{aligned} \tag{7.181}$$

where, in the interest of compactness, we have abused our earlier notation by temporarily redefining $\mu = LA/RB = +/-$. We have also set,

$$k_{LA} = pa^2, \quad k_{RB} = pb^2. \tag{7.182}$$

The gapping interaction is given by

$$\mathcal{L}_{\text{gap},1} = \mathcal{L}_{c,1} + \mathcal{L}_{n,1}, \tag{7.183}$$

$$\mathcal{L}_{c,1} = -\frac{2g}{\pi}\cos(2pab^2\phi_{LA} + 2pa^2b\phi_{RB}) \tag{7.184}$$

$$\mathcal{L}_{n,1} = u\sum_{j_1\neq j_2}\left[\cos(2\Theta_1^{j_1})\cos(2\Theta_1^{j_2}) + \cos(2\overline{\Theta}_1^{j_1})\cos(2\overline{\Theta}_1^{j_2})\right] + u\sum_{j=1}^{r}\cos(2\Theta_1^j)i\chi_{LA}\chi_{RB}, \tag{7.185}$$

where,

$$2\Theta_1^j \equiv \phi_{RB}^j - \phi_{LA}^j, \quad 2\overline{\Theta}_1^j = \overline{\phi}_{RB}^j - \overline{\phi}_{LA}^j, \tag{7.186}$$

and we take $u, g > 0$. We will also require the mode expansions

$$\begin{aligned}\phi_\mu^j &= \phi_{\mu,0}^j + 2\pi N_\mu^j\frac{x}{L} + \sum_{\mu k<0}\sqrt{\frac{2\pi}{L|k|}}\left[a_k^j e^{ikx} + (a_k^j)^\dagger e^{-ikx}\right] \\ \overline{\phi}_\mu &= \overline{\phi}_{\mu,0} + 2\pi\overline{N}_\mu^j\frac{x}{L} + \sum_{\mu k>0}\sqrt{\frac{2\pi}{L|k|}}\left[\overline{a}_k^j e^{ikx} + (\overline{a}_k^j)^\dagger e^{-ikx}\right]\end{aligned} \tag{7.187}$$

where

$$[(a_k^i)^\dagger, a_{k'}^j] = [(\overline{a}_k^i)^\dagger, \overline{a}_{k'}^j] = \delta_{k,k'}\delta_{i,j}, \tag{7.188}$$

$$[\phi_{\mu,0}^i, N_{RB}^j] = -[\overline{\phi}_{\mu,0}^i, \overline{N}_\mu^j] = -i\delta_{i,j}, \tag{7.189}$$

and we have temporarily set $\mu = LA/RB = +/-$.

Gapping Term Constraints

We now take the strong coupling limit. Without loss of generality, we expand about the vacuum defined by the expectation values

$$\begin{aligned} \langle 2pab^2\phi_{LA} + 2pa^2b\phi_{RB}\rangle &= \pi \\ \langle 2\Theta_1^j\rangle = \langle 2\Theta_1^j\rangle &= 0 \\ \langle i\chi_{LA}\chi_{RB}\rangle &< 0, \end{aligned} \tag{7.190}$$

so that

$$H_{\text{gap},1} \approx \int_0^L \left[\frac{\lambda\pi}{2}\sum_j \left[(2\Theta^j)^2 + (2\overline{\Theta}^j)^2\right] + \tilde{g}i\chi_{LA}\chi_{RB} + \frac{v_c\tilde{\lambda}\pi}{2}(b\phi_{LA} + a\phi_{RB} - \pi/(2pab))^2\right]dx. \tag{7.191}$$

Here, $\lambda, \tilde{\lambda} > 0$ and $\tilde{g} = -ru < 0$. As in the equal parity interface problem, the pinning of $b\phi_{LA} + a\phi_{RB}$ enforces the constraint Eq. (7.165), while the pinning of the $2\Theta_1^j$ and $2\overline{\Theta}_1^j$ fields enforces the constraints

$$N_{LA}^j = N_{RB}^j \in \mathbb{Z}, \quad \overline{N}_{LA}^j = \overline{N}_{RB}^j \in \mathbb{Z}. \tag{7.192}$$

Note that, at this level of our approximation, the factor of two in the argument of $\mathcal{L}_{c,1}$, which reflects the fact that we must tunnel an even number of electrons, does not play any role. This will be accounted for once we project to the physical Hilbert space.

Entanglement Entropy Calculation

We see that, in the approximated Hamiltonian, the Majorana fermion, neutral boson, and charged boson sectors all decouple. In particular, the Hamiltonians for each of these sectors have already appeared in our calculations for the equal-parity interface in Eq. (7.166). Hence, we will skip the details of the computation

and simply jump to writing down the ground state of the approximated Hamiltonian:

$$|\widehat{\psi}_{\mathbf{1},1}\rangle = |G_{b,\mathrm{zero},1}\rangle \otimes |G_{b,\mathrm{osc},1}\rangle \otimes |G_{f,\mathrm{osc},1}\rangle \otimes \prod_{j=1}^{r} |G^j_{n,\mathrm{zero},1}\rangle \otimes \prod_{j=1}^{r} |G^j_{n,\mathrm{osc},1}\rangle\,, \tag{7.193}$$

where, $|G_{b,\mathrm{osc},1}\rangle$, $|G_{f,\mathrm{osc},1}\rangle$, and $|G_{b,\mathrm{zero},1}\rangle$ are again given by Equations (7.71), (7.74), and (7.172), respectively, while the ground states for the neutral boson oscillator and zero-mode sectors of interface 1, respectively, take the form

$$|G^j_{n,\mathrm{osc},1}\rangle = \exp\left(\sum_{k>0} e^{-\frac{v_{e,n}k}{2}}[(a^j_k)^\dagger(a^j_{-k})^\dagger + (\overline{a}^j_k)^\dagger(\overline{a}^j_{-k})^\dagger]\right)|0\rangle\,, \tag{7.194}$$

$$|G^j_{n,\mathrm{zero},1}\rangle = \left(\sum_{\overline{N}^j} e^{-\frac{v_{e,n}\pi(\overline{N}^j)^2}{2L}}\,|\overline{N}^j_{RB} = \overline{N}^j, \overline{N}^j_{LA} = \overline{N}^j\rangle\right) \otimes \left(\sum_{N^j} e^{-\frac{v_{e,n}\pi(N^j)^2}{2L}}\,|N^j_{RB} = N^j, N^j_{LA} = N^j\rangle\right), \tag{7.195}$$

where the non-universal entanglement velocity $v_{e,n}$ depends on the field expectation values in an unimportant way. The corresponding state for interface 2, $|\widehat{\psi}_{\mathbf{1},2}\rangle$, is given by a similar expression.

As usual, we obtain an approximation to the physical ground state of the unapproximated gapping Hamiltonian in the $\mathbf{1}$ sector by applying a projection to $|\widehat{\psi}_{\mathbf{1}}\rangle$. Defining $\mathbb{Z}_2$ symmetry operators, Eq. (7.153), for each cylinder, $G'_{\mu\alpha}$ (where $\mu = L, R$, $\alpha = A, B$), the $\mathbf{1}$ sector is defined by the constraint $G'_{\mu\alpha} = 1$. Likewise, we define copies of the projection operators, Eq. (7.154), for each cylinder: $P_{\mathbf{1},\alpha} = P_{\mathbf{1},L\alpha}P_{\mathbf{1},R\alpha}$. We thus obtain an approximation to the ground state in the physical Hilbert space via the projection

$$|\psi_{\mathbf{1}}\rangle = P_{\mathbf{1}}\,|\widehat{\psi}_{\mathbf{1}}\rangle = P_{\mathbf{1},A}P_{\mathbf{1},B}\,|\widehat{\psi}_{\mathbf{1}}\rangle\,. \tag{7.196}$$

In contrast to our earlier calculations, however, the projection requires a bit more care, since a is even while b is odd, and so $(-1)^{aN} \neq (-1)^{bN}$ for N odd. Explicitly, we have that

$$(-1)^{N_{LA}}\,|\widehat{\psi}_{1,\mathbf{1}}\rangle = |\widehat{\psi}_{1,\mathbf{1}}\rangle\,, \tag{7.197}$$

since each state appearing in $|\widehat{\psi}_{1,\mathbf{1}}\rangle$ is an eigenstate of N_{LA} with eigenvalue aN and $(-1)^{aN} = 1$. So, $P_{\mathbf{1},LA}$ will project out all states in $|\widehat{\psi}_{1,\mathbf{1}}\rangle$ with

$$(-1)^{F_{LA}}(-1)^{\sum_j N^j_{LA}}(-1)^{\sum_j \overline{N}^j_{LA}} = -1, \tag{7.198}$$

that is, those states whose fermion parity does not match the neutral boson winding parity. However, we

can see from the explicit form of $|\widehat{\psi}_{1,\mathbf{1}}\rangle$ that

$$(-1)^{F_{RB}+\sum_j N^j_{RB}+\sum_j \overline{N}^j_{RB}} = (-1)^{F_{LA}+\sum_j N^j_{LA}+\sum_j \overline{N}^j_{LA}} \tag{7.199}$$

for each state appearing in $|\widehat{\psi}_{1,\mathbf{1}}\rangle$. Now, when we apply $P_{\mathbf{1},RB}$ to $P_{\mathbf{1},LA}\,|\psi_{1,\mathbf{1}}\rangle$, we must project out those states with $(-1)^{N_{RB}} = -1$, since all the remaining states have $(-1)^{F_{RB}+\sum_j N^j_{RB}+\sum_j \overline{N}^j_{RB}} = +1$. But, each state in $|\widehat{\psi}_{1,\mathbf{1}}\rangle$ has $N_L = bN$, with b odd, and $(-1)^{bN} = (-1)^N$. Thus, the only states remaining in the sum after projection will have $N \in 2\mathbb{Z}$ – i.e. $N_{RB} = 2bz$ and $N_{LA} = -2az$, with $z = N/2$. Physically, this reflects the fact that we are scattering an even number of electrons and holes, as manifested by the factor of two in the argument of $\mathcal{L}_{c,1}$ [Eq. (7.184)].

It is now a simple matter to deduce the entanglement spectrum and hence the entanglement partition function for, say, cylinder B. Taking into account the constraints on the fermion parity and bosonic winding number quantum numbers imposed by the projections, we can read off the entangelement spectrum from the explicit forms of $|\psi_{1,\mathbf{1}}\rangle$ and $|\psi_{2,\mathbf{1}}\rangle$, which are in Schmidt-decomposed form. Indeed, we find for the entanglement partition function,

$$Z^{RB}_{\mathbf{1},e} = \left(\sum_{N\in\text{even}} q^{pb^2(aN)^2/2}\right) q^{-\frac{1}{24}} \prod_{j=1}^{\infty}\left(1-q^j\right)^{-1} \times \left(\chi_0^{\text{Ising}}(\tilde{q}) \sum_{\substack{\{N_i\} \\ \sum_i N_i\in\text{even}}} q_n^{\sum_i N_i^2/2}\left[q_n^{-\frac{1}{24}}\prod_{j=1}^{\infty}(1-q_n^j)^{-1}\right]^{2r} + \chi_{1/2}^{\text{Ising}}(\tilde{q}) \sum_{\substack{\{N_i\} \\ \sum_i N_i\in\text{odd}}} q_n^{\sum_i N_i^2/2}\left[q_n^{-\frac{1}{24}}\prod_{j=1}^{\infty}(1-q_n^j)^{-1}\right]^{2r}\right), \tag{7.200}$$

where q and $\tilde{q}$ are again take forms given by Eq. (7.90) and we have defined $q_n \equiv \exp(2\pi i \tau_n)$, with $\tau_n \equiv i\beta v_{e,n}/L$ [$v_{e,n}$ is defined implicitly in Eqs. (7.194), (7.195)]. We have also used the fact that, since we are in the untwisted sector, we can write

$$Z_{\mathbf{1},e} = Z^{RB}_{\mathbf{1},e} Z^{LA}_{\mathbf{1},e} \tag{7.201}$$

and, as usual, $Z_{\mathbf{1},LA}$ takes a similar form to that of $Z_{\mathbf{1},RB}$. We can express the partition function in terms

of modular functions:

$$Z^{RB}_{\mathbf{1},e} = \frac{\theta^0_0(pa^2b^2\tau)+\theta^0_{1/2}(pa^2b^2\tau)}{\eta(\tau)}\times\left(\frac{1}{4}\left[\sqrt{\frac{\theta^0_0(\tilde{\tau})}{\eta(\tilde{\tau})}}+\sqrt{\frac{\theta^0_{1/2}(\tilde{\tau})}{\eta(\tilde{\tau})}}\right]\frac{\theta^0_0(\tau_n)^{2r}+\theta^0_{1/2}(\tau_n)^{2r}}{\eta(\tau_n)^{2r}}\right.$$
$$\left.+\frac{1}{4}\left[\sqrt{\frac{\theta^0_0(\tilde{\tau})}{\eta(\tilde{\tau})}}-\sqrt{\frac{\theta^0_{1/2}(\tilde{\tau})}{\eta(\tilde{\tau})}}\right]\frac{\theta^0_0(\tau_n)^{2r}-\theta^0_{1/2}(\tau_n)^{2r}}{\eta(\tau_n)^{2r}}\right). \tag{7.202}$$

Applying the usual modular transformations and taking the large length limit, we find

$$S_{\mathbf{1}} = -2\ln(4\sqrt{pa^2b^2})+\frac{\pi L}{3}\left(\frac{2r}{v_{e,n}}+\frac{1}{v_e}+\frac{1}{2\tilde{v}_e}\right). \tag{7.203}$$

Hence, the TEE for this nonuniform interface on the torus (in the vacuum sector) is given by

$$\gamma_{\mathbf{1}} = 2\ln(4\sqrt{pa^2b^2}), \tag{7.204}$$

which is another of the main results of this Chapter. Note that this differs from that of the same-parity interface [cf. Eq. (7.180)].

7.6.3 Relation to Parent Topological Phase

We now provide a physical interpretation for the values of the TEE associated with the non-uniform interface between $\mathcal{A}$ and $\mathcal{B}$, which is based on determining whether a gapped interface can be formed between phases $\mathcal{A}$ and $\mathcal{B}$ using anyon condensation. This approach has been fruitful in classifying gapped interfaces of 2D Abelian phases [81, 88] as well as the case where the bulk topological order is non-Abelian [274, 292].

Suppose $\mathcal{A}$ and $\mathcal{B}$ share a common parent phase $\mathcal{C}$ – that is to say, a phase in which condensing one set of anyons yields $\mathcal{A}$ and condensing a different set of anyons yields phase $\mathcal{B}$. Then, one can form an interface between $\mathcal{A}$ and $\mathcal{B}$ by starting with $\mathcal{C}$, condensing down to $\mathcal{A}$ in one region, and then condensing down to $\mathcal{B}$ in another region, yielding a configuration which is gapped everywhere as follows:

$$(\mathcal{A}) \quad | \quad (\mathcal{C}) \quad | \quad (\mathcal{B}) \quad . \tag{7.205}$$

Shrinking the region containing $\mathcal{C}$ yields a gapped interface between $\mathcal{A}$ and $\mathcal{B}$. Similarly, a gapped interface can be formed if $\mathcal{C}$ is a daughter phase of $\mathcal{A}$ and $\mathcal{B}$ – that is, $\mathcal{A}$ and $\mathcal{B}$ can be condensed to obtain $\mathcal{C}$.

The intermediate state $\mathcal{C}$ can be thought of as originating from $\mathcal{A}$ or $\mathcal{B}$ by gauging of an appropriate discrete symmetry, insofar as anyon condensation can be viewed as the inverse operation of gauging an

anyonic symmetry [105, 303] (related observations of the connection between boundary physics and bulk physics have been made in Ref. [304]). Consequently, the local interactions that gap the interface manifest this symmetry, which, in the Abelian case can be precisely shown to contribute to a correction to the TEE [88]. Furthermore, in Ref. [292], it was argued that the choice of $\mathcal{C}$ determines the ground state of the interface to be a particular Ishibashi state, from which the interface TEE was calculated to be $\ln \mathcal{D}_{\mathcal{C}}$, where $\mathcal{D}_{\mathcal{C}}$ is the total quantum dimension of $\mathcal{C}$. In this subsection, after first reviewing this construction for interfaces of Laughlin states, we identify the appropriate parent phases for the two classes of MR interfaces identified above, as determined by the choice of gapping interaction, and verify this relation with the TEE.

Review of Laughlin Interfaces

Let us again consider an interface between Laughlin $\nu^{-1} = pb^2$ and $\nu^{-1} = pa^2$ states, where a and b are co-prime [81]. In this case the parent topological phase is a Laughlin state at inverse filling $\nu^{-1} = pa^2b^2$:

$$(\mathcal{A}) \quad \nu = \frac{1}{pb^2} \quad \Big| \quad (\mathcal{C}) \quad \nu = \frac{1}{pa^2b^2} \quad \Big| \quad (\mathcal{B}) \quad \nu = \frac{1}{pa^2}, \tag{7.206}$$

The state $\mathcal{C}$ originates from $\mathcal{A}$ and $\mathcal{B}$ by gauging discrete $\mathbb{Z}_a$ and $\mathbb{Z}_b$ symmetries, respectively. As such, the local gapping interaction of the $\mathcal{A}-\mathcal{C}$ interface displays a discrete $\mathbb{Z}_a$ symmetry associated with the pairing of a local quasiparticles of $\mathcal{A}$ with one local quasiparticle of $\mathcal{A}$. Similarly, on the $\mathcal{B}-\mathcal{C}$ interface, the local interaction displays a $\mathbb{Z}_b$ symmetry. Consequently, as the phase "thins out," one is left with the $\mathcal{A}-\mathcal{B}$ interface where a local quasiparticles of $\mathcal{A}$ bind to b local quasiparticles of $\mathcal{B}$.

Now, the anyon content of $\mathcal{C}$ is given by

$$\mathcal{C} = \{e^{ir\phi}\}_{r=1,\ldots,pa^2b^2}. \tag{7.207}$$

These anyons have spin

$$h_r = \frac{1}{2}\frac{r^2}{pa^2b^2}. \tag{7.208}$$

Consider the anyon labelled by $r_0 = pa^2b$. It has the same spin, $h_{r_0} = \frac{1}{2}pa^2$, as the electron operator in the $\nu^{-1} = pa^2$ Laughlin state. The mutual statistics between r_0 and all other anyons is given by

$$\theta_{r_0,r} = \exp\left(2\pi i \frac{r}{b}\right). \tag{7.209}$$

So, if we condense r_0, only anyons of the form $r = bl$ will remain deconfined. These remaining anyons have

mutual statistics

$$\theta_{l,l'} = \exp\left(2\pi i \frac{ll'}{pa^2}\right). \tag{7.210}$$

This precisely describes the topological order of $\mathcal{B}$. It is easy to see that condensing $r = pab^2$ would instead give $\mathcal{A}$. Thus, $\mathcal{C}$ is indeed the parent state of $\mathcal{A}$ and $\mathcal{B}$.

Now, the total quantum dimension of a Laughlin $\nu^{-1} = pa^2b^2$ state is $\mathcal{D} = \sqrt{pa^2b^2}$, which agrees with the value of the TEE for an entanglement cut lying along the physical interface, $\gamma = \ln\sqrt{pa^2b^2}$, as computed in Ref. [91].

Extension to Moore-Read Interfaces

Let us now consider the interface between $\nu^{-1} = pb^2$ and $\nu^{-1} = pa^2$ MR states, with a and b both odd. We calculated the TEE in this scenario to be given by $\gamma = \ln(2\sqrt{pa^2b^2})$. This is precisely the TEE for a uniform $\nu^{-1} = pa^2b^2$ MR state. We thus claim that the parent phase for the $\nu^{-1} = pb^2$ and $\nu^{-1} = pa^2$ MR states, with a and b both odd, is the $\nu^{-1} = pa^2b^2$ MR state:

$$(\mathcal{A}) \quad \mathrm{MR}_{pb^2} \quad \Big| \quad (\mathcal{C}) \quad \mathrm{MR}_{pa^2b^2} \quad \Big| \quad (\mathcal{B}) \quad \mathrm{MR}_{pa^2}, \tag{7.211}$$

where we have introduced the shorthand $\mathrm{MR}_{\nu^{-1}}$ to denote the MR state at filling ν. Now, $\mathcal{C}$ has the anyon content

$$\mathcal{C} = \{e^{ir\phi}, \chi e^{ir\phi}, \sigma e^{i(r+1/2)\phi}\}_{r=1,\ldots,pa^2b^2}. \tag{7.212}$$

In order to obtain, say, phase $\mathcal{B}$, we must condense an anyon of the form $\chi e^{ir\phi}$, since this will serve as the new electron operator and we wish to obtain another MR state. From the discussion of the Laughlin interface, it is straightforward to see that condensing $\psi_{\mathcal{B}} = \chi e^{ipa^2b\phi}$ will yield the correct Laughlin quasiparticle content, as well as Majorana content (since χ has trivial braiding with itself, under a full 2π rotation).

As for the non-Abelian anyons, $\sigma e^{i(r+1/2)\phi}$, their braiding with $\psi_{\mathcal{B}}$ is given by,

$$\theta_{\sigma e^{i(r+1/2)\phi}, \psi_{\mathcal{B}}} = \exp\left[2\pi i \left(\frac{b+2r+1}{2b}\right)\right]. \tag{7.213}$$

In order for this phase to be trivial, we require

$$2r+1 = b(2m+1), \quad m \in \mathbb{Z}. \tag{7.214}$$

Both the LHS and $2m+1$ are odd, and so a solution exists if and only if b *is also odd*. If this is the case, we find that the non-Abelian anyons parameterized as

$$r = b(m+1/2) - 1/2 \implies \sigma e^{i(r+1/2)\phi} = \sigma e^{ib(m+1/2)\phi} \tag{7.215}$$

remain deconfined. These anyons have spin

$$h_r = \frac{1}{16} + \frac{1}{2}\frac{(m+1/2)^2}{pa^2}, \tag{7.216}$$

which are precisely the spins of the non-Abelian anyons in the MR_{pb^2} state. We can also compute the braiding of these anyons and the deconfined Abelian anyons, $e^{ilb\phi}$, to be

$$\theta_{\sigma e^{i(r+1/2)\phi}, e^{ilb\phi}} = \exp\left[2\pi i \frac{l(m+1/2)}{pa^2}\right]. \tag{7.217}$$

This is the expected phase for braiding of the corresponding anyons in the MR_{pb^2} state. It is straightforward to see that the correct braiding statistics between the remaining non-Abelian anyons and Majoranas will also be obtained. We thus conclude that by condensing $\chi e^{ipa^2b\phi}$ in phase $\mathcal{C}$, we obtain phase $\mathcal{B}$. *Provided a is odd*, it follows immediately that condensing $\chi e^{ipab^2\phi}$ in phase $\mathcal{C}$ will yield phase $\mathcal{A}$. We thus conclude that if both a and b are odd, we can obtain a GI between MR_{pb^2} and MR_{pa^2} states which is characterized by an intervening $\mathrm{MR}_{pa^2b^2}$ state, consistent with the fact that the TEE for this interface is $\gamma = \ln(2\sqrt{pa^2b^2})$.

Let us now consider the case where one of a and b, say a, is even and the other odd. Our claim is that the parent phase in this case is given not by a MR state, but by an Ising $\times\, U(1)_{4pa^2b^2}$ theory:

$$(\mathcal{A})\ \mathrm{MR}_{pb^2} \quad \Big| \quad (\mathcal{C})\ \text{Ising} \times U(1)_{4pa^2b^2} \quad \Big| \quad (\mathcal{B})\ \mathrm{MR}_{pa^2} \tag{7.218}$$

The anyon content of $\mathcal{C}$ is given by

$$\mathcal{C} = \{1, \chi, \sigma\} \times \{e^{il\phi}\}_{l=1,\ldots,4pa^2b^2}. \tag{7.219}$$

It is readily seen that $\mathcal{C}$ has the correct total quantum dimension, $\mathcal{D}_{\mathcal{C}} = 4\sqrt{pa^2b^2}$, given that the TEE for

this interface is given by $\gamma = \ln(4\sqrt{pa^2b^2})$.

Suppose we condense

$$\psi_{\mathcal{B}} = \chi e^{i2pa^2b\phi}. \tag{7.220}$$

This quasiparticle has spin

$$h_{\mathcal{B}} = \frac{1}{2} + \frac{1}{2}\frac{4p^2a^4b^2}{4pa^2b^2} = \frac{1}{2} + \frac{1}{2}pa^2, \tag{7.221}$$

which matches that of the electron operator in phase $\mathcal{B}$. Now, the braiding of a Laughlin quasiparticle $e^{il\phi}$ with $\psi_{\mathcal{B}}$ is given by

$$\theta_{e^{il\phi},\psi_{\mathcal{B}}} = \exp\left[2\pi i\frac{(2pa^2b)l}{4pa^2b}\right] = \exp\left[2\pi i\frac{l}{2b}\right], \tag{7.222}$$

which is trivial when $l = 2bm$, $m \in \mathbb{Z}$. So, all Laughlin quasiparticles except those of the form $e^{i2bm\phi}$ are confined. The remaining Laughlin quasiparticles have mutual statistics

$$\theta_{e^{im\phi},e^{im'\phi}} = \exp\left[2\pi i\frac{(2bm)(2bm')}{4pa^2b}\right] = \exp\left[2\pi i\frac{mm'}{pa^2}\right], \tag{7.223}$$

which are precisely the mutual statistics of the Laughlin anyons in phase $\mathcal{B}$. It immediately follows that anyons of the form $\chi e^{i2bm\phi}$ are also deconfined and reproduce the Majorana sectors of phase $\mathcal{B}$. The braiding statistics of the non-Abelian anyons, $\sigma e^{it\phi}$ with $\psi_{\mathcal{B}}$ is given by

$$\frac{1}{2\pi}\theta_{\sigma e^{it\phi},\psi_{\mathcal{B}}} = \frac{1}{2} + \frac{(2pa^2b)t}{4pa^2b^2} = \frac{1}{2} + \frac{t}{2b} = \frac{b+t}{2b}. \tag{7.224}$$

The deconfined non-Abelian anyons thus satisfy

$$b + t = 2b(r+1) \implies t = b(2r+1) \tag{7.225}$$

with $r \in \mathbb{Z}$. These deconfined anyons have spin

$$h_r = \frac{1}{16} + \frac{b^2(2r+1)^2}{4pa^2b^2} = \frac{1}{16} + \frac{(r+1/2)^2}{pa^2}, \tag{7.226}$$

which matches that of the non-Abelian anyons in phase $\mathcal{B}$. Hence, condensing $\psi_{\mathcal{B}}$ in $\mathcal{C}$ correctly reproduces

phase $\mathcal{B}$. It follows, of course, that by instead condensing $\psi_{\mathcal{A}} = \chi e^{i2pab^2\phi}$, we would have obtained phase $\mathcal{A}$. Hence, $\mathcal{C} = \text{Ising} \times U(1)_{4pa^2b^2}$ appears to be the correct intermediate phase to describe the a even, b odd interface. Note that, however, at no point was it necessary to impose that one of a and b was even and the other odd; indeed, both could have been odd as well. This is consistent with the fact that the a, b odd interface could, in principle, also be gapped using the tunneling terms of Eq. (7.159).

7.7 Discussion and Conclusion

In this Chapter, we extended the cut-and-glue approach to calculating entanglement entropy of two-dimensional topologically ordered phases to interfaces of the simplest non-Abelian fractional quantum Hall states, namely the generalized Moore-Read states. By carefully taking into account the Hilbert space structure of the MR CFT, as reviewed in Section 7.2, we first demonstrated, in Section 7.4, that we can reproduce the entanglement spectrum and hence the topological entanglement entropy for each of the topological sectors of the MR state on a torus. In Section 7.5.2, we investigated interfaces of distinct generalized MR states, identifying when and how they can be gapped out. In particular, we looked at interfaces of MR states at inverse fillings $\nu^{-1} = pa^2$ and $\nu^{-1} = pb^2$, with a and b coprime, finding that they can always be gapped, but also that the form of the gapping interaction depends on whether a and b are both odd or if one is even. We then found that this distinction manifests itself in the TEE when the entanglement cut is placed along the interface. Indeed, we found in Section 7.6 that, in the trivial sector, the TEE is given by $\gamma_{\mathbf{1}} = 2\ln(2\sqrt{pa^2b^2})$ when a and b are both odd and by $\gamma_{\mathbf{1}} = 2\ln(4\sqrt{pa^2b^2})$ when one of a and b is even. Finally, we demonstrated how this value of the TEE is connected to the existence of a parent topological phase from which both the $\nu^{-1} = pa^2$ and $\nu^{-1} = pb^2$ MR states descend.

Although we focused on the generalized MR states, in principle, the cut-and-glue approach could, in principle, be extended to other non-Abelian topological orders whose edge CFTs possess a free-field representation. Following our prescription, one can approximate a gapping term to quadratic order and then project the resulting ground state to the appropriate topological sector of the physical Hilbert space. It should be possible, for instance, to repeat our calculation for states in the Bonderson-Slingerland hierarchy [305] and for the orbifold FQH states of Barkeshli and Wen [176]. It would also be interesting to see whether our methodology could be used to investigate interfaces of Abelian and non-Abelian states.

Aside from calculations of the entanglement entropy in other systems, another open question is the extent to which the anyon condensation picture of gapped interfaces of non-Abelian states is connected to the existence of explicit gapping interactions for such interfaces. In the examples we considered, we

found that there did indeed appear to be a close correspondence between the two. For an interface of MR states at inverse fillings $\nu^{-1} = pb^2$ and $\nu^{-1} = pa^2$ with a and b both odd, we were able to write down a gapping term which simply corresponded to a local operator constructed by fusing together elements of the set of anyons to be condensed. In contrast, when one of a and b was even, we found it useful to resort to a topologically equivalent description of the MR edge theory to be able to write down an interaction which fully gapped the interface. Nevertheless, this interaction was still closely connected to the set of condensed anyons characterizing the interface. Now, for interfaces of *Abelian* states, it is known that there is a one-to-one correspondence between Lagrangian subgroups and gapping interactions, provided one allows for the introduction of additional topologically trivial edge states (physically, this corresponds to edge reconstruction). Two Abelian theories differing from one another only by the addition of such trivial edge states are said to be *stably equivalent* theories [85, 86]. At a superficial level, our construction mirrors this notion of stable equivalence, in that we write down a theory with the same topological content, but with additional degrees of freedom. However, the additional fields which are added in our case are *not* local, in contrast to the Abelian case. It is not clear how general this coset construction of topologically equivalent CFTs is, but it could perhaps be used as a basis to write down general gapping interactions for interfaces of arbitrary non-Abelian orders – or at least those with free field representations. Such a scheme could potentially be used to derive the different sets of tunneling interactions that can be used to gap out an interface between two given non-Abelian topological orders.

Lastly, as noted in the introduction, gapped interfaces of Abelian topological phases have attracted much interest in recent years, due to the possibility of realizing non-Abelian defects at terminations of said interfaces [72–81, 83]. In fact, as also noted in the introduction, the value of the TEE of an entanglement cut along an interface between Abelian topological phases has been connected to the emergence of a one-dimensional symmetry protected topological phase (SPT) along the interface [88]. The endpoints of these SPTs support parafermions, in contrast to purely one-dimensional SPTs which can only host Majorana zero modes. It would be interesting to see whether an analogous statement holds for interfaces of generalized MR states and if one can obtain bound states more exotic than parafermions.

Appendix A

Supplement to Chapter 2

A.1 Non-Interacting Model Band Structure

In Fig. A.1 we have plotted the band structure of the model Eq. (2.1) for $g = 0$, $\phi_{\pm} = \pi/2$, and $J = 1$. The lowest band, which we partially fill, has Chern number $C_0 = +1$. Note that the bandwidth of this band and the band gap are comparable in magnitude (the former is slightly smaller than the latter).

A.2 Comparison with Uniform Density Approximation

As noted in the main text our lattice Chern-Simons action explicitly breaks the lattice symmetries and as a consequence the mean-field ground state the theory predicts on the Kagome lattice breaks them as well. Previous applications of this method (e.g. the chiral spin liquid study of Ref. [96]) did not correctly solve the mean field equations (they assumed the currents to be zero) and so found uniform states. To reiterate what is said in the main text, we believe that at the full quantum level the lattice symmetries broken by our mean field solution should be restored. However this is a nontrivial calculation (presumably being a non-perturbative effect) so it is worthwhile to compare the results of our mean-field theory with those one would obtain if one assumed a uniform ground state with equal statistical fluxes through all plaquettes (which we stress is not a valid solution to the mean field equations of our theory).

In Fig. A.2 we have plotted the Hofstadter spectrum for this uniform flux approximation. Note that the spectrum here has much finer detail than Fig. 2.3(a) of the main text as in this case we are not solving the mean field equations self-consistently but rather simply computing the band structure with the aforementioned uniform fluxes. We see that Fig. 2.3(a) and Fig. A.2 are largely similar. In particular, gapped states exist at the same fillings, including the Jain sequence. The Chern numbers are mostly unchanged for the fillings we have checked; one exception is the gapped state at $n_L = 2/3$ filling. Our mean-field analysis predicts this gapped state to have $\sigma_{xy} = 1/3$ while the uniform approximation would suggest a state with $\sigma_{xy} = 2/3$. The gap of this state in both schemes is small, however, so it is unlikely that it would survive

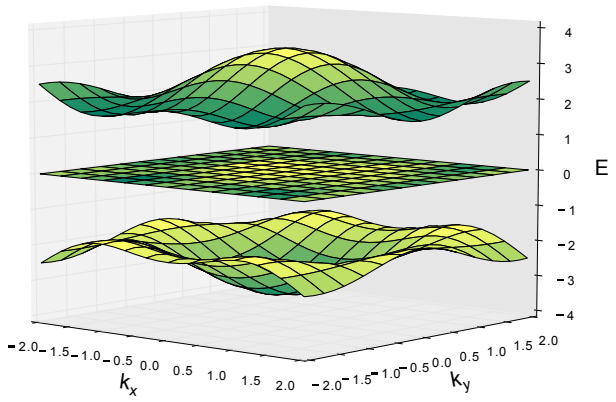

Figure A.1: Band structure of the model given by Eq. (2.1) in the absence of interactions with $\phi_\pm = \pi/2$ and $J = 1$. The lower, middle, and upper bands have $C_0 = +1, 0, -1$, respectively.

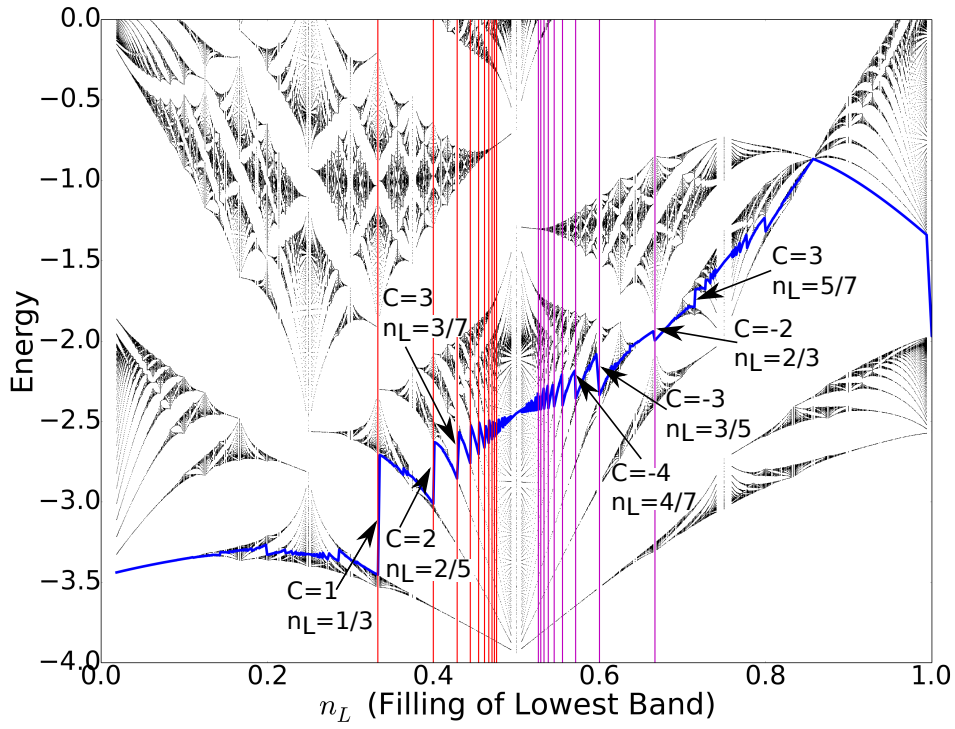

Figure A.2: Composite fermion Hofstadter spectrum on the kagome lattice with $k = 1$ and $\phi_\pm = \pi/2$ assuming a uniform density of composite fermions and equal fluxes through all plaquettes. The blue line is the Fermi energy. Some examples of gapped states are labelled with their filling and Hall conductance. Vertical red (purple) lines are drawn at fillings corresponding to the principal particle (hole) Jain sequence.

competition with other ordered states.

A.3 Full Self-Consistent Solution

In this Appendix we repeat our mean field analysis for $g \neq 0$ to check the stability of the gapped states we predict. As explained in Sec. 2.4, although the situation considered in the main text corresponds to formally taking $g = 0$, this does not mean that we neglected the role of interactions. Now, in our mean field analysis we found that even for $g = 0$, the sublattice imbalance, Δ, is generically non-zero, presumably as a result of the explicit point-group symmetry breaking of our lattice Chern-Simons action. In the case of $g \neq 0$ there is a finite energy cost associated with this imbalance and thus any finite value for the interaction strength, g, will affect the values of the sublattice densities. However, provided g is smaller than some critical g_c, we expect in general that the sublattice density will vary continuously and slowly so that the gapped states predicted in the main text remain gapped. In order to illustrate this, we perform a mean field analysis of our theory with the interaction term, Eq. (2.12), where $V_{\alpha\beta}(\mathbf{x}-\mathbf{y}) = 1$ if $(\mathbf{x}, \alpha)$ and $(\mathbf{y}, \beta)$ are nearest neighbors and $V_{\alpha\beta}(\mathbf{x} - \mathbf{y}) = 0$ otherwise. As before we focus on time independent solutions of Eq. (2.14) and Eq. (2.15) which preserve translational symmetry. Using these assumptions we note that we can re-write Eq. (2.15) as

$$\begin{aligned} \langle j_k \rangle = &-\theta(-1)^k (A_0^a - f_k A_0^c - (1 - f_k) A_0^c) \\ &- 2g\theta^2(-1)^k \left(\Phi^a - f_k \Phi^c - (1 - f_k)\Phi^b\right) \end{aligned} \tag{A.1}$$

where $f_k = 1$ for $k = 1, 5, 6$ and $f_k = 0$ for $k = 2, 3, 4$.

For simplicity we have focused on the cases of $n_L = 1/3$ and $n_L = 2/3$. In Fig. A.3 we have plotted Δ and the band gap as a function of g at these two fillings. It is clear in the case of $n_L = 1/3$ that the band gap does not close and Δ varies smoothly up to a critical value of g. Likewise in the case of $n_L = 2/3$ the imbalance Δ varies smoothly. The jump of Δ in the case of $n_L = 1/3$ appears to signal a phase transition to a nematic state. However, as discussed in the main text, since our Chern-Simons lattice action explicitly breaks the point-group symmetry we cannot trust our mean-field analysis to make accurate predictions about spontaneous rotational symmetry breaking. Nevertheless, this data suggests that we are justified in assuming that small, finite interactions will not affect the topological properties of the states predicted by our mean field analysis.

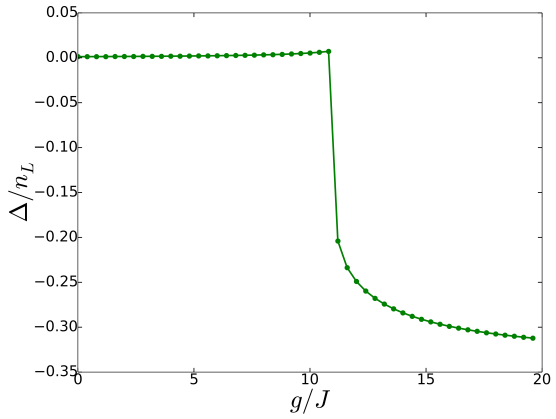

(a) $n_L = 1/3$

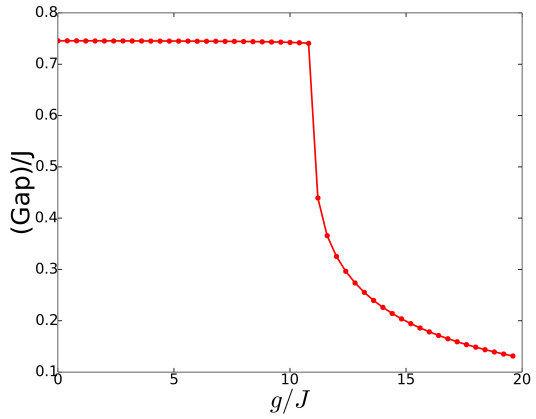

(b) $n_L = 1/3$

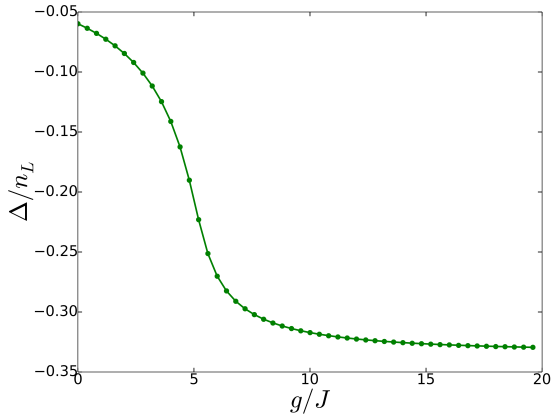

(c) $n_L = 2/3$

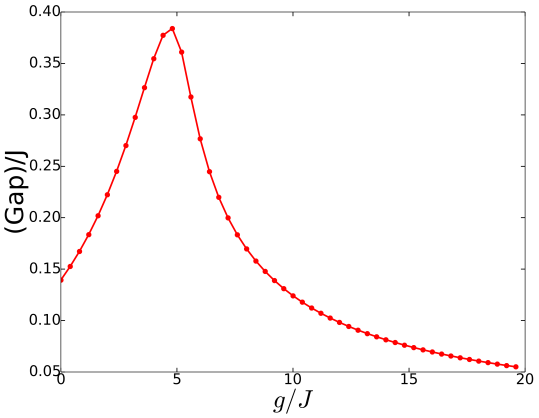

(d) $n_L = 2/3$

Figure A.3: Plots of the sublattice imbalance and band gap for (a,b) $n_L = 1/3$ and (c,d) $n_L = 2/3$ as a function of interaction strength g. Note that for small g the imbalance, Δ, and band gap vary smoothly with the latter never vanishing.

A.4 Spectrum of the $\mathcal{M}$-Matrix

Proper implementation of the lattice Chern-Simons theory requires that the matrix kernel Eq.(2.7) be non-singular, so as to guarantee that the commutation relations $[A_i(\boldsymbol{x}), A_j(\boldsymbol{y})] = -\frac{i}{\theta}\mathcal{M}^{-1}_{ij}(\boldsymbol{x}-\boldsymbol{y})$ are well defined. To access the eigenvalues of the $\mathcal{M}_{ij}(\mathbf{x}-\mathbf{y})$, we work with its Fourier transform $\mathcal{M}_{ij}(\mathbf{q})$ obtained by substituting the displacement operators s_j, $j=1,2$, by their Fourier representation $s_j(\mathbf{q}) = e^{-iq_j}$, where $q_j = \mathbf{q}\cdot\mathbf{e}_j$ is the momentum component along the direction defined by the unit vector $\mathbf{e}_j$. With that, $\mathcal{M}(\mathbf{q})$ is seen to be an anti-Hermitian matrix. Then $i\,\mathcal{M}(\mathbf{q})$ is a Hermitian 6×6 matrix, whose eigenvalues are found to be non-zero, hence $\mathcal{M}$ is invertible. To illustrate the non-singular character of the matrix kernel, we plot below the eigenvalues of $i\,\mathcal{M}(\mathbf{q})$ as function of q_1 for the choice $q_2=\pi$.

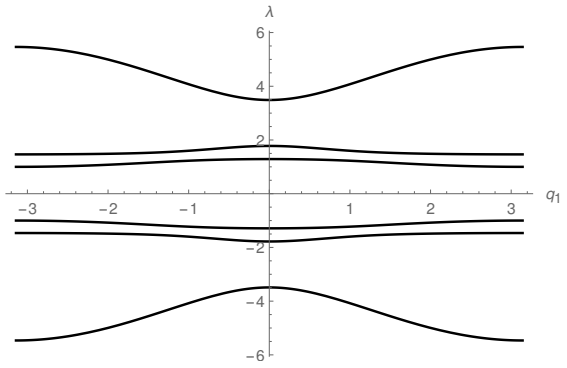

Figure A.4: Spectrum of the Hermitian 6×6 matrix $i\,\mathcal{M}(\mathbf{q})$ as function of q_1 for the choice $q_2=\pi$.

Appendix B

Supplement to Chapter 3

B.1 Details of Flux Attachment

We again direct the reader to Refs. [56, 58] for more details about the lattice Chern-Simons action of which we make use. Here, we record only for completeness the explicit form of the $\mathcal{M}$-matrix for the square lattice model under consideration, which does not play a role in our mean-field analysis:

$$\mathcal{M} = -\frac{1}{2}\begin{pmatrix} d_2\widehat{d}_2 & -2 - 2d_1 + 2\widehat{d}_2 + \widehat{d}_2 d_1 \\ 2 + 2d_2 - 2\widehat{d}_1 - \widehat{d}_1 d_2 & -d_1 - \widehat{d}_1 \end{pmatrix}. \tag{B.1}$$

As noted in Chapter 2, the form of $\mathcal{M}$ is lattice dependent and ensures that the theory is gauge invariant. We also remind the reader that the lattice Chern-Simons action of Ref. [58] can only be defined on lattices for which the number of vertices matches the number of plaquettes, of which the square lattice is one example.

B.2 Topological Properties of Period-Two Stripe Phases

B.2.1 Protection of Edge Majorana Flat Band and Bulk Nodes

We briefly detail the protection, at the level of non-interacting band theory, of the Majorana cones found in the nodal p_y stripe phase and the Majorana flat bands in both the nodal and gapped p_y stripe phases of the period-two case via reflection and particle-hole symmetries [306]. From Fig. 3.5b, we see that the unit cell of this striped phase consists of two sites, which we label as a (white, low density) sites and b (black, high density) sites. Using this notation, we can write H_F in the usual BdG form (dropping constant terms),

$$H_F = \frac{1}{2}\sum_{\boldsymbol{k}} \Psi_{\boldsymbol{k}}^\dagger h(\boldsymbol{k}) \Psi_{\boldsymbol{k}} = \frac{1}{2}\sum_{\boldsymbol{k}} \Psi_{\boldsymbol{k}}^\dagger \begin{pmatrix} h_0(\boldsymbol{k}) & \Delta(\boldsymbol{k}) \\ \Delta(\boldsymbol{k})^\dagger & -h_0(-\boldsymbol{k})^* \end{pmatrix} \Psi_{\boldsymbol{k}} \tag{B.2}$$

where we have defined the Nambu spinor

$$\Psi_{\boldsymbol{k}} = \begin{pmatrix} a_{\boldsymbol{k}} & b_{\boldsymbol{k}} & a^{\dagger}_{-\boldsymbol{k}} & b^{\dagger}_{-\boldsymbol{k}} \end{pmatrix}^{T} \tag{B.3}$$

and

$$h_0(\boldsymbol{k}) = \begin{pmatrix} 2t\cos(k_y) + 4g\rho_b - \mu & -2t\cos(k_x) \\ -2t\cos(k_x) & -2t\cos(k_y) + 4g\rho_a - \mu \end{pmatrix}, \tag{B.4}$$

$$\Delta(\boldsymbol{k}) = \begin{pmatrix} 2i\Delta_a \sin(k_y) & 0 \\ 0 & 2i\Delta_b \sin(k_y) \end{pmatrix}. \tag{B.5}$$

Here, $\rho_{a,b}$ are the average densities on the a and b sites and $\Delta_{a,b} > 0$ the pair fields on the links connecting the a and b sites, respectively. As a BdG Hamiltonian, Eq. (B.2) automatically satisfies a particle-hole symmetry:

$$Ch(\boldsymbol{k})C^{-1} = -h(-\boldsymbol{k}) \tag{B.6}$$

with

$$C = K\sigma^0\tau^x \implies C^2 = 1. \tag{B.7}$$

Here, K is the complex conjugation operator, the σ^a, $a = 0, \ldots, 3$, are the Pauli matrices acting on the band index (with $\sigma^0 = 1$), and the τ^a are Pauli matrices acting on the particle-hole sector.

The Hamiltonian is also invariant under reflection about the y-axis, under which

$$\alpha_{x,y} \to \alpha_{-x,y} \implies \alpha_{k_x,k_y} \to \alpha_{-k_x,k_y} \quad (\alpha = a, b). \tag{B.8}$$

Eq. (B.2) thus satisfies the reflection symmetry

$$R^{-1}h(k_x, k_y)R = h(-k_x, k_y) \tag{B.9}$$

where, since we are dealing with spinless fermions, $R = 1$. Defining the composite operator [306] $\tilde{C} = RC$,

we have that

$$\tilde{C}^{-1}h(k_x,k_y)\tilde{C} = -h(k_x,-k_y). \tag{B.10}$$

Hence, for fixed k_x, $h(k_x,k_y)$ describes a *one-dimensional* (particle-hole symmetric) BdG Hamiltonian in symmetry class D, for which we can define the usual $\mathbb{Z}_2$ invariant, $\mathcal{M}(k_x) = \pm 1$ [146]. The nodal points of $h(k_x,k_y)$ then correspond to critical points separating regions in k_x space with different $\mathcal{M}(k_x)$. Since $\mathcal{M}(k_x)$ takes discrete values, this means the nodal points cannot be gapped out by (local) perturbations preserving reflection symmetry. Additionally, if one imposes open boundary conditions in the y-direction, a k_x point with $\mathcal{M}(k_x) = -1$ will possess a MZM. Hence, the regions in k_x space with $\mathcal{M}(k_x) = -1$ will yield the observed edge Majorana flat bands. We note that, although H_F also possesses a time-reversal symmetry, we restrict ourselves to a consideration of the C and P symmetries, as they are sufficient to protect the single pair of nodes and non-degenerate Majorana flat bands in the period-two stripe phases.

We can compute $\mathcal{M}(k_x)$ using the usual Pfaffian expression [146], which requires us to express Eq. (B.2) in a Majorana basis. Following [307], we can define Majorana operators as

$$\begin{pmatrix} \gamma^a_{\boldsymbol{k},1} \\ \gamma^b_{\boldsymbol{k},1} \\ \gamma^a_{\boldsymbol{k},2} \\ \gamma^b_{\boldsymbol{k},2} \end{pmatrix} = \sqrt{2}U\Psi_{\boldsymbol{k}}, \qquad U = \frac{1}{\sqrt{2}}\begin{pmatrix} \sigma^0 & \sigma^0 \\ -i\sigma^0 & i\sigma^0 \end{pmatrix} \tag{B.11}$$

where $\sigma^0 = 1$ acts on the band index. In the Majorana basis the BdG Hamiltonian takes the form

$$iA(\boldsymbol{k}) = Uh(\boldsymbol{k})U^\dagger, \tag{B.12}$$

where

$$A(\boldsymbol{k}) = \begin{pmatrix} 0 & q(\boldsymbol{k}) \\ -q^\dagger(\boldsymbol{k}) & 0 \end{pmatrix}, \quad q(\boldsymbol{k}) = h_0(\boldsymbol{k}) + \Delta(\boldsymbol{k}). \tag{B.13}$$

Note that $A(\boldsymbol{k})$ is antisymmetric for $k_y = 0, \pi$. We have that [146]

$$\mathcal{M}(k_x) = \mathrm{sgn}\left[\mathrm{Pf}(A(k_x, k_y = 0))\mathrm{Pf}(A(k_x, k_y = \pi))\right] \tag{B.14}$$

where $\mathrm{Pf}(M)$ is the Pfaffian of the antisymmetric matrix M. Explicitly,

$$\begin{aligned}\mathcal{M}(k_x) = &\mathrm{sgn}\left[(4t^2\cos^2 k_x + (2t - 4g\rho_b + \mu)(2t + 4g\rho_a - \mu))\right. \\ &\left.\times\ (4t^2\cos^2 k_x + (2t - 4g\rho_a + \mu)(2t + 4g\rho_b - \mu))\right].\end{aligned} \tag{B.15}$$

In Fig. 3.6c, we have plotted $\mathcal{M}(k_x)$ on top of the BdG spectra with periodic boundary conditions in both directions as a horizontal line at $E = 0$. when $\mathcal{M}(k_x) = -1\,(+1)$, the line is purple (yellow). We see that the changes in $\mathcal{M}(k_x)$ coincide exactly with the projected positions of the bulk nodes and the Majorana flat bands, shown in Fig. 3.6b, exist in regions with $\mathcal{M}(k_x) = -1$, up to energy splittings due to the finite size of the system.

B.2.2 Majorana Zero Modes at Lattice Dislocations

We claimed in the main text that the gapped stripe phase in the period two phase diagram (see Fig. 3.5) is a weak topological superconductor and hence lattice dislocations in this phase should trap MZMs. Although this is clear from the physical picture described in the main text, we can show this more formally, following Refs. [308,309]. Indeed, we first note that, following the discussion of the previous subsection, the particle-hole conjugation operator $C = K\sigma^0\tau^x$ maps the point $(k_x, k_y) = (\pi, k_y)$ in the Brillouin zone to $(k_x, k_y) = (\pi, -k_y)$. Hence, assuming only translation symmetry, $h(k_x = \pi, k_y)$ describes a one-dimensional BdG Hamiltonian in symmetry class D. Thus, even in the absence of reflection symmetry, we can then still define a $\mathbb{Z}_2$ invariant $\mathcal{M}(k_x = \pi) = \pm 1$. This integer defines a *weak* invariant, in that if it is non-trivial, then the two-dimensional superconductor is effectively described by an array of Kitaev chains stacked along the x-direction. From Fig. 3.6c, we see that the gapped stripe phase is indeed a weak topological superconductor of composite fermions. In particular, lattice dislocations corresponding to terminating one of these effective Kitaev chains in the bulk (i.e. dislocations with Burger's vector $\boldsymbol{e}_x$) will then trap a Majorana zero mode, as discussed in Refs. [308,309].

Appendix C

Supplement to Chapter 5

C.1 Derivation of the Bosonic Parent State from Intralayer Flux Attachment

Here we describe the intra-layer flux attachment procedure described in the main text, which yields the bosonic parent state depicted in Fig. 1(b) of the main text. We start again with a trilayer of free Dirac fermions near a $\nu = 2 \to 1$ plateau transition,

$$\mathcal{L}_{\text{IQH}} = \sum_{n=1}^{3} \left[\overline{\Psi}_n (i \not{D}_A - M) \Psi_n - \frac{3}{2} \frac{1}{4\pi} A dA \right] . \tag{C.1}$$

This theory is dual to a trilayer of Wilson-Fisher composite bosons, Φ_n, coupled to fluctuating CS gauge fields, α_n, [161, 162],

$$\mathcal{L}_{\text{IQH}}[A] \leftrightarrow \sum_n \mathcal{L}_n^{\Phi}[\Phi_n, \alpha_n, A] = \sum_n \left[|D_{\alpha_n} \Phi_n|^2 - r|\Phi_n|^2 - |\Phi_n|^4 + \frac{1}{4\pi} \alpha_n d\alpha_n + \frac{1}{2\pi} A d\alpha_n - \frac{1}{4\pi} A dA \right] , \tag{C.2}$$

where $-|\Phi|^4$ again denotes tuning such that the theory is at its Wilson-Fisher fixed point when $r = 0$, and the phase diagrams of the two theories match if $\text{sgn}(r) = -\text{sgn}(M)$.

We now attach a positive flux to the electric charges on layers $n = 1$ and 3 and a negative flux to those on layer $n = 2$. This is implemented in a manifestly gauge invariant way by the following transformation on each layer's Lagrangian [207, 208],

$$\mathcal{L}_n^{\Phi}[\Phi_n, \alpha_n, A] \to \mathcal{L}_n^{\Phi}[\Phi_n, \alpha_n, \gamma_n] + \frac{1}{2\pi} \gamma_n d\beta_n + \frac{(-1)^n}{4\pi} \beta_n d\beta_n + \frac{1}{2\pi} A d\beta_n, \tag{C.3}$$

where β_n, γ_n are new fluctuating $U(1)$ gauge fields. One can easily check that the electric charges in the gapped phases of this theory have had their statistics shifted by $\pm\pi$. Because the equation of motion for γ_n

is

$$d(\alpha_n + \beta_n) = d\gamma_n \,, \tag{C.4}$$

γ_n may be integrated out while preserving flux quantization. The resulting Lagrangian on each layer is

$$\mathcal{L}_n^\Phi \equiv |D_{\alpha_n}\Phi_n|^2 - r|\Phi_n|^2 - |\Phi_n|^4 + \frac{2}{4\pi}\alpha_n d\alpha_n + \frac{1}{4\pi}\left[1+(-1)^n\right]\frac{1}{4\pi}\beta_n d\beta_n + \frac{1}{2\pi}\alpha_n d\beta_n + \frac{1}{2\pi}A d\beta_n \,, \tag{C.5}$$

where we have redefined $\mathcal{L}_n^\Phi$ to minimize the number of labels in use. On layers $n = 1, 3$, the CS term for β_n vanishes. Integrating it out therefore Higgses α_n (in other words, sets $d\alpha_n = dA$), leaving a topologically trivial theory near a superconductor-insulator transition. On layer $n = 2$, however, the CS term for β_n has level 2, meaning that the gauge theory is topologically nontrivial and has the K-matrix of the Halperin (2,2,1) state. Explicitly, renaming $\alpha_2 \equiv \alpha, \beta_2 \equiv \beta$,

$$\mathcal{L}_p^\Phi = |D_A\Phi_p|^2 - r|\Phi_p|^2 - |\Phi_p|^4 + \frac{2}{4\pi}AdA \,,\ p = 1,3 \,; \tag{C.6}$$

$$\mathcal{L}_2^\Phi = |D_\alpha\Phi_2|^2 - r|\Phi_2|^2 - |\Phi_2|^4 + \frac{2}{4\pi}\alpha d\alpha + \frac{2}{4\pi}\beta d\beta + \frac{1}{2\pi}\alpha d\beta + \frac{1}{2\pi}\beta dA \,. \tag{C.7}$$

The trilayer theory, $\sum_n \tilde{\mathcal{L}}_n^\Phi$, is the theory depicted in Fig. 1(b) of the main text.

We now check that these theories are dual to theories of composite vortices, which on clustering yield the Fibonacci state. Applying the duality used in Eq. (5.2) of the main text along with the transformation flux attachment transformation in Eq. (C.3), the dual theories of composite vortices are

$$\begin{aligned}\tilde{\mathcal{L}}_n^\phi \leftrightarrow \tilde{\mathcal{L}}_p^\phi = {} & |D_a\phi_p|^2 - \tilde{r}|\phi_n|^2 - |\phi_n|^4 + \frac{1}{4\pi}\,\mathrm{Tr}\left[a_n da_n - \frac{2i}{3}a_n^3\right] \\ & + \frac{1}{2\pi}\gamma_n d\,\mathrm{Tr}[a_n] + \frac{1}{2\pi}\gamma_n d\beta_n + \frac{(-1)^n}{4\pi}\beta_n d\beta_n + \frac{1}{2\pi}A d\beta_n \,,\end{aligned} \tag{C.8}$$

where again a_n are $U(2)$ gauge fields. In this case, both γ_n and β_n can be safely integrated out without running afoul of flux quantization: integrating out γ_n implements a constraint on (i.e. Higgses) β_n, $d\beta_n = -d\,\mathrm{Tr}[a_n]$. The resulting theories involve $U(2)_{1,-1}$ gauge theories on layers $n = 1, 3$, which is topologically trivial [199], and a $U(2)_{1,3}$ theory on the $n = 2$ layer,

$$\tilde{\mathcal{L}}_n^\phi = |D_a\phi_p|^2 - \tilde{r}|\phi_n|^2 - |\phi_n|^4 + \frac{1}{4\pi}\,\mathrm{Tr}\left[a_n da_n - \frac{2i}{3}a_n^3\right] + (-1)^n\left[\frac{1}{4\pi}\,\mathrm{Tr}[a_n]d\,\mathrm{Tr}[a_n] + \frac{1}{2\pi}A d\,\mathrm{Tr}[a_n]\right] . \tag{C.9}$$

As in the discussion in the main text, we are free to invoke charge conjugation symmetry to flip the sign of the BF term on layer $n = 2$ relative to those on layers $1, 3$. From here, it is straightforward to see that a nonzero expectation value for the clustering order parameter, $\langle \Sigma_{mn} \rangle = \langle \phi_m^\dagger \phi_n \rangle \neq 0$, sets $a_1 = a_2 = a_3 \equiv a$ and produces the Fibonacci $U(2)_{3,1}$ TQFT,

$$\mathcal{L}_{\text{Fib}} = \frac{3}{4\pi} \operatorname{Tr}\left[a_n d a_n - \frac{2i}{3} a_n^3 \right] - \frac{1}{4\pi} \operatorname{Tr}[a]\, d \operatorname{Tr}[a] + \frac{1}{2\pi} A d \operatorname{Tr}[a]\,. \tag{C.10}$$

Integrating out the ϕ_n fields but leaving the Fibonacci order parameter thus leads to the final Landau-Ginzburg theory obtained in the main text,

$$\begin{aligned} \mathcal{L} = & \sum_{m,n} \operatorname{Tr}\left[|\partial \Sigma_{mn} - i a_m \Sigma_{mn} + i \Sigma_{mn} a_n|^2 \right] - V_r[\Sigma] \\ & + \sum_n \left[\mathcal{L}_{\text{CS}}[a_n] + (-1)^n \left(\frac{1}{4\pi} \operatorname{Tr}[a_n] d \operatorname{Tr}[a_n] + \frac{1}{2\pi} A d \operatorname{Tr}[a_n] \right) \right]. \end{aligned} \tag{C.11}$$

C.2 Representation of the Fibonacci order in terms of $U(2)_{3,1}$

In this section, we demonstrate explicitly that $U(2)_{3,1} = [SU(2)_3 \times U(1)_2]/\mathbb{Z}_2$ possesses the same anyon content as that of $(G_2)_1$, namely, just the Fibonacci anyon. There are multiple ways to describe the process of enforcing the $\mathbb{Z}_2$ quotient in the definition of $U(2)_{3,1}$. From the perspective of the anyon content of the theories, this quotient amounts to condensing [286] a bosonic anyon in the $SU(2)_3 \times U(1)_2$ product theory with $\mathbb{Z}_2$ fusion rules and either 0 or π braiding statistics with all other anyons. The condensed anyon is then identified as a local quasiparticle, and so all anyons with which it braids nontrivially are projected out. In order to identify the anyon to be condensed, let us remind ourselves of the anyon content of the $SU(2)_3$ and $U(1)_2$ factors:

$$U(1)_2 : \qquad 1,\ s \tag{C.12}$$

$$SU(2)_3 : \qquad [0],\ [1/2],\ [1],\ [3/2]. \tag{C.13}$$

Here, s is the semion, which has topological spin $h_s = 1/4$ and satisfies the fusion rule $s \times s = 1$. We have labelled the anyons of $SU(2)_3$ by the representation of $SU(2)$ under which they transform. They are all

self-dual, satisfying the fusion rules

$$[0] \times [0] = [0] \tag{C.14}$$

$$[1/2] \times [1/2] = [0] + [1] \tag{C.15}$$

$$[1] \times [1] = [0] + [1] \tag{C.16}$$

$$[3/2] \times [3/2] = [0]. \tag{C.17}$$

From this, we see that [1], which has spin $h_{[1]} = 2/5$, is the Fibonacci. The only Abelian anyon is [3/2], which has spin $h_{[3/2]} = 3/4$, trivial braiding with [1], and non-trivial braiding with [1/2]. We immediately see that, in the product theory, $[3/2]s$ is an Abelian anyon with spin unity. On condensing this anyon, all anyons aside from the Fibonacci will become confined, yielding the desired $(G_2)_1$ Fibonacci topological order.

C.3 Constructing the Electron Operators

As stated in the main text, the electron operators used in constructing the Fibonacci wave function must be selected from the generators of the $(G_2)_1$ current algebra. We present the technical details of this process here. The $(G_2)_1$ current algebra has fourteen generators, twelve of which are labeled by the roots of G_2. In order to obtain explicit expressions for these operators, we make use of the duality between $(G_2)_1$ and $U(2)_{3,1} = [SU(2)_3 \times U(1)_2]/\mathbb{Z}_2$, which will allow us to write the generators in terms of operators in the $SU(2)_3$ and $U(1)_2$ conformal field theories (CFTs).

The $U(1)_2$ factor is described by a chiral boson, φ, with compactification radius $R = 1$. It supports a single anyon, the semion, represented by the vertex operator

$$s(z) \equiv e^{i\varphi(z)/\sqrt{2}}, \tag{C.18}$$

which has scaling dimension $\Delta_s = 1/4$. The operators $s^2 = e^{i\sqrt{2}\varphi}$ and $\overline{s}^2 = e^{-i\sqrt{2}\varphi}$ generate the $U(1)_2$ chiral algebra, and so correspond to local excitations.

As for $SU(2)_3$, its primary fields, like the anyons in the corresponding TQFT, fall into four topological sectors labelled by the $SU(2)$ representation under which they transform: $[j]$, $j = 0, 1/2, 1, 3/2$. In order to write down explicit forms of these fields and the current operators, we make use of the fact that the operators of $SU(2)_3$ can be expressed in terms of products of operators in the $k = 3$ parafermion and $U(1)_6$ CFTs, the former of which we will write as Parafermion$_3$. The $U(1)_6$ CFT is described by a chiral boson ϕ

at radius $R = 1$, with primary fields

$$a^l(z) \equiv e^{il\phi/\sqrt{6}}, \quad l = 0, \ldots, 5 \tag{C.19}$$

These fields have scaling dimensions $\Delta_l = l^2/12$, from which we see that the field a^6 represents a local excitation. The primary fields of the Parafermion$_3$ CFT and their scaling dimensions are given in Table C.1 while their fusion rules are given in Table C.2. The raising and lowering operators of the $SU(2)_3$ algebra are given by the operators,

$$\psi_1 a^2 = \psi_1 e^{i\sqrt{2/3}\phi}, \quad \psi_1^\dagger \overline{a}^2 = \psi_2 e^{-i\sqrt{2/3}\phi}. \tag{C.20}$$

Table C.1: Scaling dimensions of the Parafermion$_3$ primary fields.

	1	ψ_1	ψ_2	σ_1	σ_2	ϵ
Δ	0	$2/3$	$2/3$	$1/15$	$1/15$	$2/5$

Table C.2: Fusion rules of Parafermion$_3$.

$\times$	ψ_1	ψ_2	σ_1	σ_2	ϵ
ψ_1	ψ_2				
ψ_2	1	ψ_1			
σ_1	ϵ	σ_2	$\sigma_2 + \psi_1$		
σ_2	σ_1	ϵ	$1 + \epsilon$	$\sigma_1 + \psi_2$	
ϵ	σ_2	σ_1	$\sigma_1 + \psi_2$	$\sigma_2 + \psi_1$	$1 + \epsilon$

Now, in order to obtain the $(G_2)_1$ algebra from $SU(2)_3 \times U(1)_2$, we must perform the $\mathbb{Z}_2$ quotient. As in the TQFT description, this corresponds to condensing operators in the

$$\left[\frac{3}{2}\right] s \tag{C.21}$$

topological sectors. In the language of CFT, this "condensation" means that the operators in these topological sectors will be identified as generators of the $[SU(2)_3 \times U(1)_2]/\mathbb{Z}_2$ (equivalently, $(G_2)_1$) CFT. Explicitly, the operators

$$\overline{a}^3, \quad \psi_1 \overline{a}, \quad \psi_2 a, \quad a^3 \tag{C.22}$$

are all in the $[3/2]$ sector, and so are topologically equivalent. Indeed, each is related to the other by fusion with the $SU(2)_3$ generators, forming an $SU(2)_3$ quartet. Hence, performing the $\mathbb{Z}_2$ quotient means

condensing the operators

$$\begin{array}{cccc} \overline{a}^3 s, & \psi_1 \overline{a} s, & \psi_2 a s, & a^3 s \\ \overline{a}^3 \overline{s}, & \psi_1 \overline{a s}, & \psi_2 a \overline{s}, & a^3 \overline{s} \end{array} \tag{C.23}$$

This set of operators, combined with the generators of $SU(2)_3$ and $U(1)_2$ constitute the twelve generators of $(G_2)_1$ labelled by its roots [310].

Fig. C.1 depicts the G_2 root system labeled by the corresponding current generators. One can check that vector addition of the roots matches up with fusion of the corresponding current operators. Note also that the generators naturally organize themselves in terms of their transformation properties under $SU(2)$ and $U(1)$. The vertical coordinate of the root corresponds to the $U(1)$ charge and the horizontal coordinate to the $SU(2)$ spin.

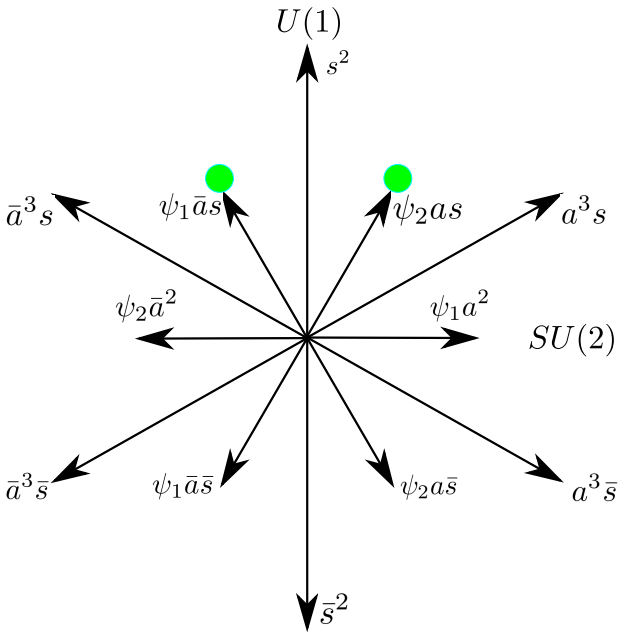

Figure C.1: Root system of G_2 labelled by the corresponding $(G_2)_1$ current generators. The green circles indicate the operators we identify as the electron operators.

It now remains to determine which generators we should identify as the physical electrons. In the spirit of Refs. [69, 214], we expect that we must choose two electron operators, by virtue of the fact that the root system is two-dimensional. The electrons should have the same positive charge, suggesting we should restrict ourselves to the upper half-plane of the root system. As described in the main text, we expect the Fibonacci wave function to describe a two-flavor system, and so the electron operators should have opposite $SU(2)$

spin. We thus claim that

$$\begin{aligned}\Psi_\uparrow &\equiv \psi_2 as = \psi_2 e^{i\phi/\sqrt{6}+i\varphi/\sqrt{2}},\\ \Psi_\downarrow &\equiv \psi_1 \overline{a} s = \psi_2 e^{-i\phi/\sqrt{6}+i\varphi/\sqrt{2}}\end{aligned} \tag{C.24}$$

are the appropriate electron operators.

We note that operators $\overline{a}^3 s$ and $a^3 s$ also satisfy our two criteria for charge and spin. In fact, $\Psi_\uparrow$ and $\Psi_\downarrow$ form an $SU(2)$ quartet with $\overline{a}^3 s$ and $a^3 s$ (as can be seen from Fig. C.1), and so one may reasonably ask whether the latter two operators constitute equally valid choices for the electron operator. As it turns out, the wave function obtained from $\overline{a}^3 s$ and $a^3 s$ describes an *Abelian* state, as we demonstrate in the following section. This suggests, *a posteriori*, that $\Psi_{\uparrow/\downarrow}$ are the correct electron operators needed to obtain a wave function describing the non-Abelian Fibonacci state.

C.4 Derivation of the Fibonacci Wave Function

In this section, we present a computation of the explicit form of the Fibonacci wave function provided in the main text. With the choice of electron operators given in Eq. (C.24), we can express the wave function as

$$\Psi(\{z_i, w_i\}) = \langle \prod_{i=1}^{N} \Psi_\uparrow(z_i)\Psi_\downarrow(w_i) O_{bg}\rangle = \langle \prod_{i=1}^{N} \psi_2 as(z_i)\psi_1 \overline{a} s(w_i) O_{bg}\rangle, \tag{C.25}$$

where z_i and w_i label the positions of the up and down spins (spin is used as a stand-in for some flavor index). Here O_{bg} is a background charge operator that ensures the correlator of the s fields is non-vanishing and yields the usual Gaussian factor on the plane [212]. Note that such an operator for the a fields is *not* necessary, since there are an equal number of a and $\overline{a}$ fields, ensuring their charge neutrality condition is satisfied. Physically, this is a consequence of the fact that it is the $U(1)_2$ sector and hence the s fields which are charged under the external electromagnetic field. We thus obtain (dropping the usual overall Gaussian factor),

$$\Psi(\{z_i, w_i\}) = \langle \prod_{i=1}^{N} \psi_2(z_i)\psi_1(w_i)\rangle \langle \prod_{i=1}^{N} e^{i\frac{1}{\sqrt{6}}\phi(z_i)} e^{-i\frac{1}{\sqrt{6}}\phi(w_i)}\rangle \langle \prod_{i=1}^{N} e^{i\frac{1}{\sqrt{2}}\varphi(z_i)} e^{i\frac{1}{\sqrt{2}}\varphi(w_i)} O_{bg}\rangle \tag{C.26}$$

$$= \langle \prod_{i=1}^{N} \psi_2(z_i)\psi_1(w_i)\rangle \prod_{i,j}(z_i - w_i)^{1/3} \prod_{i<j}(z_i - z_j)^{2/3} \prod_{i<j}(w_i - w_j)^{2/3}. \tag{C.27}$$

In order to evaluate the remaining correlator, we can use the parafermion operator product expansions (OPEs),

$$\begin{aligned}\psi_1(z)\psi_1(z') &\sim (z-z')^{-2/3}\psi_2(z') + \dots \text{ (likewise for } 1 \leftrightarrow 2)\\ \psi_1(z)\psi_2(z') &\sim (z-z')^{-4/3} + \dots .\end{aligned} \tag{C.28}$$

to effectively point-split the ψ_2 operators into products of ψ_1 operators:

$$\langle \prod_{i=1}^{N} \psi_1(z_i^1)\psi_1(z_i^2)\psi_1(w_i)\rangle = \langle \prod_{i=1}^{N} (z_i^1 - z_i^2)^{-2/3}\psi_2(z_i^2)\psi_1(w_i)\rangle + \dots , \tag{C.29}$$

where, here and in the following, the limit $z_i^1 \to z_i^2$ is taken implicitly. The ellipsis represent less singular terms in the $\psi_1 \times \psi_1$ OPE which vanish in this limit, allowing us to isolate the desired parafermion correlator when we take $z_i^1 = z_i^2 \equiv z_i$ at the end of the computation.

Now, the correlator of ψ_1 fields is precisely given in terms of the Read-Rezayi (RR) wave functions:

$$\langle \prod_{i=1}^{N} \psi_1(z_i^1)\psi_1(z_i^2)\psi_1(w_i)\rangle = \Psi_{RR}^{k=3}(\{z_i^1, z_i^2, w_i\})\Psi_{LJ}^{-2/3}(\{z_1^1, z_i^2, w_i\}). \tag{C.30}$$

Here, $\Psi_{RR}^{k=3}$ and $\Psi_{LJ}(\{z_i\}) = \prod_{i<j}(z_i - z_j)$ are the $\nu = 3/2$ bosonic RR (taking $k = 3$ and $M = 0$ in the notation of Ref. [65]) and Landau-Jastrow wave functions, respectively. Hence,

$$\langle \prod_{i=1}^{N} \psi_2(z_i^2)\psi_1(w_i)\rangle + \dots = \Psi_{RR}^{k=3}(\{z_i^1, z_i^2, w_i\})\Psi_{LJ}^{-2/3}(\{z_1^1, z_i^2, w_i\}) \prod_{i=1}^{N}(z_i^1 - z_i^2)^{2/3} \tag{C.31}$$

$$\begin{aligned} &= \Psi_{RR}^{k=3}(\{z_i^1, z_i^2, w_i\}) \prod_{i<j}(z_i^1 - z_j^1)^{-2/3}(z_i^2 - z_j^2)^{-2/3}(w_i - w_j)^{-2/3} \\ &\quad \times \prod_{i\neq j}(z_i^1 - z_j^2)^{-2/3} \prod_{i,j}(z_i^1 - w_j)^{-2/3}(z_i^2 - w_j)^{-2/3}. \end{aligned} \tag{C.32}$$

We can now safely set $z_i^1 = z_i^2 \equiv z_i$, in which case the terms contained in the ellipsis vanish identically. Combining terms and ignoring unimportant overall phase factors, we obtain

$$\Psi(\{z_i, w_i\}) = \Psi_{RR}^{k=3}(\{z_i, z_i, w_i\}) \prod_{i<j}(z_i - z_j)^{-2} \prod_{i,j}(z_i - w_j)^{-1} \tag{C.33}$$

as our Fibonacci wave function. Here, $\Psi_{RR}^{k=3}(\{z_i, z_i, w_i\})$ is the bosonic $\nu = 3/2$ RR wave function for $3N$ particles, with the coordinates of N pairs of these particles set equal to one another. As noted in the main text, the asymmetry in z_i and w_i is a consequence of having point-split the ψ_2 parafermions as opposed

to the ψ_1 parafermions. Had we instead point-split the ψ_1 parafermions into products of ψ_2 parafermions, we would have obtained the above expression with z_i and w_i exchanged. Since the expressions obtained via these two different point-splitting procedures must necessarily be equal, we can write down the wave function in a manifestly symmetric way by taking their average:

$$\Psi(\{z_i, w_i\}) = \frac{1}{2}\left(\frac{\Psi_{RR}^{k=3}(\{z_i, z_i, w_i\})}{\prod_{i<j}(z_i - z_j)^2} + \frac{\Psi_{RR}^{k=3}(\{z_i, w_i, w_i\})}{\prod_{i<j}(w_i - w_j)^2}\right)\prod_{i,j}(z_i - w_j)^{-1}. \tag{C.34}$$

Finally, we return to the remark regarding the choice of electron operators made at the end of the preceding section. Had we instead attempted to construct a wave function using $\Psi_{\uparrow\uparrow} = a^3 s$ and $\Psi_{\downarrow\downarrow} = \overline{a}^3 s$ as the electron operators, we would have obtained

$$\tilde{\Psi}(\{z_i, w_i\}) = \langle \prod_{i=1}^{N} \Psi_{\uparrow\uparrow}(z_i)\Psi_{\downarrow\downarrow}(w_i) O_{bg}\rangle = \langle \prod_{i=1}^{N} e^{i\sqrt{\frac{3}{2}}\phi(z_i)} e^{-i\sqrt{\frac{3}{2}}\phi(w_i)}\rangle \langle \prod_{i=1}^{N} e^{i\frac{1}{\sqrt{2}}\varphi(z_i)} e^{i\frac{1}{\sqrt{2}}\varphi(w_i)} O_{bg}\rangle\,. \tag{C.35}$$

The correlators of vertex operators can be straightforwardly evaluated to obtain

$$\tilde{\Psi}(\{z_i, w_i\}) = \prod_{i<j}(z_i - z_j)^2 (w_i - w_j)^2 \prod_{i,j}(z_i - w_j)^{-1}, \tag{C.36}$$

which describes the *Abelian* Halperin $(2, 2, -1)$ state, again at filling $\nu = 2$. This gives us some confidence that $\Psi(\{z_i, w_i\})$ correctly describes the Fibonacci state.

Appendix D

Supplement to Chapter 6

D.1 Details of $U(N)$ Fermion-Fermion Duality Examples

In this Appendix we provide the details of the analysis outlined in Section 6.3.6. We begin by deriving the duality between Eq. (6.27) and Eq. (6.28) and then identify the states listed in Table 6.3.

D.1.1 Derivation of the Duality

As noted in Section 6.3.6, the fermionic theories **Theory A′** and **Theory B′** are both dual to the bosonic Landau-Ginzburg theory for the $\nu = 1/k$ Laughlin state, which is described by the Lagrangian

$$\mathcal{L}_\Phi(k) = |D_b\Phi|^2 - |\Phi|^4 + \frac{k}{4\pi} bdb + \frac{1}{2\pi} bdA. \tag{D.1}$$

Here, Φ is a complex scalar field, b is a $U(1)$ gauge field, and A is the external electromagnetic field. It is straightforward to see that one obtains the Laughlin state when Φ is gapped by a mass and a trivial insulator when Φ condenses.

In order to derive these dualities, we take as our starting point the SU/U duality of Eq. (6.3),

$$|D_A\Phi|^2 - |\Phi|^4 \longleftrightarrow i\overline{\eta}\not{D}_u\eta - \frac{1/2}{4\pi}\,\mathrm{Tr}\left[udu - \frac{2i}{3}u^3\right] - \frac{1}{2\pi}\,\mathrm{Tr}[u]dA - \frac{N}{4\pi}AdA, \quad a \in U(N), \tag{D.2}$$

where u is a $U(N)$ gauge field and η is a fermion in the fundamental representation of $U(N)$. Note that the rank N can be an *arbitrary* integer, and so the above equation implies that the Wilson-Fisher theory is dual to an infinite number of fermionic $U(N)$ gauge theories. Now, one can derive new dualities from old ones by applying the modular transformations [208]

$$\mathcal{S} : \mathcal{L}[A] \mapsto \mathcal{L}[b] + \frac{1}{2\pi}Adb\,, \qquad \mathcal{T} : \mathcal{L}[A] \mapsto \mathcal{L}[A] + \frac{1}{4\pi}AdA\,, \tag{D.3}$$

to both sides of a duality, where again A is the background EM field and b is a new dynamical $U(1)$ gauge

field. Here, $\mathcal{S}$ is the operation of promoting a background gauge field to a dynamical one, while $\mathcal{T}$ corresponds to the addition of a Landau level. Applying $\mathcal{S}\mathcal{T}^k$ to the SU/U duality yields,

$$\mathcal{L}_\Phi(k) \longleftrightarrow i\bar{\eta}\not{D}_u\eta - \frac{1/2}{4\pi}\,\mathrm{Tr}\left[udu - \frac{2i}{3}u^3\right] - \frac{1}{2\pi}\,\mathrm{Tr}[u]db - \frac{N-k}{4\pi}bdb + \frac{1}{2\pi}bdA = \mathcal{L}_{B'}(k,N)\,. \tag{D.4}$$

On the other hand, we can also consider the Abelian bosonization duality [161, 162],

$$|D_A\Phi|^2 - |\Phi|^4 \longleftrightarrow i\overline{\psi}\not{D}_a\psi - \frac{1}{2}\frac{1}{4\pi}ada + \frac{1}{2\pi}adA - \frac{1}{4\pi}AdA\,, \tag{D.5}$$

where a is an emergent $U(1)$ gauge field and ψ a Dirac fermion. Applying $\mathcal{S}\mathcal{T}^k$ to this duality, we find

$$\mathcal{L}_\Phi(k) \longleftrightarrow i\overline{\psi}\not{D}_a\psi - \frac{1}{2}\frac{1}{4\pi}ada + \frac{1}{2\pi}adv + \frac{k-1}{4\pi}vdv + \frac{1}{2\pi}vdA = \mathcal{L}_{A'}(k). \tag{D.6}$$

We thus arrive at the desired dualities

$$\mathcal{L}_{A'}(k) \longleftrightarrow \mathcal{L}_\Phi(k) \longleftrightarrow \mathcal{L}_{B'}(k,N). \tag{D.7}$$

We emphasize that these dualities hold true for any value of the rank, $N > 0$, of the gauge group $U(N)$ of **Theory B′**.

D.1.2 Examples Involving Gapless States

Let us now investigate the states predicted by the dual theories, **Theory A′** and **Theory B′**, at fractional electronic filling fractions, following the logic in our study of the dual fermionic theories in the $SU(2)$ quadrality in Section 6.3. We define the filling fraction of the ψ composite fermions as

$$\nu_\psi = \frac{2\pi\langle\psi^\dagger\psi\rangle}{\langle\varepsilon^{ij}\partial_i a_j\rangle}. \tag{D.8}$$

Using the equations of motion of $\mathcal{L}_{A'}$, we find the following relationship between the electronic and ψ filling fractions

$$\nu_\psi = \frac{1}{2} + \frac{1}{-1/\nu + (k-1)} \iff \nu = \frac{2\nu_\psi - 1}{2(k-1)\nu_\psi - k - 1}. \tag{D.9}$$

As for the composite fermions of the non-Abelian **Theory B′**, to define the η filling fraction, we first decompose the $U(N)$ gauge field as $u = u_{SU(N)} + \tilde{u}\mathbf{1}$, where $\mathbf{1}$ is the $N \times N$ identity matrix, $\tilde{u}$ is a $U(1)$

gauge field, and $u_{SU(N)}$ is an $SU(N)$ gauge field. In the presence of a non-zero $U(1)$ flux, $\langle \varepsilon^{ij}\partial_i \tilde{u}_j\rangle$, the η fermion Landau level degeneracy is given by

$$d_{LL} = \frac{\langle \varepsilon^{ij}\partial_i \tilde{u}_j\rangle A}{2\pi} \times (\text{color degeneracy}) \times (\text{charge}) = \frac{\langle \varepsilon^{ij}\partial_i \tilde{u}_j\rangle A}{2\pi} \times N \times 1 = \frac{N\langle \varepsilon^{ij}\partial_i \tilde{u}_j\rangle A}{2\pi}. \tag{D.10}$$

Hence, the η fermion filling fraction is given by[1]

$$\nu_\eta = -\frac{2\pi\langle \eta^\dagger \eta\rangle}{N\langle \varepsilon^{ij}\partial_i \tilde{u}_j\rangle}. \tag{D.11}$$

Using the equations of motion of $\mathcal{L}_{B'}$, we find

$$\nu_\eta = -\frac{1}{2} + \frac{N}{1/\nu + N - k} \iff \nu = \frac{2\nu_\eta + 1}{2(k-N)\nu_\eta + (k+N)}. \tag{D.12}$$

Let us suppose the ψ fermions fill up an integer number of LLs, so that $\nu_\psi = p - 1/2$. Then, from Eq. (D.9), we have

$$\nu = \frac{p-1}{(p-1)(k-1)-1}, \tag{D.13}$$

which is simply the Jain sequence of states.

We are interested in seeing whether a gapped state of the ψ fermions ever corresponds to a metallic state of the η fermions (i.e. with $\nu_\eta \to \infty$). From Eq. (D.12), we see that the η fermions form a metallic state when $1/\nu = -N + k \in \mathbb{Z}$. We must therefore look for solutions of the equation

$$k - 1 - (p-1)^{-1} = -N + k. \tag{D.14}$$

The only valid solution with $N > 0$ is $(N, p) = (2, 2)$. So, when $N = 2$ and the ψ fermions fill the $p = 2$ Landau level, the η fermions form a metallic state. The electronic filling fraction is $\nu_* = 1/(k-2)$. At this filling, we can integrate out the ψ fermions in **Theory A′** to obtain the effective action

$$\mathcal{L}_{A',\text{eff}} = \frac{k-2}{4\pi} v dv + \frac{1}{2\pi} v dA\,. \tag{D.15}$$

We thus have two cases to consider: $k = 2$ and $k \neq 2$. When $k = 2$, **Theory A′** yields the usual dual theory for a superfluid (recall that there is an implicit Maxwell term in the action for c). This is not surprising,

[1] We add the minus sign for consistency with the definition of the χ filling fraction ν_χ of Eq. (6.19) when $N = k = 2$.

as the filling fraction of the electrons (which are bosons for $k = 2$) is $\nu = \infty$, which is to say they see no magnetic field. Hence, for $k = 2$, both **Theory A′** and **Theory B′** predict compressible states. In contrast, for $k \neq 2$, **Theory A′** describes the incompressible $\nu = 1/(k-2)$ Laughlin state, while **Theory B′** again describes a metallic state of the η fermions.

Let us now consider the inverse scenario in which the η fermions fill an integer number of LLs, so that $\nu_\eta = s - 1/2$. Hence,

$$\nu = \frac{s}{s(k-N)+N}, \tag{D.16}$$

From Eq. (D.9), we see that the ψ-fermions are in a metallic state when $1/\nu = k - 1$. This implies

$$\frac{s-1}{s} = N > 0, \tag{D.17}$$

for which the only solution is $(N, s) = (2, 2)$. In this case, the electronic filling fraction is $\nu_* = 1/(k-1)$. This simply corresponds to the usual sequence of incompressible states for the fermionic (k odd) and bosonic (k even) Jain sequences. At these fillings, we can integrate out the η fermions in **Theory B′** to obtain the effective action

$$\mathcal{L}_{B',\text{eff}} = \frac{-2}{4\pi}\,\text{Tr}\left[udu - \frac{2i}{3}u^3\right] + \frac{k-2}{4\pi}bdb - \frac{1}{2\pi}\,\text{Tr}[u]db + \frac{1}{2\pi}bdA\,, \tag{D.18}$$

describing a non-Abelian topological order. Specifically, this is the Lagrangian for the $[U(2)^{\text{spin}}_{-2}\times U(1)_{4(k-1)}]/\mathbb{Z}_2$ $\leftrightarrow [SU(2)_2 \times U(1)_{4(k-1)}]/\mathbb{Z}_2 = U(2)_{2,2(k-1)}$ Chern-Simons theory.

In order to understand how one arrives at this identification of the Lagrangian as that for a quotient theory, let us start with a decoupled $U(2)^{\text{spin}}_{-2} \times U(1)_{4(k-1)}$ Chern-Simons theory:

$$\mathcal{L} = \frac{-2}{4\pi}\,\text{Tr}\left[\widehat{u}d\widehat{u} - \frac{2i}{3}\widehat{u}^3\right] + \frac{4(k-1)}{4\pi}\widehat{b}d\widehat{b} + \frac{2}{2\pi}\widehat{b}dA\,. \tag{D.19}$$

Now, taking the $\mathbb{Z}_2$ quotient of this theory amounts to declaring that $\widehat{u}$ and $\widehat{b}$ are no longer "good" gauge fields but the linear combinations

$$u = \widehat{u} - \widehat{b}\mathbf{1} \tag{D.20}$$

$$b = 2\widehat{b} \tag{D.21}$$

are [143]. That is to say, we declare u and b to satisfy the appropriate flux quantization conditions. In more

formal terms, taking the $\mathbb{Z}_2$ quotient means we gauge the common $\mathbb{Z}_2$ one-form symmetry of the $U(2)^{\text{spin}}_{-2}$ and $U(1)_{4(k-1)}$ factors [143, 217] (which is to say, we project out all Wilson lines which have non-trivial braiding with respect to the Wilson line generating the $\mathbb{Z}_2$ one-form symmetry). Rewriting $\mathcal{L}$ in terms of these gauge fields, we arrive at Eq. (D.18), as desired.

D.1.3 Examples Involving Gapped States

Lastly, we can look for filling fractions at which both the ψ and η fermions form IQH states. Setting Eqs. (D.13) and (D.16) equal to one another, we find that this happens when

$$N = \frac{s}{s-1}\frac{p}{p-1} \tag{D.22}$$

The topological orders predicted by **Theory A′** and **Theory B′** at these filling fractions are described by, respectively, the low energy actions

$$\mathcal{L}_{A',\text{eff}} = \frac{p-1}{4\pi} ada + \frac{1}{2\pi} adv + \frac{k-1}{4\pi} vdv + \frac{1}{2\pi} vdA\,, \tag{D.23}$$

$$\mathcal{L}_{B',\text{eff}} = -\frac{s}{4\pi}\,\text{Tr}\left[udu - \frac{2i}{3}u^3\right] + \frac{k-2}{4\pi} bdb - \frac{1}{2\pi}\,\text{Tr}[u]db + \frac{1}{2\pi} bdA\,. \tag{D.24}$$

One integer solution to the above equation is given by $(s, p, N) = (3, 4, 2)$, corresponding to an electronic filling fraction of $\nu_* = 3/(3k-4)$. Here, **Theory A′** predicts a $U(1)^{\text{spin}} \times U(1)$ theory (note a is a spin_c connection while v is a regular gauge field) describing the Abelian Jain state at $\nu_* = 2k/(2k-3)$. Using the same quotient construction as in the previous subsection, we can see that **Theory B′** describes a $[U(2)^{\text{spin}}_{-3} \times U(1)_{3(3k-4)}]/\mathbb{Z}_3 \leftrightarrow [SU(3)_2 \times U(1)_{3(3k-4)}]/\mathbb{Z}_3 = U(3)_{2,3k-4}$ topological order. A second integer solution is given by $(s, p, N) = (4, 3, 2)$, corresponding to an electronic filling fraction of $\nu_* = 2/(2k-3)$. **Theory A′** again predicts an Abelian Jain state, whereas **Theory B′** predicts a non-Abelian $[U(2)^{\text{spin}}_{-4} \times U(1)_{8(2k-3)}]/\mathbb{Z}_4 \leftrightarrow [SU(4)_2 \times U(1)_{8(2k-3)}]/\mathbb{Z}_4 = U(4)_{2,2(2k-3)}$ topological order.

Appendix E

Supplement to Chapter 7

E.1 Modular Functions

In this appendix we collect the definitions and basic properties of the θ and η functions. First, we introduce the notation

$$q = e^{2\pi i \tau}, \tag{E.1}$$

where $\tau \in \mathbb{C}$ is the modular parameter. The Dedekind η function is defined as

$$\eta(\tau) = q^{1/24} \prod_{n=1}^{\infty} (1 - q^n). \tag{E.2}$$

Under modular transformations, the η function satisfies

$$\eta(\tau + 1) = e^{\pi i/12} \eta(\tau), \tag{E.3}$$

$$\eta(-1/\tau) = \sqrt{-i\tau}\, \eta(\tau). \tag{E.4}$$

We also make use of the θ functions,

$$\theta^{\alpha}_{\beta}(\tau) = \sum_{n \in \mathbb{Z}} q^{\frac{1}{2}(n+\alpha)^2} e^{2\pi i (n+\alpha)\beta}. \tag{E.5}$$

Under modular transformations, these functions satisfy

$$\theta^{\alpha}_{\beta}(\tau + 1) = e^{-\pi i \alpha(\alpha - 1)} \theta^{\alpha}_{\alpha+\beta-\frac{1}{2}}(\tau), \tag{E.6}$$

$$\theta^{\alpha}_{\beta}(-1/\tau) = \sqrt{-i\tau}\, e^{2\pi i \alpha\beta} \theta^{\beta}_{-\alpha}(\tau). \tag{E.7}$$

The standard Jacobi θ functions (see, for instance, Ref. [311]) can be expressed in terms of these more general functions:

$$\theta_2(\tau) = \sum_{n\in\mathbb{Z}} q^{(n+1/2)^2/2} = \theta_0^{1/2}(\tau), \tag{E.8}$$

$$\theta_3(\tau) = \sum_{n\in\mathbb{Z}} q^{n^2/2} = \theta_0^0(\tau), \tag{E.9}$$

$$\theta_4(\tau) = \sum_{n\in\mathbb{Z}} (-1)^n q^{n^2/2} = \theta_{1/2}^0(\tau). \tag{E.10}$$

Lastly, we note that for $\tau = i\tau_2$, with $\tau_2 \in \mathbb{R}^+$, we have that

$$\lim_{\tau_2\to\infty} \eta(\tau) = q^{1/24}\,. \tag{E.11}$$

$$\lim_{\tau_2\to\infty} \theta_\beta^\alpha(\tau) = \delta_{\alpha,0}\,. \tag{E.12}$$

E.2 Details of Projected Ground States

E.2.1 Untwisted Sectors

For completeness, we can write down the explicit form of the ground state in, say, the $e^{ir\phi}$ sector:

$$|\psi_{e^{ir\phi}}\rangle = P_{e^{ir\phi},B}\,|\widehat{\psi}_{e^{ir\phi}}\rangle = |\psi_{e^{ir\phi},1}\rangle \otimes |\psi_{e^{ir\phi},2}\rangle\,, \tag{E.13}$$

where we made use of Eq. (7.80). Following Section 7.3.1, we further rewrite $P_{e^{ir\phi},B} = P_{e^{ir\phi},RB}P_{e^{ir\phi},LB}$ so that we can express the exact interface ground states as

$$|\psi_{e^{ir\phi},1}\rangle = P_{e^{ir\phi},RB}\,|\widehat{\psi}_{e^{ir\phi},1}\rangle = \frac{1}{2}(1+(-1)^{F_{RB}}(-1)^{N_{RB}+r/n})\,|\widehat{\psi}_{e^{ir\phi},1}\rangle\,, \tag{E.14}$$

$$|\psi_{e^{ir\phi},2}\rangle = P_{e^{ir\phi},LB}\,|\widehat{\psi}_{e^{ir\phi},2}\rangle = \frac{1}{2}(1+(-1)^{F_{LB}}(-1)^{N_{LB}-r/n})\,|\widehat{\psi}_{e^{ir\phi},2}\rangle\,. \tag{E.15}$$

As is evident from the above expression, the effect of the projection on, say, $|\widehat{\psi}_{e^{ir\phi},1}\rangle$, is to annihilate all states not satisfying $(-1)^{F_{RB}}(-1)^{N_{RB}+r/n} = 1$. As discussed in the main text, the form of $|\widehat{\psi}_{e^{ir\phi},1}\rangle$ is such that the remainig states will also satisfy $(-1)^{F_{LA}}(-1)^{N_{LA}-r/n} = 1$. Analogous statements hold for the action of the projection on $|\widehat{\psi}_{e^{ir\phi},2}\rangle$. Note that these expressions for the projections require that $|\widehat{\psi}_{e^{ir\phi},1/2}\rangle$ already

obey the correct quantization of the winding numbers, $N_{\mu B}$ for sector $e^{ir\phi}$. Explicitly, we can write

$$|\psi_{e^{ir\phi},1}\rangle = \frac{1}{2}\Bigg[|G_{b,\mathrm{osc},1}\rangle \otimes \sum_{N\in\mathbb{Z}-\frac{r}{n}} e^{-\frac{v_e\pi n N^2}{2L}} |N_{RB}=N\rangle\,|N_{LA}=-N\rangle \otimes \prod_{k>0}\left(1+ie^{-\tilde{v}_e k/2}d^\dagger_{-k}c^\dagger_k\right)|0\rangle$$
$$+\,|G_{b,\mathrm{osc},1}\rangle \otimes \sum_{N\in\mathbb{Z}-\frac{r}{n}} (-1)^{N+\frac{r}{n}} e^{-\frac{v_e\pi n N^2}{2L}} |N_{RB}=N\rangle\,|N_{LA}=-N\rangle \otimes \prod_{k>0}\left(1-ie^{-\tilde{v}_e k/2}d^\dagger_{-k}c^\dagger_k\right)|0\rangle\Bigg], \tag{E.16}$$

with $|\psi_{e^{ir\phi},2}\rangle$ taking a similar form. Focusing on the explicit expression for $|\psi_{e^{ir\phi},1}\rangle$, we see that every state appearing in the second line of Eq. (E.16) with $(-1)^{F_{RB}}(-1)^{N_{RB}+r/n}=-1$ will indeed cancel with a corresponding state in the first line.

E.2.2 Twisted Sectors

Ground State

We present here the explicit form of the approximated ground state in the $a=\sigma e^{i(r+1/2)\phi}$ sector:

$$|\psi_a\rangle = P_B\,|\widehat{\psi}_a\rangle = \frac{1}{2}(1+(-1)^{F_B}(-1)^{N_{RB}+N_{LB}})\,|\widehat{\psi}_a\rangle\,, \tag{E.17}$$

where we used Eq. (7.106) to write $P\,|\widehat{\psi}_a\rangle = P_B\,|\widehat{\psi}_a\rangle$. As in the untwisted sector case of the previous subsection, we made use of the fact that all the states appearing in $|\widehat{\psi}_a\rangle$ obey the correct quantization of the winding modes, $N_{\mu\alpha}$, appropriate to the $a=\sigma e^{i(r+1/2)\phi}$ sector to write down a closed form expression for $P_B\,|\widehat{\psi}_a\rangle$. The effect of the projection is to annihilate all states not satisfying $(-1)^{F_B}(-1)^{N_{RB}+N_{LB}}=1$. Again, as discussed in the main text, the remaining states will also automatically satisfy $(-1)^{F_A}(-1)^{N_{RA}+N_{LA}}=1$.

Explicitly evaluating the above expression for $|\psi_a\rangle$, we can write

$$
\begin{aligned}
|\psi_a\rangle = &\frac{1}{2}\left[|G_{b,\mathrm{osc},1}\rangle \otimes \sum_{N\in\mathbb{Z}-\frac{r+1/2}{n}} e^{-\frac{v_e\pi n N^2}{2L}} |N_{RB}=N\rangle\,|N_{LA}=-N\rangle \otimes \prod_{k>0}\left(1+ie^{-\tilde{v}_e k/2} d^\dagger_{-k}c^\dagger_k\right)|0\rangle\right] \\
&\otimes\left[|G_{b,\mathrm{osc},2}\rangle \otimes \sum_{N\in\mathbb{Z}-\frac{r+1/2}{n}} e^{-\frac{v_e\pi n N^2}{2L}} |N_{LB}=-N\rangle\,|N_{RA}=N\rangle \otimes \prod_{k>0}\left(1+ie^{-\tilde{v}_e k/2} \tilde{c}^\dagger_{-k}\tilde{d}^\dagger_k\right)|0\rangle\right] \\
&\otimes \frac{1}{\sqrt{2}}(|0_A,0_B\rangle + i\,|1_A,1_B\rangle) \\
&+\frac{1}{2}\left[|G_{b,\mathrm{osc},1}\rangle \otimes \sum_{N\in\mathbb{Z}-\frac{r+1/2}{n}} (-1)^{N+\frac{r+1/2}{n}} e^{-\frac{v_e\pi n N^2}{2L}} |N_{RB}=N\rangle\,|N_{LA}=-N\rangle \otimes \prod_{k>0}\left(1-ie^{-\tilde{v}_e k/2} d^\dagger_{-k}c^\dagger_k\right)|0\rangle\right] \\
&\otimes\left[|G_{b,\mathrm{osc},2}\rangle \otimes \sum_{N\in\mathbb{Z}-\frac{r+1/2}{n}} (-1)^{-N-\frac{r+1/2}{n}} e^{-\frac{v_e\pi n N^2}{2L}} |N_{LB}=-N\rangle\,|N_{RA}=N\rangle \otimes \prod_{k>0}\left(1-ie^{-\tilde{v}_e k/2} \tilde{c}^\dagger_{-k}\tilde{d}^\dagger_k\right)|0\rangle\right] \\
&\otimes \frac{1}{\sqrt{2}}(|0_A,0_B\rangle - i\,|1_A,1_B\rangle).
\end{aligned}
\tag{E.18}
$$

Although this is a rather cumbersome expression, we can parse its meaning as follows. The first three lines are simply a re-expression of $|\widehat{\psi}_a\rangle$. The last three lines correspond to the state obtained by acting on $|\widehat{\psi}_a\rangle$ with $(-1)^{F_B}(-1)^{N_{RB}+N_{LB}}$. Every state appearing in the last three lines for which $(-1)^{F_B}(-1)^{N_{RB}+N_{LB}}=-1$ will thus cancel with a state in the first three lines, leaving only states with $(-1)^{F_B}(-1)^{N_{RB}+N_{LB}}=1$, as desired.

Zero Mode Fermion Parity

Now, as alluded to in the main text, there is a subtlety regarding how to interpret the fermion parity of the zero mode. We constructed the fermion f_A from the MZMs d_0 and $\tilde{d}_0$ as $f_A=(d_0+i\tilde{d}_0)/\sqrt{2}$. However, we can also define $f'_A=(\tilde{d}_0+id_0)/\sqrt{2}$, so that

$$
|0,\tilde{0}\rangle = \frac{1}{\sqrt{2}}(|0_A,0_B\rangle + i\,|1_A,1_B\rangle) = \frac{1}{\sqrt{2}}(|1'_A,0_B\rangle - |0'_A,1_B\rangle). \tag{E.19}
$$

In other words, f_A being occupied is equivalent to saying that f'_A is unoccupied and vice versa. The point at issue is that the $\mathbb{Z}_2$ symmetry operators, G_α [see Eq. (7.41)], are defined in terms of the total fermion parities, $(-1)^{F_\alpha}$, and one must decide whether this parity is measured relative to the occupation of f_A or f'_A. Indeed, if we measured it with respect to f'_A, one would find that $P_a|\widehat{\psi}_a\rangle=0$ since, for each state appearing

in $|\widehat{\psi}_a\rangle$, the total fermion parities of A and B would be opposite to one another.

In order to remove this ambiguity in the definition of the fermion parity, it is necessary to resort to physical arguments which can provide additional input, which we now provide. Before physically cutting the torus into the cylinders A and B, the torus starts in the ground state with a $\sigma e^{i(r+1/2)\phi}$ Wilson loop wrapping around the y-cycle (i.e. the cycle perpendicular to the entanglement cut). On performing the physical cut of the torus into two cylinders, the Wilson loop is cut into two Wilon lines with endpoints at the edges of the cylinders. Physically, this configuration corresponds to having a $\sigma e^{i(r+1/2)\phi}$ anyon on one end of each cylinder and the corrsponding conjugate anyon on the other end of each cylinder.

Let us label these anyons as $\sigma_{A,r} \equiv \sigma_A e^{i(r+1/2)\phi_A}$, $\overline{\sigma}_{A,r} \equiv \overline{\sigma}_A e^{i(r+1/2)\overline{\phi}_A}$, $\sigma_{B,r} \equiv \sigma_B e^{i(r+1/2)\phi_B}$, and $\overline{\sigma}_{B,r} \equiv \overline{\sigma}_B e^{i(r+1/2)\overline{\phi}_B}$. We claim that the pairs of anyons at each interface must fuse to the identity, and not to a neutral Majorana:

$$\sigma_{A,r} \times \overline{\sigma}_{B,r} = \sigma_{B,r} \times \overline{\sigma}_{A,r} = 1. \tag{E.20}$$

Physically, we can think of the electron tunneling terms which glue the edges together as hybridizations of $\sigma_{A,r}$ with $\overline{\sigma}_{B,r}$ and $\sigma_{B,r}$ with $\overline{\sigma}_{A,r}$. This would make it energetically preferable for each pair of these anyons to fuse into the identity, as opposed to a Majorana fermion. In particular, when we expanded the tunneling term about one of its minima, we did so assuming that this corresponded to the ground state, which one should interpret as the vacuum.

Now, we wish to identify what the allowed fusion possibilities for $\sigma_A \times \overline{\sigma}_A$ and $\sigma_B \times \overline{\sigma}_B$ should be. From the previous paragraph, we see that fusing all four of the twist anyons should yield the vacuum. This requires that either $\sigma_A \times \overline{\sigma}_A = \sigma_B \times \overline{\sigma}_B = 1$ *or* $\sigma_A \times \overline{\sigma}_A = \sigma_B \times \overline{\sigma}_B = \chi$. This suggests that we should define the complex fermions $f_{1,2}$ on cylinders A and B to be such that we can express the ground state as

$$|0, \tilde{0}\rangle = \frac{1}{\sqrt{2}}(|0_1, 0_2\rangle + \alpha\,|1_1, 1_2\rangle), \tag{E.21}$$

where α is some unimportant phase. Hence, our choice of measuring the fermion parity relative to f_A and f_B is consistent with this physical picture. We note that this line of reasoning is similar to more carefully constructed arguments for determining the ground state degeneracy of the Moore-Read state on the torus – see, for instance, Refs. [312, 313].

E.3 Alternative Representation of the Ising CFT

In this section, we consider the edge theory of the Ising topological order which, conventionally, is described by the Ising CFT. We first write down a CFT description of the edge which is topologically equivalent to the Ising CFT, in a sense to be made more precise shortly. We then show how we can write down an explicit gapping interaction for the interface of two Ising edges using this alternative CFT description, which does not appear possible (at least based on a superficial analysis) in the standard Ising CFT description of the edge.

E.3.1 Coset Construction and Hilbert Space Structure

In the usual free-field representation, the Ising edge theory contains a single chiral Majorana:

$$\mathcal{L}' = \psi \frac{i}{2}(\partial_t - \partial_x)\psi. \tag{E.22}$$

The three topological sectors in the theory are 1, σ, and ψ – the vacuum, twist operator, and Majorana sectors, respectively. Gapping an interface between two Ising topological orders thus appears difficult, as any local tunneling operator would have to involve terms quadratic in both the left- and right-moving Majoranas, which naïvely would square to unity.

We instead make use of the coset representation,

$$\text{Ising} = \frac{SO(N+1)_1}{SO(N)} \sim SO(N+1)_1 \boxtimes \overline{SO(N)}_1. \tag{E.23}$$

Here we take $N = 2r$, $1 < r \in \mathbb{Z}$. On the left hand side of the equivalence, we have a theory of $N+1$ chiral Majoranas in which we gap out N of them. On the right hand side, we have a theory of $N+1$ chiral Majoranas and N anti-chiral Majoranas in which we have condensed a certain set of bosonic anyons so as to identify certain topological sectors. Now, the Ising CFT is identical to the coset $SO(N+1)_1/SO(N)$, in that they have the same primary operator content as well as total and chiral central charges. In contrast,we will say the Ising CFT and the $SO(N+1)_1 \boxtimes \overline{SO(N)}_1$ CFT are *topologically* equivalent, in that they possess the same primary operator content (i.e. topological sectors) and chiral central charge, but not the same total central charge [286, 314].

Let us now outline in detail the structure of the $SO(N+1)_1 \boxtimes \overline{SO(N)}_1$ theory. Placing the Ising

topological order on a cylinder, as in Fig. 7.1, the $\mu = L, R = +, -$ edges are described by the Lagrangians

$$\mathcal{L}_\mu = \sum_{\alpha=0}^{N} \psi_\mu^\alpha \frac{i}{2}(\partial_t - \mu\partial_x)\psi_\mu^\alpha + \sum_{a=1}^{N} \overline{\psi}_\mu^a \frac{i}{2}(\partial_t + \mu\partial_x)\overline{\psi}_\mu^a. \tag{E.24}$$

So, on edge L (R), there are $N+1$ chiral (anti-chiral) Majoranas, ψ_μ^α and N anti-chiral (chiral) Majoranas, $\overline{\psi}_\mu^a$. For simplicity, we have set all velocities to unity. Additionally, we adopt the convention that Greek indices α, β run from 0 to N and the Latin indices a, b from 1 to N. This theory possesses the currents

$$J_\mu^{\alpha\beta} = i\psi_\mu^\alpha \psi_\mu^\beta, \quad \overline{J}_\mu^{ab} = i\overline{\psi}_\mu^a \overline{\psi}_\mu^b, \tag{E.25}$$

which generate the $SO(N+1)_1$ and $\overline{SO(N)}_1$ Kac-Moody algebras of the two edges, respectively. Additionally, the operators

$$M_\mu^{\alpha a} = i\psi_\mu^\alpha \overline{\psi}_\mu^a \tag{E.26}$$

correspond to the condensed bosons encoded in the tensor product, $\boxtimes$, and hence, like the currents, are local-electronic objects. Using these expressions, we can see that this theory is in fact topologically equivalent to the Ising CFT. For instance, starting with one Majorana fermion, say, ψ^α, we can obtain any other Majorana ψ^β or $\overline{\psi}^a$ by fusing it with $J^{\alpha\beta}$ or $M^{\alpha a}$. Hence, there is only *one* distinct Majorana fermion sector, as in the Ising theory.

Although not strictly necessary, it will prove convenient for our purposes to bosonize as many of the fermions as possible. Since we have taken $N = 2r$ to be even, we can pair up all the Majoranas in the $\overline{SO(N)}_1$ factor into Dirac fermions and bosonize them:

$$\overline{c}_\mu^j = (\overline{\psi}_\mu^{2j-1} + i\overline{\psi}_\mu^{2j})/\sqrt{2} \sim e^{i\overline{\phi}_\mu^j}, \quad j = 1, \ldots, r. \tag{E.27}$$

Hence,

$$\overline{\psi}_\mu^{2j-1} \sim \cos(\overline{\phi}_\mu^j), \quad \overline{\psi}_\mu^{2j} \sim \sin(\overline{\phi}_\mu^j). \tag{E.28}$$

As for the $SO(N+1)$ factor, we can bosonize all but one of the Majoranas, say the $\mu = 0$ one:

$$c_\mu^j = (\psi_\mu^{2j-1} + i\psi_\mu^{2j})/\sqrt{2} \sim e^{i\phi_\mu^j}, \quad j = 1, \ldots, r. \tag{E.29}$$

Hence

$$\psi_\mu^{2j-1} \sim \cos(\phi_\mu^j), \quad \psi_\mu^{2j} \sim \sin(\phi_\mu^j). \tag{E.30}$$

The $\mu = L, R = +, -$ edges are then described by the Lagrangians

$$\mathcal{L}_\mu = \frac{1}{4\pi} \sum_{j=1}^{r} \left[\partial_x \phi_\mu^j (\mu \partial_t - \partial_x) \phi_\mu^j + \partial_x \overline{\phi}_\mu^j (-\mu \partial_t - \partial_x) \overline{\phi}_\mu^j \right] + \psi_\mu \frac{i}{2} (\partial_t - \mu \partial_x) \psi_\mu, \tag{E.31}$$

where we have relabelled $\psi_\mu^{\alpha=0} \equiv \psi_\mu$. In this partially bosonized language, the currents are given by

$$J^{\alpha\beta} \sim \begin{cases} \cos(\phi^{(\alpha+1)/2}) \cos(\phi^{(\beta+1)/2}), \ \alpha \text{ odd}, \ \beta \text{ odd} \\ \cos(\phi^{(\alpha+1)/2}) \sin(\phi^{\beta/2}), \ \alpha \text{ odd}, \ \beta \text{ even} \\ \sin(\phi^{\alpha/2}) \sin(\phi^{\beta/2}), \ \alpha \text{ even}, \ \beta \text{ even} \end{cases} \tag{E.32}$$

for $\alpha, \beta \neq 0$, while,

$$J^{0\beta} \sim \begin{cases} \psi \cos(\phi^{(\beta+1)/2}), \ \beta \text{ odd} \\ \psi \sin(\phi^{\beta/2}), \ \beta \text{ even} \end{cases}, \tag{E.33}$$

for $\beta \neq 0$, and

$$\overline{J}^{ab} \sim \begin{cases} \cos(\overline{\phi}^{(a+1)/2}) \cos(\overline{\phi}^{(b+1)/2}), \ a \text{ odd}, \ b \text{ odd} \\ \cos(\overline{\phi}^{(a+1)/2}) \sin(\overline{\phi}^{b/2}), \ a \text{ odd}, \ b \text{ even} \\ \sin(\overline{\phi}^{a/2}) \sin(\overline{\phi}^{b/2}), \ a \text{ even}, \ b \text{ even}. \end{cases} \tag{E.34}$$

The local-electronic operators, $M^{\alpha a}$, are likewise given by

$$M^{\alpha a} \sim \begin{cases} \cos(\phi^{(\alpha+1)/2}) \cos(\overline{\phi}^{(a+1)/2}), \ \alpha \text{ odd}, \ a \text{ odd} \\ \cos(\phi^{(\alpha+1)/2}) \sin(\overline{\phi}^{a/2}), \ \alpha \text{ odd}, \ a \text{ even} \\ \sin(\phi^{\alpha/2}) \sin(\overline{\phi}^{a/2}), \ \alpha \text{ even}, \ a \text{ even} \end{cases} \tag{E.35}$$

for $\alpha \neq 0$, and by

$$M^{0a} \sim \begin{cases} \psi \cos(\overline{\phi}^{(a+1)/2}), \ a \text{ odd} \\ \psi \sin(\overline{\phi}^{a/2}), \ a \text{ even.} \end{cases} \tag{E.36}$$

We have suppressed the $\mu = L, R$ edge subscript for compactness in the above expressions.

Now, as discussed in Section 7.2 for the MR theory, it is important that we understand the organization of the Hilbert space as dictated by the currents. Let us first work in the fermionic language of Eq. (E.24) and Eq. (E.25). As described above, there are three topological sectors: 1, ψ, and σ. Since the currents are all bilinears in the Majorana fields, it immediately follows that all states within a topological sector have the same total fermion parity, $(-1)^F$, where $(-1)^F$ anti-commutes with *all* the Majorana fields.

Similar statements hold in the (partially) bosonized language. From Equations (E.32)-(E.36) we see that the current operators either change the bosonic winding number parity of two bosonic fields, or change the bosonic winding number parity of one field and the Majorana fermion parity. In other words, in the identity sector, the total bosonic winding number parity (of both the barred and unbarred fields) must much that of the fermion parity – note the similarity with the "gluing" constraint in the Moore-Read CFT.

In order to express this Hilbert space organization more formally, let us identify the operator which generates the underlying $\mathbb{Z}_2$ gauge symmetry. As usual, we write the bosonic winding numbers as

$$N_\mu^j = \int_0^L \frac{\partial_x \phi_\mu^j}{2\pi} dx, \quad \overline{N}_\mu^j = \int_0^L \frac{\partial_x \overline{\phi}_\mu^j}{2\pi} dx, \tag{E.37}$$

which have *integer* eigenvalues. We then define the operator

$$I = (-1)^F (-1)^{\sum_j (N_R^j + N_L^j)} (-1)^{\sum_j (\overline{N}_R^j + \overline{N}_L^j)}, \tag{E.38}$$

where $(-1)^F$ anti-commutes with the Majorana fields ψ_L and ψ_R. This generates the $\mathbb{Z}_2$ transformation,

$$\psi^\mu \to -\psi_\mu, \quad \phi_\mu^j \to \phi_\mu^j + \mu\pi, \quad \overline{\phi}_\mu^j \to \overline{\phi}_\mu^j - \mu\pi, \tag{E.39}$$

under which the currents are manifestly invariant. The physical Hilbert space is defined by the constraint $I = 1$, which simply states the total number of fermionic excitations (recalling that the vertex operators $e^{i\phi_\mu^j}$ and $e^{i\overline{\phi}_\mu^j}$ obey fermionic statistics) is even.

E.3.2 Gapping Term

Let us now return to the question which motivated the search for an alternative representation of the Ising edge theory, namely, how to gap out an interface of Ising edges. For instance, suppose we would like to glue the two edges of the cylinder in Fig. 7.1 together by bringing them close together and adding an interaction to gap them out. To do so, we can simply write down a current-current interaction, which is local by definition and takes the form of a Gross-Neveu interaction [302]:

$$H_{\text{gap}} = u \sum_{\alpha,\beta} J_R^{\alpha\beta} J_L^{\alpha\beta} + u \sum_{a,b} J_R^{ab} J_L^{ab} = -u(\boldsymbol{\psi}_R \cdot \boldsymbol{\psi}_L)^2 - u(\overline{\boldsymbol{\psi}}_R \cdot \overline{\boldsymbol{\psi}}_L)^2. \tag{E.40}$$

In the language of the standard Ising edge theory (i.e. the usual Ising CFT), this interaction heuristically corresponds to $(\psi_L \psi_R)^2$, as one would expect on the basis of an anyon condensation picture of the gapped interface. Indeed, condensing $\psi_L \psi_R$ in the Ising $\times$ $\overline{\text{Ising}}$ theory yields the Toric code topological order, which can further be condensed to a trivial order. In the partially bosonized language, this Gross-Neveu interaction becomes (dropping terms which only renormalize velocities)

$$H_{\text{gap}} = -u \sum_{j_1 \neq j_2} \left[\cos(2\Theta^{j_1}) \cos(2\Theta^{j_2}) + \cos(2\overline{\Theta}^{j_1}) \cos(2\overline{\Theta}^{j_2}) \right] - u \sum_{j=1}^{r} \cos(2\Theta^j) i\psi_L \psi_R \tag{E.41}$$

where we have defined

$$2\Theta^j \equiv \phi_R^j - \phi_L^j, \quad 2\overline{\Theta}^j = \overline{\phi}_R^j - \overline{\phi}_L^j. \tag{E.42}$$

It is straightforward to see that Eq. (E.41) will gap out the interface – the sine-Gordon terms will pin the angle variables, which in turn will result in a mass term for the remaining Majoranas.

Appendix F

Chern-Simons conventions for Chapters 4, 5, and 6

Here we lay out our conventions for non-Abelian Chern-Simons gauge theories. We define $U(N)$ gauge fields $a_\mu = a_\mu^b t^b$, where t^b are the (Hermitian) generators of the Lie algebra of $U(N)$, which satisfy $[t^a, t^b] = i f^{abc} t^c$, where f^{abc} are the structure constants of $U(N)$. The generators are normalized so that $\mathrm{Tr}[t^b t^c] = \frac{1}{2}\delta^{bc}$. The trace of a is a $U(1)$ gauge field, which we require to satisfy the Dirac quantization condition,

$$\int_\Sigma \frac{d\,\mathrm{Tr}[a]}{2\pi} = n \in \mathbb{Z}\,. \tag{F.1}$$

where $\Sigma \subset X$ is an oriented 2-cycle in spacetime, which we denote X. If a_μ couples to fermions, then it is a spin$_c$ connection, and it satisfies a modified flux quantization condition

$$\int_\Sigma \frac{d\,\mathrm{Tr}[a]}{2\pi} = \int_\Sigma \frac{w_2}{2} + n\,,\, n \in \mathbb{Z}\,, \tag{F.2}$$

where w_2 is the second Stiefel-Whitney class of X. In general, the Chern-Simons levels for the $SU(N)$ and $U(1)$ components of a can be different. We therefore adopt the standard notation [68],

$$U(N)_{k,k'} = \frac{SU(N)_k \times U(1)_{Nk'}}{\mathbb{Z}_N}\,. \tag{F.3}$$

By taking the quotient with $\mathbb{Z}_N$, we are restricting the difference of the $SU(N)$ and $U(1)$ levels to be an integer multiple of N,

$$k' = k + nN\,, n \in \mathbb{Z}\,. \tag{F.4}$$

This enables us to glue the $U(1)$ and $SU(N)$ gauge fields together to form a gauge invariant theory of a single $U(N)$ gauge field $a = a_{SU(N)} + \tilde{a}\,\mathbf{1}$, with $\mathrm{Tr}[a] = N\tilde{a}$ having quantized fluxes as in Eq. (F.1). The

Lagrangian for the $U(N)_{k,k'}$ theory can be written as

$$\mathcal{L}_{U(N)_{k,k'}} = \frac{k}{4\pi}\,\mathrm{Tr}\left[ada - \frac{2i}{3}a^3\right] + \frac{k'-k}{4\pi N}\,\mathrm{Tr}[a]d\,\mathrm{Tr}[a] \tag{F.5}$$

$$= \frac{k}{4\pi}\,\mathrm{Tr}\left[a_{SU(N)}da_{SU(N)} - \frac{2i}{3}a^3_{SU(N)}\right] + \frac{Nk'}{4\pi}\tilde{a}d\tilde{a}\,. \tag{F.6}$$

For the case $k = k'$, we simply refer to the theory as $U(N)_k$.

Throughout this thesis, we implicitly regulate non-Abelian (Abelian) gauge theories using Yang-Mills (Maxwell) terms, as opposed to dimensional regularization [99, 315]. In Yang-Mills regularization, there is a one-loop exact shift of the $SU(N)$ level, $k \to k+\mathrm{sgn}(k)N$, that does not appear in dimensional regularization. Consequently, to describe the same theory in dimensional regularization, one must start with a $SU(N)$ level $k_{\mathrm{DR}} = k + \mathrm{sgn}(k)N$. The dualities discussed in this thesis e.g. Eqs. (4.13)-(4.15), therefore would take a somewhat different form in dimensional regularization.

References

[1] G. Moore and N. Read, Nonabelions in the fractional quantum Hall effect, Nuclear Physics B **360**, 362 (1991).

[2] E. Fradkin, *Field Theories of Condensed Matter Systems, Second Edition* (Cambridge University Press, Cambridge, U.K., 2013).

[3] K. v. Klitzing, G. Dorda, and M. Pepper, New method for high-accuracy determination of the fine-structure constant based on quantized hall resistance, Phys. Rev. Lett. **45**, 494 (1980).

[4] D. C. Tsui, H. L. Stormer, and A. C. Gossard, Two-dimensional magnetotransport in the extreme quantum limit, Phys. Rev. Lett. **48**, 1559 (1982).

[5] P. H. Bonderson, *Non-Abelian anyons and interferometry*, PhD thesis, California Institute of Technology, 2007.

[6] C. Nayak, S. H. Simon, A. Stern, M. Freedman, and S. Das Sarma, Non-Abelian anyons and topological quantum computation, Rev. Mod. Phys. **80**, 1083 (2008).

[7] J. Nakamura, S. Liang, G. C. Gardner, and M. J. Manfra, Direct observation of anyonic braiding statistics, Nature Physics **16**, 931 (2020).

[8] H. Bartolomei *et al.*, Fractional statistics in anyon collisions, Science **368**, 173 (2020), https://science.sciencemag.org/content/368/6487/173.full.pdf.

[9] M. Banerjee *et al.*, Observation of half-integer thermal Hall conductance, Nature **559**, 205 (2018), 1710.00492.

[10] R. B. Laughlin, Anomalous Quantum Hall Effect: An Incompressible Quantum Fluid with Fractionally Charged Excitations, Phys. Rev. Lett. **50**, 1395 (1983).

[11] J. K. Jain, Composite-fermion approach for the fractional quantum Hall effect, Phys. Rev. Lett. **63**, 199 (1989).

[12] A. López and E. Fradkin, Fractional quantum Hall effect and Chern-Simons gauge theories, Phys. Rev. B **44**, 5246 (1991).

[13] S. C. Zhang, T. H. Hansson, and S. Kivelson, Effective-Field-Theory Model for the Fractional Quantum Hall Effect, Phys. Rev. Lett. **62**, 82 (1989).

[14] X.-G. Wen, Topological orders and edge excitations in fractional quantum Hall states, Advances in Physics **44**, 405 (1995).

[15] R. Sohal, L. H. Santos, and E. Fradkin, Chern-Simons composite fermion theory of fractional Chern insulators, Phys. Rev. B **97**, 125131 (2018).

[16] R. Sohal and E. Fradkin, Intertwined order in fractional Chern insulators from finite-momentum pairing of composite fermions, Phys. Rev. B **101**, 245154 (2020).

[17] H. Goldman, R. Sohal, and E. Fradkin, Landau-Ginzburg theories of non-Abelian quantum Hall states from non-Abelian bosonization, Phys. Rev. B **100**, 115111 (2019).

[18] H. Goldman, R. Sohal, and E. Fradkin, A composite particle construction of the Fibonacci fractional quantum Hall state, 2020, arxiv:2012.11611.

[19] H. Goldman, R. Sohal, and E. Fradkin, Non-Abelian fermionization and the landscape of quantum Hall phases, Phys. Rev. B **102**, 195151 (2020).

[20] R. Sohal, B. Han, L. H. Santos, and J. C. Y. Teo, Entanglement entropy of generalized Moore-Read fractional quantum Hall state interfaces, Phys. Rev. B **102**, 045102 (2020).

[21] F. D. M. Haldane, Model for a quantum hall effect without landau levels: Condensed-matter realization of the "parity anomaly", Phys. Rev. Lett. **61**, 2015 (1988).

[22] D. J. Thouless, M. Kohmoto, M. P. Nightingale, and M. den Nijs, Quantized Hall Conductance in a Two-Dimensional Periodic Potential, Phys. Rev. Lett. **49**, 405 (1982).

[23] T. Neupert, L. Santos, C. Chamon, and C. Mudry, Fractional Quantum Hall States at Zero Magnetic Field, Phys. Rev. Lett. **106**, 236804 (2011).

[24] D. Sheng, Z.-C. Gu, K. Sun, and L. Sheng, Fractional quantum Hall effect in the absence of Landau levels, Nat. Comm. **2**, 389 (2011).

[25] E. Tang, J.-W. Mei, and X.-G. Wen, High-Temperature Fractional Quantum Hall States, Phys. Rev. Lett. **106**, 236802 (2011).

[26] K. Sun, Z. Gu, H. Katsura, and S. Das Sarma, Nearly Flatbands with Nontrivial Topology, Phys. Rev. Lett. **106**, 236803 (2011).

[27] N. Regnault and B. A. Bernevig, Fractional Chern Insulator, Phys. Rev. X **1**, 021014 (2011).

[28] Z. Liu, E. J. Bergholtz, H. Fan, and A. M. Läuchli, Fractional Chern Insulators in Topological Flat Bands with Higher Chern Number, Phys. Rev. Lett. **109**, 186805 (2012).

[29] Y.-L. Wu, B. A. Bernevig, and N. Regnault, Zoology of fractional Chern insulators, Phys. Rev. B **85**, 075116 (2012).

[30] A. M. Läuchli, Z. Liu, E. J. Bergholtz, and R. Moessner, Hierarchy of Fractional Chern Insulators and Competing Compressible States, Phys. Rev. Lett. **111**, 126802 (2013).

[31] T. Liu, C. Repellin, B. A. Bernevig, and N. Regnault, Fractional chern insulators beyond laughlin states, Phys. Rev. B **87**, 205136 (2013).

[32] E. J. Bergholtz and Z. Liu, Topological Flat Band Models and Fractional Chern Insulators, Int. J. Mod. Phys. B **27**, 1330017 (2013).

[33] S. A. Parameswaran, R. Roy, and S. L. Sondhi, Fractional quantum Hall physics in topological flat bands, Comptes Rendus Physique **14**, 816 (2013).

[34] A. Kol and N. Read, Fractional quantum Hall effect in a periodic potential, Phys. Rev. B **48**, 8890 (1993).

[35] M. Barkeshli and X.-L. Qi, Topological Nematic States and Non-Abelian Lattice Dislocations, Phys. Rev. X **2**, 031013 (2012).

[36] A. Sterdyniak, C. Repellin, B. A. Bernevig, and N. Regnault, Series of abelian and non-abelian states in $c > 1$ fractional chern insulators, Phys. Rev. B **87**, 205137 (2013).

[37] A. M. Essin and M. Hermele, Classifying fractionalization: Symmetry classification of gapped $\mathbb{Z}_2$ spin liquids in two dimensions, Phys. Rev. B **87**, 104406 (2013).

[38] X. Chen, Symmetry fractionalization in two dimensional topological phases, Reviews in Physics **2**, 3 (2017).

[39] N. Manjunath and M. Barkeshli, Crystalline gauge fields and quantized discrete geometric response for abelian topological phases with lattice symmetry, Phys. Rev. Research **3**, 013040 (2021).

[40] N. Manjunath and M. Barkeshli, Classification of fractional quantum Hall states with spatial symmetries, 2020, 2012.11603.

[41] J. Y. Lee, C. Wang, M. P. Zaletel, A. Vishwanath, and Y.-C. He, Emergent multi-flavor qed_3 at the plateau transition between fractional chern insulators: Applications to graphene heterostructures, Phys. Rev. X **8**, 031015 (2018).

[42] S. Kourtis and M. Daghofer, Combined Topological and Landau Order from Strong Correlations in Chern Bands, Phys. Rev. Lett. **113**, 216404 (2014).

[43] S. Kourtis, Symmetry breaking and the fermionic fractional Chern insulator in topologically trivial bands, Phys. Rev. B **97**, 085108 (2018).

[44] E. M. Spanton *et al.*, Observation of fractional Chern insulators in a van der Waals heterostructure, Science **360**, 62 (2018).

[45] Y. Cao *et al.*, Correlated insulator behaviour at half-filling in magic-angle graphene superlattices, Nature **556**, 80 (2018).

[46] Y. Cao *et al.*, Unconventional superconductivity in magic-angle graphene superlattices, Nature **556**, 43 (2018).

[47] A. L. Sharpe *et al.*, Emergent ferromagnetism near three-quarters filling in twisted bilayer graphene, Science **365**, 605 (2019).

[48] G. Chen *et al.*, Tunable correlated Chern insulator and ferromagnetism in a moiré superlattice, Nature **579**, 56 (2020).

[49] M. Serlin *et al.*, Intrinsic quantized anomalous Hall effect in a moiré heterostructure, Science (2019).

[50] M. Aidelsburger *et al.*, Realization of the Hofstadter Hamiltonian with Ultracold Atoms in Optical Lattices, Phys. Rev. Lett. **111**, 185301 (2013).

[51] H. Miyake, G. A. Siviloglou, C. J. Kennedy, W. C. Burton, and W. Ketterle, Realizing the Harper Hamiltonian with Laser-Assisted Tunneling in Optical Lattices, Phys. Rev. Lett. **111**, 185302 (2013).

[52] M. Aidelsburger *et al.*, Measuring the Chern number of Hofstadter bands with ultracold bosonic atoms, Nature Physics **11**, 162 (2015).

[53] G. Jotzu *et al.*, Experimental realization of the topological Haldane model with ultracold fermions, Nature **515**, 237 (2014).

[54] N. R. Cooper, J. Dalibard, and I. B. Spielman, Topological bands for ultracold atoms, Rev. Mod. Phys. **91**, 015005 (2019).

[55] X.-L. Qi, Generic wave-function description of fractional quantum anomalous hall states and fractional topological insulators, Phys. Rev. Lett. **107**, 126803 (2011).

[56] D. Eliezer and G. W. Semenoff, Anyonization of lattice Chern-Simons theory, Annals of Physics **217**, 66 (1992).

[57] D. Eliezer and G. W. Semenoff, Intersection forms and the geometry of lattice Chern-Simons theory, Physics Letters B **286**, 118 (1992).

[58] K. Sun, K. Kumar, and E. Fradkin, Discretized Abelian Chern-Simons gauge theory on arbitrary graphs, Phys. Rev. B **92**, 115148 (2015).

[59] G. Möller and N. R. Cooper, Composite Fermion Theory for Bosonic Quantum Hall States on Lattices, Phys. Rev. Lett. **103**, 105303 (2009).

[60] G. Möller and N. R. Cooper, Fractional Chern Insulators in Harper-Hofstadter Bands with Higher Chern Number, Phys. Rev. Lett. **115**, 126401 (2015).

[61] N. Read and D. Green, Paired states of fermions in two dimensions with breaking of parity and time-reversal symmetries and the fractional quantum Hall effect, Phys. Rev. B **61**, 10267 (2000).

[62] D. F. Agterberg *et al.*, The physics of pair-density waves: Cuprate superconductors and beyond, Annual Review of Condensed Matter Physics **11**, 231 (2020), https://doi.org/10.1146/annurev-conmatphys-031119-050711.

[63] C. Nayak and F. Wilczek, 2n-quasihole states realize 2n1-dimensional spinor braiding statistics in paired quantum hall states, Nuclear Physics B **479**, 529 (1996).

[64] B. I. Halperin, P. A. Lee, and N. Read, Theory of the half-filled Landau level, Phys. Rev. B **47**, 7312 (1993).

[65] N. Read and E. Rezayi, Beyond paired quantum Hall states: Parafermions and incompressible states in the first excited Landau level, Phys. Rev. B **59**, 8084 (1999).

[66] O. Aharony, G. Gur-Ari, and R. Yacoby, d = 3 bosonic vector models coupled to Chern-Simons gauge theories, J. High Energy Phys. **03**, 37 (2012).

[67] S. Giombi *et al.*, Chern-Simons theory with vector fermion matter, Eur. Phys. J. C **72**, 1 (2012).

[68] O. Aharony, Baryons, monopoles and dualities in Chern-Simons-matter theories, J. High Energy Phys. **02**, 93 (2016).

[69] E. Ardonne and K. Schoutens, New Class of Non-Abelian Spin-Singlet Quantum Hall States, Phys. Rev. Lett. **82**, 5096 (1999).

[70] Y. Fuji and P. Lecheminant, Non-abelian $su(n-1)$-singlet fractional quantum hall states from coupled wires, Phys. Rev. B **95**, 125130 (2017).

[71] B. Blok and X. Wen, Many-body systems with non-abelian statistics, Nuclear Physics B **374**, 615 (1992).

[72] M. Barkeshli and X.-L. Qi, Topological nematic states and non-abelian lattice dislocations, Phys. Rev. X **2**, 031013 (2012).

[73] N. H. Lindner, E. Berg, G. Refael, and A. Stern, Fractionalizing majorana fermions: Non-abelian statistics on the edges of abelian quantum hall states, Phys. Rev. X **2**, 041002 (2012).

[74] D. J. Clarke, J. Alicea, and K. Shtengel, Exotic non-abelian anyons from conventional fractional quantum hall states, Nature Communications **4**, 1348 EP (2013).

[75] M. Cheng, Superconducting proximity effect on the edge of fractional topological insulators, Phys. Rev. B **86**, 195126 (2012).

[76] A. Vaezi, Fractional topological superconductor with fractionalized majorana fermions, Phys. Rev. B **87**, 035132 (2013).

[77] M. Barkeshli, C.-M. Jian, and X.-L. Qi, Twist defects and projective non-abelian braiding statistics, Phys. Rev. B **87**, 045130 (2013).

[78] M. Barkeshli, C.-M. Jian, and X.-L. Qi, Classification of topological defects in abelian topological states, Phys. Rev. B **88**, 241103 (2013).

[79] R. S. K. Mong *et al.*, Universal topological quantum computation from a superconductor-abelian quantum hall heterostructure, Phys. Rev. X **4**, 011036 (2014).

[80] M. N. Khan, J. C. Y. Teo, and T. L. Hughes, Anyonic symmetries and topological defects in abelian topological phases: An application to the *ade* classification, Phys. Rev. B **90**, 235149 (2014).

[81] L. H. Santos and T. L. Hughes, Parafermionic wires at the interface of chiral topological states, Phys. Rev. Lett. **118**, 136801 (2017).

[82] J. May-Mann and T. L. Hughes, Families of gapped interfaces between fractional quantum hall states, Phys. Rev. B **99**, 155134 (2019).

[83] L. H. Santos, Parafermions in hierarchical fractional quantum hall states, Phys. Rev. Research **2**, 013232 (2020).

[84] Ö. Gül *et al.*, Induced superconductivity in the fractional quantum Hall edge, 2020, 2009.07836.

[85] M. Levin, Protected edge modes without symmetry, Phys. Rev. X **3**, 021009 (2013).

[86] M. Barkeshli, C.-M. Jian, and X.-L. Qi, Theory of defects in abelian topological states, Phys. Rev. B **88**, 235103 (2013).

[87] J. C. Wang and X.-G. Wen, Boundary degeneracy of topological order, Phys. Rev. B **91**, 125124 (2015).

[88] L. H. Santos, J. Cano, M. Mulligan, and T. L. Hughes, Symmetry-protected topological interfaces and entanglement sequences, Phys. Rev. B **98**, 075131 (2018).

[89] A. Kitaev and J. Preskill, Topological entanglement entropy, Phys. Rev. Lett. **96**, 110404 (2006).

[90] M. Levin and X.-G. Wen, Detecting Topological Order in a Ground State Wave Function, Phys. Rev. Lett. **96**, 110405 (2006).

[91] J. Cano, T. L. Hughes, and M. Mulligan, Interactions along an entanglement cut in $2+1$D abelian topological phases, Phys. Rev. B **92**, 075104 (2015).

[92] Y.-M. Lu and Y. Ran, Symmetry-protected fractional Chern insulators and fractional topological insulators, Phys. Rev. B **85**, 165134 (2012).

[93] G. Murthy and R. Shankar, Hamiltonian theory of fractionally filled chern bands, Phys. Rev. B **86**, 195146 (2012).

[94] G. Murthy and R. Shankar, Gauge choices in the hamiltonian theory of fractionally filled chern bands, Phys. Rev. B **89**, 195107 (2014).

[95] E. Fradkin, Jordan-Wigner transformation for quantum-spin systems in two dimensions and fractional statistics, Phys. Rev. Lett. **63**, 322 (1989).

[96] K. Kumar, K. Sun, and E. Fradkin, Chern-Simons theory of magnetization plateaus of the spin-$\frac{1}{2}$ quantum XXZ Heisenberg model on the kagome lattice, Phys. Rev. B **90**, 174409 (2014).

[97] D. Green, L. Santos, and C. Chamon, Isolated flat bands and spin-1 conical bands in two-dimensional lattices, Phys. Rev. B **82**, 075104 (2010).

[98] E. Fradkin, *Field Theories of Condensed Matter Physics, 2nd Edition* (Cambridge University Press, Cambridge, UK, 2013).

[99] E. Witten, Quantum field theory and the Jones polynomial, Commun. Math. Phys. **121**, 351 (1989).

[100] A. López and E. Fradkin, Universal structure of the edge states of the fractional quantum Hall states, Phys. Rev. B **59**, 15323 (1999).

[101] G. Horowitz, Exactly Soluble Diffeomorphism Invariant Theories, Comm. Math. Phys. **125**, 417 (1989).

[102] T. Fukui, Y. Hatsugai, and H. Suzuki, Chern Numbers in Discretized Brillouin Zone: Efficient Method of Computing (Spin) Hall Conductances, J. Phys. Soc. Japan **74**, 1674 (2005).

[103] X. G. Wen and A. Zee, Classification of Abelian quantum Hall states and matrix formulation of topological fluids, Phys. Rev. B **46**, 2290 (1992).

[104] S. Dong, E. Fradkin, R. G. Leigh, and S. Nowling, Topological Entanglement Entropy in Chern-Simons Theories and Quantum Hall Fluids, JHEP-J. High Energy Phys. **05**, 016 (2008).

[105] M. Barkeshli, P. Bonderson, M. Cheng, and Z. Wang, Symmetry fractionalization, defects, and gauging of topological phases, Phys. Rev. B **100**, 115147 (2019).

[106] M. Cheng, M. Zaletel, M. Barkeshli, A. Vishwanath, and P. Bonderson, Translational Symmetry and Microscopic Constraints on Symmetry-Enriched Topological Phases: A View from the Surface, Phys. Rev. X **6**, 041068 (2016).

[107] Y.-M. Lu, Y. Ran, and M. Oshikawa, Filling-enforced constraint on the quantized Hall conductivity on a periodic lattice, Annals of Physics **413**, 168060 (2020).

[108] Y.-F. Wang, H. Yao, Z.-C. Gu, C.-D. Gong, and D. N. Sheng, Non-Abelian Quantum Hall Effect in Topological Flat Bands, Phys. Rev. Lett. **108**, 126805 (2012).

[109] Z. Liu and E. J. Bergholtz, From fractional Chern insulators to Abelian and non-Abelian fractional quantum Hall states: Adiabatic continuity and orbital entanglement spectrum, Phys. Rev. B **87**, 035306 (2013).

[110] Z. Liu, E. J. Bergholtz, and E. Kapit, Non-Abelian fractional Chern insulators from long-range interactions, Phys. Rev. B **88**, 205101 (2013).

[111] D. Wang, Z. Liu, W.-M. Liu, J. Cao, and H. Fan, Fermionic non-Abelian fractional Chern insulators from dipolar interactions, Phys. Rev. B **91**, 125138 (2015).

[112] P. Fulde and R. A. Ferrell, Superconductivity in a Strong Spin-Exchange Field, Phys. Rev. **135**, A550 (1964).

[113] A. Larkin and Y. Ovchinnikov, Nonuniform State of Superconductors, Sov. Phys. JETP **20**, 762 (1965).

[114] E. Berg, E. Fradkin, S. A. Kivelson, and J. M. Tranquada, Striped superconductors: how spin, charge and superconducting orders intertwine in the cuprates, New Journal of Physics **11**, 115004 (2009).

[115] H. Zhai, R. O. Umucal ılar, and M. O. Oktel, Pairing and Vortex Lattices for Interacting Fermions in Optical Lattices with a Large Magnetic Field, Phys. Rev. Lett. **104**, 145301 (2010).

[116] M. Iskin, Stripe-ordered superfluid and supersolid phases in the attractive Hofstadter-Hubbard model, Phys. Rev. A **91**, 011601(R) (2015).

[117] R. O. Umucalılar and M. Iskin, Superfluid transition in the attractive Hofstadter-Hubbard model, Phys. Rev. A **94**, 023611 (2016).

[118] H. Guo *et al.*, Unconventional pairing symmetry of interacting dirac fermions on a π-flux lattice, Phys. Rev. B **97**, 155146 (2018).

[119] M. M. Fogler, A. A. Koulakov, and B. I. Shklovskii, Ground state of a two-dimensional electron liquid in a weak magnetic field, Phys. Rev. B **54**, 1853 (1996).

[120] R. Moessner and J. T. Chalker, Exact results for interacting electrons in high Landau levels, Phys. Rev. B **54**, 5006 (1996).

[121] A. A. Koulakov, M. M. Fogler, and B. I. Shklovskii, Charge Density Wave in Two-Dimensional Electron Liquid in Weak Magnetic Field, Phys. Rev. Lett. **76**, 499 (1996).

[122] E. Fradkin and S. A. Kivelson, Liquid-crystal phases of quantum Hall systems, Phys. Rev. B **59**, 8065 (1999).

[123] E. Fradkin, S. A. Kivelson, E. Manousakis, and K. Nho, Nematic Phase of the Two-Dimensional Electron Gas in a Magnetic Field, Phys. Rev. Lett. **84**, 1982 (2000).

[124] D. T. Son, Is the composite fermion a dirac particle?, Phys. Rev. X **5**, 031027 (2015).

[125] N. Samkharadze *et al.*, Observation of a transition from a topologically ordered to a spontaneously broken symmetry phase, Nature Physics **12**, 191 (2016).

[126] K. A. Schreiber *et al.*, Onset of quantum criticality in the topological-to-nematic transition in a two-dimensional electron gas at filling factor $\nu = 5/2$, Phys. Rev. B **96**, 041107(R) (2017).

[127] K. A. Schreiber *et al.*, Electron-electron interactions and the paired-to-nematic quantum phase transition in the second Landau level, Nature Comm. **9**, 2400 (2018).

[128] L. H. Santos, Y. Wang, and E. Fradkin, Pair-Density-Wave Order and Paired Fractional Quantum Hall Fluids, Phys. Rev. X **9**, 021047 (2019).

[129] E. Fradkin, S. A. Kivelson, and J. M. Tranquada, Colloquium: Theory of intertwined orders in high temperature superconductors, Rev. Mod. Phys. **87**, 457 (2015).

[130] A. Abouelkomsan, Z. Liu, and E. J. Bergholtz, Particle-hole duality, emergent fermi liquids, and fractional chern insulators in moiré flatbands, Phys. Rev. Lett. **124**, 106803 (2020).

[131] P. J. Ledwith, G. Tarnopolsky, E. Khalaf, and A. Vishwanath, Fractional chern insulator states in twisted bilayer graphene: An analytical approach, Phys. Rev. Research **2**, 023237 (2020).

[132] C. Repellin and T. Senthil, Chern bands of twisted bilayer graphene: Fractional chern insulators and spin phase transition, Phys. Rev. Research **2**, 023238 (2020).

[133] Z. Liu, A. Abouelkomsan, and E. J. Bergholtz, Gate-Tunable Fractional Chern Insulators in Twisted Double Bilayer Graphene, 2020, arXiv:2004.09522, unpublished.

[134] P. G. Harper, Single Band Motion of Conduction Electrons in a Uniform Magnetic Field, Proceedings of the Physical Society. Section A **68**, 874 (1955).

[135] M. Y. Azbel, Energy spectrum of a conduction electron in a magnetic field, Sov. Phys. JETP **19**, 634 (1964).

[136] D. R. Hofstadter, Energy levels and wave functions of Bloch electrons in rational and irrational magnetic fields, Phys. Rev. B **14**, 2239 (1976).

[137] J. Zak, Magnetic Translation Group, Phys. Rev. **134**, A1602 (1964).

[138] N. E. Bonesteel, Singular Pair Breaking in the Composite Fermi Liquid Description of the Half-Filled Landau Level, Phys. Rev. Lett. **82**, 984 (1999).

[139] S. A. Parameswaran, S. A. Kivelson, S. L. Sondhi, and B. Z. Spivak, Weakly Coupled Pfaffian as a Type I Quantum Hall Liquid, Phys. Rev. Lett. **106**, 236801 (2011).

[140] B. I. Halperin, Theory of the Quantized Hall Conductance, Helv. Phys. Acta **56**, 75 (1983).

[141] E. Fradkin and S. H. Shenker, Phase diagrams of lattice gauge theories with Higgs fields, Phys. Rev. D **19**, 3682 (1979).

[142] T. H. Hansson, V. Oganesyan, and S. L. Sondhi, Superconductors are topologically ordered, Annals of Physics **313**, 497 (2004).

[143] N. Seiberg and E. Witten, Gapped boundary phases of topological insulators via weak coupling, Prog. Theor Exp. Phys. (PTEP) **2016**, 12C101 (2016).

[144] D. F. Agterberg and H. Tsunetsugu, Dislocations and vortices in pair-density-wave superconductors, Nature Physics **4**, 639 (2008).

[145] M. Sato, Y. Tanaka, K. Yada, and T. Yokoyama, Topology of Andreev bound states with flat dispersion, Phys. Rev. B **83**, 224511 (2011).

[146] A. Y. Kitaev, Unpaired Majorana fermions in quantum wires, Physics-Uspekhi **44**, 131 (2001).

[147] C. L. Kane, A. Stern, and B. I. Halperin, Pairing in Luttinger Liquids and Quantum Hall States, Phys. Rev. X **7**, 031009 (2017).

[148] J. Koepsell *et al.*, Robust Bilayer Charge-Pumping for Spin- and Density-Resolved Quantum Gas Microscopy, 2020, arXiv:2002.07577, unpublished.

[149] Z. Liu, G. Möller, and E. J. Bergholtz, Exotic Non-Abelian Topological Defects in Lattice Fractional Quantum Hall States, Phys. Rev. Lett. **119**, 106801 (2017).

[150] S. L. Sondhi and K. Yang, Sliding phases via magnetic fields, Phys. Rev. B **63**, 054430 (2001).

[151] C. L. Kane, R. Mukhopadhyay, and T. C. Lubensky, Fractional Quantum Hall Effect in an Array of Quantum Wires, Phys. Rev. Lett. **88**, 036401 (2002).

[152] J. C. Y. Teo and C. L. Kane, From Luttinger liquid to non-Abelian quantum Hall states, Phys. Rev. B **89**, 085101 (2014).

[153] M. Storni, R. H. Morf, and S. Das Sarma, Fractional quantum hall state at $\nu = \frac{5}{2}$ and the moore-read pfaffian, Phys. Rev. Lett. **104**, 076803 (2010).

[154] M. P. Zaletel, R. S. K. Mong, F. Pollmann, and E. H. Rezayi, Infinite density matrix renormalization group for multicomponent quantum hall systems, Phys. Rev. B **91**, 045115 (2015).

[155] E. H. Rezayi, Landau level mixing and the ground state of the $\nu = 5/2$ quantum hall effect, Phys. Rev. Lett. **119**, 026801 (2017).

[156] R. V. Mishmash, D. F. Mross, J. Alicea, and O. I. Motrunich, Numerical exploration of trial wave functions for the particle-hole-symmetric pfaffian, Phys. Rev. B **98**, 081107 (2018).

[157] E. Ardonne, R. Kedem, and M. Stone, Filling the Bose sea: symmetric quantum Hall edge states and affine characters, Journal of Physics A: Mathematical and General **38**, 617 (2004).

[158] X. G. Wen, Non-Abelian statistics in the fractional quantum Hall states, Phys. Rev. Lett. **66**, 802 (1991).

[159] X.-G. Wen, Projective construction of non-Abelian quantum Hall liquids, Phys. Rev. B **60**, 8827 (1999).

[160] M. Barkeshli and X.-G. Wen, Effective field theory and projective construction for Z_k parafermion fractional quantum Hall states, Phys. Rev. B **81**, 155302 (2010).

[161] N. Seiberg, T. Senthil, C. Wang, and E. Witten, A Duality Web in 2+1 Dimensions and Condensed Matter Physics, Annals of Physics **374**, 395 (2016).

[162] A. Karch and D. Tong, Particle-Vortex Duality from 3D Bosonization, Phys. Rev. X **6**, 031043 (2016).

[163] C. Wang and T. Senthil, Dual Dirac liquid on the surface of the electron topological insulator, Phys. Rev. X **5**, 041031 (2015).

[164] M. A. Metlitski and A. Vishwanath, Particle-vortex duality of two-dimensional Dirac fermion from electric-magnetic duality of three-dimensional topological insulators, Phys. Rev. B **93**, 245151 (2016).

[165] D. Radicevic, D. Tong, and C. Turner, Non-Abelian 3d Bosonization and Quantum Hall States, JHEP **12**, 067 (2016), 1608.04732.

[166] H. Goldman, M. Mulligan, S. Raghu, G. Torroba, and M. Zimet, Two-dimensional conductors with interactions and disorder from particle-vortex duality, Phys. Rev. B **96**, 245140 (2017), 1709.07005.

[167] A. Hui, E.-A. Kim, and M. Mulligan, Non-abelian bosonization and modular transformation approach to superuniversality, Phys. Rev. B **99**, 125135 (2019).

[168] C. Wang, A. Nahum, M. A. Metlitski, C. Xu, and T. Senthil, Deconfined quantum critical points: Symmetries and dualities, Phys. Rev. X **7**, 031051 (2017).

[169] A. Thomson and S. Sachdev, Fermionic Spinon Theory of Square Lattice Spin Liquids near the Néel State, Phys. Rev. X **8**, 011012 (2018).

[170] H. Goldman and E. Fradkin, Dirac Composite Fermions and Emergent Reflection Symmetry about Even Denominator Filling Fractions, Phys. Rev. **B98**, 165137 (2018), 1808.09314.

[171] X.-G. Wen, Continuous Topological Phase Transitions between Clean Quantum Hall States, Phys. Rev. Lett. **84**, 3950 (2000).

[172] D. C. Cabra, E. Fradkin, G. L. Rossini, and F. A. Schaposnik, Non-Abelian fractional quantum Hall states and chiral coset conformal field theories, International Journal of Modern Physics A **15**, 4857 (2000), http://www.worldscientific.com/doi/pdf/10.1142/S0217751X00002354.

[173] D. Cabra, A. Lopez, and G. Rossini, Transition from abelian to non-abelian fqhe states, The European Physical Journal B **19**, 21 (2001).

[174] E. Rezayi, X.-G. Wen, and N. Read, Condensation of fractional excitons, non-Abelian states in double-layer quantum Hall systems and Z_4 parafermions, arXiv e-prints , arXiv:1007.2022 (2010), 1007.2022.

[175] M. Barkeshli and X.-G. Wen, Anyon Condensation and Continuous Topological Phase Transitions in Non-Abelian Fractional Quantum Hall States, Phys. Rev. Lett. **105**, 216804 (2010).

[176] M. Barkeshli and X.-G. Wen, Bilayer quantum hall phase transitions and the orbifold non-abelian fractional quantum hall states, Phys. Rev. B **84**, 115121 (2011).

[177] A. Vaezi and M. Barkeshli, Fibonacci anyons from abelian bilayer quantum hall states, Phys. Rev. Lett. **113**, 236804 (2014).

[178] E. H. Fradkin, C. Nayak, and K. Schoutens, Landau-Ginzburg theories for nonAbelian quantum Hall states, Nucl. Phys. **B546**, 711 (1999), cond-mat/9811005.

[179] A. Cappelli, L. S. Georgiev, and I. T. Todorov, Parafermion hall states from coset projections of abelian conformal theories, Nuclear Physics B **599**, 499 (2001).

[180] E. Ardonne, P. Bouwknegt, and P. Dawson, K-matrices for 2d conformal field theories, Nuclear Physics B **660**, 473 (2003).

[181] Z. Papić, M. O. Goerbig, N. Regnault, and M. V. Milovanović, Tunneling-driven breakdown of the 331 state and the emergent pfaffian and composite fermi liquid phases, Phys. Rev. B **82**, 075302 (2010).

[182] M. R. Peterson *et al.*, Abelian and non-abelian states in $\nu = 2/3$ bilayer fractional quantum hall systems, Phys. Rev. B **92**, 035103 (2015).

[183] S. Geraedts, M. P. Zaletel, Z. Papić, and R. S. K. Mong, Competing abelian and non-abelian topological orders in $\nu = 1/3 + 1/3$ quantum hall bilayers, Phys. Rev. B **91**, 205139 (2015).

[184] Z. Liu, A. Vaezi, K. Lee, and E.-A. Kim, Non-abelian phases in two-component $\nu = 2/3$ fractional quantum hall states: Emergence of fibonacci anyons, Phys. Rev. B **92**, 081102 (2015).

[185] W. Zhu, S. S. Gong, D. N. Sheng, and L. Sheng, Possible non-abelian moore-read state in double-layer bosonic fractional quantum hall system, Phys. Rev. B **91**, 245126 (2015).

[186] W. Zhu, Z. Liu, F. D. M. Haldane, and D. N. Sheng, Fractional quantum hall bilayers at half filling: Tunneling-driven non-abelian phase, Phys. Rev. B **94**, 245147 (2016).

[187] V. Crépel, B. Estienne, and N. Regnault, Variational Ansatz for an Abelian to non-Abelian Topological Phase Transition in $\nu = 1/2 + 1/2$ Bilayers, 2019, arXiv:1904.01589.

[188] S. G. Naculich and H. J. Schnitzer, Duality between $SU(N)_k$ and $SU(k)_N$ WZW models, Nuclear Physics B **347**, 687 (1990).

[189] S. Naculich, H. Riggs, and H. Schnitzer, Group-level duality in WZW models and Chern-Simons theory, Physics Letters B **246**, 417 (1990).

[190] M. Camperi, F. Levstein, and G. Zemba, The large N limit of Chern-Simons gauge theory, Physics Letters B **247**, 549 (1990).

[191] J. W. Reijnders, F. J. M. van Lankvelt, K. Schoutens, and N. Read, Quantum hall states and boson triplet condensate for rotating spin-1 bosons, Phys. Rev. Lett. **89**, 120401 (2002).

[192] E. Ardonne, N. Read, E. Rezayi, and K. Schoutens, Non-abelian spin-singlet quantum Hall states: wave functions and quasihole state counting, Nuclear Physics B **607**, 549 (2001).

[193] D. Gepner, New conformal field theories associated with lie algebras and their partition functions, Nuclear Physics B **290**, 10 (1987).

[194] E. Fradkin and L. P. Kadanoff, Disorder variables and para-fermions in two-dimensional statistical mechanics, Nuclear Physics B **170**, 1 (1980).

[195] J. W. Reijnders, F. J. M. van Lankvelt, K. Schoutens, and N. Read, Rotating spin-1 bosons in the lowest landau level, Phys. Rev. A **69**, 023612 (2004).

[196] N. Read, Excitation structure of the hierarchy scheme in the fractional quantum Hall effect, Phys. Rev. Lett. **65**, 1502 (1990).

[197] J. Fröhlich and A. Zee, Large scale physics of the quantum Hall fluid, Nuclear Physics B **364**, 517 (1991).

[198] R. Jackiw and P. Rossi, Zero modes of the vortex-fermion system, Nuclear Physics B **190**, 681 (1981).

[199] P.-S. Hsin and N. Seiberg, Level/rank Duality and Chern-Simons-Matter Theories, JHEP **09**, 095 (2016), 1607.07457.

[200] O. Aharony, F. Benini, P.-S. Hsin, and N. Seiberg, Chern-Simons-matter dualities with SO and USp gauge groups, JHEP **02**, 072 (2017), arXiv:1611.07874.

[201] M. Barkeshli and J. McGreevy, Continuous transition between fractional quantum Hall and superfluid states, Phys. Rev. B **89**, 235116 (2014).

[202] D. F. Mross, J. Alicea, and O. I. Motrunich, Symmetry and duality in bosonization of two-dimensional Dirac fermions, Phys. Rev. X **7**, 041016 (2017).

[203] H. Goldman and E. Fradkin, Loop Models, Modular Invariance, and Three Dimensional Bosonization, Phys. Rev. B **97**, 195112 (2018), 1801.04936.

[204] F. Benini, P.-S. Hsin, and N. Seiberg, Comments on global symmetries, anomalies, and duality in (2 + 1)d, JHEP **04**, 135 (2017), 1702.07035.

[205] C. Cordova, P.-S. Hsin, and N. Seiberg, Global Symmetries, Counterterms, and Duality in Chern-Simons Matter Theories with Orthogonal Gauge Groups, SciPost Phys. **4**, 021 (2018), 1711.10008.

[206] S. Chatterjee *et al.*, Field-induced transition to semion topological order from the square-lattice Néel state, 2019, 1903.01992.

[207] S. Kivelson, D.-H. Lee, and S.-C. Zhang, Global phase diagram in the quantum Hall effect, Phys. Rev. B **46**, 2223 (1992).

[208] E. Witten, SL(2,Z) Action On Three-Dimensional Conformal Field Theories With Abelian Symmetry, 2003, arXiv:0307041, published in *From Fields to Strings* vol. 2, p. 1173, M. Shifman *et al*, eds., World Scientific, 2005.

[209] M. E. Peskin, Mandelstam-'t Hooft duality in abelian lattice models, Annals of Physics **113**, 122 (1978).

[210] C. Dasgupta and B. I. Halperin, Phase Transition in a Lattice Model of Superconductivity, Phys. Rev. Lett. **47**, 1556 (1981).

[211] K. Schoutens, E. Ardonne, and F. J. M. van Lankvelt, *Paired and Clustered Quantum Hall States* (Springer Netherlands, Dordrecht, 2002), pp. 305–316.

[212] P. Di Francesco, P. Mathieu, and D. Sénéchal, *Conformal Field Theory* (Springer-Verlag, Berlin, 1997).

[213] A. Karch, B. Robinson, and D. Tong, More Abelian Dualities in 2+1 Dimensions, JHEP **01**, 017 (2017), 1609.04012.

[214] E. Ardonne, F. J. M. v. Lankvelt, A. W. W. Ludwig, and K. Schoutens, Separation of spin and charge in paired spin-singlet quantum hall states, Phys. Rev. B **65**, 041305 (2002).

[215] C. Cordova, P.-S. Hsin, and K. Ohmori, Exceptional Chern-Simons-Matter Dualities, arXiv e-prints , arXiv:1812.11705 (2018), 1812.11705.

[216] A. Kapustin and N. Seiberg, Coupling a qft to a tqft and duality, Journal of High Energy Physics **2014**, 1 (2014).

[217] D. Gaiotto, A. Kapustin, N. Seiberg, and B. Willett, Generalized global symmetries, Journal of High Energy Physics **2015**, 172 (2015).

[218] C. Chamon, D. E. Freed, S. A. Kivelson, S. L. Sondhi, and X. G. Wen, Two point-contact interferometer for quantum Hall systems, Phys. Rev. B **55**, 2331 (1997).

[219] E. Fradkin, C. Nayak, A. Tsvelik, and F. Wilczek, A Chern-Simons effective field theory for the Pfaffian quantum Hall state, Nuclear Physics B **516**, 704 (1998).

[220] P. Bonderson, A. Kitaev, and K. Shtengel, Detecting non-abelian statistics in the $\nu = 5/2$ fractional quantum Hall state, Phys. Rev. Lett. **96**, 016803 (2006).

[221] A. Stern and B. I. Halperin, Proposed Experiments to Probe the Non-Abelian $\nu = 5/2$ Quantum Hall State, Phys. Rev. Lett. **96**, 016802 (2006).

[222] W. Bishara, P. Bonderson, C. Nayak, K. Shtengel, and J. K. Slingerland, Interferometric signature of non-Abelian anyons, Phys. Rev. B **80**, 155303 (2009).

[223] J. Nakamura, S. Liang, G. C. Gardner, and M. J. Manfra, Direct observation of anyonic braiding statistics, Nature Physics **16**, 931 (2020).

[224] I. P. Radu *et al.*, Quasi-Particle Properties from Tunneling in the v = 5/2 Fractional Quantum Hall State, Science **320**, 899 (2008).

[225] M. Dolev, M. Heiblum, V. Umansky, A. Stern, and D. Mahalu, Observation of a quarter of an electron charge at the $\nu = 5/2$ quantum Hall state, Nature **452**, 829 (2008).

[226] R. L. Willett, L. N. Pfeiffer, and K. W. West, Measurement of filling factor 5/2 quasiparticle interference with observation of charge e/4 and e/2 period oscillations, Proceedings of the National Academy of Sciences **106**, 8853 (2009).

[227] R. L. Willett, C. Nayak, K. Shtengel, L. N. Pfeiffer, and K. W. West, Magnetic-Field-Tuned Aharonov-Bohm Oscillations and Evidence for Non-Abelian Anyons at $\nu = 5/2$, Phys. Rev. Lett. **111**, 186401 (2013).

[228] M. H. Freedman, M. Larsen, and Z. Wang, A Modular Functor Which is Universal for Quantum Computation, Communications in Mathematical Physics **227**, 605 (2002).

[229] K. Pakrouski, M. Troyer, Y.-L. Wu, S. Das Sarma, and M. R. Peterson, Enigmatic 12/5 fractional quantum Hall effect, Phys. Rev. B **94**, 075108 (2016).

[230] R. S. K. Mong, M. P. Zaletel, F. Pollmann, and Z. Papić, Fibonacci anyons and charge density order in the 12/5 and 13/5 quantum Hall plateaus, Phys. Rev. B **95**, 115136 (2017).

[231] R. S. K. Mong *et al.*, Universal topological quantum computation from a superconductor-abelian quantum hall heterostructure, Phys. Rev. X **4**, 011036 (2014).

[232] Y. Hu and C. L. Kane, Fibonacci Topological Superconductor, Phys. Rev. Lett. **120**, 066801 (2018).

[233] P. L. S. Lopes, V. L. Quito, B. Han, and J. C. Y. Teo, Non-Abelian twist to integer quantum Hall states, Phys. Rev. B **100**, 085116 (2019).

[234] A. C. Balram, M. Barkeshli, and M. S. Rudner, Parton construction of particle-hole-conjugate Read-Rezayi parafermion fractional quantum Hall states and beyond, Phys. Rev. B **99**, 241108 (2019).

[235] P. Fendley and E. Fradkin, Realizing non-abelian statistics in time-reversal-invariant systems, Phys. Rev. B **72**, 024412 (2005).

[236] C. Chen, L.-Y. Hung, Y. Li, and Y. Wan, Entanglement entropy of topological orders with boundaries, Journal of High Energy Physics **2018**, 113 (2018), 1804.05725.

[237] A. Hui, E.-A. Kim, and M. Mulligan, Non-Abelian bosonization and modular transformation approach to superuniversality, Phys. Rev. B **99**, 125135 (2019), 1712.04942.

[238] D. J. Clarke and C. Nayak, Chern-simons-higgs transitions out of topological superconducting phases, Phys. Rev. B **92**, 155110 (2015).

[239] A. Zamoldchikov and V. Fateev, Nonlocal (parafermion) currents in two-dimensional conformal quantum field theory and self-dual critical points in zn-symmetric statistical systems, Sov. Phys. JETP **62**, 215 (1985).

[240] S.-S. Lee, S. Ryu, C. Nayak, and M. P. A. Fisher, Particle-hole symmetry and the $\nu = \frac{5}{2}$ quantum hall state, Phys. Rev. Lett. **99**, 236807 (2007).

[241] M. Levin, B. I. Halperin, and B. Rosenow, Particle-hole symmetry and the pfaffian state, Phys. Rev. Lett. **99**, 236806 (2007).

[242] Z. Komargodski and N. Seiberg, A symmetry breaking scenario for QCD_3, JHEP **01**, 109 (2018), 1706.08755.

[243] R. Argurio, M. Bertolini, F. Mignosa, and P. Niro, Charting the phase diagram of QCD_3, JHEP **08**, 153 (2019), 1905.01460.

[244] A. Baumgartner, Phases of flavor broken QCD_3, JHEP **10**, 288 (2019), 1905.04267.

[245] A. Armoni, T. T. Dumitrescu, G. Festuccia, and Z. Komargodski, Metastable vacua in large-N QCD_3, JHEP **01**, 004 (2020), 1905.01797.

[246] A. Baumgartner, Flavor broken QCD_3 at large N, Journal of High Energy Physics **2020**, 145 (2020), 2005.11339.

[247] N. Read, Lowest-landau-level theory of the quantum hall effect: The fermi-liquid-like state of bosons at filling factor one, Phys. Rev. B **58**, 16262 (1998).

[248] C. Wang and T. Senthil, Composite fermi liquids in the lowest landau level, Phys. Rev. B **94**, 245107 (2016).

[249] E. H. Fradkin, C. Nayak, A. Tsvelik, and F. Wilczek, A Chern-Simons effective field theory for the Pfaffian quantum Hall state, Nucl. Phys. **B516**, 704 (1998), cond-mat/9711087.

[250] N. R. Cooper, N. K. Wilkin, and J. M. F. Gunn, Quantum phases of vortices in rotating bose-einstein condensates, Phys. Rev. Lett. **87**, 120405 (2001).

[251] Z. Dong and T. Senthil, Noncommutative field theory and composite fermi liquids in some quantum hall systems, Phys. Rev. B **102**, 205126 (2020).

[252] R. Ma and Y.-C. He, Emergent QCD_3 Quantum Phase Transitions of Fractional Chern Insulators, 2020, 2003.05954.

[253] C. Cordova, P.-S. Hsin, and K. Ohmori, Exceptional Chern-Simons-Matter Dualities, SciPost Phys. **7**, 56 (2019).

[254] O. Aharony, F. Benini, P.-S. Hsin, and N. Seiberg, Chern-Simons-matter dualities with SO and USp gauge groups, Journal of High Energy Physics **2017**, 72 (2017), 1611.07874.

[255] I. Halder and S. Minwalla, Matter Chern Simons theories in a background magnetic field, Journal of High Energy Physics **2019**, 89 (2019), 1904.07885.

[256] B. Yang, Y.-H. Wu, and Z. Papić, Effective abelian theory from a non-abelian topological order in the $\nu = 2/5$ fractional quantum hall effect, Phys. Rev. B **100**, 245303 (2019).

[257] B. Andrews, M. Mohan, and T. Neupert, Abelian topological order of $\nu = 2/5$ and $3/7$ fractional quantum Hall states in lattice models, 2020, 2007.08870.

[258] C. Cordova, P.-S. Hsin, and N. Seiberg, Global Symmetries, Counterterms, and Duality in Chern-Simons Matter Theories with Orthogonal Gauge Groups, SciPost Phys. **4**, 21 (2018).

[259] H. Li and F. D. M. Haldane, Entanglement spectrum as a generalization of entanglement entropy: Identification of topological order in non-abelian fractional quantum hall effect states, Phys. Rev. Lett. **101**, 010504 (2008).

[260] R. Thomale, A. Sterdyniak, N. Regnault, and B. A. Bernevig, Entanglement gap and a new principle of adiabatic continuity, Phys. Rev. Lett. **104**, 180502 (2010).

[261] L. Fidkowski, Entanglement spectrum of topological insulators and superconductors, Phys. Rev. Lett. **104**, 130502 (2010).

[262] A. Chandran, M. Hermanns, N. Regnault, and B. A. Bernevig, Bulk-edge correspondence in entanglement spectra, Phys. Rev. B **84**, 205136 (2011).

[263] X.-L. Qi, H. Katsura, and A. W. W. Ludwig, General relationship between the entanglement spectrum and the edge state spectrum of topological quantum states, Phys. Rev. Lett. **108**, 196402 (2012).

[264] B. Swingle and T. Senthil, Geometric proof of the equality between entanglement and edge spectra, Phys. Rev. B **86**, 045117 (2012).

[265] J. Dubail, N. Read, and E. H. Rezayi, Edge-state inner products and real-space entanglement spectrum of trial quantum hall states, Phys. Rev. B **86**, 245310 (2012).

[266] R. Lundgren, Y. Fuji, S. Furukawa, and M. Oshikawa, Entanglement spectra between coupled tomonaga-luttinger liquids: Applications to ladder systems and topological phases, Phys. Rev. B **88**, 245137 (2013).

[267] S. Furukawa and Y. B. Kim, Entanglement entropy between two coupled tomonaga-luttinger liquids, Phys. Rev. B **83**, 085112 (2011).

[268] X. Chen and E. Fradkin, Quantum entanglement and thermal reduced density matrices in fermion and spin systems on ladders, Journal of Statistical Mechanics: Theory and Experiment **2013**, P08013 (2013).

[269] L. Zou and J. Haah, Spurious long-range entanglement and replica correlation length, Phys. Rev. B **94**, 075151 (2016).

[270] J. R. Fliss *et al.*, Interface contributions to topological entanglement in abelian chern-simons theory, Journal of High Energy Physics **2017**, 56 (2017).

[271] V. Crépel, N. Claussen, B. Estienne, and N. Regnault, Model states for a class of chiral topological order interfaces, Nature Communications **10**, 1861 (2019), 1806.06858.

[272] V. Crépel, N. Claussen, N. Regnault, and B. Estienne, Microscopic study of the Halperin-Laughlin interface through matrix product states, Nature Communications **10**, 1860 (2019), 1904.11023.

[273] V. Crépel, B. Estienne, and N. Regnault, Variational ansatz for an abelian to non-abelian topological phase transition in $\nu = 1/2 + 1/2$ bilayers, Phys. Rev. Lett. **123**, 126804 (2019).

[274] F. A. Bais, J. K. Slingerland, and S. M. Haaker, Theory of topological edges and domain walls, Phys. Rev. Lett. **102**, 220403 (2009).

[275] S. Beigi, P. W. Shor, and D. Whalen, The Quantum Double Model with Boundary: Condensations and Symmetries, Communications in Mathematical Physics **306**, 663 (2011), 1006.5479.

[276] A. Kitaev and L. Kong, Models for Gapped Boundaries and Domain Walls, Communications in Mathematical Physics **313**, 351 (2012), 1104.5047.

[277] J. Fuchs, C. Schweigert, and A. r. Valentino, Bicategories for Boundary Conditions and for Surface Defects in 3-d TFT, Communications in Mathematical Physics **321**, 543 (2013), 1203.4568.

[278] L. Kong, Anyon condensation and tensor categories, Nuclear Physics B **886**, 436 (2014), 1307.8244.

[279] T. Lan, J. C. Wang, and X.-G. Wen, Gapped domain walls, gapped boundaries, and topological degeneracy, Phys. Rev. Lett. **114**, 076402 (2015).

[280] L.-Y. Hung and Y. Wan, Ground-state degeneracy of topological phases on open surfaces, Phys. Rev. Lett. **114**, 076401 (2015).

[281] W. Ji and X.-G. Wen, Noninvertible anomalies and mapping-class-group transformation of anomalous partition functions, Phys. Rev. Research **1**, 033054 (2019).

[282] T. Lan, X. Wen, L. Kong, and X.-G. Wen, Gapped domain walls between 2+1D topologically ordered states, arXiv e-prints , arXiv:1911.08470 (2019), 1911.08470.

[283] M. Milovanović and N. Read, Edge excitations of paired fractional quantum hall states, Phys. Rev. B **53**, 13559 (1996).

[284] Y. Zhang, T. Grover, A. Turner, M. Oshikawa, and A. Vishwanath, Quasiparticle statistics and braiding from ground-state entanglement, Phys. Rev. B **85**, 235151 (2012).

[285] P. Fendley, M. P. A. Fisher, and C. Nayak, Topological Entanglement Entropy from the Holographic Partition Function, Journal of Statistical Physics **126**, 1111 (2007).

[286] F. A. Bais and J. K. Slingerland, Condensate-induced transitions between topologically ordered phases, Phys. Rev. B **79**, 045316 (2009).

[287] F. Burnell, Anyon condensation and its applications, Annual Review of Condensed Matter Physics **9**, 307 (2018), https://doi.org/10.1146/annurev-conmatphys-033117-054154.

[288] N. Ishibashi, The Boundary and Crosscap States in Conformal Field Theories, Mod. Phys. Lett. **A4**, 251 (1989).

[289] J. Cardy, Boundary conformal field theory, in *Encyclopedia of Mathematical Physics*, edited by J.-P. Franoise, G. L. Naber, and T. S. Tsun, pp. 333 – 340, Academic Press, Oxford, 2006.

[290] X. Wen, S. Matsuura, and S. Ryu, Edge theory approach to topological entanglement entropy, mutual information, and entanglement negativity in chern-simons theories, Phys. Rev. B **93**, 245140 (2016).

[291] D. Das and S. Datta, Universal features of left-right entanglement entropy, Phys. Rev. Lett. **115**, 131602 (2015).

[292] J. Lou, C. Shen, and L.-Y. Hung, Ishibashi states, topological orders with boundaries and topological entanglement entropy. part i, Journal of High Energy Physics **2019**, 17 (2019).

[293] J. R. Fliss and R. G. Leigh, Interfaces and the extended Hilbert space of Chern-Simons theory, 2020, 2004.05123.

[294] A. Kapustin and N. Saulina, Topological boundary conditions in abelian chernsimons theory, Nuclear Physics B **845**, 393 (2011).

[295] C. L. Kane and M. P. A. Fisher, Quantized thermal transport in the fractional quantum hall effect, Phys. Rev. B **55**, 15832 (1997).

[296] A. Cappelli, M. Huerta, and G. R. Zemba, Thermal transport in chiral conformal theories and hierarchical quantum hall states, Nuclear Physics B **636**, 568 (2002).

[297] A. Kitaev, Anyons in an exactly solved model and beyond, Annals of Physics **321**, 2 (2006).

[298] F. D. M. Haldane, Stability of chiral luttinger liquids and abelian quantum hall states, Phys. Rev. Lett. **74**, 2090 (1995).

[299] A. Cappelli and E. Randellini, Stability of topological insulators with non-abelian edge excitations, Journal of Physics A: Mathematical and Theoretical **48**, 105404 (2015).

[300] M. Levin and A. Stern, Classification and analysis of two-dimensional abelian fractional topological insulators, Phys. Rev. B **86**, 115131 (2012).

[301] A. Zamolodchikov, From tricritical ising to critical ising by thermodynamic bethe ansatz, Nuclear Physics B **358**, 524 (1991).

[302] D. J. Gross and A. Neveu, Dynamical symmetry breaking in asymptotically free field theories, Phys. Rev. D **10**, 3235 (1974).

[303] J. C. Y. Teo, T. L. Hughes, and E. Fradkin, Theory of Twist Liquids: Gauging an Anyonic Symmetry, arXiv e-prints , arXiv:1503.06812 (2015), 1503.06812.

[304] T. Lichtman, R. Thorngren, N. H. Lindner, A. Stern, and E. Berg, Bulk Anyons as Edge Symmetries: Boundary Phase Diagrams of Topologically Ordered States, arXiv e-prints , arXiv:2003.04328 (2020), 2003.04328.

[305] P. Bonderson and J. K. Slingerland, Fractional quantum hall hierarchy and the second landau level, Phys. Rev. B **78**, 125323 (2008).

[306] C.-K. Chiu and A. P. Schnyder, Classification of reflection-symmetry-protected topological semimetals and nodal superconductors, Phys. Rev. B **90**, 205136 (2014).

[307] J. C. Budich and E. Ardonne, Equivalent topological invariants for one-dimensional Majorana wires in symmetry class D, Phys. Rev. B **88**, 075419 (2013).

[308] D. Asahi and N. Nagaosa, Topological indices, defects, and majorana fermions in chiral superconductors, Phys. Rev. B **86**, 100504 (2012).

[309] J. C. Teo and T. L. Hughes, Topological defects in symmetry-protected topological phases, Annual Review of Condensed Matter Physics **8**, 211 (2017), https://doi.org/10.1146/annurev-conmatphys-031016-025154.

[310] K. Schoutens and X.-G. Wen, Simple-current algebra constructions of 2+1-dimensional topological orders, Phys. Rev. B **93**, 045109 (2016).

[311] P. Di Francesco, P. Mathieu, and D. Snchal, *Conformal field theory*Graduate texts in contemporary physics (Springer, New York, NY, 1997).

[312] M. Oshikawa, Y. B. Kim, K. Shtengel, C. Nayak, and S. Tewari, Topological degeneracy of non-abelian states for dummies, Annals of Physics **322**, 1477 (2007).

[313] T. Iadecola, T. Neupert, C. Chamon, and C. Mudry, Ground-state degeneracy of non-abelian topological phases from coupled wires, Phys. Rev. B **99**, 245138 (2019).

[314] G. Moore and N. Seiberg, Taming the conformal zoo, Physics Letters B **220**, 422 (1989).

[315] W. Chen, G. W. Semenoff, and Y.-S. Wu, Two loop analysis of nonAbelian Chern-Simons theory, Phys. Rev. **D46**, 5521 (1992), hep-th/9209005.